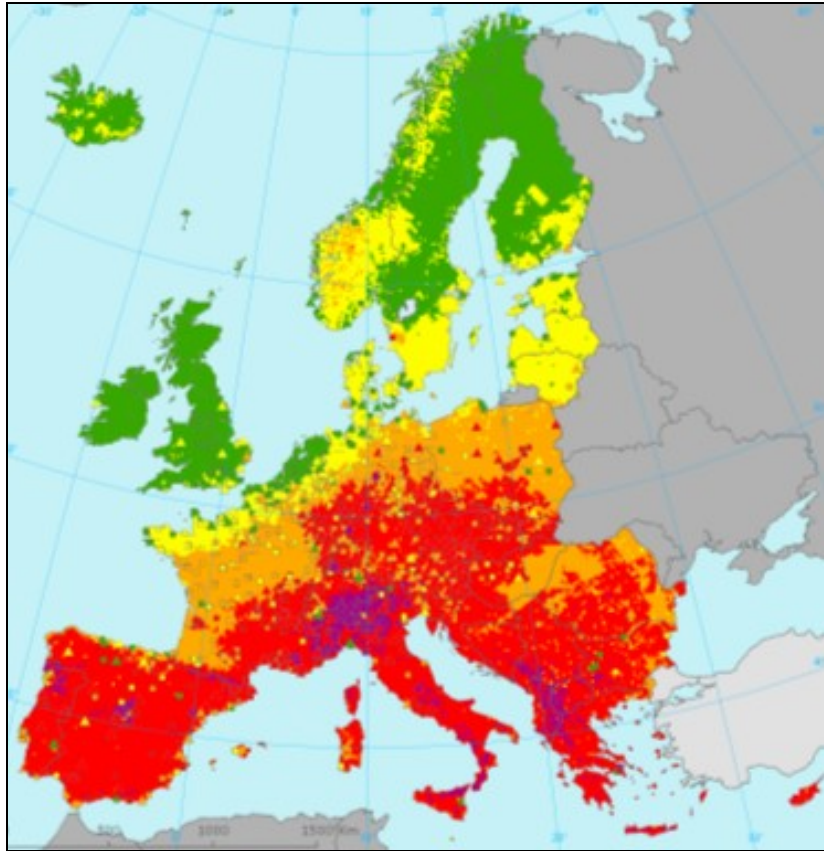


European air quality maps for 2005 including uncertainty analysis



ETC/ACC Technical Paper 2007/7

March 2008

Final version

*Jan Horálek, Peter de Smet, Frank de Leeuw,
Bruce Denby, Pavel Kurfürst, Rob Swart*



The European Topic Centre on Air and Climate Change (ETC/ACC)
is a consortium of European institutes under contract of the European Environmental Agency
MNP UBA-D UBA-V NILU AEAT AUTH CHMI MET.NO ÖKO TNO REC

Front page picture: The combined rural and urban concentration map of ozone health indicators 26th highest daily maximum 8-hour value in $\mu\text{g}\cdot\text{m}^{-3}$ for the year 2005. (Figure 4.1 (top) of this paper.)

ETC/ACC Technical Paper 2007/7

March 2008

Final version

Jan Horálek¹, Peter de Smet², Frank de Leeuw², Bruce Denby³, Pavel Kurfürst¹, Rob Swart²

¹ *Czech Hydrometeorological Institute (CHMI), Praha*

² *Netherlands Environmental Assessment Agency (MNP), Bilthoven*

³ *Norwegian Institute of Air Research (NILU), Kjeller*

EEA project managers: Jaroslav Fiala, Anke Lükewille

DISCLAIMER

<p>This ETC/ACC Technical Paper has not been subjected to European Environment Agency (EEA) member country review. It does not represent the formal views of the EEA.</p>

Contents

1 Introduction	5
2 Interpolation methodologies, supplementary data selection, and uncertainty analysis.....	9
2.1 <i>Interpolation methodologies and supplementary data selection.....</i>	9
2.2 <i>Interpolation uncertainty analysis</i>	10
2.3 <i>Exceedance probability mapping.....</i>	12
3 PM₁₀ maps for 2005	17
3.1 <i>PM₁₀ annual average</i>	17
3.1.1 <i>Population exposure and health impacts.....</i>	18
3.1.2 <i>Uncertainties.....</i>	21
3.2 <i>PM₁₀ 36th highest daily average.....</i>	22
3.2.2. <i>Uncertainties.....</i>	24
4 Ozone maps for 2005.....	27
4.1 <i>Ozone health related indicators</i>	27
4.1.1 <i>Population exposure and health impacts.....</i>	29
4.1.2 <i>Uncertainties.....</i>	32
4.2 <i>Ozone vegetation indicators.....</i>	34
4.2.1 <i>Vegetation and forest exposure</i>	34
4.2.2 <i>Uncertainties.....</i>	39
5 SO₂ maps for 2005	43
5.1 <i>SO₂ vegetation indicators.....</i>	43
5.1.1 <i>Natural vegetation exposure</i>	43
5.1.2 <i>Uncertainties.....</i>	45
6 NO_x maps for 2005	47
6.1 <i>NO_x annual average vegetation indicator</i>	47
6.1.1 <i>Natural vegetation exposure</i>	47
6.1.2 <i>Uncertainties.....</i>	48
7 Discussion, recommendations and conclusions.....	51
7.1 <i>Introduction.....</i>	51
7.2 <i>Recommended interpolation methods for regular updating</i>	52
7.3 <i>Interpolation without dispersion model output</i>	53
7.4 <i>Final conclusions relating to the mapping methodology.....</i>	58
References	63
Annexes	65
Annex 1 Input data.....	67
A1.1 <i>Introduction</i>	67
A1.2 <i>Measured air quality data</i>	67
A1.3 <i>Unified EMEP model output.....</i>	68
A1.4 <i>LOTOS-EUROS model output</i>	68
A1.5 <i>Altitude</i>	69
A1.6 <i>Meteorological parameters</i>	69
A1.7 <i>Population density</i>	69
A1.8 <i>Land cover</i>	69

Annex 2 PM₁₀ spatial analysis	71
<i>General introduction to the spatial analysis</i>	<i>71</i>
<i>A2.1 Rural maps.....</i>	<i>72</i>
A2.1.1 Linear regression analysis.....	72
A2.1.2 Spatial interpolation.....	73
A2.1.3 Uncertainty analysis	76
<i>A2.2 Urban maps</i>	<i>84</i>
A2.2.1 Linear regression analysis.....	84
A2.2.2 Spatial interpolation.....	85
A2.2.3 Uncertainty analysis	88
Annex 3 Ozone spatial analysis	97
<i>A3.1 Rural maps.....</i>	<i>97</i>
A3.1.1 Linear regression analysis.....	97
A3.1.2 Spatial interpolation.....	98
A3.1.2 Uncertainty analysis	103
<i>A3.2 Urban maps</i>	<i>114</i>
A3.2.1 Linear regression analysis.....	114
A3.2.2 Spatial interpolation.....	115
A3.2.3 Uncertainty analysis	118
Annex 4 SO₂ spatial analysis	127
<i>A4.1 Rural maps.....</i>	<i>127</i>
A4.1.1 Linear regression analysis.....	127
A4.1.2 Spatial interpolation.....	128
A4.1.3 Uncertainty analysis	130
Annex 5 NO_x spatial analysis.....	137
<i>A5.1 Rural maps.....</i>	<i>137</i>
A5.1.1 Linear regression analysis.....	137
A5.1.2 Spatial interpolation.....	138
A5.1.3 Uncertainty analysis	140
Annex 6 Formulas of statistical indicators and other calculations	145
<i>Kriging and variograms.....</i>	<i>146</i>
<i>Merging criteria of rural and urban maps into combined concentration maps</i>	<i>148</i>
<i>Combining criteria of rural and urban uncertainty map for the combined probability map.....</i>	<i>148</i>
Annex 7 PM_{2,5} in relation to PM₁₀.....	149

1 Introduction

General objectives

This is the first of two technical papers describing air quality mapping activities performed by the European Topic Centre on Air and Climate Change (ETC/ACC) for the European Environment Agency (EEA) in 2007. The objective of this report is (a) the updating and refinement of European air quality maps based on annual statistics of the 2005 observational data reported by EEA Member countries in 2006, and (b) the further improvement of the interpolation methodologies. The paper presents the results achieved and an uncertainty analysis of the interpolated maps and builds upon earlier reports from Horálek et al. (2005; 2007).

In the second report (Denby et al., 2008) the focus is on the use of daily statistical data, i.e. creating interpolated fields on a daily basis and combining these fields to derive the air quality indicators. This report builds upon the methodology described in Horálek et al. (2007) Chapter 6.

The products of this work are mainly intended to be used for the assessment of European air quality by the EEA and for public information purposes through the EEA website.

Air pollutants selected

This work builds upon the deliberation with EEA and recommendations summarized in Horálek et al. (2007), in which earlier spatial interpolation methodology developments and mapping activities have been documented. Again five pollutants have been taken into account, namely PM₁₀, PM_{2.5}, ozone, SO₂ and NO_x. However, PM_{2.5} maps are not created because the number of the relevant measuring stations continues to be too small to arrive at reliable results, as concluded in Annex 7 of this document.

General methodology

The mapping methods are, in principle, the same as described in Horálek et al. (2007): the rural and the urban areas are mapped separately; and the final maps are created by merging these together, using a weighting based on the population density. For rural mapping, the recommended methodology by Horálek et al (2007) is followed. I.e., “Methodologies based on linear regression models, using supplementary data, are generally preferred to pure interpolation methods as the pure interpolation methods give highly uncertain results far from monitoring sites.” Following this recommendation, not only data from measured air quality is used in the mapping procedure, but also supplementary data, such as output from chemical transport models (CTMs), altitude and the meteorological parameters. By making use of their correlation to air quality they contribute to improvements in the quality of Europe-wide air quality assessment through spatial interpolation, especially for areas further away from the measurement sites and where measurements are lacking, including urbanised areas without measurements. This paper examines whether the use of the same supplementary parameters for 2004 data (Horálek et al., 2007) is also the best for 2005 data. In addition, a number of specific questions regarding uncertainty are addressed.

Comparing four different interpolation methodologies

To carry out a proper evaluation of the improvements in interpolation results, by pursuing different types of input data in three subsequent steps and including their involved uncertainties, we employed a type-wise analysis. The extension with the CTM model comparison is considered as the fourth type. The resulting four types of interpolation methodologies analysed and compared are:

1. Using monitoring data only (by geostatistical methods based on kriging)
2. Combining monitoring data and EMEP model data (using a linear regression model followed by kriging of its residual)
3. Combining monitoring data, EMEP model data and other supplementary data (using a multiple linear regression model followed by kriging of its residual)
4. Combining monitoring data and LOTOS-EUROS model data (using a linear regression model followed by kriging of its residual)

The reason for the comparison of these types of methods is to examine their respective level of performance and interpolation improvement by adding additional information to that of the monitoring data. From the results, the statistically best or operationally preferred method is selected for the final creation of interpolated European maps of air quality. When different methods arrive at comparable statistical results, the associated air quality maps can be considered as being more robust.

Mapping uncertainty of the interpolations

The interpolation uncertainty of the preferred method used for the mapping is assessed quantitatively. As compared to Horálek et al. (2007), the interpolation uncertainty analysis of the maps has been applied for all air quality indicators and improved. To conclude on the most robust and suitable method for the operational mapping, Horálek et al (2007) recommended carrying out inter-annual comparisons of different methods and already provided such comparisons for *rural* areas. The preferred method derived from this analysis has been applied in the 2005 mapping. In the current paper this comparison has been extended to the *urban* areas. Based on the current and previous comparison results we conclude for every indicator on the most robust and preferred method for both the rural and urban areas. Those methods we ultimately used for producing the rural, the urban and their combined 2005 maps.

In this paper, an additional comparison as recommended by Horálek et al. (2007) is made, using output from the Unified EMEP model and from an alternative CTM as source of the supplementary information. The hypothesis is that (a) the performance of the models in the spatial interpolations should lead to comparable improved results, confirming the robustness and justification of using the EMEP model as source of supplementary data, and that (b) the use of CTMs in general improves interpolation results. As representative substitute for the output of the EMEP model we selected the LOTOS-EUROS dispersion model, a well established regional scale CTM applied in Europe from which data was readily available. To effectively examine the performance of the model contribution itself, we used dispersion model data as only data source additional to the air quality measurements and are reflected by above mentioned methodologies 2 and 4.

Mapping probability of exceedance

From a political point of view, a key question is to what extent air quality is either above or below a particular limit value in a certain area. But because of the significant scientific uncertainties, this question can not be answered very accurately for any particular location. Therefore, it is interesting to evaluate the probability that limit values will be exceeded, taking into account the scientific uncertainties. In this paper, trials of maps with the probability of exceedances of limit values are constructed. From the uncertainties in the interpolation methods and from the actual concentrations in each grid cell the probability of an exceedance of the limit value has been estimated. The resulting maps may guide further action with respect to implementation of abatement measures and design of the monitoring network.

Paper outline

Chapter 2 describes the methodological aspects in more detail. Chapters 3, 4, 5, and 6 present and discuss the mapping results for PM₁₀, ozone, SO₂ and NO_x, respectively. Final maps for each pollutant and indicator will be presented at the end of each of these chapters. Chapter 7 discusses the selection of the preferred interpolation methodologies for the European mapping of air quality pollutant indicators. In Annex 1 the input data sources and their detailed parameters used in the interpolations and mapping are presented. Annexes 2-5 discuss for each pollutant the comparison of maps created by different methods, leading to the selection of best or preferred mapping method. In Annex 6 the equations of the used statistical indicators are given. In Annex 7 the assessment of the feasibility of creating European PM_{2.5} maps based on PM₁₀-PM_{2.5} ratio of measurements is presented, discussed and concluded.

2 Interpolation methodologies, supplementary data selection, and uncertainty analysis

2.1 Interpolation methodologies and supplementary data selection

Air pollution measurements from ground stations are the most accurate source of air quality information. As the number of measuring sites is limited, the information obtained from these measurements has to be generalized to improve the spatial coverage. There are various ways to arrive at spatial maps on the basis of the data from the monitoring stations. The most straightforward type of interpolation methods is through spatial interpolation of monitoring data. If spatial interpolation does not use any further information (except the coordinates and altitude of the measurement stations) in addition to the measurements, we speak about spatial *interpolation using primarily monitoring data*, i.e. the type 1 of interpolation methods evaluated.

The second type of methods considered focuses on ground-based measurements as primary information using output of chemistry transport models (CTMs) as secondary, supplementary sources. This is in contrast to the work supporting the development of the European Thematic Strategy on Air Pollution, which gives prominence to modelling as primary source of information, using monitoring data to calibrate the model. While some of the methods and data sources are similar, to some extent the two approaches can be regarded as complementary. The CTMs have the advantage of full coverage of the whole territory, but they are generally less reliable than the measured data. The combination of the monitoring data with the dispersion modelling data represents the second type of the interpolation methods, being *linear regression models using monitoring and modelling data followed by interpolation of its residuals*. As explained in Chapter 1 we further examine and compare the performance of the same method using two different CTMs: the Unified EMEP model and the LOTOS-EUROS model.

Finally, the third type of method is an extension of the second type by the inclusion of supplementary parameters, spatially resolved, which show statistical correlation with the air quality data, providing more spatially resolved information on the whole territory than the pure air quality measurements. Examples of such supplementary data considered are meteorology, topography, population density and emissions. The linear regression analysis is primarily interested in identifying and selecting the most descriptive supplementary parameters to be used in this third type, the multiple *linear regression models using monitoring, modelling and other supplementary data followed by interpolation of their residuals*. The linear regression models and their use to select the most significantly correlating supplementary parameters for the interpolations is explained in Horálek et al. (2007), Sections 2.4 and 2.5. The supplementary data sources we considered here are described in more detail in Annex 1.

As concluded in Horálek et al. (2007), different geo-statistical interpolation techniques can be applied at each of the four types of methodologies, each with its specific level of performance per pollutant indicator field. The four techniques selected for type 1 were considered as promising with the recommendation to assess its inter-annual performance. Therefore, these are selected for examination on the 2005 data again. The simpler Inverse Distance Weighting (IDW) is not considered in this paper, since this method proved to be the weakest interpolator. It was recommended to drop it from any further interpolation improvement effort. For the three types where the interpolation is preceded by linear regression only ordinary kriging is used, since Horálek et al (2007) recommend dropping the IDW for its weak performance in general. Details on the interpolation kriging techniques used in this paper are described in Horálek et al. (2007), sections 2.2 to 2.4.

In summary, the four types of methodologies examined are the following:

1. Interpolation methods using primarily monitoring data
 - a. ordinary kriging (OK)
 - b. lognormal kriging (LK)
 - c. ordinary cokriging, using the altitude of the measuring stations (OC)
 - d. lognormal cokriging, using the altitude of the measuring stations (LC)
2. Linear regression model using monitoring and EMEP modelling data, followed by interpolation of its residuals by using ordinary kriging
3. Linear regression models using monitoring, EMEP modelling data and other supplementary data, followed by interpolation of their residuals by using ordinary kriging
4. Linear regression model using monitoring and LOTOS-EUROS modelling data, followed by interpolation of its residuals by using ordinary kriging

For all interpolation methods, i.e. OK, LK, OC and LC, variogram parameters are estimated by the minimization of the cross-validation RMSE (Horálek et al. 2007, Section 2.3.5).

For all four types of methods, the mutual comparison and uncertainty analysis is executed using cross-validation, for all considered pollutants and their indicators. For the purpose of this comparison and uncertainty analyses the specific methods (using specific supplementary data) of the methodology type 3 had to be selected. Thus we made an additional sub-selection: we first took the linear regression submodel performing best on 2005 data with the set of supplementary parameters contributing most, selected through a stepwise regression with a backward elimination. If the preferred method with particular supplementary data turned out to be different from the 2004 analysis, the method used by Horálek et al. (2007) for mapping of 2004 data was applied as well for the relevant pollutant indicator and the type of area as a basis for comparison.

Based on the cross-validation analysis the preferred method is selected. In case the selected methods for 2004 and 2005 mapping result to be different, both are compared for the 2005 data. The best is selected as the preferred method for the mapping of 2005 data. In case the same method is selected as best for both years, it is considered to be the best or at least as the preferred method to be used for mapping. Especially for cases when the same method performs best in both years, it gives some confidence in the robustness of the method for further application on the specific pollutant indicator.

The above described approach and methods are applied separately for the rural and urban areas. The merging of the selected rural and urban into one combined map is done based on the aggregated 10 x 10 km population density grid, using the criterion as described in Horálek et al. (2007), Chapter 3 and Annex.

2.2 Interpolation uncertainty analysis

The interpolation uncertainty of each interpolation method used for the mapping and the maps themselves are assessed quantitatively. Compared to Horálek et al. (2007), Chapter 7, similar interpolation uncertainty analyses of the maps are done, however this is now extended to each of the air pollutant indicators. Also, the cross-validation scatter plots were extended also for the methods of types 2, 3 and 4.

Four approaches are applied: (i) comparison of the maps created by the selected and alternative methods, using the difference of these maps (ii) cross-validation analysis, using statistical indicators and their scatter plots, (iii) non cross-validation scatter plots for comparison measured with estimated values, and (iv) the creation of uncertainty maps additional to the interpolated maps produced with the preferred interpolation method. Cross-validation analysis is executed for all examined methods, whilst the other approaches for selected method only.

Next to the aim of selecting an optimal set of supplementary data, cross-validation analysis also serve as a basis to estimate the level of uncertainty in the interpolation methods (or the interpolation-part of the methods of type 2 to 4). The statistical *cross-validation* consists of a spatial interpolation carried out for a measurement point using all the available measurement points (resp. information associated with them) except the data from that one point, i.e., it withholds one data point and then makes a prediction at the spatial location of that point. This procedure is repeated for all measurement points of the available set. The predicted and the measured values are then compared with help of statistical indicators. The statistical uncertainty indicators of the cross-validation are: the root mean squared error (*RMSE*), the mean prediction error (*MPE*), the mean absolute error (*MAE*), the standard deviation of error (*SDE*), the minimum error, the maximum error, the median of absolute error (*MedAE*), the mean prediction standard error (*MPSE*) and parameters of the cross-validation scatter plot, i.e. slope a , intercept c and the coefficient of determination R^2 . See Annex 6 or Horálek et al. (2007) Section 2.6 for more details on their definitions and their role as indicator. The cross-validation scatter plots are created by plotting the actual measurement indicator values (x axis) against the cross-validation predicted indicator values (y axis). The scatter plot of the cross-validation predicted indicator values plotted against the measurement based indicator values serve as a mean uncertainty indicator for the interpolation method itself. It provides an estimate of the level of uncertainty for the predicted interpolation values at locations without measurements.

In this paper an additional comparison between the interpolation uncertainty of the method using the EMEP dispersion model and the same method using the LOTOS-EUROS model is performed to explore uncertainties resulting from the choice of a particular model. This comparison is also carried out using cross-validation.

Alternatively to the cross-validation approach, a simple comparison between the measured and interpolated values in the points of measurement is made, using scatter plots (resp. the parameters of the fitted regression line, i.e. R^2 , slope a and intercept c). This comparison differs from cross-validation in two ways: First, the comparison is constructed from all stations, including the measured value in the examined point. Second, the interpolated values are the mean values of the 10x10 grid cells obtained by kriging (whereas in cross-validation the predicted value is computed in the exact location of the monitoring station). The principle of this type of kriging is described in detail in Annex 6. This comparison shows the uncertainty at the monitoring location; while cross-validation simulates the behaviour of interpolation in the places with no measurement (the cross-validation approach does not use the measured value in the examined point).

Two different sources of uncertainty are present in this approach: Firstly, uncertainty caused by the method. The values estimated by kriging are mostly smoothed in comparison with the measured values. Secondly, the spatial uncertainty related to the differences in representativity: the values of each grid are the estimated value of the mean of the 10x10 km area, whilst the measured values are station-related measurements.

The uncertainty maps show the predicted standard error of estimation, following the principles of spatial statistics (see Cressie, 1993). The statistical term *standard error of estimation* of a particular method is defined as the estimated standard deviation of the value estimated by that method in a relevant point. Uncertainty maps are computed together with air quality interpolation maps. As in the case of concentration maps, the interpolation is executed first and then aggregated into the 10x10 km grid. The uncertainty analyses are done for urban and rural areas separately.

2.3 Exceedance probability mapping

In addition to the uncertainty maps, one can construct maps with the probability of exceedance (PoE) of a specific threshold value (e.g. limit or target value).

The maps of PoE of limit value exceedance are constructed using the concentration and uncertainty maps:

$$PoE(x) = 1 - \Phi\left(\frac{LV - C_c(x)}{\delta_c(x)}\right) \quad (2.1)$$

where $PoE(x)$ is the probability of limit value (LV) exceedance in the grid cell x ,

$\Phi()$ is the cumulative distribution function of the normal distribution,

LV is the limit value of the relevant indicator,

$C_c(x)$ is the estimated combined concentration value in the grid cell x ,

$\delta_c(x)$ is the combined standard error of the estimation in the grid cell x .

For the probability map of the combined (rural and urban) map, the standard error is calculated from the standard errors of the composing rural and urban maps:

$$\delta_c = \sqrt{A^2 \cdot \delta_r^2 + (1 - A)^2 \cdot \delta_u^2 + 2A \cdot (1 - A) \cdot \delta_r \cdot \delta_u \cdot r_{ru}} \quad (2.2)$$

where δ_c is the combined uncertainty (standard deviation) in the grid cell

A is the weight factor based on population density for the rural grid cells (see Annex 6)

δ_r and δ_u are the uncertainties in the corresponding rural resp. urban grid cell

r_{ru} is the correlation coefficient of the rural and urban concentration fields.

In the case of the perfect correlation the equation becomes

$$\delta_c = A \cdot \delta_r + (1 - A) \cdot \delta_u \quad (2.3)$$

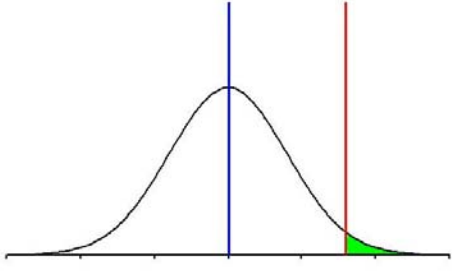
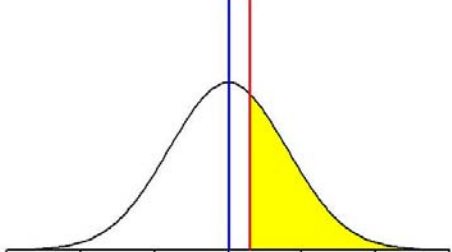
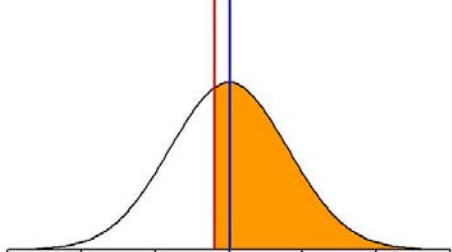
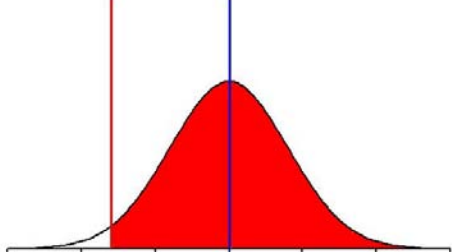
In the case of no correlation it is

$$\delta_c = \sqrt{A^2 \cdot \delta_r^2 + (1 - A)^2 \cdot \delta_u^2} \quad (2.4)$$

At areas with a population density less than 100 inhabitants per km² the weight factor $A = 1$, meaning the concentration and uncertainty of the rural map is assigned to the corresponding grid cell of the final map. At areas with more than 500 inhbs.km⁻² the weight factor $A = 0$, meaning the concentration and uncertainty of the rural map is assigned to the corresponding grid cell of the final map. At areas with a population density within the range of 100 - 500 inhbs.km⁻² the combined concentration C_c is derived according equation A6.13 and its related combined standard error uncertainty δ_c according equation 2.2.

To get an impression on the size of the area per population density 'class' the number of 10x10 km⁻² grid cells are counted. From the total number of 50918 cells the terrestrial mapping domain consists of there are 40942 cells classified as rural (< 100 inhbs.km⁻²), 1831 cells as urban (> 500 inhbs.km⁻²) and 8145 cells as combined rural and urban (100 – 500 inhbs.km⁻²).

In the probability maps the relation between the predicted value in a cell and the limit value (or target value) is grouped in four cases which are illustrated below.

	<p>The graph shows the predicted concentration value in the grid cell (blue line) and the normal distribution centered around the grid cell value. The limit value is given by the red line. In this situation the grid value is much lower than the limit value. However, when considering the uncertainties in the concentration value, an exceedance is unlikely but there is still a small change on exceedance. When the total probability of exceedance is less than 25% the cells are green coloured in the probability maps.</p>
	<p>In this situation the concentration value is slightly lower than the limit value. There is no exceedance but when considering the uncertainty ranges, exceedance of the limit value is possible. The change of an exceedance is up to 50% when concentration and limit value are equal. In the map the areas where the probability of exceedance is between 25% and 50% are coloured yellow.</p>
	<p>Here the concentration is larger than the limit value: such a situation is defined as an exceedance but as the graph shows that compliance with the limit value is possible. This kind of situations where the probability of exceedance is between 50 and 75% are given by an orange colour.</p>
	<p>Here the concentration is much larger than the limit value. Exceedance of the limit value is most likely. In the probability maps areas where the change of exceedance is more than 75% are coloured red.</p>

The four probability classes can be defined in terms of the standard error $\sigma(x)$ and predicted concentration value C in the grid:

if the limit value is more than $C + 0.675 \sigma(x)$ then the PoE is less than 25%

if the limit value is between C and $C + 0.675 \sigma(x)$ then the PoE is between 25 and 50%

if the limit value is between $C - 0.675 \sigma(x)$ and C then the PoE is between 50 and 75%

if the limit value is less than $C - 0.675 \sigma(x)$ then the PoE is more than 75%.

The difference between the predicted value and the limit value and the level of interpolation uncertainty play a combined role in the level of probability of exceedance. This is illustrated in Figure 2.1. Here the distribution around the predicted value is given for two cases with a low and high uncertainty.

With increasing uncertainty, (that is with increasing standard error of the predicted value in the grid cell) the curve broadens. The predicted value is below the limit value; the probability of an exceedance is given by the area on the right hand side of the red line of the limit value. Although the difference between predicted value and limit value is the same in the high and low uncertainty case, it is clear that in the high uncertainty case the probability of exceedance is must larger than in the low uncertainty case. For the situation sketched in Figure 2.1 the grid cell may even fall in different probability classes: in the low uncertainty case the cell would be green, in the high uncertainty case the cell would be yellow.

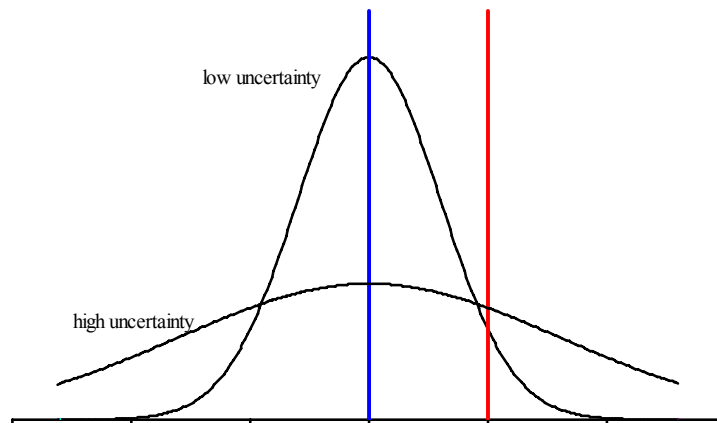


Figure 2.1 Distribution around the predicted value (blue) given for two cases with a low and high uncertainty. Red is the limit or target value.

Next to the estimation of the probability of the limit value exceedance, the real measured values at the stations are presented in the probability maps: stations with the measured values above the limit value or target value are marked red, whereas the station measurements below the limit value are marked green. (Neither orange nor yellow is applied on the stations, since that classification is related to the *interpolation uncertainty* only and not to the measurement uncertainty at the stations).

The probability map may guide further action with respect to implementing of abatement measures and to monitoring network design. In regions with a high uncertainty in the indicator value there might be no need to reduce this uncertainty (e.g. by establishing additional stations) when the probability map indicates that exceedance is most unlikely. On the other hand, there will be areas where the concentration is below the limit value but the probability map indicates that exceedance is likely. Although these areas are formally speaking in compliance, one may conclude that, in order to avoid non-compliance in another year, abatement measure should be considered.

Both the uncertainty and probability maps presented in this report accounts only for the interpolation error. Other sources of uncertainty (e.g. measuring errors, representativeness, and model uncertainty) have not been included. Therefore, it should be stressed that these maps are the estimates only.

The exceedance probability maps show that relationship between the actual, the interpolated value and the associated uncertainty is much more complex than is often assumed. This calls for a careful consideration of the selection of the particular output indicator to be presented and the way of presenting it, especially in view of the message to be communicated.

3 PM₁₀ maps for 2005

For PM₁₀ the two health-related indicators annual average and 36th highest maximum daily average are considered. The analyses and determination of the best and/or preferring interpolation method for mapping out of the set of methods of the different types of methodologies takes place for the rural and urban areas separately. Based on the selected method for each indicator for both the rural and urban maps are produced. Out of these maps a combined European covering interpolated PM₁₀ indicator map is created using a population density relation as criteria.

The preparation of the separate rural and urban maps is discussed in Annex 2. Details on the process of selecting the best interpolation method are also given in this Annex.

3.1 PM₁₀ annual average

The combined interpolated map for the 2005 PM₁₀ annual averages in Figure 3.1 is created by combining the rural and urban maps using a 10x10 km grid aggregated population density field, according the criterion as described in Horálek et al. (2007).

The rural map has been created by combining the annual averages from the measured PM₁₀ concentrations from the rural background stations with supplementary data from the EMEP model output, altitude field, wind speed and surface solar radiation in a linear regression model, followed by the interpolation of its residuals by ordinary kriging. This method (abbreviated as 3-P.Eawr-a) is the same as used for the 2004 mapping (Horálek et al, 2007). Although the methods based on lognormal cokriging with altitude gives slightly better results, this method has been selected as it gives a better

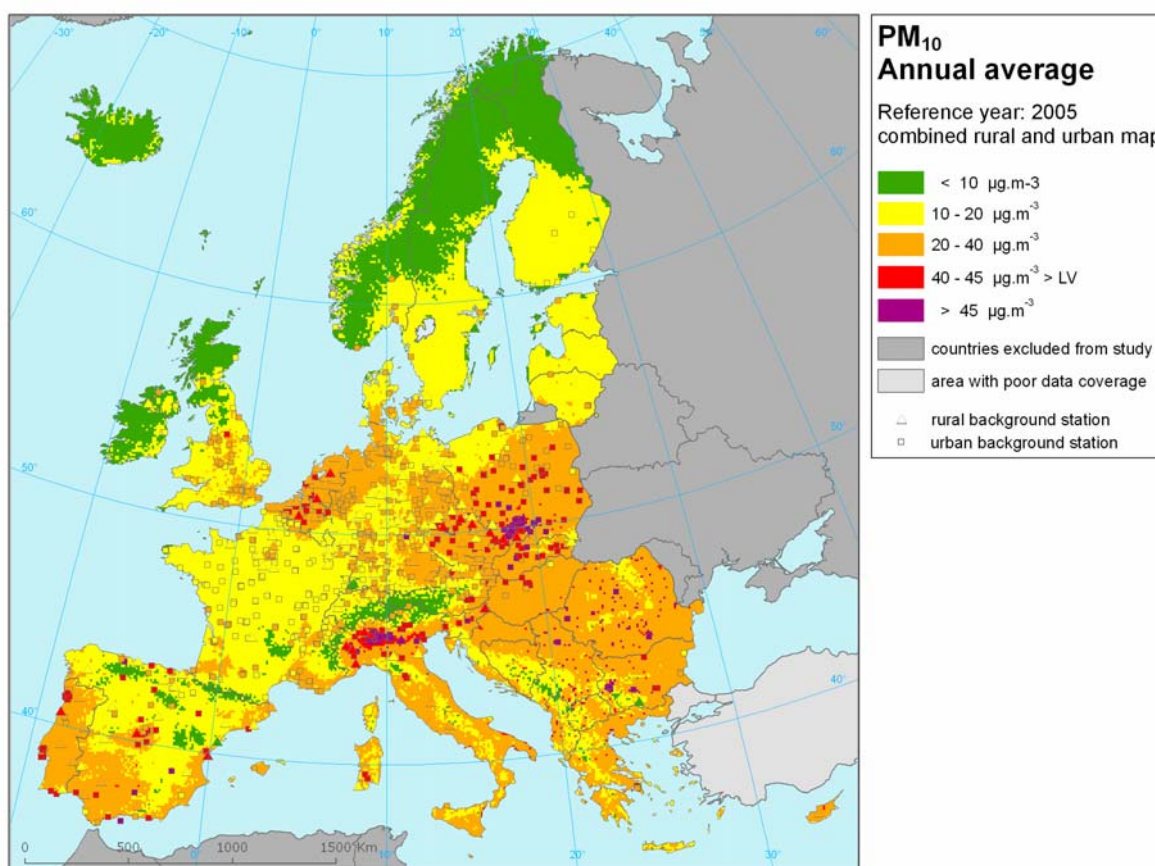


Figure 3.1 Combined rural and urban concentration map of PM₁₀ – annual average, year 2005. Spatial interpolated concentration field and the measured values in the measuring points. Units: µg.m⁻³.

European coverage.

The urban map is created by combining the measured PM10 annual averages from the urban and suburban background stations with the EMEP model output only in a linear regression, followed by the interpolation of its residuals by ordinary kriging (abbreviated as 2-UP.E-a), while on the 2004 data the method of ordinary kriging on monitoring data only (method 1-a) was applied in TP 2006/6 with the disadvantage of a limited European coverage. The performance of other mapping methods is similar but the method 2-UP.E-a is selected for its better European coverage.

The areas and stations in the combined map where the limit value (LV) of 40 $\mu\text{g}\cdot\text{m}^{-3}$ is exceeded are coloured red and purple. Comparing this map with the 2004 concentration map (Horálek et al, 2007), a similar spatial pattern is observed but the concentration in 2005 tends to be slightly higher than in 2004. A similar small increase is also noted in the monitoring data alone (Mol et al. 2007).

3.1.1 Population exposure and health impacts

The final concentration map of the annual PM10 mean concentration shows increased concentrations in the urbanized areas. In comparison to its neighbouring countries the concentration in France are relatively low. It can not be excluded that these low levels to the fact that these data are not corrected despite they were obtained by non-reference measuring configurations (mostly TEOM) (de Leeuw, 2005).

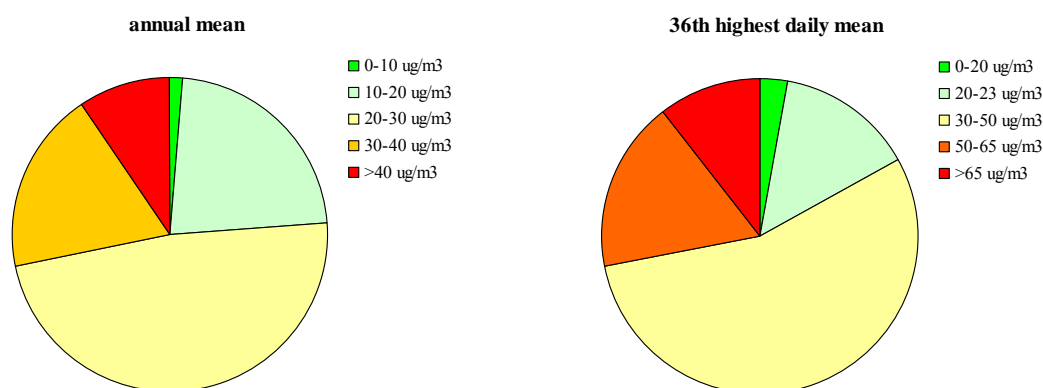


Figure 3.2 Exposure of the European population to PM10 concentrations, annual mean (left) and 36th highest daily mean (right), (reference year 2005).

Table 3.1 and Figure 3.2 give the population frequency distribution for a limited number of exposure classes. Note that, in contrast to Table 3.1, Figure 3.2 includes all countries shown in Figure 3.1. Almost a quarter (23%) of the European population is exposed to concentrations below the stage-2 indicative limit value of 20 $\mu\text{g}\cdot\text{m}^{-3}$. About two-third of the European population lived in 2005 in areas where the PM10 concentration is estimated to be between 20 and 40 $\mu\text{g}\cdot\text{m}^{-3}$. About 9% of the population lives in areas where the PM10 annual limit value is exceeded. However, as the current mapping methodology tends to underestimate high values, the number of 9% is probably higher. The frequency distribution shows a large variability over Europe; in six countries (Albania, Bulgaria, Cyprus, FYR of Macedonia, Greece, and Romania) it is estimated that more than a quarter of the population is exposed to concentrations above the limit value. In a number of countries in north and north-west Europe the LV seems not to be exceeded at the 10x10 km² level applied in the mapping.

Table 3.1 Population exposure and population weighted concentration – PM₁₀, annual average, year 2005.

Country	Population x1000	2005 Percent [%]					Population- weighted conc. µg.m ⁻³
		< 10 µg.m ⁻³	10 - 20 µg.m ⁻³	20 - 40 µg.m ⁻³	40 - 45 µg.m ⁻³	> 45 µg.m ⁻³	
Austria	8286	5.8	16.9	77.4	0	0	23.5
Belgium	10542	0	2.8	97.2	0	0	28.9
Bulgaria	8055	0.3	4.5	65.3	3.2	26.7	37.2
Croatia	4366	0	4.4	87.5	8.1	0	30.6
Czech Rep.	10155	0	1.5	88.8	2.9	6.8	31.5
Denmark	5006	1.2	40.8	58.0	0	0	19.7
Estonia	1301	2.4	83.7	14.0	0	0	16.3
Finland	5179	7.9	92.1	0.0	0	0	13.3
France	58286	0.5	60.9	38.5	0	0	19.1
Germany	81889	0.1	22.7	77.2	0	0	22.1
Greece	10655	0.1	7.2	48.7	35.4	8.5	34.7
Hungary	10107	0	0	98.0	2	0	33.5
Ireland	3652	40.0	60.0	0.0	0	0	11.4
Italy	57119	0.6	5.1	71.8	10.1	12.4	32.7
Latvia	2243	1.3	58.6	40.1	0	0	18.7
Liechtenstein	32	0	0	100	0	0	21.4
Lithuania	3567	0	54.0	46.0	0	0	20.3
Luxembourg	451	0	100	0.0	0	0	18.4
Malta	394	0	0	100	0	0	36.5
Netherlands	15153	0	0.2	99.8	0	0	29.1
Poland	38182	0	8.1	75.6	4.1	12.2	30.5
Portugal	10024	0	1.8	85.3	12.9	0.0	30.6
Romania	22228	0	1.9	59.2	12.3	26.7	37.4
San Marino	19	0	0	100	0	0	24.9
Slovakia	5265	0	2.0	92.6	5.4	0	31.4
Slovenia	2034	0.1	11.5	88.4	0	0	27.5
Spain	39884	0.6	15.8	82.7	0.8	0	27.4
Sweden	8666	8.8	84.6	6.6	0	0	15.0
United Kingdom	58204	2.3	30.5	67.2	0	0	20.8
Albania	3767	1	13.5	39.5	32.9	12.9	33.8
Andorra	59	18	16.1	65.7	0.0	0.0	16.2
Bosnia-Herzegovina	4000	0.6	17.7	60.7	20.9	0.0	30.1
Island	101	47.4	52.6	0.0	0	0	9.5
Macedonia, FYR of	2214	1.2	9.9	25.5	5.2	58.2	42.7
Norway	2907	15.6	53.2	31.1	0.0	0.0	16.5
Serbia&Montenegro	10996	0	6	47	7	40	38.7
Switzerland	6801	3	42.0	54.8	0.0	0	19.8
Total	511787	1.3	22.7	66.8	3.9	5.4	26.3

Note: Countries with the values based on ORNL population data with uncertain quality: AD, AL, BA, CH, CS, IS, MK, NO. Countries with the lack of air quality or population density data are excluded from calculations in this paper: CY, TR.

From Figure 3.2 it is clear that the daily limit value of PM₁₀ has been exceeded in a much larger part of Europe, see also the map in Figure 3.5 and Table 3.2 given below.

In a health impact assessment the number of premature deaths attributable to long-term exposure to PM₁₀ has been estimated. A similar approach as described in Horálek et al. (2007) has been applied. An update of country-specific demographic data has been taken from the UN population Division (UN, 2006). The health impact assessment is performed according to standard population attributive principles (WHO, 2001). A relative risk of 4.3% per 10 µg.m⁻³ PM₁₀ for total mortality (excluding violent deaths, adults 30 years and older) has been used (Künzli et al., 2000). A uniform non-anthropogenic background concentration of 5 µg/m³ has been subtracted.

The estimated number of premature deaths per million inhabitants attributable to PM₁₀ exposure is given in Figure 3.3. The observed range is partly caused by the differences in PM₁₀ concentration over Europe and partly by the differences in age distributions and baseline mortalities. The

uncertainties in the numbers caused by the uncertainties in the relative risk factor are relatively large: for the EU27 as a whole the number ranges from 510 to 1150 deaths per million with a best estimate of 830.

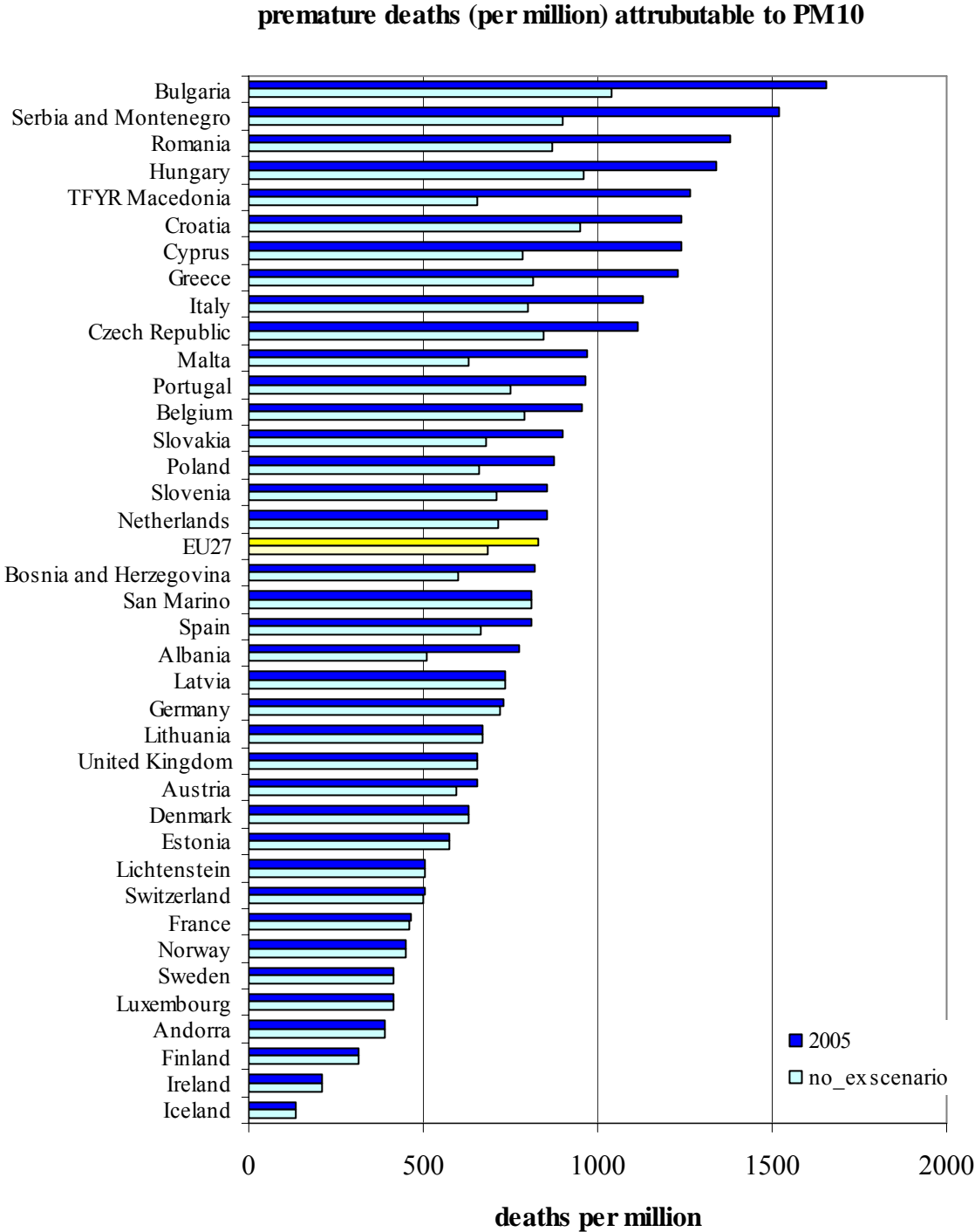


Figure 3.3 Number of premature deaths per million inhabitants attributable to PM10 exposure, reference year 2005. The “no_ex scenario” corresponds to the (hypothetical) situation that the daily limit value is not exceeded at European hot-spot locations.

The results in Figure 3.3 labelled as “no_ex scenario” correspond to a sensitivity calculation in which it is assumed that the daily limit value (a daily mean of $50 \mu\text{g}\cdot\text{m}^{-3}$ may not be exceeded on more than 35 days per year) is nowhere in Europe, not even at hot-spot location, exceeded. This situation has been simulated by truncating the annual mean concentration calculated for each 10×10 km grid cell to $25 \mu\text{g}\cdot\text{m}^{-3}$ and re-estimating the number of premature deaths using the truncated concentration field. The rationale of the truncation value of $25\mu\text{g}\cdot\text{m}^{-3}$ is as follows: the monitoring data shows that the daily PM10 limit value is equivalent with an annual average concentration of $31 \mu\text{g}\cdot\text{m}^{-3}$ (see e.g. Buijsman et al. (2005) and Stedman et al. (2007)). In our mapping exercise the concentration in the 10×10 km grid cell is assumed to be representative for the rural or urban background situation. On the average the annual average concentration at a traffic hot-spot is 20-25% higher than at an urban background station (see e.g. Mol et al, 2007). Therefore, with a background concentration of $25 \mu\text{g}\cdot\text{m}^{-3}$ exceedance of the daily limit value at hot spots will largely be avoided.

In this “no_ex scenario” the reduction in premature deaths is particularly large in the central eastern countries. For the EU27 as an average we estimate a reduction of about 17%. Even when the limit values are met in the whole EU27 territory a substantial number of premature deaths are to be expected.

3.1.2 Uncertainties

The absolute and relative mean interpolation uncertainty in the combined map, summarised from Sections A.2.1.3 and A2.2.3, are for the rural areas - taken from the rural map - $5.5 \mu\text{g}\cdot\text{m}^{-3}$, and about 26% respectively, of the mean of the measurement based PM10 annual averages at all rural background stations. For the urban areas - taken from the urban map – they are $5.5 \mu\text{g}\cdot\text{m}^{-3}$, and about 20% respectively, at all urban and suburban background stations

Based on the concentration maps (Figure A2.1 left, rural; Figure A2.11 left, urban) and uncertainty maps (Figures A2.9 left, rural; Figure A2.18 left, urban) and the limit values for the annual average PM10 the maps of the probability of the limit value (LV) exceedance have been constructed.

The combined map of probability of exceedance is composed from the combined map of concentrations (Figure 3.1) and combination uncertainty map according a merging criterion as described in Section 2.3 leading to a combined map. The uncertainty in the probability maps accounts only from the uncertainties caused by the interpolation and innate spatial variability of concentrations within the grid cell. Uncertainties in the measurements, the supplementary data and those caused by the urban/rural combination are not included. This combined map of uncertainty is derived according the standard error propagation calculation on the level of grid cells according Section 2.3.

After constructing the combined uncertainty map, the combined probability map can be constructed again: given the concentration value at each grid cell from the combined concentration map (Figure 3.1) and its corresponding combined uncertainty value, and given the limit value we can estimate the exceedance for that grid cell assuming a Gaussian distribution. Figure 3.4 shows the combined map of estimated probability of exceedance of the PM10 annual average and the 36th maximum daily mean.

Areas with the probability of limit value exceedance above 75% are marked in red; areas below 25% are marked in green. The red areas indicate areas for which exceedance may occur very likely due to high concentration close to or already above LV, including such enclosed uncertainty that exceedance is likely. Or lower concentrations with such high uncertainty levels reaching above the LV that exceedance is very likely. Vice versa, in the green areas it is not very likely to have predicted concentration values showing exceedance and/or such enclosed uncertainties that reaching above the LV not very likely.

Next to the estimation of the probability of the limit value exceedance, the real measured values at the stations are presented in the maps: stations with the measured values above the limit value or target value are marked red, whereas the station measurements below the limit value are marked green. (Neither orange nor yellow is applied on the stations, since that classification is related to the *interpolation uncertainty* and not to the measurement uncertainty).

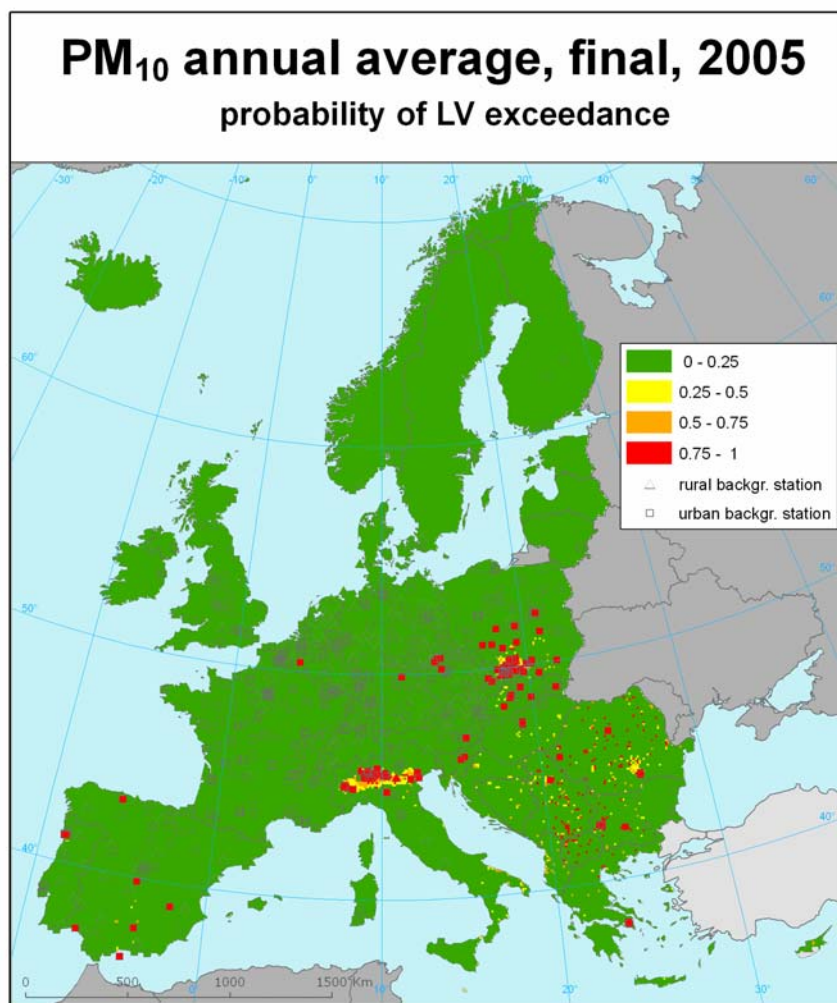


Figure 3.4 Map with the probability of the limit value exceedance for PM₁₀ indicators annual average, in $\mu\text{g}\cdot\text{m}^{-3}$ on the European scale in 2005, on the 10 x 10 km grid resolution. (Stations with annual averaged measurement values above the limit value are marked red; station measurements below the limit value are marked green).

The estimated probability of exceedance for the PM₁₀ annual averages are moderate to considerable at urban areas in the Balkan region at urban locations (red grid cells, i.e. larger than 75 % probability). To less extent this occurs in south Poland, Czech Republic, Hungary and south Spain. Again in the Balkan and south Poland, but also in the Italian Po Valley one encounter larger continues areas with exceedance probability ranging from 25 to 50 % with increased levels from 50 to 75 % or even higher at their centre. At these areas PM₁₀ annually based exceedances are very likely and considerable reductions may be needed to reach non-exceedance levels in the future. The north-western and northern countries of Europe do not show such increased (larger then 25%) probability exceedances, indicating policy targets are or may be reached for the larger background areas. The map does not indicate locally bound exceedance effects. The low probability percentages for France may have their caused by the low measurement correction factor applied in the French networks.

3.2 PM₁₀ 36th highest daily average

The combined map for the 2005 PM₁₀ 36th highest daily averages is created by the same interpolation methods as the annual mean map: the rural maps uses the 3-P.Eawr-a method and the urban map

method 2-UP.E-a .In mapping of the 2004 concentration fields the same method has been used for the rural maps but not for the urban maps. Because methods 3-P.Eawr-a for rural and 2-UP.E-a for urban areas are the close best (rural) and best (urban) performers on the 2005 data and their differences with the best methods on the 2004 data were small, as well as its good European coverage makes them the preferred and recommended method as “standard” in future applications for both indicators.

The areas and stations in the combined map where the limit value (LV) of $50 \mu\text{g.m}^{-3}$ is exceeded are coloured red and purple. Compared to the situation in 2004, the 2005-concentrations in central-eastern Europe and Po valley seem to be higher than last year while along the coast of the Atlantic and the North Sea lower levels are observed. The population exposure is given in Figure 3.2. More than 25% of the European population has been exposed to ambient concentrations above $50 \mu\text{g.m}^{-3}$, that is, to concentrations above the LV of daily concentrations.

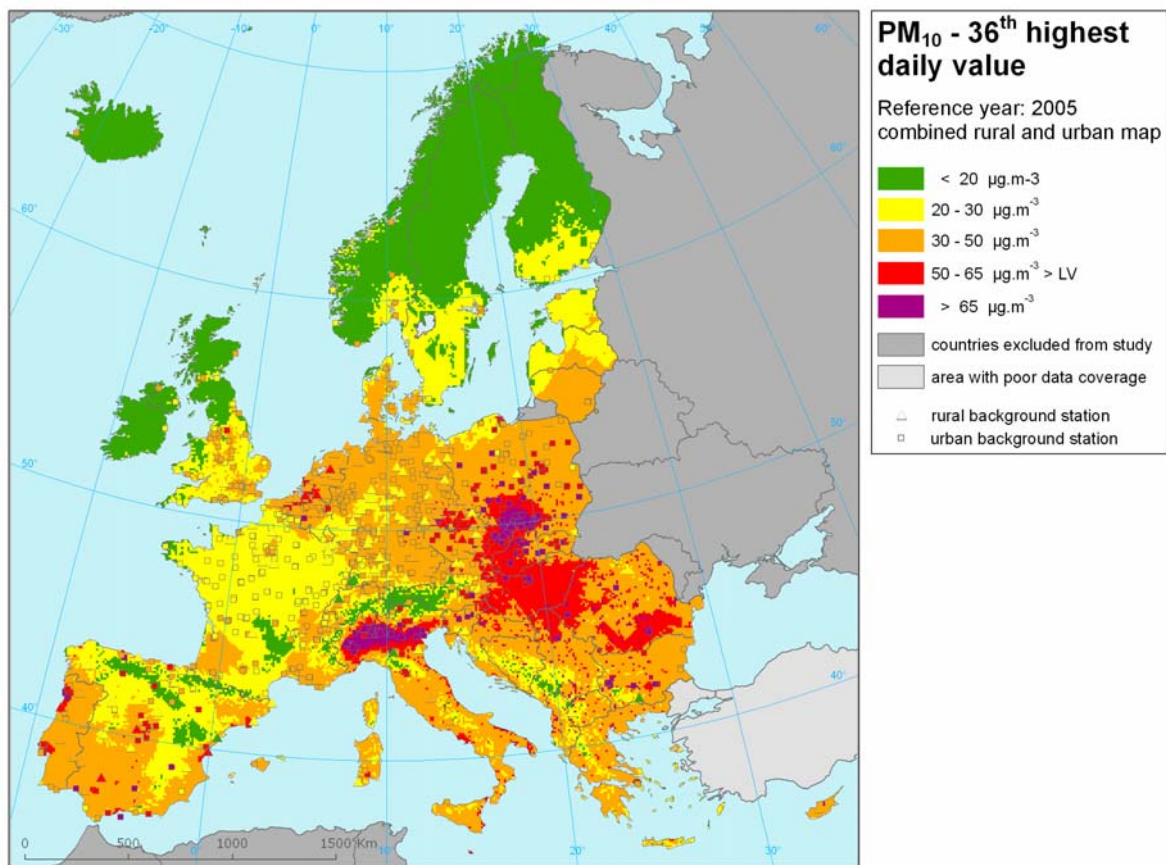


Figure 3.5 Combined rural and urban concentration map of PM₁₀ – 36th maximum daily average value, year 2005. Units: $\mu\text{g.m}^{-3}$.

Table 3.2 Population exposure and population weighted concentration – PM₁₀, 36th maximum daily average value, year 2005.

Country	Population x1000	2005 Percent [%]					Population- weighted conc. µg.m ⁻³
		< 20 µg.m ⁻³	20 - 30 µg.m ⁻³	30 - 50 µg.m ⁻³	50 - 65 µg.m ⁻³	> 65 µg.m ⁻³	
Austria	8286	5.4	7.4	54.9	30.0	2.3	42.3
Belgium	10542	0	2.3	71.7	26.0	0	46.5
Bulgaria	8055	0.1	2.1	54.6	9.5	33.7	62.7
Croatia	4366	0.0	2.2	46.8	31.2	19.7	52.0
Czech Rep.	10155	0	0.0	31.3	49.5	19.3	57.5
Denmark	5006	2.9	15.2	81.9	0	0	32.7
Estonia	1301	5.3	52.9	41.8	0	0	28.8
Finland	5179	33.1	66.9	0	0	0	22.1
France	58286	1.9	51.9	46.2	0	0	29.6
Germany	81889	0.1	7.5	90.9	1.5	0	37.2
Greece	10655	0.3	5.7	37.9	42.0	14.2	54.1
Hungary	10107	0	0	9.1	66.0	24.8	59.1
Ireland	3652	63.6	36.4	0	0	0	14.8
Italy	57119	0.5	2.9	39.2	30.6	26.9	56.2
Latvia	2243	1.8	33.6	64.6	0	0	33.6
Liechtenstein	32	0	0	100	0	0	36.2
Lithuania	3567	1.2	9.3	89.4	0	0	36.8
Luxembourg	451	0	30.7	69.3	0	0	30.6
Malta	394	0	0	14.5	85.5	0	61.6
Netherlands	15153	0	0	76.6	23.4	0	47.4
Poland	38182	0.1	2.0	49.5	27.4	21.0	54.7
Portugal	10024	0	0.3	44.6	37.9	17.3	51.7
Romania	22228	0.0	0.3	29.6	29.3	40.8	63.9
San Marino	19	0	0	100	0	0	39.8
Slovakia	5265	0	0.1	27.6	59.7	12.6	55.3
Slovenia	2034	0.0	1.6	53.8	44.6	0	48.4
Spain	39884	1.2	10.2	50.2	38.2	0.2	43.7
Sweden	8666	25.8	50.7	23.5	0	0	24.0
United Kingdom	58204	6.3	22.9	70.9	0	0	31.4
Albania	3767	1.1	10.2	29.6	13.3	45.8	55.4
Andorra	59	18.3	16.1	65.7	0	0	28.7
Bosnia-Herzegovina	4000	0.9	11.2	42.8	14.6	30.5	50.1
Island	101	100	0	0	0	0	9.6
Macedonia, FYR of	2214	1.2	5.2	28.9	0	64.7	71.4
Norway	2907	31.6	32.5	35.9	0	0	26.1
Serbia&Montenegro	10996	0.6	4.2	27.0	20.7	47.6	63.9
Switzerland	6801	2.3	13.6	82.0	1.2	1.0	33.9
Total	511787	2.7	14.3	54.8	17.5	10.6	43.8

Note: Countries with the values based on ORNL population data with uncertain quality: AD, AL, BA, CH, CS, IS, MK, NO. Countries with the lack of air quality or population density data are excluded from calculations in this paper: CY, TR.

3.2.2. Uncertainties

The absolute and relative mean interpolation uncertainty in the combined map, summarised from Section A2.1.3 and A2.2.3, are for the rural areas in the combined map 9.7 µg.m⁻³, and about 26% respectively, of the mean of the measured PM₁₀ 36th maximum daily average at all rural background stations. For the urban areas in the combined map they are 9.9 µg.m⁻³, and about 21% respectively, at all urban and suburban background stations.

The combined probability map for PM₁₀ 36th maximum daily average is shown in Figure 3.6. It is derived the same way as described in Section 3.1.2. As input served the concentration maps (Figure A2.1 right, rural; Figure A2.11 right, urban), the uncertainty maps (Figures A2.9 right, rural; Figure A2.18 right, urban) and the limit values used to construct the maps of the probability of the limit value exceedance (Figure A2.10 right, rural; Figure A2.19 right, urban).

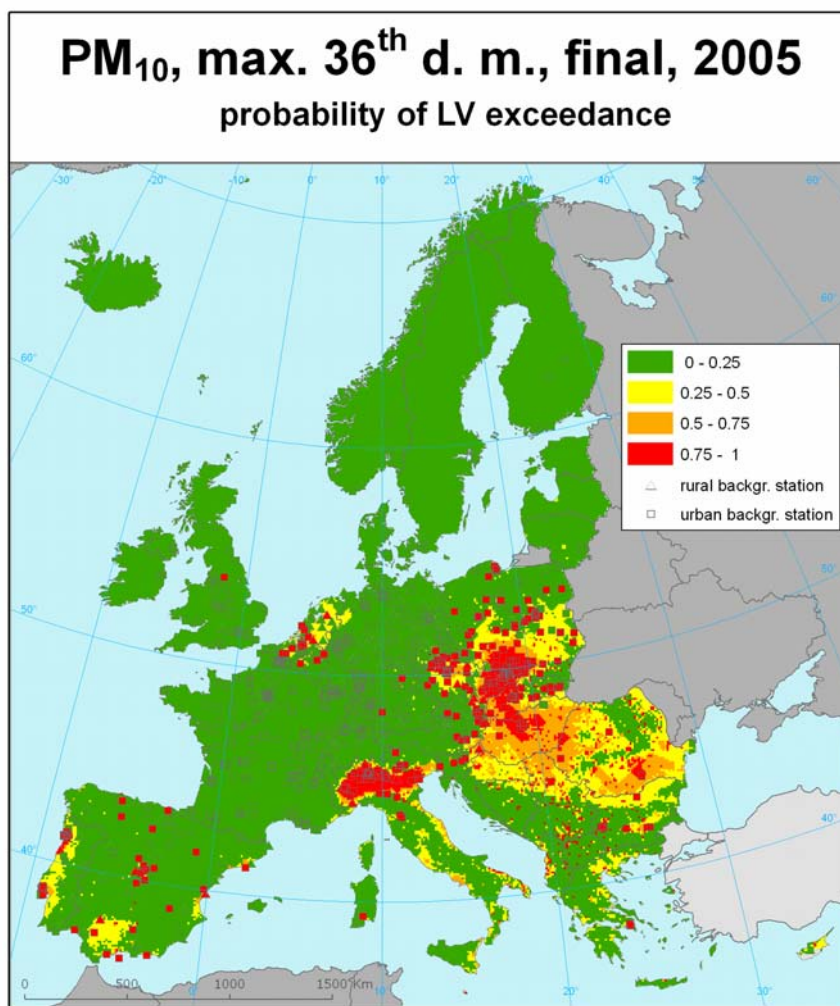


Figure 3.6 Map with the probability of the limit value exceedance for PM₁₀ indicators 36th maximum daily mean, in $\mu\text{g}\cdot\text{m}^{-3}$ on the European scale in 2005, on the 10 x 10 km grid resolution. (Stations with annual averaged measurement values above the limit value are marked red; station measurements below the limit value are marked green).

The estimated probability of exceedance in Figure 3.6 for the PM₁₀ 36th maximum daily average are considerable at large areas in the eastern European countries and the whole Po Valley (red areas indicating larger than 75 % probability of exceedances). At these areas PM₁₀ daily based exceedances are very likely and considerable reductions may be needed to reach non-exceedance levels in the future. To less extend this occurs in Spain, Portugal, Italy, Greece, some Balkan countries and the Benelux, where the probability ranges from 25 to 50 % with increased levels of 50 – 75 % at the more urbanised centres of the regions. The remaining of north-western and northern countries of Europe do not show such increased (larger than 25%) probability exceedances, indicating policy targets are or may be reached for the larger background areas. The map does not indicate locally bound exceedance effects. France may show low probability percentages possibly caused by the low measurement correction factor applied in the French networks.

4 Ozone maps for 2005

The ozone indicators examined are for human health the 26th highest daily maximum 8-hour average concentration and SOMO35, and for vegetation the AOT40 for crops and AOT40 for forests. For the health-related indicators the most suitable and preferred method for interpolated mapping of each indicator of the rural and urban areas have been analysed again separately. For the vegetation-related indicators only rural maps have been considered for the selection of preferred method for mapping, since no relevant vegetation is assumed to exist in urban areas).

The preparation of the separate rural and urban maps is discussed in Annex 3. Details on the process of selecting the best interpolation method are also given in this Annex.

4.1 Ozone health related indicators

The combined interpolated map for both ozone health indicators 26th highest daily maximum 8-hour average ozone concentrations and SOMO35 are presented in Figure 4.1. Both have been created by combining the rural and urban maps (Horálek et al. 2007).

For both indicators the rural maps (see Annex 3) have been created by combining the measurement data from rural background stations with the EMEP model output, altitude and surface solar radiation in a linear regression model (O.Ear), followed by the interpolation of its residuals by ordinary kriging (method 3-O.Ear-a). Although this method does not give the best statistical results it is close to the best method. This method is preferred here, and recommended for next year's application because its better geographical coverage and consistency with the ozone indicators related to vegetation protections: all rural ozone maps are made with the same method.

For both indicators the urban maps (Annex 3) have been created by combining the measurement data from the urban and suburban background stations with the EMEP model output, wind speed and surface solar radiation in a linear regression model (UO.Ewr), followed by interpolation of its residuals by ordinary kriging (method 3-UO.Ewr-a). In mapping the 2004 data a different method (ordinary kriging with the model results as only source of supplementary parameters) for the 26th highest daily maximum 8-hour average has been used. In the 2005 analysis (see Annex) the results are similar for both approaches. Method 3-UO.Ewr-a is to be preferred because of the better spatial coverage. This method is recommended for future applications.

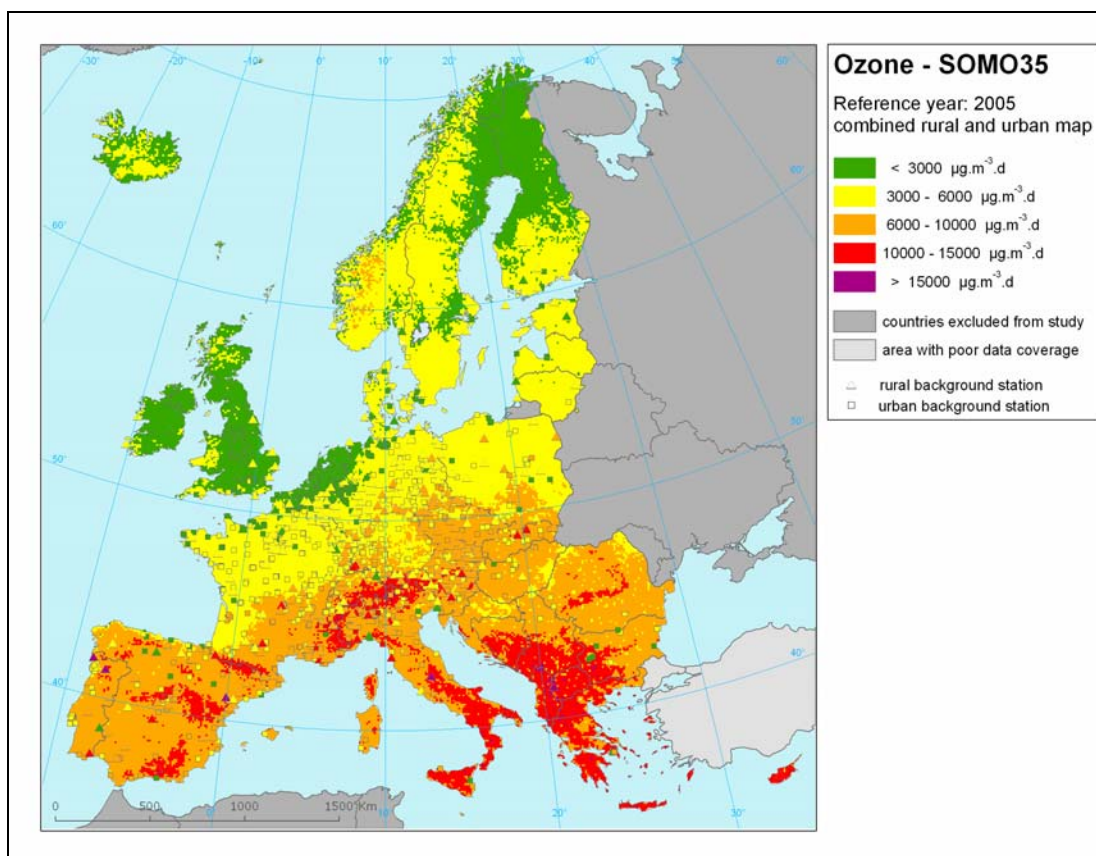
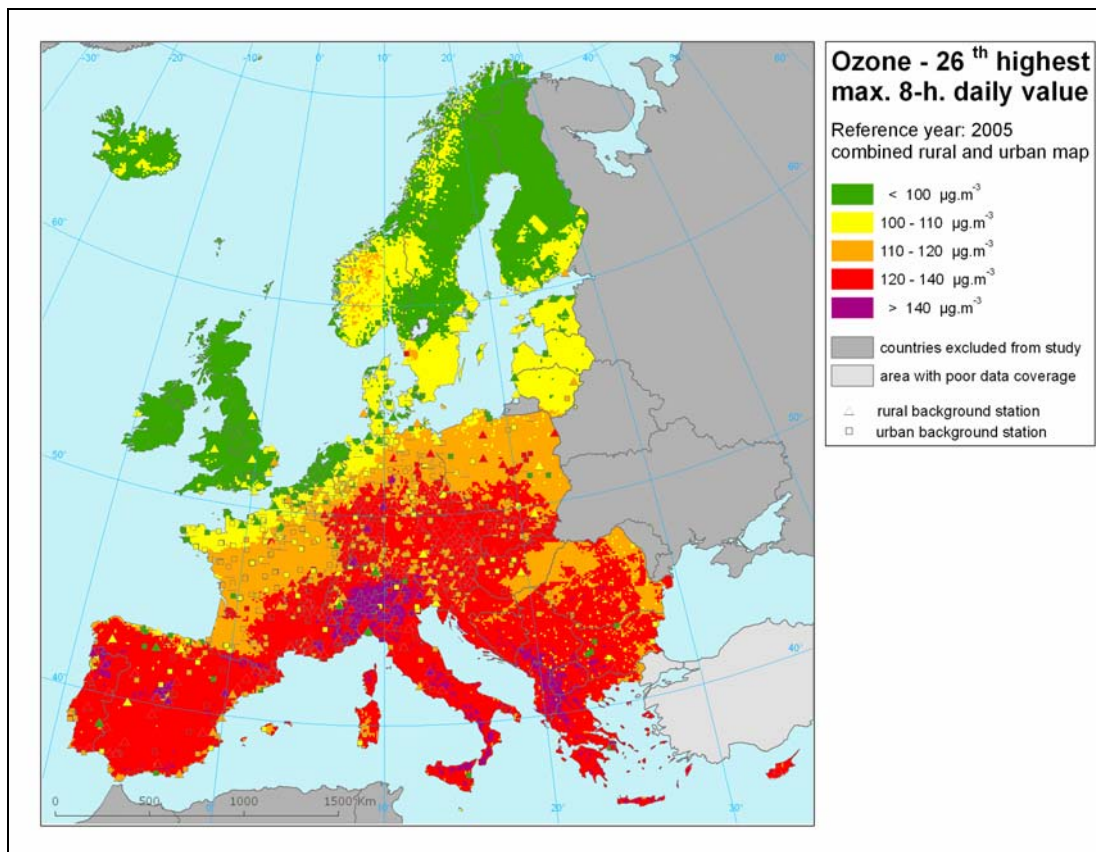


Figure 4.1 Combined rural and urban concentration map of ozone health indicators 26th highest daily maximum 8-hour value in $\mu\text{g.m}^{-3}$ (top) and SOMO35 in $\mu\text{g.m}^{-3}.\text{days}$ (bottom) for the year 2005.

4.1.1 Population exposure and health impacts

The final SOMO35 map is given in Figure 4.1 (bottom). The concentrations in 2005 are both in magnitude and spatial distribution similar to the concentrations in 2004 although in 2005 there is an increase in SOMO35 values in south-east Europe and eastern Mediterranean. The map of the 26th highest maximum daily value (Figure 4.1 top) shows also somewhat higher values in the central and eastern part of Europe, but lower levels in the northern region. The population exposure of both parameters is shown in Figure 4.2. Note that, in contrast to Table 4.1 and 4.2, Figure 4.2 includes all countries shown in Figure 4.1. Of the European population 38% is exposed to ozone levels above the target value ($120 \mu\text{g}\cdot\text{m}^{-3}$, 26th highest daily maximum 8-hour average). As Table 4.1 shows, this fraction varies strongly from country to country. In the Mediterranean in general more than half of the population lives in non-compliance areas, while in the northern part there is no exceedance at all. No limit or target values are set for SOMO35. Table 4.2 shows strongly varying values from country to country as well.

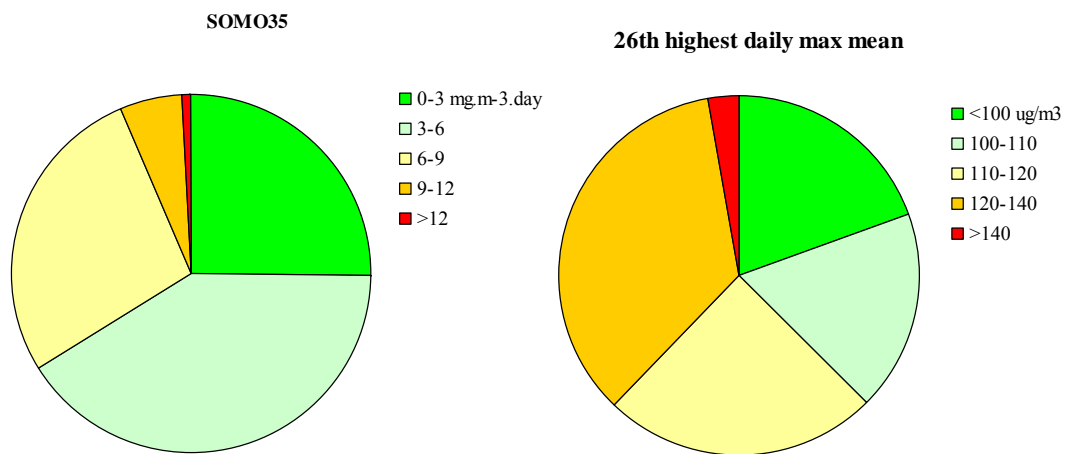


Figure 4.2 Exposure of the European population to ozone concentrations, SOMO35 (left) and 26th highest daily mean (right), (reference year 2005).

Table 4.1 Population exposure and population weighted concentration – ozone, 26th highest daily maximum 8-hour value, year 2005.

Country	Population x1000	2005 Percent [%]					Population- weighted conc. µg.m ⁻³
		< 100 µg.m ⁻³	100 - 110 µg.m ⁻³	110 - 120 µg.m ⁻³	120 - 140 µg.m ⁻³	> 140 µg.m ⁻³	
Austria	8286	0	2.4	18.4	78.6	0.6	122.6
Belgium	10542	16.6	74.1	9.1	0.1	0	104.1
Bulgaria	8055	14.3	24.5	18.2	42.3	0.6	115.0
Croatia	4366	0	0	18.4	81.1	0.4	120.7
Czech Rep.	10155	0	0	15.5	84.5	0	122.3
Denmark	5006	48.0	51.3	0.8	0	0	97.0
Estonia	1301	62.1	37.9	0	0	0	92.9
Finland	5179	84.4	15.6	0	0	0	93.9
France	58286	2.5	36.3	33.6	27.3	0.3	114.1
Germany	81889	3.2	27.2	36.6	33.0	0	114.9
Greece	10655	0	1.6	24.1	72.2	2.1	125.8
Hungary	10107	0	0	34.7	65.3	0	120.0
Ireland	3652	100	0	0	0	0	84.8
Italy	57119	0	0.6	7.0	72.1	20.3	132.2
Latvia	2243	48.1	51.9	0	0	0	92.3
Liechtenstein	32	0	100	0	0	0	106.6
Lithuania	3567	24.5	73.8	1.7	0	0	103.2
Luxembourg	451	0	0	54.3	45.7	0	120.2
Malta	394	0	85.5	9.5	5.0	0	107.0
Netherlands	15153	82.4	17.6	0	0	0	92.8
Poland	38182	2.6	11.8	72.0	13.5	0	114.9
Portugal	10024	1.1	14.6	33.6	48.4	2.3	119.0
Romania	22228	1.4	24.8	47.6	26.1	0.1	115.0
San Marino	19	0	0	0	100	0	134.8
Slovakia	5265	0	0	18.0	81.9	0.0	122.4
Slovenia	2034	0	0	13.3	86.7	0.0	123.6
Spain	39884	4.1	17.1	22.5	55.9	0.3	117.9
Sweden	8666	57.4	39.4	3.2	0	0	95.5
United Kingdom	58204	98.4	1.6	0	0	0	87.2
Andorra	59	20.4	18.1	24.6	34.3	2.6	130.6
Albania	3767	0	2.7	45.9	39.4	12.0	125.1
Bosnia-Herzegovina	4000	0	0	40.5	59.0	0.6	122.2
Serbia&Montenegro	10996	0	19.6	31.7	47.1	1.7	119.3
Switzerland	6801	0	4.2	16.1	74.2	5.5	123.4
Island	101	96.0	4.0	0	0	0	90.9
Macedonia, FYR of	2214	0	40.2	23.3	29.6	7.0	120.0
Norway	2907	74.1	25.3	0.7	0	0	98.2
Total	511787	19.6	17.9	24.8	35.1	2.7	112.9

Note: Countries with the values based on ORNL population data with uncertain quality: AD, AL, BA, CH, CS, IS, MK, NO. Countries with the lack of air quality or population density data are excluded from calculations in this paper: CY, TR.

Table 4.2 Population exposure and population weighted concentration – ozone, SOMO35, year 2005.

Country	Population x1000	2005 Percent [%]					Population- weighted conc. $\mu\text{g.m}^{-3}.\text{d}$
		< 3000 $\mu\text{g.m}^{-3}.\text{d}$	3000 - 6000 $\mu\text{g.m}^{-3}.\text{d}$	6000 - 10000 $\mu\text{g.m}^{-3}.\text{d}$	10000 - 15000 $\mu\text{g.m}^{-3}.\text{d}$	> 15000 $\mu\text{g.m}^{-3}.\text{d}$	
Austria	8286	0	33.9	62.8	3.4	0	6576
Belgium	10542	71.1	28.9	0	0	0	2787
Bulgaria	8055	13.7	27.5	49.2	9.6	0.0	6669
Croatia	4366	0	41.1	56.1	2.8	0	6667
Czech Rep.	10155	0	47.5	52.5	0	0	6087
Denmark	5006	43.5	56.5	0	0	0	3019
Estonia	1301	53.5	46.5	0	0	0	2722
Finland	5179	63.5	36.5	0	0	0	2580
France	58286	16.0	61.9	21.5	0.5	0.0	4756
Germany	81889	24.6	70.0	5.4	0.0	0	4164
Greece	10655	0	13.6	58.4	27.8	0.1	9062
Hungary	10107	0	41.4	58.6	0	0	5965
Ireland	3652	97.8	2.2	0	0	0	1852
Italy	57119	0	4.0	83.8	12.2	0.0	8134
Latvia	2243	46.0	54.0	0	0	0	2739
Liechtenstein	32	0	100	0	0	0	5699
Lithuania	3567	6.8	93.2	0	0	0	3790
Luxembourg	451	0	100	0	0	0	4796
Malta	394	0	0	95.0	5.0	0	7140
Netherlands	15153	99.5	0.5	0	0	0	1920
Poland	38182	2.2	87.4	10.4	0	0	5037
Portugal	10024	1.1	54.5	43.6	0.8	0	5824
Romania	22228	0	48.6	50.2	1.1	0	6062
San Marino	19	0	0	100	0	0	8612
Slovakia	5265	0	17.5	82.2	0.3	0	6622
Slovenia	2034	0	24.3	75.5	0.3	0	6669
Spain	39884	4.6	29.2	63.9	2.2	0.0	6514
Sweden	8666	47.3	52.7	0.0	0	0	3083
United Kingdom	58204	97.8	2.2	0	0	0	1634
Albania	3767	0	21.8	42.7	33.7	1.7	8563
Andorra	59	0	0.0	65.7	34.3	0	9023
Bosnia-Herzegovina	4000	0	40.2	44.5	15.3	0	7490
Island	101	94.5	5.5	0	0	0	1887
Macedonia, FYR of	2214	0	51.6	14.7	32.3	1.4	7738
Norway	2907	72.5	27.0	0.5	0	0	2697
Serbia&Montenegro	10996	0	43.6	41.6	14.8	0.0	6978
Switzerland	6801	0	61.0	34.4	4.6	0.0	6150
Total	511787	25.4	40.7	30.5	3.4	0.0	5047

Note: Countries with the values based on ORNL population data with uncertain quality: AD, AL, BA, CH, CS, IS, MK, NO. Countries with the lack of air quality or population density data are excluded from calculations in this paper: CY, TR.

Following a similar procedure as described in Horálek et al (2007) the number of premature deaths attributable to ozone has been estimated, see Figure 4.3. Taking the difference in concentrations into account the estimates are in correspondence with the estimates made for 2004. The impact on health from ozone seems to be an order of magnitude lower than the PM10 impact.

premature deaths (per million) attributable to ozone

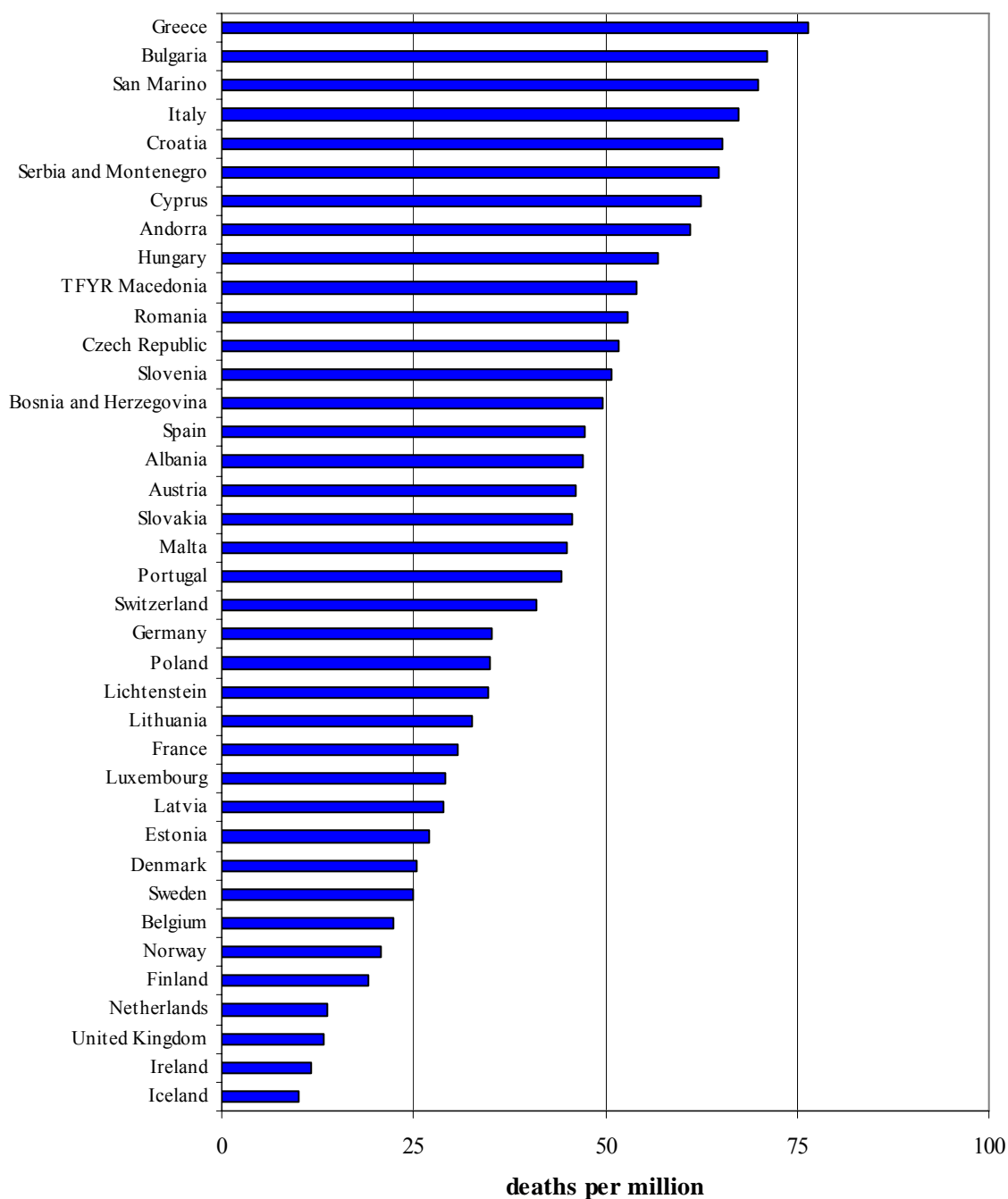


Figure 4.3 Number of premature deaths per million inhabitants attributable to ozone exposure, reference year 2005.

4.1.2 Uncertainties

The 26th highest daily maximum 8-hour average ozone concentrations for the rural areas in the combined map show an absolute and relative mean interpolation uncertainty of 12.3 $\mu\text{g.m}^{-3}$, i.e. about 10 %. For the urban map it is 10.0 $\mu\text{g.m}^{-3}$, i.e. about 9 % of the average of the measured indicator at all urban and suburban stations. For SOMO35 in rural areas in the combined map it is 2200 $\mu\text{g.m}^{-3}.\text{days}$,

i.e. 35.5 % of the average of SOMO35 values measured at all rural background stations. For the urban map is 1500 $\mu\text{g}\cdot\text{m}^{-3}\cdot\text{days}$, i.e. about 32 % of the average of measured SOMO35 values at all urban and suburban stations.

Based on the concentration maps (Figures A3.1 left, rural; Figure A3.16 left, urban), the uncertainty maps (Figures A3.13 left, rural; Figure A3.23 left, urban) and the target value (TV of 120 $\mu\text{g}\cdot\text{m}^{-3}$ for 26th highest daily maximum 8-hour average) the map of the probability of the target value exceedance has been constructed. The probability map is presented in Figure A3.15-left for the rural areas and Figure A3.24 for the urban areas. Areas with the probability of limit value exceedance above 75% are marked in red; areas below 25% are marked in green. The red areas indicate areas for which exceedance may occur very likely due to high concentration close to or already above the TV, including such enclosed uncertainty that exceedance is likely. Or lower concentrations with such high uncertainty levels reaching above the TV that exceedance is very likely. Vice versa, in the green areas it is not very likely to have predicted concentration values showing exceedance and/or such enclosed uncertainties that reaching above the TV not very likely.

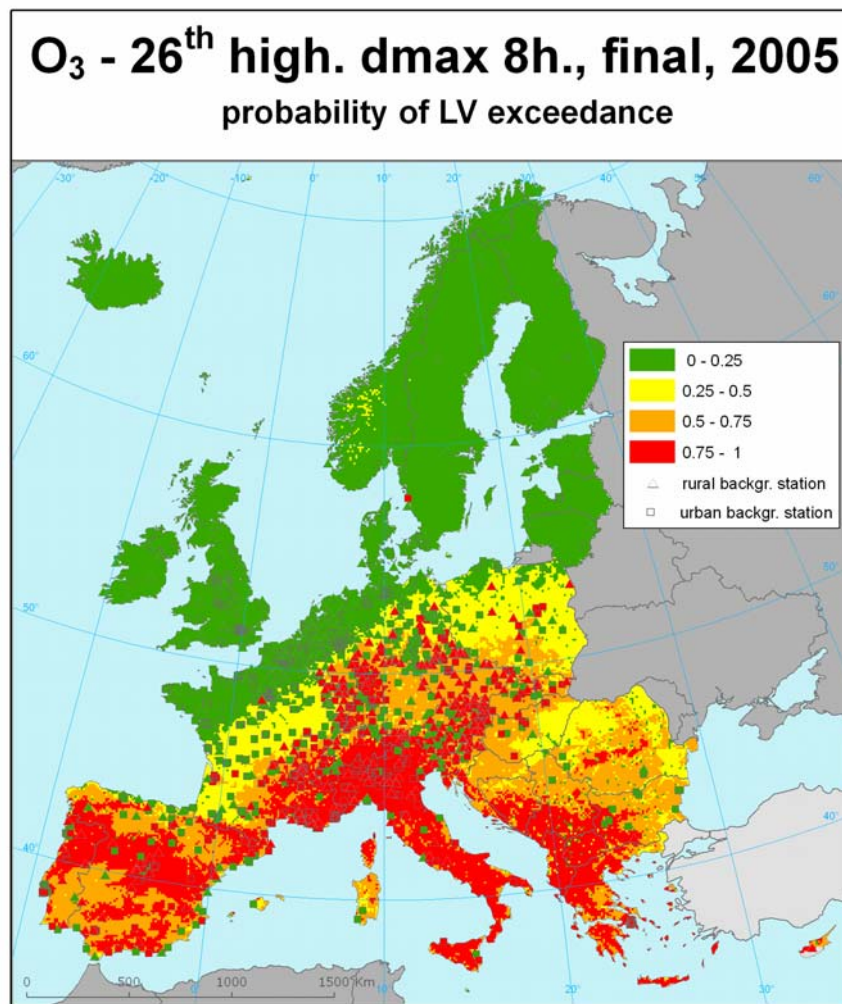


Figure 4.4 Map with the probability of the limit value exceedance for ozone indicator 26th highest daily maximum 8-hour average values (in $\mu\text{g}\cdot\text{m}^{-3}$) on European scale in 2005, 10 x 10 km grid resolution. (Stations with annual averaged measurement values above the limit value are marked red; station measurements below the limit value are marked green).

The estimated probability of target value exceedance (PoE) for the ozone 26th highest daily maximum 8-hour average is moderate to considerable south of the line Biarritz – Basel – Luxemburg – Hannover - Polish/Belarusian border (orange grid cells > 50 % and red cells > 75 % probability). In this area the levels of exceedance probability follow the European altitudes highly correlated: fluctuations in the probability relief are well reflected by the fluctuation of in the altitude relief map. It is to be expected that for these regions the target value will not be met easily.

North of the line the exceedance probability reduces to levels of about 25 – 50 % meaning that target values could be met here more easily. While levels lower than 25 % do widely occur north of the line La Rochelle - Rostock – Vilnius, except some local higher altitudes in southern Norway (25 - 50 % PoE), indicating policy targets are or may be reached for the larger background areas. The map does not indicate locally bound exceedance effects.

The visual impression of the map pattern seems to be dominated by the rural map pattern of Figure A3.14, but remarkable is the relative frequent number of red marked rural background stations with measurements above the limit value in areas with a PoE of 25 – 50 %. This indicates that in the rural areas local contrast in even increased probability of exceedances may play an important role which is not covered by the resolution of the interpolation. In addition a frequent number of green marked urban and suburban background stations with measurements below the limit value seem to be located in areas with a PoE of 50 – 75 % as well, indicating local urban air quality is likely not always covered well in by the resolution of the interpolation. The interpolated concentration field is ultimately a spatially smoothed representation of the background stations in the mapping domain, not necessarily reflecting the higher resolution local air quality status.

4.2 Ozone vegetation indicators

The interpolated map for both vegetation indicators AOT40 for crops and AOT40 for forests are presented in Figure 4.5. Only rural maps are presented here as it is assumed that there is no relevant vegetation in urban areas.

For both indicators the maps have been created by combining measurement data from the rural background stations with the EMEP model output, altitude field and surface solar radiation in a linear regression model (O.Ear), followed by the interpolation of its residuals by ordinary kriging (method 3-O.Ear-a). As discussed above, it is recommended for future applications because of consistency reasons.

Up to present both ozone vegetation indicators for rural areas were created in the trend analysis based an interpolation method of type 1, using an ordinary cokriging of the rural background station measurements stations combined with altitude as supplementary information. The Balkan region was excluded from the mapping calculations due to its poor measurement station coverage. These maps are in use at the EEA Core Set Indicator 005 (CSI 005, 2006) and in EEA air pollution assessment reports. For consistency in the indicator assessment over the years (1996 – 2004) the type 1 method was still prolonged. However, current comparison with 2005 data confirms method 3-O.Ear-a to be the best, leading to the decision to switch methods for the indicator CSI005 analyses. To assure that possible discontinuities in the trend of vegetation exposure, is recommended to re-calculated a few recent years using both ‘old’ and ‘new’ method in parallel.

4.2.1 Vegetation and forest exposure

In the ozone directive a target value (TV) and a long-term objective (LTO) for the protection of vegetation have been defined. TV and LTO are defined as AOT40, calculated from 1-hour values (daylight hours only, defined as the period between 8:00 and 20:00 CET) from May to July. The TV for 2010 is 18,000 $\mu\text{g}\cdot\text{m}^{-3}\cdot\text{h}$; the LTO is 6,000 $\mu\text{g}\cdot\text{m}^{-3}\cdot\text{h}$. The term *vegetation* is not further defined in the ozone directive. Comparing the definitions in the Mapping Manual (UNECE, 2004) and those in the ozone directive suggests that we have to interpret the term *vegetation* in the ozone directive as

agricultural crops. The exposure of *agricultural crops* has been evaluated here on basis of the AOT40 for vegetation as defined in the ozone directive.

In addition, exposure of *forests* has been estimated on the basis of the corresponding definition in the Mapping Manual: critical level of 10 mg.m⁻³.h (corresponding to 5 ppm.h), accumulation over the full vegetation period, April 1 – September 30.

Agricultural crops

The rural map for ozone, AOT40 for vegetation, is given in Figure 4.5. This map has been combined with the land cover CLC2000 map. Following a similar procedure as described in Horálek et al (2007) the exposure of agricultural areas, defined as the Corine Land Cover level-1 class 2 *Agricultural areas* (encompassing the level-2 classes 2.1 *Arable land*, 2.2 *Permanent crops*, 2.3 *Pastures* and 2.4 *Heterogeneous agricultural areas*) has been calculated at the country-level. Table 4.3 gives the absolute and relative agricultural area for each country and for four European regions where the target value and long-term objective for ozone are exceeded. The table presents the frequency distribution of the agricultural area per country over the exposure classes as well.

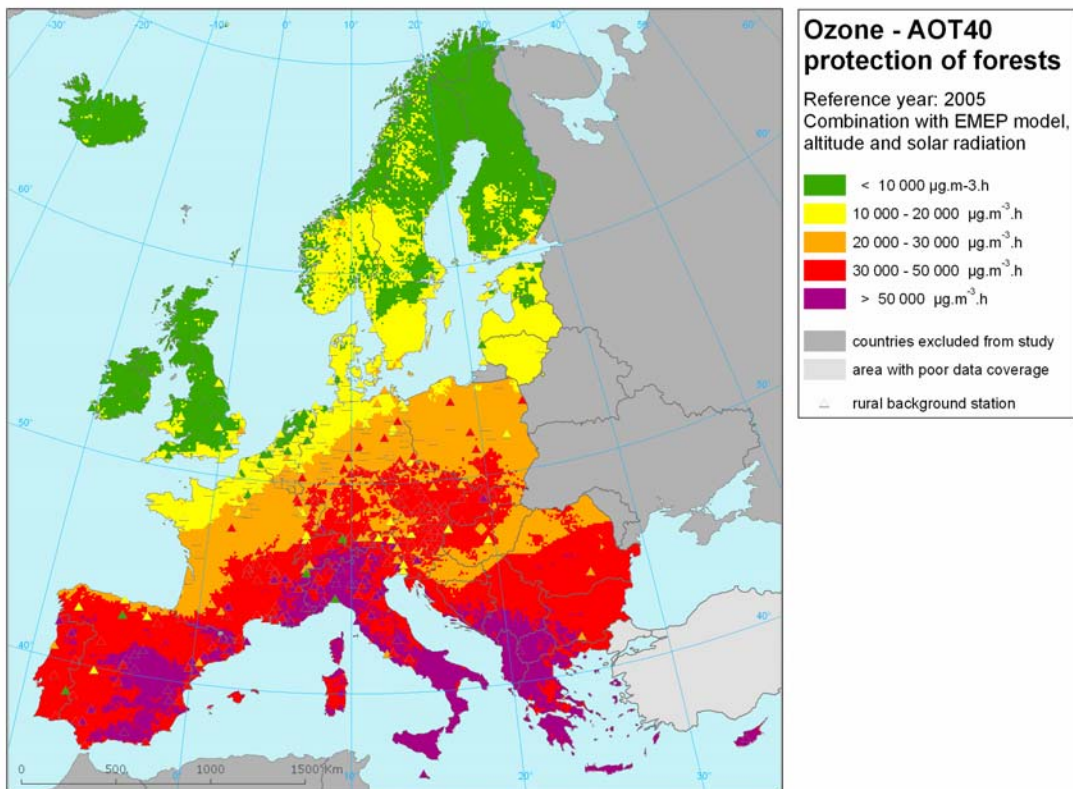
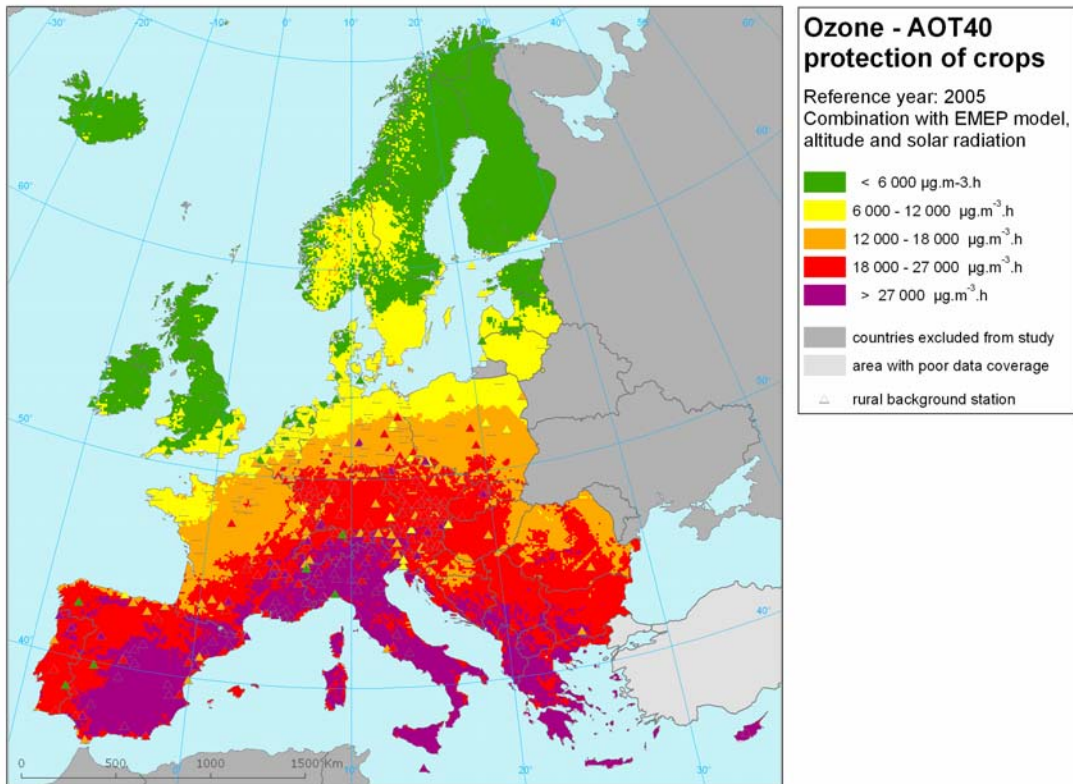


Figure 4.5 Rural concentration map of ozone vegetation indicators AOT40 for crops (top) and AOT40 for forests (bottom) for the year 2005. Units: $\mu\text{g}\cdot\text{m}^{-3}\cdot\text{hours}$.

Table 4.3 Agricultural area exposure and exceedance (Long Term Objective, LTO, and Target Value, TV) for ozone, AOT40 for crops, year 2005.

Country	Agricultural area					2005 Percent [%]				
	total km ²	above LTO (6 mg.m-3.h)		above TV (18 mg.m-3.h)		< 6000 µg.m ⁻³ .h	6000 - 12000 µg.m ⁻³ .d	12000 - 18000 µg.m ⁻³ .d	18000 - 27000 µg.m ⁻³ .d	> 27000 µg.m ⁻³ .d
		km ²	%	km ²	%					
Albania	7109	7109	100	7109	100	0	0	0	32.3	67.7
Austria	27450	27450	100	27069	99	0	0	1.4	93.6	5.0
Belgium	17623	17500	99	1129	6	0.7	45.7	47.2	6.4	0
Bosnia-Herzegovina	19251	19251	100	15026	78	0	0	21.9	64.5	13.5
Bulgaria	57208	57208	100	56635	99	0	0	1.0	95.4	3.6
Croatia	23745	23745	100	17602	74	0	0	25.9	64.1	10.1
Cyprus	4088	4088	100	4088	100	0	0	0	3.1	96.9
Czech Republic	45550	45550	100	37063	81	0	0	18.6	81.4	0
Denmark (ex.Faroes)	30798	22946	75	0	0	25.5	72.1	2.4	0	0
Estonia	14418	962	7	0	0	93.3	6.7	0	0	0
Finland	28582	837	3	0	0	97.1	2.9	0	0	0
France	327337	327337	100	110461	34	0	16.2	50.1	28.1	5.6
FYR of Macedonia	9515	9515	100	9515	100	0	0	0	66.6	33.4
Germany	212360	210699	99	72072	34	0.8	28.7	36.5	33.9	0
Greece	48918	48918	100	48918	100	0	0	0	33.3	66.7
Hungary	63054	63054	100	47441	75	0	0	24.8	75.2	0
Ireland	45312	1552	3	0	0	96.6	3.4	0	0	0
Italy	153591	153591	100	153193	100	0	0	0.3	14.7	85.0
Latvia	28053	19733	70	0	0	29.7	70.3	0	0	0
Liechtenstein	42	42	100	42	100	0	0	0.0	100	0
Lithuania	39656	37554	95	0	0	5.3	94.7	0.0	0	0
Luxembourg	1410	1410	100	1347	96	0	0	4.4	95.6	0
Malta	91	91	100	91	100	0	0	0	0	100
Netherlands	24347	22391	92	0	0	8.0	89.2	2.8	0	0
Poland	199623	199623	100	12031	6	0	32.1	61.8	6.0	0.0
Portugal	42351	42351	100	41799	99	0	0	1.3	95.3	3.4
Romania	134314	134314	100	66285	49	0	0.7	50.0	49.3	0.0
San Marino	44	44	100	44	100	0	0	0	0	100
Slovakia	24248	24248	100	18534	76	0	0	23.6	76.4	0.1
Slovenia	7133	7133	100	6176	87	0	0	13.4	84.1	2.5
Spain	251487	251487	100	248108	99	0	0	1.3	44.7	54.0
Sweden	37737	18174	48	0	0	14.8	85.2	0	0	0
United Kingdom	137813	33353	24	0	0	75.8	24.2	0.0	0	0
Total	2064257	1833258	89	1001777	49	10.4	16.0	24.1	32.7	16.8
France over 45N	259908	259908	100	51786	20	0	20.4	59.7	18.8	1.2
France below 45N	67429	67429	100	58675	87	0	0	13.0	64.1	22.9
Northern	179245	100206	56	0	0					
North-western	486412	336113	69	54263	11					
Central & eastern	763849	762189	100	337171	44					
Southern	634751	634751	100	610342	96					
Total	2064257	1833258	89	1001777	49					

Note: Countries not included due to lack of land cover data: Andorra, Iceland, Norway, Serbia and Montenegro, Switzerland and Turkey.

The table indicates the country grouping with corresponding colours of the region. *Northern Europe*: Sweden, Finland, Estonia, Lithuania, Latvia and Denmark. *North-western Europe*: United Kingdom, Ireland, the Netherlands, Belgium, Luxembourg and France north of 45 degrees latitude. *Central and Eastern Europe*: Germany, Poland, Czech Republic, Slovakia, Hungary, Austria, Liechtenstein, Bulgaria and Romania. *Southern Europe*: Albania, Bosnia-Herzegovina, France south of 45 degrees latitude, Portugal, Spain, Italy, San Marino, Slovenia, Croatia, Greece, Cyprus, F.Y.R. of Macedonia and Malta.

Table 4.3 illustrates that about 50 % of all agricultural land is exposed to ozone exceeding the target value of 18 mg.m⁻³.h and about 90 % is exposed to levels in excess of the long-term objective of 6

mg.m⁻³.h. In southern countries about 95 % is exceeding the target values. In northern Europe the ozone levels are below the target value for nearly 100 % of the agricultural area.

Forests

The ozone directive does not give a target value or a long-term objective for the protection of forest. However, Annex III - which defines the information to be submitted to the Commission - mentions a level of 20 mg.m⁻³.h. Following a similar procedure as in Horálek et al (2007), in this paper we will use again this level (indicated as: reporting value or *RV*) as reference in combination with the critical level (*CL*) of 10 mg.m⁻³.h as defined in the Mapping Manual. The forest areas are defined as the Corine Land Cover level-2 classes *3.1. Forests* and *3.2 Scrub and/or herbaceous vegetation associations* as the two out of the three of level-1 class *3. Forests and semi-natural areas*, and is different from what has been used (level-2 class 3.1) in Horálek et al. (2007).

The rural ozone map for ozone, AOT40 for forest, is given in Figure 4.5. The same country grouping is used as at AOT40 for crops. The gradients in this map are very similar to those in the map of AOT40 for vegetation: increasing concentrations from north to south. Table 4.4 gives the forest area where the critical level for ozone is exceeded. Similar to the finding in CAFE, we observe for the year 2005 - and similar to 2004 - that in many countries, except for the UK and some of the northern countries, all forest area is exposed to levels above the critical level (*CL*). The reporting level (*RV*) is exceeded in 2005 with about 60 % - with 50 % in 2004 - of the European forest area. The frequency distribution of forest exposure is per country given in the table as well.

It is clear that in northern Europe the reporting level of 20 mg.m⁻³.h is not exceeded, in central and eastern almost everywhere and southern Europe everywhere.

Table 4.4 Forest area exposure and exceedance (CL and RV) – ozone, AOT40 forests, year 2005.

Country	Area of forests					2005 Percent [%]				
	Total km ²	above CL (10 mg.m-3.h)		above RV (20 mg.m-3.h)		< 10000 µg.m ⁻³ .h	10000 - 20000 µg.m ⁻³ .d	20000 - 30000 µg.m ⁻³ .d	30000 - 50000 µg.m ⁻³ .d	> 50000 µg.m ⁻³ .d
		km ²	%	km ²	%					
Albania	7738	7738	100	7738	100	0	0	0	0.5	99.5
Austria	37608	37608	100	37608	100	0	0	12.7	85.5	1.8
Belgium	6100	6094	100	4535	74	0.1	25.6	74.3	0	0
Bosnia-Herzegovina	22815	22815	100	22815	100	0	0	7.2	74.9	17.9
Bulgaria	34660	34660	100	34660	100	0	0	0	79.6	20.4
Croatia	19762	19762	100	19762	100	0	0	38.3	53.2	8.5
Cyprus	1498	1498	100	1498	100	0	0	0	1.7	98.3
Czech Republic	25501	25501	100	25501	100	0	0	11.2	88.8	0
Denmark (ex.Faroes)	3408	3349	98	202	6	1.8	92.3	5.9	0	0
Estonia	20317	16010	79	0	0	21.2	78.8	0	0	0
Finland	191690	28748	15	0	0	85.0	15.0	0	0	0
France	144521	144514	100	133827	93	0.0	7.4	44.8	37.4	10.4
FYR of Macedonia	8619	8619	100	8619	100	0	0	0	2.8	97.2
Germany	103589	103542	100	91770	89	0.0	11.4	56.4	32.2	0
Greece	22978	22978	100	22978	100	0	0	0	21.1	78.9
Hungary	17331	17331	100	17331	100	0	0	35.2	64.8	0
Ireland	2892	142	5	0	0	95.1	4.9	0	0	0
Italy	78497	78497	100	78497	100	0	0	0.2	32.9	66.9
Latvia	26512	25052	94	0	0	5.5	94.5	0	0	0
Liechtenstein	63	63	100	63	100	0	0	41.1	58.9	0
Lithuania	18468	18468	100	55	0	0	99.7	0.3	0	0
Luxembourg	904	904	100	904	100	0	0	100	0	0
Malta	2	2	100	2	100	0	0	0	0	100
Netherlands	3074	2475	81	0	0	19.5	80.5	0	0	0
Poland	91182	91182	100	87305	96	0	4.3	84.1	11.7	0.0
Portugal	24190	24190	100	24190	100	0	0	0	98.3	1.7
Romania	69660	69660	100	69660	100	0	0	25.4	73.9	0.7
San Marino	6	6	100	6	100	0	0	0	86.5	13.5
Slovakia	19248	19248	100	19248	100	0	0	12.7	87.2	0.1
Slovenia	11469	11469	100	11469	100	0	0	20.5	79.4	0.2
Spain	91489	91489	100	91463	100	0	0.0	6.9	59.2	33.9
Sweden	248597	111768	45	567	0	55.0	44.7	0.2	0	0
United Kingdom	19158	3598	19	0	0	81.2	18.8	0	0	0
Total	1373545	1048978	76	812271	59	23.6	17.2	18.8	29.5	10.8
France north of 45N	89453	89446	100	78871	88	0.0	11.8	57.5	29.1	1.5
France south of 45N	55068	55068	100	54957	100	0	0.2	24.1	50.8	24.9
Northern	508993	203395	40	824	0					
North-western	121580	102658	84	84309	69					
Central & eastern	398842	398795	100	383146	96					
South	344130	344130	100	343992	100					
Total	1373545	1048978	76	812271	59					

Note: Countries not included due to lack of land cover data: Andorra, Iceland, Norway, Serbia and Montenegro, Switzerland and Turkey.

4.2.2 Uncertainties

The absolute and relative mean interpolation uncertainty of the map of AOT40 for crops, expressed by the RMSE from the cross-validation, is 7700 µg.m⁻³.hours, i.e. about 41 % of the average of AOT40 crops values measured at all stations. For the map of AOT40 for forests it is 12500 µg.m⁻³.hours, i.e. about 42 % of the average of AOT40 forest values measured at all stations.

Based on the concentration map (Figures A3.2), the uncertainty maps (Figures A3.13) and the target value (TV, i.e. 18,000 µg.m⁻³.h) the map of the probability of the target value exceedance has been constructed. The probability map is presented in Figure 4.6. (Areas with the probability of limit value exceedance above 75% are marked in red; areas below 25% are marked in green. The red areas

indicate areas for which exceedance may occur very likely due to high concentration close to or already above the TV, including such enclosed uncertainty that exceedance is likely. Or lower concentrations with such high uncertainty levels reaching above the TV that exceedance is very likely. Vice versa, in the green areas it is not very likely to have predicted concentration values showing exceedance and/or such enclosed uncertainties that reaching above the TV not very likely).

While no ozone limit or target values for forests are defined in the ozone directive, no probability map has been prepared for the AOT40 for forests.

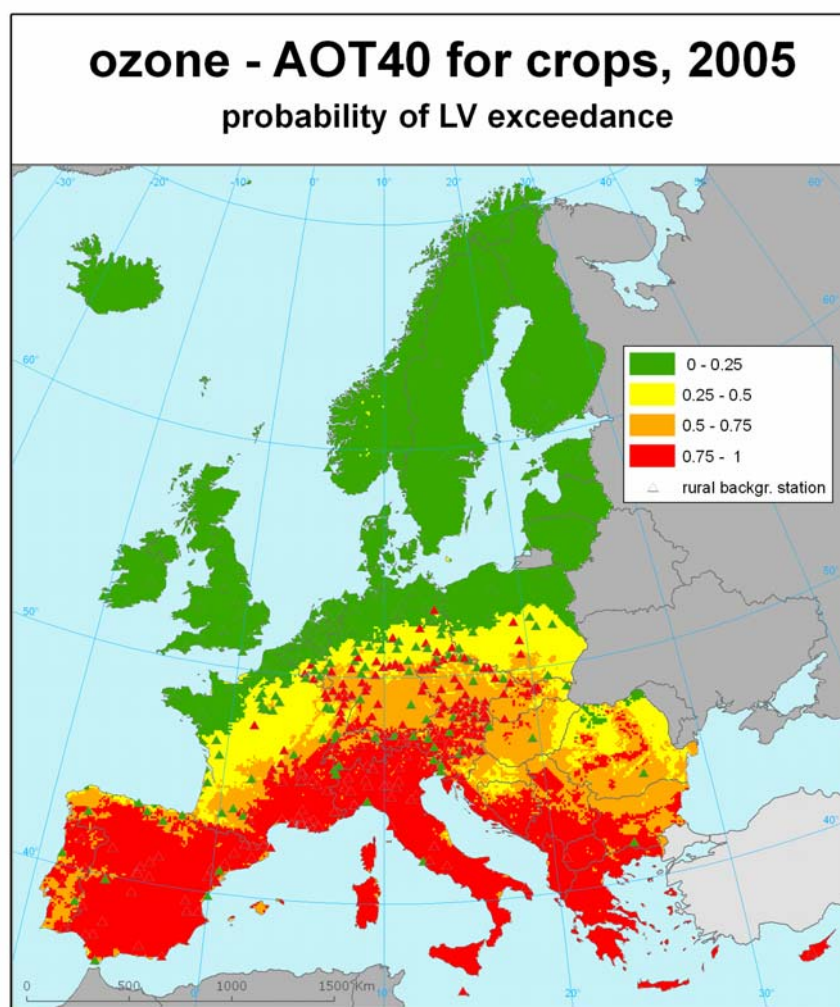


Figure 4.6 Map with the probability of the target value exceedance for ozone vegetation indicator AOT40 for crops, in $\mu\text{g}\cdot\text{m}^{-3}$ on the European scale in 2005, on the 10 x 10 km grid resolution.

The estimated probability of target value exceedance (PoE) for the ozone vegetation indicator AOT40 for crops is moderate to considerable south of the line Biarritz – Basel – Luxemburg – Krakow (orange grid cells > 50 % and red cells > 75 % probability). In this area the levels of exceedance probability follow the European altitudes highly correlated: fluctuations in the probability relief are well reflected by the fluctuation of in the altitude relief map. It is to be expected that for these regions the target value will not be met easily.

North of the line the exceedance probability reduces to levels of about 25 – 50 % meaning that target values could be met here more easily. While levels lower than 25 % do widely occur north of the line

La Rochelle – Hannover - Polish/Belarusian border, indicating policy targets are or may be reached for the larger background areas. The map does not indicate locally bound exceedance effects.

The visual impression of map pattern seems to be dominated by the map pattern of Figure 4.5 (top), but remarkable is the relative frequent number of green marked stations below limit in areas with a PoE above 50 % and also some red marked stations above limit in areas with a PoE of 25-50 %. This indicates that in the rural areas local contrast in even increased probability of exceedances may play an important role which is not covered by the resolution of the interpolation. The interpolated concentration field is ultimately a spatially smoothed representation of the background stations in the mapping domain, not necessarily reflecting the higher resolution local air quality status.

5 SO₂ maps for 2005

5.1 SO₂ vegetation indicators

The interpolated map for the annual average SO₂ and the winter average SO₂ concentrations are presented in Figure 5.1. As the limit value of the SO₂ annual and winter mean are set for the protection of vegetation, only rural maps have been made

For both indicators the maps have been created by combining the 2005 measurement data at rural background stations with the EMEP model output in a linear regression model (S.E), followed by the interpolation of its residuals by ordinary kriging (method 2-S.E-a). As the same method has been selected for the preparation of the 2004-map, it is also recommended to be used in future mapping activities.

5.1.1 Natural vegetation exposure

For both the annual mean as well as the winter mean the limit value (LV) is set at 20 µg.m⁻³. Inspecting Figure 5.1 learns that the annual limit value has not been exceeded in 2005. The probability map given below in Figure 5.2 (left) indicates that exceedance is unlikely except for a small area in Bulgaria where exceedance might be possible. In winter the SO₂ emission are higher and dispersion is less than in summertime. The winter average will therefore be higher than the annual mean. Especially in eastern Europe increase levels are seen in Figure 5.2 (right). Although the winter LV is more stringent than the annual LV, exceedances of the winter LV are not observed with exception of one small area near Katowice in Poland.

The exposure of natural vegetation (Corine Land Cover level-2 classes "3.1. Forests" and "3.2 Scrub and/or herbaceous vegetation associations") is given in Table 5.1. From this table it is clear that non-compliance with the LVs is only at a few locations. Due to the meteorological variability it might well be that in another year exceedance might be observed over larger areas but it unlikely that it is in more than 1-2% of the total area. It is therefore recommended not to map these indicators on a routine basis.

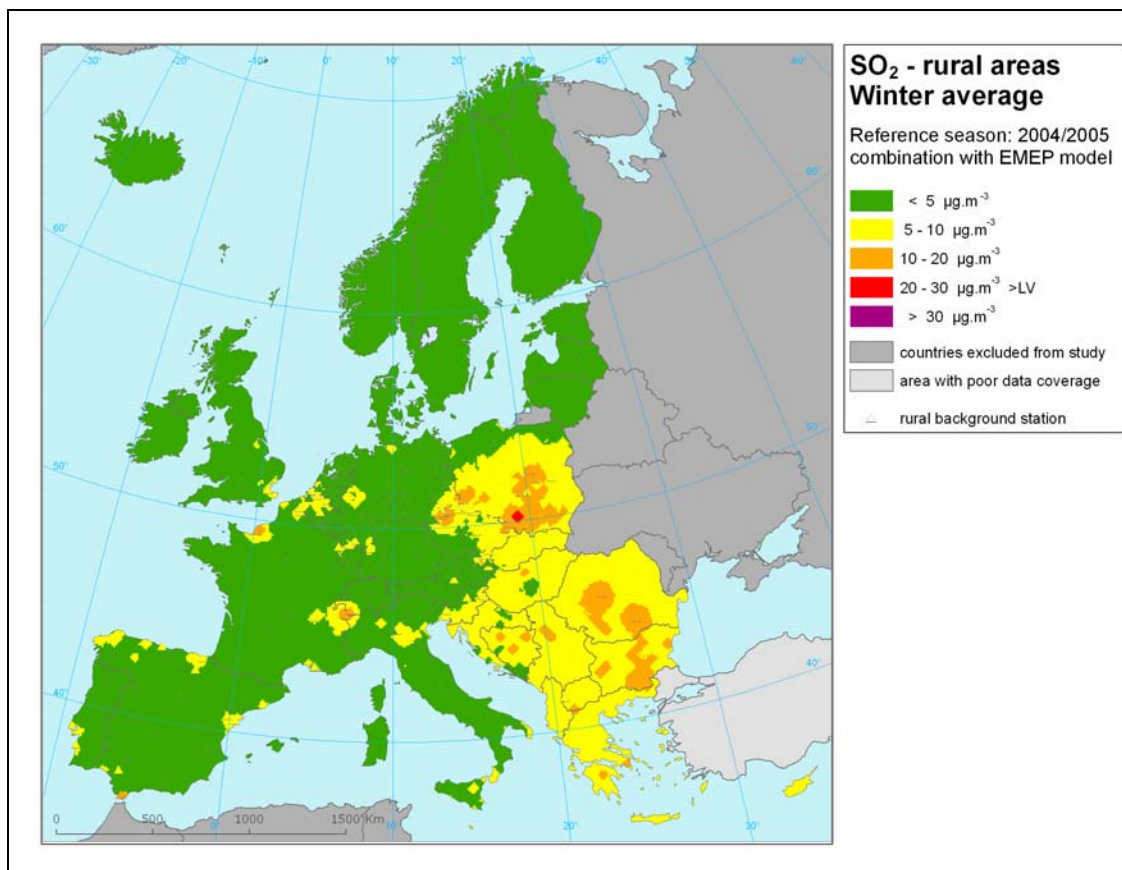
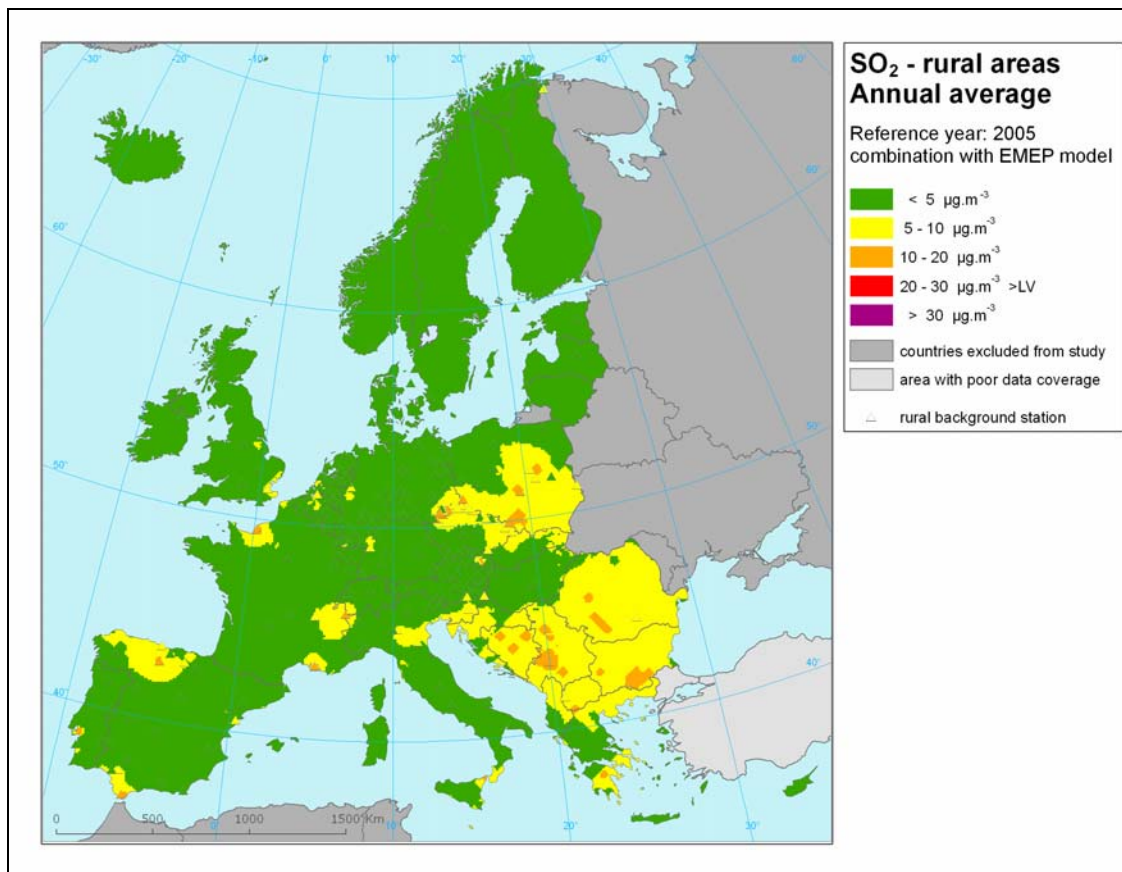


Figure 5.1 Rural concentration map of the SO₂ vegetation indicators annual average (top) and winter average (bottom) for the year 2005. Units: µg.m⁻³.

Table 5.1 Vegetation area exposure to SO₂ – annual average 2005 and winter season 2004/2005, (LV 20µg.m⁻³).

Country	Natural vegetation area km ²	SO2 annual average, 2005 [%]					SO2 winter season average 2004/2005 [%]				
		< 5 µg.m ⁻³	5 - 10 µg.m ⁻³	10 - 20 µg.m ⁻³	20 - 30 µg.m ⁻³	> 30 µg.m ⁻³	< 5 µg.m ⁻³	5 - 10 µg.m ⁻³	10 - 20 µg.m ⁻³	20 - 30 µg.m ⁻³	> 30 µg.m ⁻³
Albania	20321	36.4	63.4	0.1	0	0	0	99.9	0.1	0	0
Austria	52015	98.9	1.1	0	0	0	96.2	3.8	0	0	0
Belgium	6462	97.8	2.2	0	0	0	83.9	16.1	0	0	0
Bosnia-Herzegovina	30936	3.0	86.2	10.8	0	0	16.3	73.5	10.2	0	0
Bulgaria	47028	1.8	86.6	11.6	0	0	0	70.3	29.7	0	0
Croatia	28679	34.3	65.7	0.0	0	0	16.0	84.0	0	0	0
Cyprus	3963	100	0	0	0	0	0	100	0	0	0
Czech Republic	27758	47.0	51.0	2.0	0	0	34.0	55.7	10.2	0	0
Denmark (exc.Faroes)	5064	100	0	0	0	0	100	0	0	0	0
Estonia	25269	100	0	0	0	0	100	0	0	0	0
Finland	246040	100	0	0	0	0	100	0	0	0	0
France	186891	89	10.7	0.1	0	0	93.0	5.8	1.2	0	0
FYR of Macedonia	15003	0	97.2	2.8	0	0	0	96.2	3.8	0	0
Germany	108772	95.9	4.1	0.0	0	0	92.9	6.3	0.8	0	0
Greece	71419	55.5	42.6	1.9	0	0	0.0	95.4	4.6	0	0
Hungary	21809	96.7	3.3	0	0	0	8.9	89.6	1.5	0	0
Ireland	8113	100	0	0	0	0	100.0	0	0	0	0
Italy	125913	94	5.4	0.2	0	0	94	5	0.6	0	0
Latvia	32506	100	0	0	0	0	100	0	0	0	0
Liechtenstein	105	100	0	0	0	0	100	0	0	0	0
Lithuania	20955	100	0	0	0	0	100	0	0	0	0
Luxembourg	934	100	0	0	0	0	100	0	0	0	0
Malta	42	0	100	0	0	0	0	100	0	0	0
Monaco	5	100	0	0	0	0	100	0	0	0	0
Netherlands	3790	97.4	2.6	0	0	0	95.0	5.0	0	0	0
Poland	94994	49.0	48.2	2.8	0	0	26.6	52.8	19.8	0.7	0
Portugal	42678	97.0	2.0	1.0	0	0	95.9	4.1	0	0	0
Romania	80549	3.7	93.2	3.1	0	0	0	78.1	21.9	0	0
San Marino	10	100	0	0	0	0	100	0	0	0	0
Slovakia	21500	53.7	46.3	0	0	0	0.5	98.8	0.7	0	0
Slovenia	12628	46.8	53.2	0	0	0	24.8	75.2	0	0	0
Spain	233153	84.3	15.1	0.7	0	0	92.9	6.8	0.3	0	0
Sweden	333915	100	0	0	0	0	100	0	0	0	0
United Kingdom	73474	99.6	0.4	0.0	0	0	99.6	0.4	0.0	0	0
Total	1982692	81.5	18.6	1.0	0	0	76.0	20.7	3.3	0.0	0

Note: Countries not included due to lack of land cover data: Andorra, Iceland, Norway, Serbia and Montenegro, Switzerland and Turkey.

5.1.2 Uncertainties

The absolute and relative mean interpolation uncertainty of the map of the annual averages, expressed by the cross-validation RMSE, is 1.9 µg.m⁻³, i.e. about 53 % of the average of the values measured at all rural stations. For the map of the winter averages it is 2.3 µg.m⁻³, i.e. about 54 % of the average of the values measured at all rural stations.

In case one would like to aim for one indicator for inter-annual trend analysis of the reduction of SO₂ exceedances, one should consider using the winter season average preferable to the annual averages. Despite its higher concentrations and their slightly worse performance on the error statistics, they show statistically a more accurate behaviour when comparing predicted values against measured values.

The maps of the probability of the limit value exceedance are constructed, using concentration (Figure 5.1), uncertainty maps (Figures A4.6) and the limit values (i.e. $20 \mu\text{g}\cdot\text{m}^{-3}$ in the case of both SO_2 vegetation-related indicators), see Figure 5.2. The maps show that there is only a small location in Bulgaria where the limit value of the annual average may be exceeded with a probability of 25 - 50 %. The other small location is at Katowice, south Poland, where the limit value for the winter season average may be exceeded with a probability larger than 75 %.

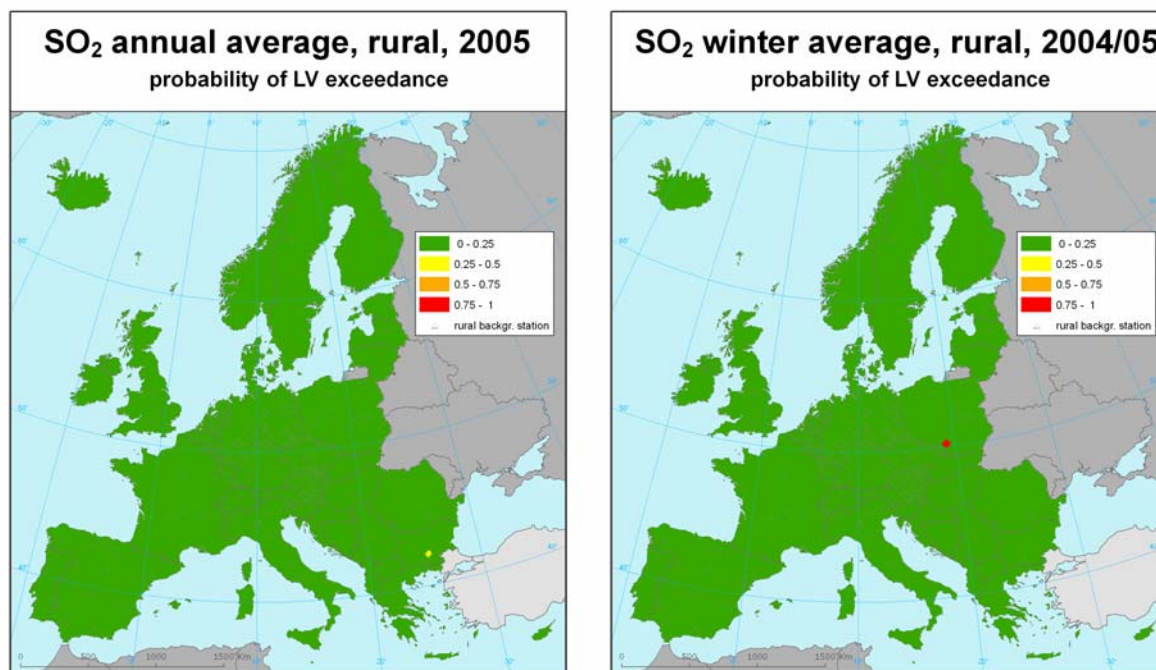


Figure 5.2 Probability of the limit value exceedance map for the SO_2 indicators annual average concentration in the year 2005 (left) and winter average concentration for the season 2004/2005 (in $\mu\text{g}\cdot\text{m}^{-3}$) on European scale for rural areas, 10 x 10 km grid resolution, as a result of interpolation method 3-S.E-a. (Stations with annual averaged measurement values above the limit value are marked red; station measurements below the limit value are marked green).

6 NO_x maps for 2005

6.1 NO_x annual average vegetation indicator

The interpolated map for the vegetation indicator annual average NO_x concentrations are presented in Figure 6.1. The rural NO_x map has been created by combining monitoring data from rural background monitoring stations with the EMEP model output, altitude field, wind speed, solar radiation in a linear regression model (N.Eawr), followed by the interpolation of its residuals with ordinary kriging (method 3-N.Eawr-a). Measurement were used from rural background stations which reported either NO_x or NO + NO₂ monitoring data, with inclusion of an additional 23 rural background stations for which the NO_x concentrations were estimated from the available NO₂ measurements.

Compared to the 2004 mapping exercise where altitude was included as the only regression parameter, this time the regression model has been extended with wind speed and solar radiation. The performance of the extended model is improved and for further work it is recommended to use the 3N-Eawr-a method.

6.1.1 Natural vegetation exposure

The NO_x limit value (LV) for the protection of vegetation is set on 30 µg.m⁻³. Figure 6.1 shows exceedances in Northern Italy, southern France, and the Benelux area and around large urban agglomerations (London, Paris, Barcelona, and Lyon). In these regions large fractions of the natural vegetation is exposed to concentrations above the LV (see Table 6.1). For the whole of Europe, exceedances are estimated in 2.2% of the natural vegetation area.

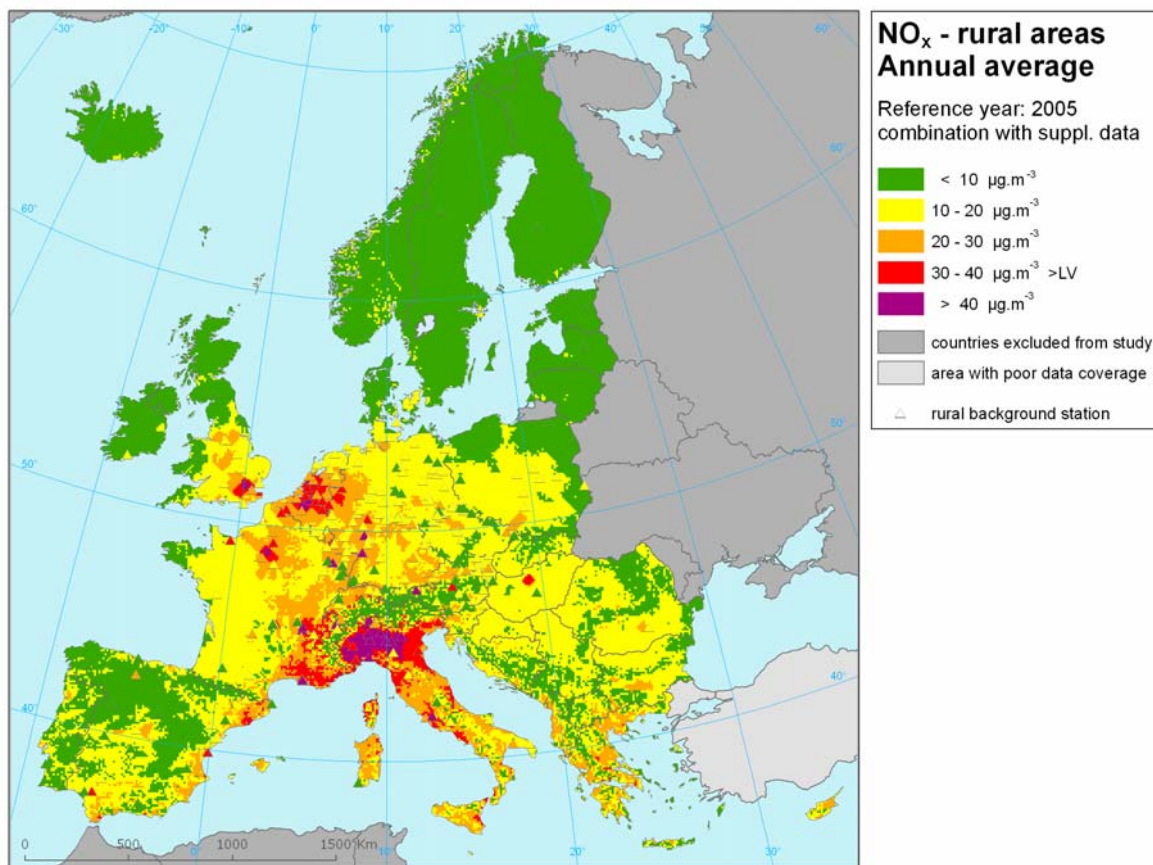


Figure 6.1 Rural concentration map of NO_x - annual average, year 2005. Units: µg.m⁻³.

Table 5.1 Vegetation area exposure to NO_x – annual average 2005, (LV 30 µg.m⁻³).

Country	Natural vegetation [km ²]	2005 Percent [%]				
		< 10 µg.m ⁻³	10 - 20 µg.m ⁻³	20 - 30 µg.m ⁻³	30 - 40 µg.m ⁻³	> 40 µg.m ⁻³
Albania	20036	50.4	35.2	14.4	0	0
Austria	52015	55.1	37.8	7.1	0	0
Belgium	6453	0.2	56.2	27.6	14.0	2.0
Bosnia-Herzegovina	30936	53.0	46.8	0.2	0	0
Bulgaria	46977	51.0	48.2	0.7	0	0
Croatia	27708	14.7	76.4	8.9	0	0
Cyprus	3629	11.3	69.1	19.6	0	0
Czech Republic	27758	20.1	77.1	2.8	0	0
Denmark (ex.Faroes)	4551	79.9	20.1	0	0	0
Estonia	24173	98.2	1.8	0	0	0
Finland	244587	99.7	0.3	0	0	0
France	185821	9.9	51.7	29.6	8.5	0.3
FYR of Macedonia	15003	59.6	39.4	1.0	0	0
Germany	108461	1.7	74.8	23.4	0.2	0
Greece	67621	32.9	45.6	21.5	0.0	0
Hungary	21809	3.3	94.3	0.4	2.0	0
Ireland	7740	99.6	0.4	0	0	0
Italy	124912	15.4	30.5	37.3	12.1	4.6
Latvia	32070	92.4	7.6	0	0	0
Liechtenstein	105	0	30.7	69.3	0	0
Lithuania	20852	81.5	18.5	0.0	0	0
Luxembourg	934	0	38.1	61.9	0	0
Malta	22	0	100.0	0	0	0
Netherlands	3607	1.0	14.7	56.9	26.1	1.3
Poland	94799	46.8	52.2	1.0	0	0
Portugal	42267	59.9	38.8	1.3	0	0
Romania	80498	61.5	38.1	0.4	0	0
San Marino	10	0	0	98.1	1.9	0
Slovakia	21500	52.0	48.0	0.0	0	0
Slovenia	12628	10.6	67.1	22.2	0.0	0
Spain	231893	62.6	30.2	6.2	1.0	0.1
Sweden	331266	97.8	2.2	0	0	0
United Kingdom	69716	88.2	7.8	3.0	0.8	0.1
Total	1962355	58.5	30.2	9.1	1.9	0.3

Note: Countries not included due to lack of land cover data: Andorra, Iceland, Norway, Serbia and Montenegro, Switzerland and Turkey.

6.1.2 Uncertainties

The absolute and relative mean interpolation uncertainty of this map of the annual averages, expressed in the RMSE from the cross-validation, is 9.7 µg.m⁻³, i.e. about 55.9 % of the average of the values measured at all rural stations.

The map of the probability of the NO_x limit value exceedance is constructed, using the concentration map (Figure 6.1), the uncertainty map (Figure A5.5) and the limit value (i.e. 30 µg.m⁻³), see Figure 6.2. The highest probability of limit value exceedance is at locations and regions with large agglomerations, such as London, Ruhr Gebiet, Paris, French Rhone Valley, German Rhine Valley, Italian Po Valley, and Benelux. Also the Italian, French and Spanish Mediterranean coastal zone elevated probability of exceedance. It is to be expected that the likelihood of limit value exceedances in these areas will continue to occur in the years to come due to significant NO_x emissions from human activities, not leading easily to non-exceedance levels.

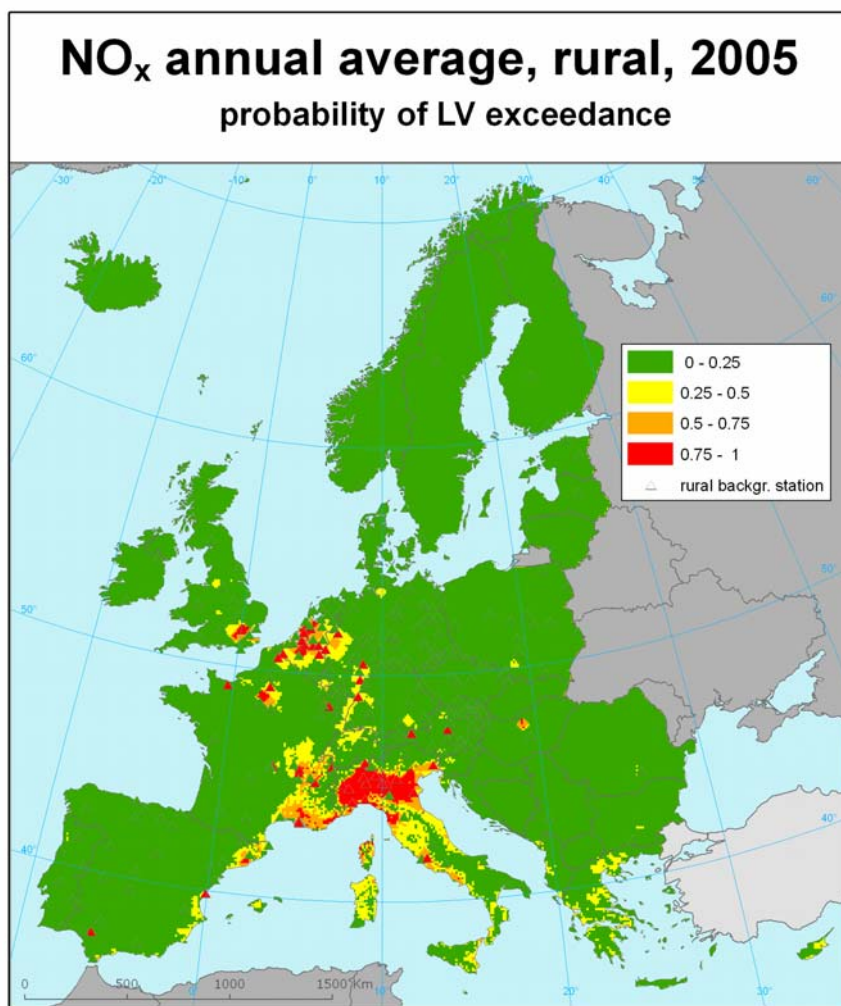


Figure 6.2 Probability of the limit value exceedance map for the annual average NO_x concentration (in $\mu\text{g}\cdot\text{m}^{-3}$) on European scale for rural areas in 2005, 10 x 10 km grid resolution, as a result of interpolation method 3-N.Eawr-a. (Stations with annual averaged measurement values above the limit value are marked red; station measurements below the limit value are marked green).

7 Discussion, recommendations and conclusions

7.1 Introduction

This report presents the updated European interpolated air quality indicator maps based on the 2005 monitoring data as reported by EU Member States in 2006 for pollutants PM₁₀, ozone NO_x and SO₂. It represents a follow-up from similar activities on 2004 data in 2006 (Horálek et al., 2007). In addition to analysing a new year of data, improvements of the interpolation methodologies have been examined with the intention to come to recommendations on which interpolation method to be used best or preferred on a more regular basis for the production and updating of such indicator maps. These maps are intended to serve as input into EEA's state and impact indicators and assessments at a European scale, e.g., population and ecosystem exposure assessment.

The focus of this work is on ground-based measurements as primary information, using results from chemistry transport modeling (CTM) and other data as secondary, supplementary sources. This is in contrast to the work supporting the development of the European Thematic Strategy on Air Pollution, which gives prominence to modelling as primary source of information, using monitoring data to calibrate the model. While some of the methods and data sources are similar, to some extent the two methods can be regarded as complementary.

In this report, similar methodologies as in Horálek et al. (2007) are applied to the 2005 datasets for the same pollutants. The maps of air quality are produced at a resolution of 10 x 10 km, covering all of Europe, and include both rural background and urban and suburban background monitoring data retrieved from the AirBase database. Spatially resolved supplementary data are used in the interpolation methodologies to improve the spatial assessment.

Reassessed are the interpolations of the annual averaged values for the indicators as defined in the EU Directives. In addition, the same supplementary data sources (altitude, meteorological parameters, EMEP dispersion model output) as used for the 2004 maps have been reselected for their positive contribution to the regressions and interpolations. We reassessed their usage for the 2005 data. In most cases, the same parameters appeared to be selected for achieving the best fit in the regression analysis, confirming the robustness of using them routinely. Additional to previous work, this comparison between years has been done now for both the rural and the urban areas. Attention is also given to the question of the uncertainty and variability related to the interpolations and to the 10x10 km gridded resolution, applied for mapping of the interpolated concentration fields.

To examine the hypothesis that the use of CTMs in general improves interpolation results, something that we concluded in Horálek et al. (2007) only for the Unified EMEP model, we introduced a comparison with another CTM. As representative substitute we selected the LOTOS-EUROS dispersion model output, since this is also a well established regional scale CTM applied in Europe, and from which data was readily available. For this study the comparison was limited to the interpolation method that does not include other supplementary data in addition to the CTM and the air quality measurements. The hypothesis was confirmed. The spatial interpolations led to comparable results in most cases. This supports the justification of using such well established models for air quality mapping.

Parallel to this, a study concerning the temporal resolution of the assessment was performed. Denby et al. (2008) - ETC/ACC Technical Paper 2007/8 – assesses for PM₁₀ and ozone indicators the interpolation performances using daily interpolations averaged to annual values and compared their behaviour for several data years and compared them to those obtained by the annual averages based interpolations.

This chapter further provides a more detailed summary of the conclusions of this study, as well as providing recommendations for usage of specific methods for mapping of particular air quality indicators. Next to this, the majority of recommendations given in Horálek et al. (2007) are still valid.

From a political point of view, a key question is to what extent air quality is either above or below a particular limit value in a certain area. But because of the significant scientific uncertainties, this question can not be answered very accurately for any particular location. Therefore, it was interesting to evaluate the probability that limit values would be exceeded, taking into account the scientific uncertainties. Section 7.4 includes several conclusions on the found uncertainties and experiences from the exceedance probability mapping trials.

7.2 Recommended interpolation methods for regular updating

Chapters 3 to 6 describe the mapping of air quality monitoring data for the year 2005 on the basis of the preferred interpolation method. Included is an assessment of the interpolation uncertainty and the exceedance probability in case of limit or target values or objectives as defined by the air quality directives. Additionally, the chapters present some examples of health and vegetation impact assessment for the year 2005. The selection of the interpolation method used as the preferred method was based on several criteria. Taking the best statistical fit as the starting point, also other criteria were considered, such as correspondence with the (close to) best performers for other indicators of the same pollutant, extent of coverage of the European mapping domain, the best performer for the on 2004-data, and furthermore practical and pragmatic reasons like continuity in the indicator updating over the (past) years, facilitating trend analyses. If a method would score better on these other criteria and did not have a much worse statistical fit, this was selected. In this way subjective expert judgment is considered to lead to an acceptable determination of “best” methods.

Table 7.1 provides an overview per pollutant indicator and per type of area for the preferred interpolation method as has been used for the 2004 air quality data (Horálek et al. (2007) and for the 2005 data (this paper). For each of the entities a recommendation is given for a specific method for future use in EEA assessments and (core set) indicators, especially for those produced and updated on a regular basis. Also, the motivation for the choice is given, based on the selection criteria.

Up to now, both ozone vegetation indicators for rural areas were created using the trend analysis using ordinary cokriging of the rural background measurements, combined with altitude. Maps for the EEA Core Set Indicator 005 (CSI 005, 2006) and in EEA air pollution assessment reports are based on this method. However, both 2004 and 2005 show for these indicators that the linear regression with EMEP model output, altitude field and surface solar radiation in a linear regression model (O.Ear), followed by the interpolation of its residuals by ordinary kriging (method 3-O.Ear-a) convincingly appears to be a better method. Nevertheless, for consistency over the years (1996 – 2004) the earlier method was still prolonged. However, comparison with 2005 data confirms that the linear regression with EMEP model output, altitude field and surface solar radiation in a linear regression model (O.Ear), followed by the interpolation of its residuals by ordinary kriging (3-O.Ear-a) appears to be the best, leading to the proposal to switch methods for the indicator CSI005 analyses. To avoid discontinuities in the trend of vegetation exposure, it is recommended to recalculate the indicators for a few recent years using both ‘old’ and ‘new’ method in parallel.

For both SO₂ natural vegetation indicators the maps have been created by combining the 2005 measurement data at rural background stations with the EMEP model output in a linear regression model (S.Ea), followed by the interpolation of its residuals by ordinary kriging (method 2-O.E-a). As the same method has been selected for the preparation of the 2004-map, it is also recommended to be used in future mapping activities. However, it is clear that non-compliance with the LVs only occurs at a few locations. Due to the meteorological variability it might well be that in another year exceedance might be observed over larger areas but it is unlikely that this would happen in more than 1-2% of the total area. Therefore, it is recommended not to map these indicators on a routine basis.

For the NO_x vegetation indicator where at the 2004 mapping exercise altitude was included as the only regression parameter, for 2005 mapping the regression model was extended with wind speed and solar radiation. The performance of the extended model was better and for further work it is recommended to use the new (3-N.Eawr-a) method.

7.3 Interpolation without dispersion model output

Dispersion modelling output data are frequently included as supplementary data source in the best or preferred interpolation methods. Advantage of using this data source as supplementary data to the monitoring data is its positive contribution to the interpolation results and its large European coverage. A drawback, however, could be its delayed availability compared to the monitoring data and the other supplementary data sources (meteorology and altitude, available even before the monitoring data). Excluding the dispersion modelling output data from the interpolation would allow a delivery of interpolated maps about half a year earlier and provide more timely support to (indicator) assessments if timeliness would be considered as more important than accuracy and a complete European coverage. The delivery would be able in April of year+2 instead of November of year+2. However, this requires alternative interpolation methods than those recommended in Table 7.1. Table 7.2 presents for the 2005 data the best performing interpolation methods not using dispersion modelling data. This table also presents the preferred methods for the year 2004 of which most were also the best performers. Based on the almost full correspondence between methods used in the two data-years we would recommend to use the method as is listed at 2005 in case no modelling data is applied.

Table 7.1 Summary table on best or preferred interpolation methods.

Substance	Urban /rural	Indicator	Preferred method on 2004 data (Horálek et al. 2007)	Preferred method on 2005 data (this paper)	Motivation on selected preferred method	Advice on specific method for future
PM10	Rural	Annual average	2 nd best: Ordinary kriging of residuals of linear regression model using EMEP model output, altitude, solar radiation and wind speed	2 nd best: Ordinary kriging of residuals of linear regression model using EMEP model output, altitude, solar radiation and wind speed	Same 1 st and 2 nd best in 2004 and 2005. 2004: 2 nd best solution as to fit preferred because of better coverage of areas without measurements, continuity with earlier work and its performance close to best results. 2005: 2 nd best selected for the same reasons.	Ordinary kriging of residuals of linear regression model using EMEP model output, altitude, solar radiation and wind speed (3-P.Eawr-a)
		36 th maximum daily average	See previous row	See previous row		
	Urban	Annual average	Close 2 nd best: Ordinary kriging on monitoring data only	Best: Ordinary kriging of residuals of linear regression model using EMEP model	2004: 2 nd best preferred: close to best, in line with best and used method at urban 36 th max. daily average indicator, simpler to generate. 2005: Different method preferred: better fit and better coverage of areas without stations.	Ordinary kriging of residuals of linear regression model using EMEP model (2-UP.E-a)
		36 th maximum daily average	Best: See previous row	Best: See previous row	2004: Best. 2005: See previous row	
Ozone	Rural	26th highest maximum 8-hour running average	Ordinary cokriging on monitoring data, including altitude ^(*)	Close 2 nd best: Ordinary kriging of residuals of linear regression model using EMEP model output, altitude and solar radiation	2004: ^(*) No EMEP model data available leading to limited comparison; spatial methods perform better than linear regression. 2005: EMEP data now available. Best is OC, but 2 nd best is preferred: close to best, better coverage of area without stations, overall (close) best performer at all other O3 indicators (both rural and urban) and therefore considered to be robust.	Ordinary kriging of residuals of linear regression model using EMEP model output, altitude and solar radiation (3-O.Ear-a)

Substance	Urban /rural	Indicator	Preferred method on 2004 data (Horálek et al. 2007)	Preferred method on 2005 data (this paper)	Motivation on selected preferred method	Advice on specific method for future
		SOMO35	Best: Ordinary kriging of residuals of linear regression model using EMEP model output, altitude and solar radiation.	Close 2 nd best: Ordinary kriging of residuals of linear regression model using EMEP model output, altitude and solar radiation.	Appears robust method over the years. 2005: Close 2 nd best preferred: used last year and see above and below.	
		AOT40 crops	2 nd best: Ordinary cokriging on monitoring data, including altitude	Best: Ordinary kriging of residuals of linear regression model using EMEP model output, altitude and solar radiation.	2004: Best was ordinary kriging of residuals of linear regression using EMEP model output, altitude, solar radiation and rel. humidity. 2 nd best used for consistency with AOT40forest's best performer and with previous years. 2005: Different method preferred: best fit, similar to 2004's best performer, better area coverage, preferred and used at all other O3 indicators and appears to be robust.	Ordinary kriging of residuals of linear regression model using EMEP model output, altitude and solar radiation (3-O.Ear-a)
		AOT40 forests	Best: Ordinary cokriging on monitoring data, including altitude	Best: Ordinary kriging of residuals of linear regression model using EMEP model output, altitude and solar radiation.	2005: Different best method preferred: in line with AOT40crops' best performer and arguments above.	
Ozone (cont.)	Urban	26th highest maximum 8-hour running average	Best: Ordinary cokriging on monitoring data, including altitude	Best: Ordinary Kriging of residuals of linear regression model using EMEP model output, wind speed and solar radiation	2004: with very close 2 nd best OK with altitude. 2005: Different best method preferred: better fit and better methodological consistency with all other ozone indicator maps (both rural and urban).	
		SOMO35	Close 2 nd best: Ordinary kriging of monitoring data	Best: Ordinary Kriging of residuals of linear regression model using EMEP model output, wind speed and solar radiation	2004: best is OC with altitude. 2 nd best preferred: close to best and materials were ready to use. 2005: See previous row	

Substance	Urban /rural	Indicator	Preferred method on 2004 data <i>(Horálek et al. 2007)</i>	Preferred method on 2005 data <i>(this paper)</i>	Motivation on selected preferred method	Advice on specific method for future
SO ₂	Rural	Annual average	Ordinary kriging of residuals of linear regression model using EMEP model output	Ordinary kriging of residuals of linear regression model using EMEP model output	Appears robust method.	Ordinary kriging of residuals of linear regression model using EMEP model output (2-S.E-a) <i>Little to no exceedance in Europe therefore recommended not to map these indicators on a routine basis.</i>
		Winter average	Not done	Ordinary kriging of residuals of linear regression model using EMEP model output	In line with annual average results: methodology appears consistent and robust.	
NO _x	Rural	Annual average	Ordinary kriging of residuals of linear regression model using EMEP and altitude	Ordinary kriging of residuals of linear regression model using EMEP, altitude, wind speed, solar radiation	2005: addition of meteorological parameters appears to improve performance significantly.	Ordinary kriging of residuals of linear regression model using EMEP, altitude, wind speed, solar radiation (3-N.Eawr-a)
PM2.5			Not pursued because of data scarcity.	Not pursued because of data scarcity.	2004: linking to PM10 mon. data or EMEP model PM2.5 output gives poor fit. 2005: See Annex PM10-PM2.5 assessment feasibility study. Re-assess in 2009 with more reported PM2.5 stations.	n/a

Table 7.2 Summary of advised interpolation methods when no dispersion model output data is used in the interpolated mapping. Advice is based on results from the application on 2004 and 2005 monitoring data.

Substance	Urban /rural	Indicator	Preferred interpolation when not using dispersion modelled data on 2004 data (Horálek et al. 2007)	Preferred interpolation when not using dispersion modelled data on 2005 data (this paper)
PM10	Rural	Annual average	Lognormal cokriging on monitoring data, including altitude	Lognormal cokriging on monitoring data, including altitude (1-d)
		36 th max. daily avg		
	Urban	Annual average	Ordinary kriging on monitoring data only (Used for final mapping as close 2 nd best.)	Indifferent: Ordinary kriging or Lognormal kriging on monitoring data only (1-a or 1-b)
		36 th max daily avg		
Ozone	Rural	26th h. max 8-hr avg	Ordinary cokriging on monitoring data, including altitude (Used at AOT40crops and urban SOMO35 for final mapping, but was close 2 nd best)	Ordinary cokriging on monitoring data, including altitude (1-c)
		SOMO35		
		AOT40 crops		
		AOT40 forests		
Ozone (cont.)	Urban	26th h. max 8-hr avg		
		SOMO35		
SO ₂	Rural	Annual average	Lognormal kriging on monitoring data only	Lognormal kriging on monitoring data only (1-b)
		Winter average	Not done	
NO _x	Rural	Annual average	Lognormal cokriging on monitoring data, including altitude	Lognormal cokriging on monitoring data, including altitude (1-d)
PM2.5			Not pursued because of data scarcity.	Not pursued because of data scarcity.

7.4 Final conclusions relating to the mapping methodology

Mapping methodology

1. There appears to be a reasonable agreement between the analyses using EMEP and LOTOS-EUROS modelling results. Even the fact that in some cases LOTOS-EUROS provides a better fit, the differences are sufficiently small to justify for the time being the usage of the EMEP-model as we did for the final mapping with the argument of its somewhat larger mapping domain and on its more established updating cycle. This does not exclude the use of LOTOS-EUROS in the near future when its data availability has become better established. It would allow making use of its better fit on the PM₁₀ indicators and its advantage of having a grid resolution scaling feature providing zoom-in options to more regional areas in Europe.
2. For some substances and indicators (rural PM₁₀, rural SOMO₃₅, SO₂) the preferred method is the same in 2005 as in 2004 (see Table 7.1), suggesting that in those cases the methods are relatively robust and an annual comparison between methods does not appear to be necessary. Frequent comparison and changing of methods for indicators updated within the EEA regular production processes should be avoided to guarantee better the stability in the messages to be send out and limits production resources. It is recommended to fix the method for some years and change it only when EEA and ETC experts believes in the robustness to move from one method to another method resulting from a parallel development process. The frequency will depend on the methodological and expertise developments in this area.
3. For other substances (rural ozone vegetation indicators, urban PM₁₀ and urban ozone, NO_x) the new analysis suggests that a different method is to be preferred. We recommended using the new method from now onward.
4. A multi-annual analysis with data of some past 10 yrs of EMEP model runs should be done to map and explain trends on aspects of stations density influences and method or model influences for ozone and PM₁₀ to determine more definitely the level of inter-annual variability of the best performing method.
5. To ensure that discontinuities in the indicator trend analysis are avoided due to a switch between interpolation methods in case of vegetation exposure (for CSI005), it is recommended to recalculate the trends for a few recent years and in addition, to use both the 'old' and 'new' methods in parallel for the coming years, however, leading to about half a year later delivery of the ozone indicator update due to the later model data availability.
6. Like for the 2004 maps, not always the "best" method in terms of fit was selected, because other criteria were considered to be more important than the best statistical fit. For example, spatial interpolation methods using additional data (e.g., EMEP) can have the advantage of larger spatial coverage in areas where monitoring stations are missing. Also consistency between all indicators of one pollutant can be an argument not to choose the method that performs best statistically. In such cases, the statistical performance levels should not differ too much.
7. If one would consider timeliness more important than accuracy and Europe-wide coverage, half a year can be gained by creating maps only based on monitoring data, without usage of

EMEP model results. In that case Table 7.2 gives recommendations depending on the indicator on which method is best to use. The recommendations are given using similar criteria as those of Table 7.1.

8. Improvements in the regression, through the use of other regression parameters, may ultimately lead to improvements in the residual kriging. The use of other data sources such as other land use characteristics next to altitude, or air pollutant satellite imagery, or even more directly high resolution emission estimates, may provide similar improvements to the multiple regression and hence the residual kriging.

Mapping results

9. For PM₁₀, health exposure assessment reveals exposure above the limit values in a number of areas of Europe. In comparison to its neighbouring countries, the concentrations in France are relatively low. It can not be excluded that these low levels are caused by the low correction factor applied in the French networks for correcting the data for non-reference measuring configurations (de Leeuw, 2005). The number of Europeans exposed to annual mean concentrations of PM₁₀ above the limit value of 40 ug.m⁻³ is 9% of the total population; in the case of the limit value of 50 ug.m⁻³ it is 28%. The numbers of premature deaths on European and regional scales have been estimated and show a range that is partly caused by the differences in PM₁₀ concentration over Europe and partly by the differences in age distributions and baseline mortalities. The uncertainties in the numbers caused by the uncertainties in the relative risk factor are relatively large.
10. Similar assessments and estimates have been executed for the ozone human health indicators, ozone vegetation (crops and forests) indicators, natural vegetation SO₂ indicators and vegetation NO_x indicator. Striking are the high likelihood in exceeding the ozone health target value in southern and south-eastern Europe. Furthermore, there are the higher exposure exceedances of crops and forests to ozone in 2005 compared to 2004: almost 50 % of all agricultural land may be exposed to ozone exceeding the target value of 18 mg.m⁻³.h and almost 90 % may be exposed to levels in excess of the long-term objective of 6 mg.m⁻³.h. The difference in comparison with 2004 results has its cause not only in the higher ozone concentrations, but also in the switch to an improved interpolation method leading to presenting the larger area.
11. Little to no exceedance is observed for both annual and winter season SO₂ in Europe. Therefore it is recommended not to map these indicators on a routine basis. Nevertheless, In case one would like to aim for one indicator for inter-annual trend analysis of the SO₂ exceedances, one should consider using the winter season average preferable to the annual averages. Despite its higher concentrations and its slightly worse performance on the error statistics, it shows statistically a more accurate behaviour when comparing predicted values against measured values.
12. For NO_x the regression model method extended with wind speed and solar radiation was selected, while the 2004 mapping exercise included altitude as the only regression parameter. The performance of the extended model gives better results and for future updates it is recommended to use the new (3N-Eawr-a) method.

Uncertainties

13. The following conclusions relating to the uncertainties for the mapping of different substances can be drawn:
 - The relative uncertainty of rural PM₁₀ maps is about 26%, the relative uncertainty of urban PM₁₀ maps is about 20%
 - The relative uncertainty of rural ozone maps is different for different indicators: about 10% in the case of 26th highest daily maximum 8-hour average, about 35% in case of SOMO35 and about 40% in case of both AOT40 indicators
 - The relative uncertainty of urban ozone maps is 9% in the case of 26th highest daily maximum 8-hour average and 32% in case of SOMO35
 - The relative uncertainty of rural SO₂ and NO_x maps is about 50-55%.

14. Both the uncertainty and probability maps presented in this report accounts only for the interpolation error. Other sources of uncertainty (e.g. measuring errors, representativeness, and model uncertainty) have not been included. It is recommended to identify and quantify the sources of uncertainty external to the interpolation methodologies as well as to study of effects of impacts of monitoring uncertainties on mapping.

15. The approach, the weighting function and its related criterion used to combine and merge the concentration and uncertainty of the rural and urban maps into final concentration and probability of exceedance maps need to be addressed further on its validity, leading to improvements and being better be able describing its involved uncertainty.

16. The following more general conclusions related to the probability of limit or target value exceedances (PoE) and their maps can be drawn:
 - Resulting PoE maps may guide further action with respect to implementation of abatement measures and to the design of the monitoring network.
 - In regions with a high uncertainty in the indicator value there might be no need to reduce this uncertainty (e.g. by establishing additional stations) when the probability map indicates that exceedance is most unlikely.
 - On the other hand, there will be areas where the concentration is below the limit value but the probability map indicates that exceedance is likely. Although these areas are formally speaking in compliance, one may conclude that, in order to avoid non-compliance in another year, abatement measure should be considered.
 - The exceedance probability maps show that relationship between the *actual* and the *interpolated* value and the associated *uncertainty* is much more complex than is often assumed. This calls for a careful consideration of the selection of the particular output indicator to be presented and the way of presenting it, especially in view of the message to be communicated.

17. The concentration maps in general underestimate the high values in at areas with no measurement, as is indicated by the cross-validation scatter plots. The underestimation of interpolation is smaller in the urban areas for both PM₁₀ and ozone. This is probably caused by the higher number of urban/suburban stations in comparison to the number of the rural stations. The level of underestimation is visible from the scatter plots in the Annexes).

18. Next to the concentration maps, the uncertainty maps were constructed. The maps show higher uncertainty in areas with low density of stations. The areas with the highest uncertainty are southern Italy, west Balkan (or the whole Balkan for some pollutants), Iceland and the northern Scandinavia.

19. Based on the concentration and uncertainty maps, the maps of probability of limit value exceedances (PoE) have been estimated.

References

- AirBase, European air quality database, <http://airbase.eionet.europa.eu>
- Buijsman E, Beck JP, Bree L van, Cassee FR, Koelemeijer RBA, Matthijssen J, Thomas R, Wieringa K (2005). Particulate Matter: a closer look. MNP report no. 500037011, Bilthoven, the Netherlands. <http://www.mnp.nl/bibliotheek/rapporten/500037011.pdf> (Dutch version: Fijn stof nader bekeken. MNP report 500037008, <http://www.mnp.nl/bibliotheek/rapporten/500037008.pdf>)
- Cressie N (1993). Statistics for spatial data. Wiley series, New York.
- Denby B, Horálek J, Walker SE, Eben K, Fiala J (2005). Interpolation and assimilation methods for European scale air quality assessment and mapping. Part I: Review and recommendations. ETC/ACC Technical paper 2005/7. http://air-climate.eionet.europa.eu/docs/ETCACC_TechPaper_2005_7_SpatAO_Interpol_Part_I.pdf
- Denby B, Horálek J, Walker SE, Eben K, Fiala J (2008). European scale exceedance mapping for PM10 and ozone based on daily interpolation fields. ETC/ACC Technical Paper 2007/8. http://air-climate.eionet.europa.eu/docs/ETCACC_TP_2007_8_daily_interpol_spatAOmaps_fnl.pdf
- ECMWF: Meteorological Archival and Retrieval System (MARS). It is the main repository of meteorological data at ECMWF (European Centre for Medium-Range Weather Forecasts; <http://www.ecmwf.int/>).
- Fagerli H, Simpson D, Tsyro S (2004). Unified EMEP model: Updates. In: EMEP Report 1/2004. MSC-W, Oslo, Norway. www.emep.int/publ/reports/2004/Status_report_int_dell.pdf
- Horálek J, Denby B, de Smet PAM, de Leeuw FAAM, Kurfürst P, Swart R, van Noije T (2007). Spatial mapping of air quality for European scale assessment. ETC/ACC Technical paper 2006/6. http://air-climate.eionet.europa.eu/docs/ETCACC_TechPaper_2006_6_Spat_AO.pdf
- Künzli N, Kaiser R, Medina S, Studnicka M, Chanel O, Filliger P, Herry M, Horak F, Jr, Puybonnieux-Texier V, Querel P, Schneider J, Seethaler R, Vergnaud JC, Sommer H (2000). Public-health impact of outdoor and traffic-related air pollution: a European assessment. *Lancet* 2000;356(9232):795-801. <http://linkinghub.elsevier.com/retrieve/pii/S0140673601067630>
- Leeuw, FAAM de (2005). PM10 measurement methods and correction factors in AIRBASE 2004 status report, ETC/ACC Technical Paper 2005/6. http://air-climate.eionet.europa.eu/reports/docs/ETCACC_TechPaper_2005_6_PM10_Corr_factors_2004.pdf
- Mol, WMA, van Hooydonk PR, de Leeuw FAAM (2007), European exchange of monitoring information and state of the air quality in 2005, ETC/ACC Technical Paper 2007/1. http://air-climate.eionet.europa.eu/reports/docs/ETCACC_TP_2007_1_eoi2006_2005aqdata.pdf
- Sandnes Lenschow H, Tsyro S (2002). Meteorological input data for EMEP/MSW-W air pollution models. EMEP MSC-W Note 2/2000. http://www.emep.int/publ/reports/2000/dnmi_note_2_2000.pdf
- Schaap M, Timmermans RMA, Roemer M, Boersen GAC, Bultjes PJH, Sauter FJ, Velders GJM, Beck JP (2008). The LOTOS-EUROS model: description, validation and latest developments. *International Journal Environment and Pollution*, Vol. 32, No. 2, pp.270-290. <http://www.inderscience.com/browse/index.php?journalID=9&year=2008&vol=32&issue=2> and <http://www.lotos-euros.nl>
- Simpson D, Fagerli H, Jonson JE, Tsyro S, Wind P, Tuovinen J-P (2003). Transboundary acidification and eutrophication and ground level ozone in Europe: Unified EMEP model description. EMEP Status Report 1/03 Part I. MNP, Oslo, Norway. http://www.emep.int/publ/reports/2003/emep_report_1_part1_2003.pdf
- Stedman JR, Kent AJ Grice S, Bush TJ, Derwent RG (2007) A consistent method for modeling PM10 and PM2.5 concentrations across the United Kingdom in 2004 for air quality assessment. *Atmospheric Environment* 41, 161-172. <http://linkinghub.elsevier.com/retrieve/pii/S1352231006008168>
- UN (2006). United Nations, Department of Economic and Social Affairs, Population Division (2007). World Population Prospects: The 2006 Revision. CD-ROM Edition - Extended Dataset (United Nations publications, ST/ESA/SER.A/266). http://unstats.un.org/unsd/cdb/cdb_source_xrxx.asp?source_code=15
- UNECE (2004). United Nations – Economic Commission for Europe, LRTAP Convention. Mapping Manual 2004. Manual on methodologies and criteria for Modelling and Mapping Critical Loads and Levels and Air Pollution Effects, Risks and Trends. http://www.oekodata.com/icpmapping/htm/manual/manual_eng.htm
- Vestreng V, Mareckova K, Kakareka S, Malchukhina A, Kukharchyk T (2007). Inventory Review 2007; Emission Data reported to LRTAP Convention and NEC Directive, MSC-W Technical Report 1/07 http://www.emep.int/mscw/mscw_publications.html#2007
- WHO (2001). Quantification of health effects of exposure to air pollution. EUR/01/5026342, E74256, WHO Regional office for Europe, Copenhagen. <http://www.euro.who.int/document/e74256.pdf>

Annexes

Annex 1 Input data	67
Annex 2 PM10 spatial analysis	71
Annex 3 Ozone spatial analysis	97
Annex 4 SO2 spatial analysis	127
Annex 5 NOx spatial analysis	137
Annex 6 Formulas of statistical indicators and other calculations	145
Annex 7 PM2.5 in relation to PM10	149

Annex 1 Input data

A1.1 Introduction

The input data used depends on the mapping methodology applied. Chapter 4 of Horálek et al. (2007) provides a complete overview on sources and specifications of the input data. For clarity and readability of this paper we provide here the full list of the used data. The interpolation methods of type 1 use measured air pollution data, together with the coordinates and altitude of the measurement stations. The advanced mapping methods use also supplementary parameters, such as output from the dispersion models, altitude data covering the whole study area, meteorological parameters and population density. The resolution of such input data should be, if possible, higher than or comparable to the resolution of the maps constructed, which is 10 x 10 km.

A1.2 Measured air quality data

The air quality data were extracted from the European monitoring database AirBase, supplemented by several rural EMEP stations which are not reported to AirBase. Only data from stations classified by AirBase and/or EMEP as *rural*, *suburban* and *urban background* stations has been used. *Industrial* and *traffic* station types are not considered, since they represent local scale concentration levels not applicable at the mapping resolution employed. The following components and their indicators were considered:

- PM₁₀ – annual average [$\mu\text{g}\cdot\text{m}^{-3}$], year 2005
– 36th maximum daily average value [$\mu\text{g}\cdot\text{m}^{-3}$], year 2005
- Ozone – 26th highest daily maximum 8-hour average value [$\mu\text{g}\cdot\text{m}^{-3}$], year 2005
– SOMO35 [$\mu\text{g}\cdot\text{m}^{-3}\cdot\text{day}$], year 2005
– AOT40 for crops [$\mu\text{g}\cdot\text{m}^{-3}\cdot\text{hour}$], year 2005
– AOT40 for forests [$\mu\text{g}\cdot\text{m}^{-3}\cdot\text{hour}$], year 2005
- SO₂ – annual average [$\mu\text{g}\cdot\text{m}^{-3}$], year 2005
– winter average [$\mu\text{g}\cdot\text{m}^{-3}$], winter 2004-2005
- NO_x – annual average [$\mu\text{g}\cdot\text{m}^{-3}$], year 2005
- NO₂ – annual average [$\mu\text{g}\cdot\text{m}^{-3}$], year 2005 (for purposes of NO_x mapping only)
- NO – annual average [$\mu\text{g}\cdot\text{m}^{-3}$], year 2005 (for purposes of NO_x mapping only)

SOMO35 is the annual sum of maximum daily 8-hour concentrations above 35 ppb (i.e. 70 $\mu\text{g}\cdot\text{m}^{-3}$). Winter average is the average over the six months from October to March.

In case of components affecting human health (i.e. PM₁₀, and the ozone parameters 26th highest daily maximum 8-hour average value and SOMO35) data from *rural*, *urban* and *suburban* background stations are considered. In case of components affecting vegetation (SO₂, NO_x and both AOT40 parameters for ozone) only *rural* background stations are considered. The paucity of PM_{2.5} data available from AirBase precludes further analysis of this pollutant, see Annex 7.

Only the stations with annual data coverage of at least 75 percent are used. The stations from French overseas areas (departments) have been excluded. Additionally, one Greek ozone station (GR0110R) with highly questionable data has been excluded from the analysis.

Table A1.1 shows the number of the measurement stations selected for the individual pollutants and their respective indicators.

Table A1.1 Number of the stations selected for the individual indicators and areas. For rural areas the rural background stations and for urban areas the urban and suburban background stations are used.

	PM ₁₀		ozone		SO ₂		NO _x direct	NO & NO ₂	NO ₂ only	NO _x direct & derived
	annual average	36 th max. daily mean	SOMO35	26 th highest max. daily 8h	annual average	winter average	annual average	annual average	annual average	annual average
rural	214	206	440	442	283	271	132	+ 126	+ 67	= 325
urban	800	800	843	841	-	-	-	-	-	-

In addition to the AirBase data, 8 additional rural PM₁₀ stations from the EMEP database have been used to reach a more extended spatial coverage by measurement data.

For a considerable number of stations NO_x is measured, however not reported as such but separately as NO and NO₂. For these 126 rural background stations reporting NO and NO₂ separately, the NO_x concentrations were derived according the equation

$$\text{NO}_x = \text{NO}_2 + 46/30 \cdot \text{NO} \quad (3.1)$$

where all components are expressed in $\mu\text{g}\cdot\text{m}^{-3}$, with a molecular mass for NO of 30 and for NO₂ of 46 $\text{g}\cdot\text{mol}^{-1}$. For the NO_x mapping these stations were added to the set with reported NO_x concentrations resulting in a extended set of 258 stations. For the remaining 67 stations with NO₂ data reported only, the NO_x values were estimated according Horálek et al. (2007), Section 5.4.1, increasing the total ultimately to a set of 325 stations.

A1.3 Unified EMEP model output

The well established European chemistry transport model we used is the photochemical version of the Unified EMEP model (revision rv2_5_beta2), which is a Eulerian model with a resolution of 50 x 50 km. The disaggregation to the 10x10km grid cells is done as described in Section 4.4 of Horálek et al. (2007). Output from this model (2005 data extracted in October 2007) is used for the same parameter set as the set of measurement parameters in Section 3.2:

- PM₁₀ – annual average [$\mu\text{g}\cdot\text{m}^{-3}$], year 2005
- 36th maximum daily average value [$\mu\text{g}\cdot\text{m}^{-3}$], year 2005
- Ozone – 26th highest daily maximum 8-hour average value [$\mu\text{g}\cdot\text{m}^{-3}$], year 2005
- SOMO35 [$\mu\text{g}\cdot\text{m}^{-3}\cdot\text{day}$], year 2005
- AOT40 for crops [$\mu\text{g}\cdot\text{m}^{-3}\cdot\text{hour}$], year 2005
- AOT40 for forests [$\mu\text{g}\cdot\text{m}^{-3}\cdot\text{hour}$], year 2005
- SO₂ – annual average [$\mu\text{g}\cdot\text{m}^{-3}$], year 2005
- winter average [$\mu\text{g}\cdot\text{m}^{-3}$], season 2004/2005
- NO_x – annual average [$\mu\text{g}\cdot\text{m}^{-3}$], year 2005

The model is described by Simpson et al. (2003) and Fagerli et al. (2004). The model results are based on the emissions for the relevant year (Vestreng et al., 2007) and actual meteorological data (from PARLAM-PS, i.e. special dedicated 2000 version of HIRLAM numerical weather prediction model, with parallel architecture, see Sandnes Lenschow and Tsyro, 2000).

A1.4 LOTOS-EUROS model output

As comparable air chemistry transport model for interpolated air quality mapping of the health-related pollutant indicators the following 2005 data output of LOTOS-EUROS model (Schaap et al., 2007) was used:

- PM₁₀ – annual average [$\mu\text{g}\cdot\text{m}^{-3}$], year 2005
- 36th maximum daily average value [$\mu\text{g}\cdot\text{m}^{-3}$], year 2005
- Ozone – 26th highest daily maximum 8-hour average value [$\mu\text{g}\cdot\text{m}^{-3}$], year 2005
- SOMO35 [$\mu\text{g}\cdot\text{m}^{-3}\cdot\text{day}$], year 2005

The data were extracted on 17-19 October 2007 by TNO in netCDF for the years 2004 and 2005. The pollutant parameters extracted are PM₁₀ daily averages and ozone hourly averages in a grid resolution of 25x25km for the whole modeling domain, which is somewhat less extended than that of EMEP. The same disaggregation as with the EMEP data has been applied to meet the 10x10 km grid interpolation resolution.

A1.5 Altitude

The station altitude from AirBase (or EMEP) is only considered in this study at the interpolation cokriging techniques using primarily monitoring data (methodology type 1).

For the methodologies of type 3, using as supplementary information the altitude in their linear regression model we used the European covering altitude data field (in meters) of GTOPO30, original grid resolution of 30 x 30 arcsec. For details, see Horálek et al (2007).

A1.6 Meteorological parameters

Actual meteorological surface layer parameters are extracted from the Meteorological Archival and Retrieval System (MARS) of the ECMWF (European Centre for Medium-range Weather Forecasts). The derived parameters currently used extracted from the ECMWF variables, specified in detail in Horálek et al. (2007) Section 4.5, are:

- Wind speed – annual average [m.s⁻¹], year 2005
- Surface solar radiation – annual average [MWs.m⁻²], year 2005
- Temperature (in 2 meters) – annual average [°C], year 2005
- Relative humidity – annual average [%], year 2005

Next to this, we tested the use of surface pressure (according to the recommendation of Horálek et al., 2007), but finally we decided to ignore this parameter, because of almost no improvement of the results in the case of its use at the pollutant, except NO_x (see Section A5.1.1).

A1.7 Population density

Population density [inhbs.km⁻²] is based on JRC data for the majority countries (Source EEA, pop01c00v3int, official version Aug. 2006; Owner: JRC). For the countries which are not included in this database (i.e. for Andorra, Albania, Bosnia-Herzegovina, Cyprus, Island, Lichtenstein, FYR of Macedonia, Norway, Serbia and Montenegro, Switzerland, and Turkey) we used population density data from an alternative source, the ORNL LandScan (2002) Global Population Dataset. However, these data were not available for the southern part of Cyprus. See Horálek et al. (2007) Section 4.9 for the detailed specification and the aggregation executed on the population density data.

As mentioned in Horálek et al. (2007), preliminary comparisons between the ORNL LandScan and the JRC datasets for countries covered by both datasets demonstrated significant differences between these two databases. Thus we compared the aggregated data for the individual countries with the official UN population data (<http://www.un.org/popin/data.html>) for these countries. This comparison showed good agreement of JRC and UN data, but underestimation of ORNL data. Based on this comparison the multiplied factor 1.65 was applied for all ORNL data.

For the health impact assessment, performed according to standard population attributive principles (WHO, 2001), an update of country-specific demographic data has been taken from the UN population Division (UN, 2006).

A1.8 Land cover

The input data from CORINE Land Cover 2000 (CLC2000) – grid 250 x 250 m, version 8/2005 version 2, (Source and owner: EEA, lceugr250_00) is used. The countries missing in this database are Iceland, Norway, Switzerland, Serbia and Montenegro, and Turkey.

In an effort to reduce the time demanding calculations on large data quantity involved with the 250 x 250 m grid resolution an aggregation to a 500 x 500 m grid resolution is performed first, before the exceedance mapping and table extraction takes place. The ultimate map and table results are not influenced by this resolution aggregation.

Annex 2 PM₁₀ spatial analysis

General introduction to the spatial analysis

For both rural and urban maps the examination and selection process is described in three subsections:

1. supplementary data selection for linear regression model and its analysis
2. spatial interpolation comparison and selection of interpolation method for mapping
3. the interpolation uncertainty analysis of the selected mapping method

The first subsection concentrates on determining whether a linear regression model using supplementary parameters next to modelling data would improve the fit of predicted and measurement values. Simultaneously, the set of most significant contributing parameters is selected. This analysis is based on the 2005 data. It leads to a nomination of the best performing linear regression model to be used for selecting the best method of methodology type 3. Next to this, the linear regression model used on 2004 data (Horálek et al., 2007) is nominated for further comparison as well. The model selected could be the same for 2004 and 2005 data, if possible. Also, both the linear regression models of methodology type 2 (using EMEP model output only) and methodology type 4 (using LOTOS-EUROS model output only) are included in the comparison for reasons given in chapter 1. The nominated linear regression models are examined and compared with statistical indicators. The goal is to rank and select the best fitting linear regression model from the group of methods belonging to methodologies 2, 3 and 4. A good performing regressions model as part of a whole interpolation mapping methodology directs the selection of the best or preferred method for mapping. However, the subsequent interpolation of the regression residuals plays the major role in the ultimate selection of the best or preferred interpolation mapping method.

The second subsection describes the comparison of these subsequent residual interpolations by means of cross-validation and statistical indicators, including the interpolation methodology type 1, using the monitoring data only as well. The main comparison criterion is RMSE, followed by MAE, MPE, MedAE and other indicators. RMSE, SDE, MAE, MedAE and MPSE should be as small as possible, see Annex 6 for a further description. MPE, minimum error and maximum error should be as near to zero as possible. The SDE is not included in the comparison tables since it is almost equal to the RMSE; inherent to the fact that at all cases the MPE (being part of SDE equation) is close to zero. The R^2 should be as close to 1 as possible. All the statistical indicators, with exception of R^2 , are expressed in the same unit as the interpolated parameter (generally $\mu\text{g}\cdot\text{m}^{-3}$; for AOT40 in $(\mu\text{g}\cdot\text{m}^{-3})\cdot\text{h}$ and for SOMO35 in $(\mu\text{g}\cdot\text{m}^{-3})\cdot\text{day}$). The method selected on basis of these criteria as being or preferred is used to create interpolation maps for each indicator.

The third section is to examine the level of uncertainties in the ultimately selected interpolation mapping method of the air pollution indicator throughout Europe, especially for areas without measurement stations. Firstly, differences in the concentration maps resulting from the preferred method with those of the other interpolation methods are compared and briefly discussed.

Cross-validation analysis evaluates by RMSE the absolute and relative mean uncertainty of the map based on the selected interpolation method and the linear regression of the cross-validation scatter plots for provides insight in the over- or under-estimation of the predicted values compared to the measured values of each indicator. The level of the smoothing effect of the interpolation is demonstrated by the parameters of linear regression $y = a \cdot x + c$: a high intercept c means overestimated predicted values at low air pollution indicator measurements, and a low slope a means underestimation of the predicted values at high measurement values. The R^2 indicates the level of correlation of the predicted values of the interpolation method with the measurement values: The closer R^2 is to 1, the better the correlation.

Alternatively to the cross-validation approach, a simple comparison between the measured and interpolated values in the points of measurement is made, using scatter plots (resp. the parameters of the fitted regression line, i.e. R^2 , slope a and intercept c). This comparison of measured and interpolated values shows the uncertainty at the stations locations (points) itself, while the cross-

validation simulates the behaviour of the interpolation at locations and areas without measurement. The uncertainty at measurement locations is caused partly by the smoothing effect of interpolation and partly by the spatial averaging of the values in 10x10 km grid.

Additionally to the concentration maps, the uncertainty maps are constructed representing the maps of the predicted standard error of estimation. Based on concentration and uncertainty maps, the maps of probability of the limit value exceedance are constructed.

The same procedures as described above are followed for the ozone, SO₂ and NO_x indicators. For particulate matter rural, urban and combined maps are constructed for the annual mean and the 36th highest daily mean. The available PM_{2.5} data is insufficient for preparing PM_{2.5} maps, see Annex 7.

A2.1 Rural maps

A2.1.1 Linear regression analysis

In Horálek et al. (2007) the linear regression model selected for rural PM₁₀ mapping of 2004 data was for both indicators the model using, apart from air pollution modelling output data, the supplementary parameters altitude, wind speed, surface solar radiation (coded below as P.Eawr).

With the 2005 data, the selection of supplementary data parameters considered in the stepwise regression with backward elimination are altitude, meteorological parameters (i.e. wind speed, surface solar radiation, temperature, relative humidity, surface pressure) and EMEP model output. The selected parameters, apart from EMEP model output, best fitting the regression model are altitude, relative humidity and temperature (coded as P.Eaht). The models using EMEP and LOTOS-EUROS modelling output only (coded P.E resp. P.L) are examined as well.

Thus, the following linear regression models to be examined are:

Submodel	Input parameters
P.E	EMEP model output
P.Eaht	EMEP model output, altitude, relative humidity, temperature
P.Eawr	EMEP model output, altitude, wind speed, surface solar radiation
P.L	LOTOS-EUROS model output

The statistical performance of these four different linear regression models is presented in Table A2.1 for both indicators.

Table A2.1 Statistical indicator values of the selected linear regression models indicating the correlation between supplementary data and the annual average and 36th daily maximum mean of the 2005 measurement PM₁₀ concentrations in the rural areas.

Indicator	PM10 annual average, 2005				PM10 max. 36th daily mean, 2005			
	R ²	adjusted R ²	st. error [µg.m ⁻³]	RMSE [µg.m ⁻³]	R ²	adjusted R ²	st. error [µg.m ⁻³]	RMSE [µg.m ⁻³]
P.E	0.111	0.107	7.512	7.477	0.152	0.148	13.318	13.255
P.Eaht	0.306	0.292	6.687	6.608	0.341	0.329	11.822	11.683
P.Eawr	0.289	0.276	6.764	6.685	0.304	0.291	12.150	12.007
P.L	0.164	0.160	7.285	7.251	0.164	0.160	7.285	7.251

Table A2.1 shows the results for the PM₁₀ annual average concentration. The values of R² and RMSE for the models of the methodology type 2 (i.e. P.E) and 3 (P.Eaht and P.Eawr) show quite clearly that the addition of supplementary parameters substantially improves the closeness of the regression relation by an increased R² of about 0.2 and a decreased RMSE by approximately 0.8µg.m⁻³, i.e. one tenth. Similarly, the R² and RMSE for the models of types 2 (P.E) and 4 (P.L) indicate that the closeness of regression is higher when the LOTOS-EUROS modelled concentration field is used, instead of the EMEP modelled field.

The results in the table for the 36th maximum daily average PM₁₀ value are quite similar to those of the annual average. The addition of supplementary parameters substantially improves the closeness of the regression relation by an increased R² of 0.19 and a decreased RMSE of about one ninth. The closeness of the regression improves when output from the LOTOS-EUROS model is used, instead of EMEP model output.

Conclusions:

- At both indicators the addition of supplementary parameters substantially improves the closeness of the linear regression relation with the indicator values of the PM₁₀ measurements.
- At both indicators the closeness of the linear regression is higher when using the LOTOS-EUROS modelled concentration field instead of the EMEP modelled field.

However, these conclusions do not determine which method of methodology type 2, 3 and 4 (methods with or without supplementary data next to modelling data) would be best or preferred for the interpolation mapping method. They do indicate that the methods using linear regressions most likely will perform better by including additional supplementary parameter next to modelling data.

A2.1.2 Spatial interpolation

As explained in Section 2.1, from the four methodological types we examined several promising interpolation methods on their performance by comparing the RMSE and other statistical indicators from cross-validation:

1. Interpolation using primarily monitoring data

- a. Ordinary kriging (OK)
- b. Lognormal kriging (LK)
- c. Ordinary cokriging (OC)
- d. Lognormal cokriging (LC)

2. Interpolation using monitoring data and EMEP modelling data

Linear regression using EMEP model output (P.E), followed by interpolation of its residuals using OK.

3. Interpolation using monitoring data, EMEP model data and other supplementary data

Linear regression model using EMEP model output, altitude, relative humidity and temperature (P.Eaht), followed by interpolation of its residuals using OK

Linear regression model using EMEP model output, altitude, relative humidity and temperature (P.Eawr), followed by interpolation of its residuals using OK

4. Interpolation using monitoring data and LOTOS-EUROS modelling data

Linear regression using LOTOS-EUROS model output (P.L) plus interpolation of its residuals using OK.

The statistical indicators of the cross-validation of the methods are presented in Table A2.2 for the annual averages and in Table A2.3 for the 36th maximum daily averages. In the same tables the resulting linear regression equations and correlation coefficient R² from the cross-validation scatter plots with the measurements on the *x* axis, and the predicted values on the *y* axis are also presented.

Table A2.2 Comparison of different interpolation methods showing RMSE and the other statistics and linear regression parameters from the cross-validation scatter plots of the predicted values for the PM₁₀ annual averages for 2005 in rural areas. Apart from R² and a, all statistical indicators are in µg.m⁻³.

mapping method		annual average PM ₁₀ [µg.m ⁻³]									
		RMSE	MPE	min. error	max. error	MAE	MedAE	MPSE	linear regr. y = a.x + c		
									a	c	R ²
1-a	interp. OK	6.44	0.45	-23.26	20.57	4.72	3.50	6.67	0.365	13.97	0.344
1-b	interp. LK	6.45	0.47	-25.94	18.61	4.74	3.54	6.61	0.356	14.20	0.342
1-c	interp. OC	5.53	0.43	-21.36	14.76	4.03	2.94	5.93	0.468	11.76	0.522
1-d	interp. LC	5.45	0.12	-23.64	13.87	3.88	2.64	4.95	0.461	11.61	0.541
2-P.E-a	lin. regr. P.E + OK	6.15	0.20	-21.54	22.16	4.48	3.34	6.77	0.398	13.04	0.400
3-P.Eaht-a	lin. r. P.Eaht + OK	5.64	0.07	-26.04	24.04	3.92	2.76	5.67	0.535	9.98	0.498
3-P.Eawr-a	lin. r. P.Eawr + OK	5.52	0.13	-19.24	25.34	3.98	2.83	5.67	0.539	9.95	0.517
4-P.L-a	lin. regr. P.L + OK	5.87	0.15	-20.81	21.15	4.25	3.37	6.34	0.437	12.14	0.454

Table A2.3 Comparison of different interpolation methods showing RMSE and the other statistics and linear regression parameters from the cross-validation scatter plots of the predicted values for the PM₁₀ indicator 36th maximum daily averages for 2005 in rural areas. Apart from R² and a, all other statistical indicators are in µg.m⁻³.

mapping method		36 th maximum daily average PM ₁₀ [µg.m ⁻³]									
		RMSE	MPE	min. error	max. error	MAE	MedAE	MPSE	linear regr. y = a.x + c		
									a	c	R ²
1-a	interp. OK	11.03	0.93	10.99	-50.30	32.67	8.05	6.06	0.442	21.52	0.418
1-b	interp. LK	10.97	0.79	10.94	-51.19	29.54	7.99	6.04	0.428	21.92	0.422
1-c	interp. OC	10.18	0.92	10.14	-48.31	26.98	7.50	5.56	0.465	20.66	0.508
1-d	interp. LC	9.86	-0.12	9.86	-49.73	23.43	7.04	4.82	0.462	19.76	0.543
2-P.E-a	lin. regr. P.E + OK	10.36	0.40	10.35	-48.35	34.26	7.40	5.21	0.489	19.27	0.483
3-P.Eaht-a	lin. r. P.Eaht + OK	9.86	0.08	9.86	-45.46	34.94	6.86	5.08	0.585	15.41	0.535
3-P.Eawr-a	lin. r. P.Eawr + OK	9.70	0.16	9.70	-46.48	38.21	6.93	5.35	0.584	15.53	0.548
4-P.L-a	lin. regr. P.L + OK	10.1594	0.47	10.149	-47.81	33.42	7.32	5.38	0.495	19.12	0.503

A number of comparison conclusions can be drawn from the results provided in Tables A2.2 and A2.3 for the rural areas:

- When ranking of the statistics on their performance at both indicators, the best results for methods of methodology type 1, interpolation with monitoring data only, are obtained by lognormal cokriging, method 1-d. This confirms the results from Horálek et al. (2007).
- When ranking of the statistics RMSE (and also SDE and R²) at both indicators, the best results for methods of type 3, linear regression followed by interpolation of its residuals, are obtained by ordinary kriging of the residuals of the linear regression model P.Eawr, which uses EMEP model output, altitude, solar radiation and wind speed (method 3-P.Eawr-a). The same was concluded in Horálek et al. (2007) on the 2004 data. This confirms the suitability of these parameters for interpolation purposes.
- The comparison of the method of the types 2 and 4 (i.e. use of EMEP or LOTOS-EUROS model) shows slightly better results for the type 4 (i.e. use of LOTOS-EUROS), based on RMSE (and also SDE, MAE and R²). However, the difference is 2-5 % and the performance of both models is similar.
- The comparison of the method of the types 2 and 3 shows better results for the type 3 (i.e. including other supplementary parameter), based on RMSE (and also MPE, SDE, MAE, R² and MPSE). The addition of supplementary parameters improves the interpolation, which confirms the findings of Horálek et al. (2007) on 2004 data.

- The comparison of the scatter plots of the methods of type 1 and 3 shows that the method of type 3 (3-P.Eawr-a) gives at both indicators better results for slope (highest), i.e. it is expected this method will show the smaller underestimations for high values in areas with no measurements. Its intercept at both indicators is smallest, i.e. expected is the method will show the smallest overestimations of predicted values at low values in areas without measurements. Method 3-P.Eawr shows just a bit higher R^2 values than method 1-d, meaning method 3-P.Eawr provides also the best correlation with the measured values and expectedly the best representation of predicted for areas without measurements.
- An inter-comparison of the methods of the types 1, 2 and 3 shows that the best results for 2005 data are given by method 1-d (lognormal cokriging on monitoring data only) and 3-P.Eawr-a (linear regression model using the EMEP model output, altitude, wind speed and surface solar radiation, P.Eawr, followed by ordinary kriging of its residuals). Method 1-d gives slightly better results for the case of annual average, whereas method 3-P.Eawr-a does for the 36th maximum daily average.
- As observed with the 2004 data (Horálek et al., 2007), good results of lognormal cokriging are obtained with the 2005 data again, even though it is no more than an interpolation of measured data only. This can be explained by the fact that this method uses logarithmic transformation which corresponds to a logarithmic-normal distribution of PM_{10} . For future applications it is still recommended to examine methods that enable logarithmic transformation of PM_{10} values and the use of supplementary parameters.

The conclusions on the linear regression and interpolation analysis confirm method 3-P.Eawr-a (linear regression model using EMEP model output, altitude, wind speed and surface solar radiation, followed by interpolation of its residuals by ordinary kriging) on the 2005 data as the preferred method for PM_{10} rural mapping for both indicators. It is the same as used for the 2004 mapping in Horálek et al. (2007) and as such an additional motivation for its continued use. Even though for the annual average method 1-d performs slightly better (same as with the 2004 data), method 3-P.Eawr-a is preferred for its European coverage with its supplementary data of areas without measurements.

The resulting rural maps for the annual mean PM_{10} concentrations and 36th maximum daily average PM_{10} using the selected interpolation method 3-P.Eawr-a are shown in Figure A2.1, values of the key parameters (see Annex 6 for variogram definitions) used for mapping are given in Table A2.4.

Table A2.4 Parameters of the linear regression model and variogram of method 3-P.Eawr-a used for final mapping of PM_{10} indicators annual average (left) and 36th maximum daily mean (right) for 2005 in the rural areas, i.e. linear regression model P.Eawr following by the interpolation on its residuals using ordinary kriging (OK).

linear regr. model P.Eawr + OK on its residuals	annual average	36 th max. d. m.
	coeff.	coeff.
c (constant)	15.0	19.2
a1 (EMEP model 2005)	1.02	1.11
a2 (altitude GTOPO)	-0.0098	-0.0118
a3 (wind speed 2005)	-2.76	-5.39
a4 (s. solar radiation 2005)	0.80	1.49
nugget	20	55
sill	40	135
range [km]	250	250

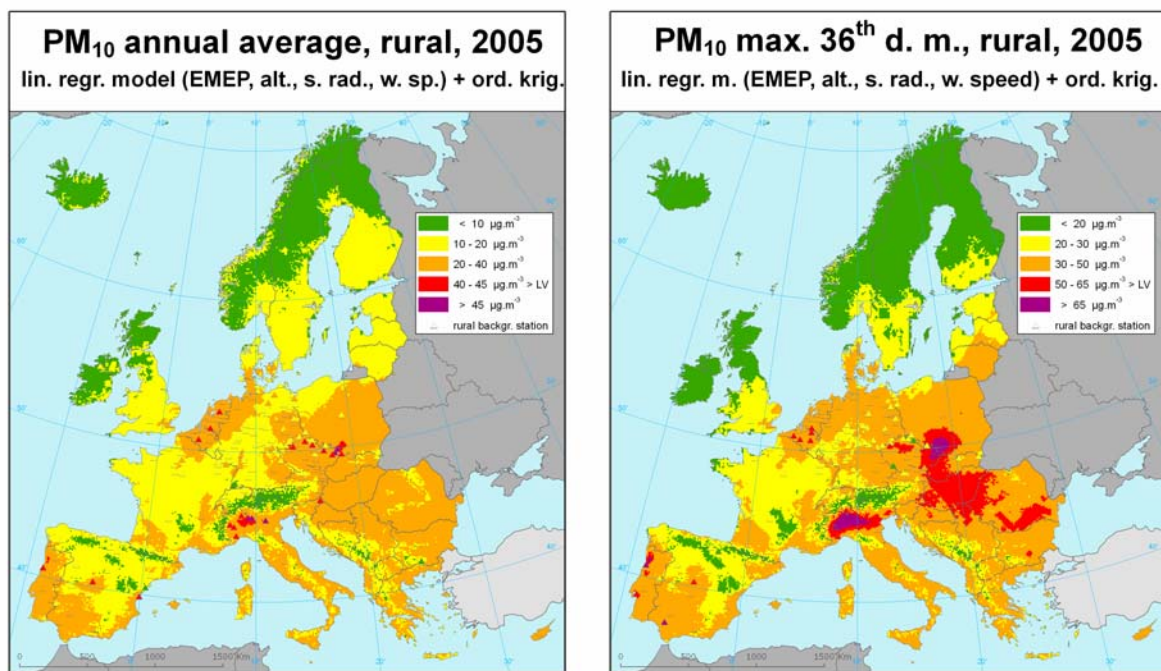


Figure A2.1 Maps showing the PM_{10} indicators annual average (left) and 36th maximum daily mean (right), in $\mu\text{g}\cdot\text{m}^{-3}$ on the European scale for rural areas in 2005, 10 x 10 km grid resolution, as a result of the linear regression model P.Eawr and ordinary kriging of its residuals. Absolute and relative mean uncertainty of these maps expressed by RMSE is $5.5 \mu\text{g}\cdot\text{m}^{-3}$ and 25.9 % (left), and $9.7 \mu\text{g}\cdot\text{m}^{-3}$ and 26.3 % (right).

A2.1.3 Uncertainty analysis

Comparing concentration maps of the interpolation methods

The interpolated maps of rural PM_{10} based on the preferred method 3-P.Eawr-a as well as methods 1-d, 2P.E-a and 4P.L-a are shown in Figure A2.2 for the annual average and Figure A2.3 for the 36th maximum daily averages. In Figures A2.4 and A2.5 the differences between the selected method 3-P.Eawr-a and the other methods are shown. The maps based on the preferred method 3P.Eawr-a clearly show the impact of using altitude in the regression: lower levels are seen in the Alps and Pyrenees. The largest differences between method 1-d at one hand and the other three at the other hand are the concentrations in the north-west part of Europe: concentrations in UK, Ireland and Scandinavia are higher estimated by method 1-d than by the other. The overestimation of PM_{10} in these areas by method 1-d, i.e. the method using measurement data only, is caused by the lack of stations in these areas.

Figure A2.6 illustrates for both indicators the differences between method 2-P.E-a (EMEP) and the corresponding method 4-P.L-a (LOTOS-EUROS). The annual mean pattern in the methods is very similar: EMEP shows only slightly lower concentration in Scandinavia. In the 36th maximum daily averages maps the EMEP model tends to give higher values in south and east Europe.

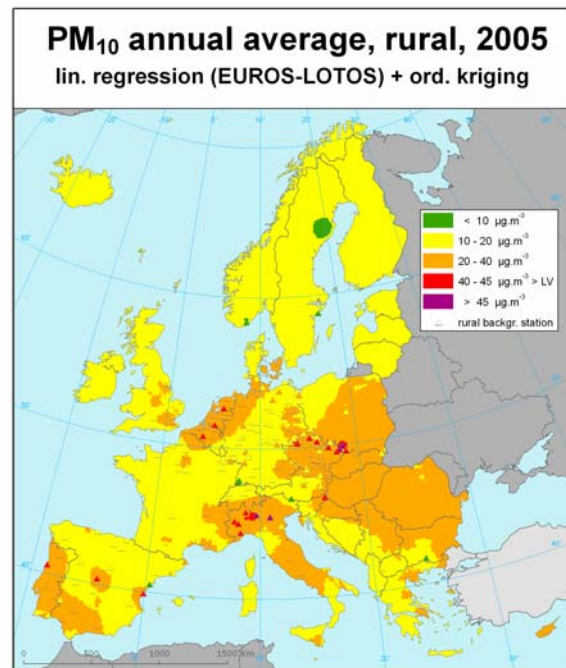
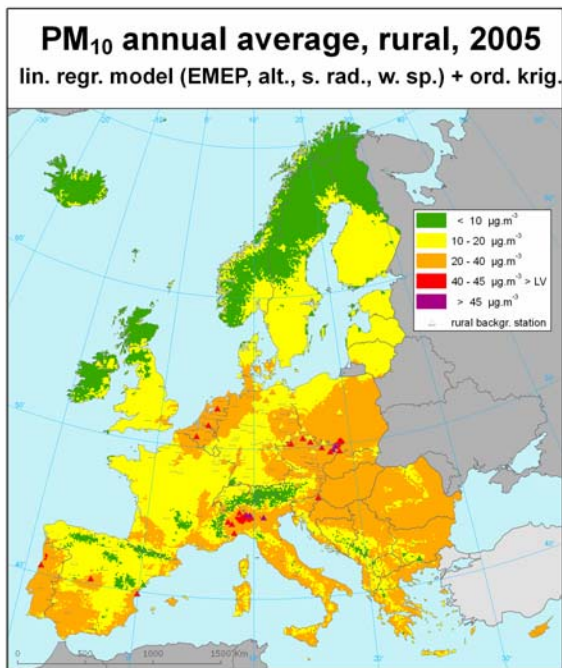
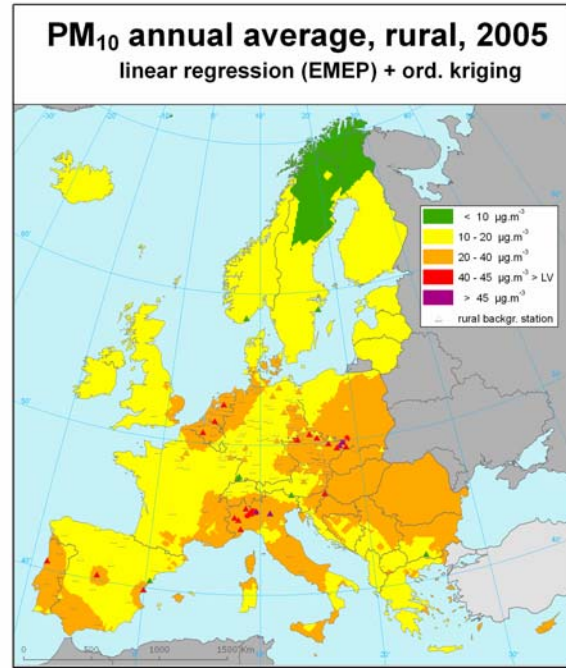
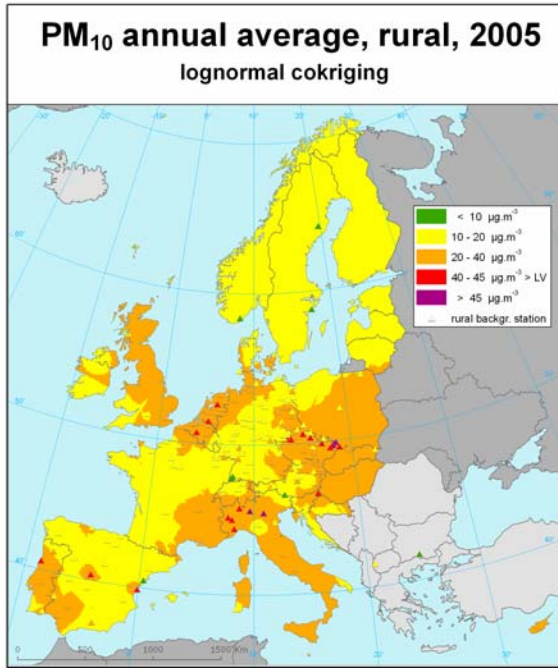


Figure A2.2 Maps showing the annual average PM₁₀ concentration (in $\mu\text{g}\cdot\text{m}^{-3}$) on the European scale for rural areas in 2005, 10 x 10 km grid resolution, as a result of the interpolation methods 1-d (top left), 2P.E-a (top right), 3P.Eawr-a (bottom left) and 4P.L-a (bottom right).

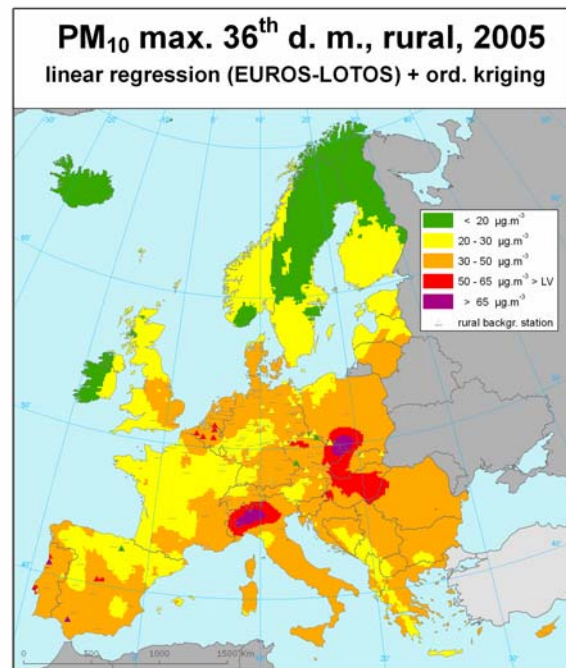
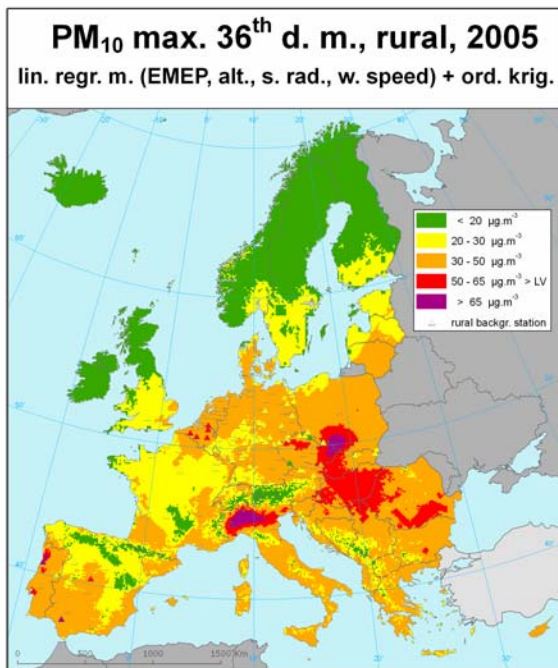
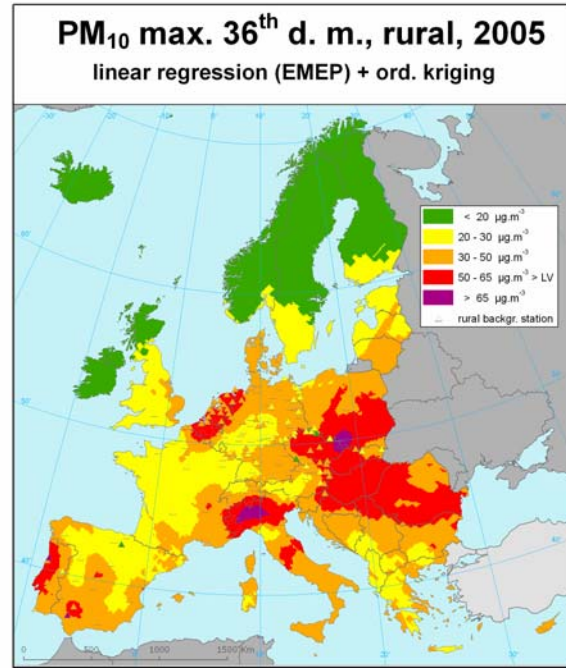
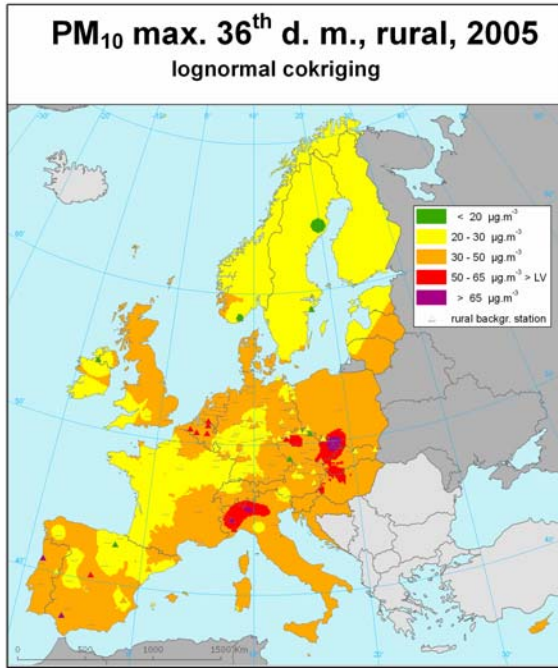


Figure A2.3 Maps showing 36th maximum daily mean PM₁₀ concentration (in $\mu\text{g}\cdot\text{m}^{-3}$) on the European scale for rural areas in 2005, 10 x 10 km grid resolution, as a result of the interpolation methods 1-d (top left), 2P.E-a (top right), 3P.Eawr-a (bottom left) and 4P.L-a (bottom right).

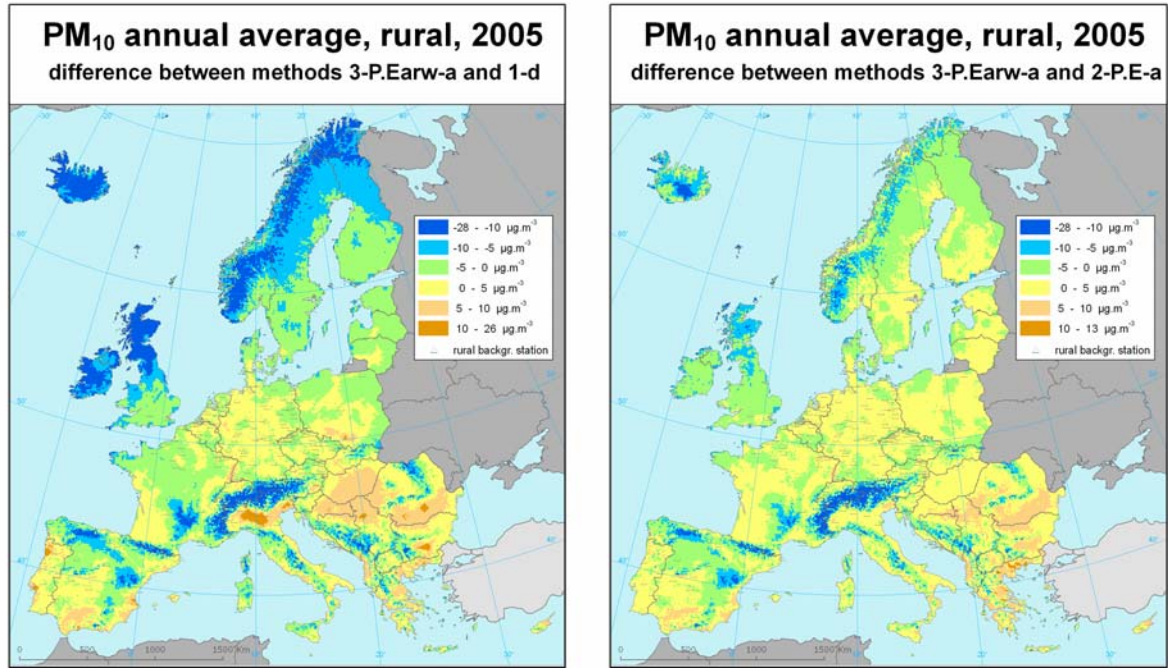


Figure A2.4 Maps showing the difference of the selected method 3-P.Earw-a and the method 1-d (left), resp. 2-P.E-a (right) for annual average PM₁₀ concentration (in $\mu\text{g.m}^{-3}$) on the European scale for rural areas in 2005, 10 x 10 km grid resolution. Negative values show up at areas with higher concentrations of the alternative method (1-d left, 2-P.E-a right) compared to the preferred method 3-P.Earw-a.

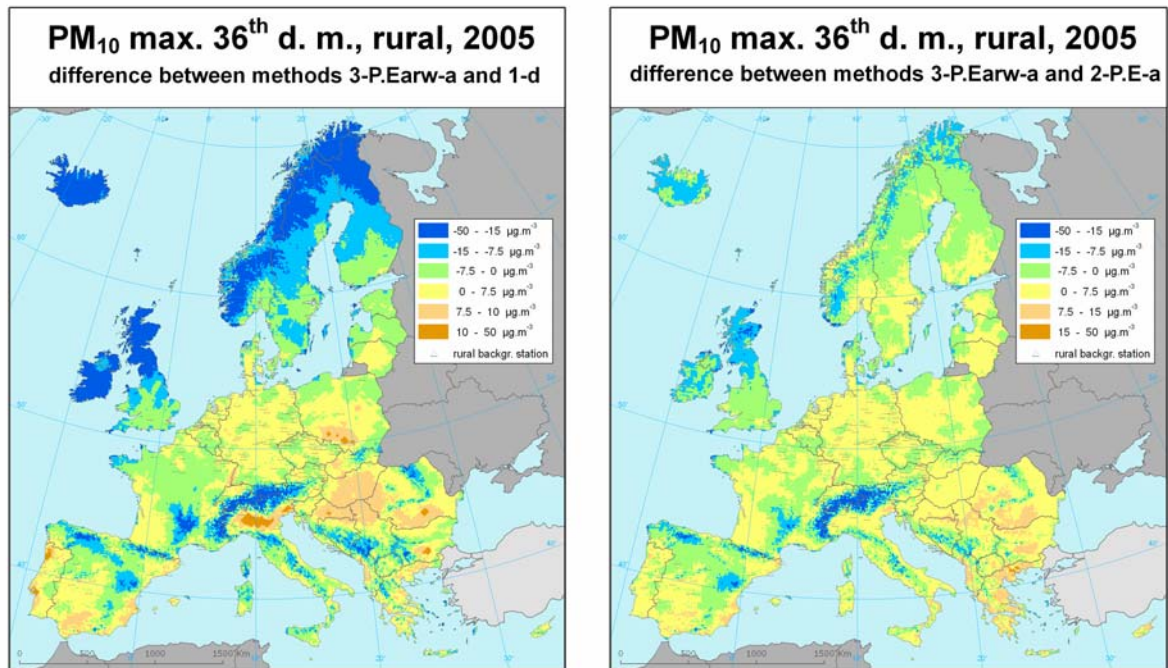


Figure A2.5 Maps showing the difference of the selected method 3-P.Earw-a and the method 1-d (left), resp. 2-P.E-a (right) for PM₁₀ indicator 36th maximum daily value (in $\mu\text{g.m}^{-3}$) on the European scale for rural areas in 2005, 10 x 10 km grid resolution. Negative values show up at areas with higher concentrations of the alternative method (1-d left, 2-P.E-a right) compared to the preferred method 3-P.Earw-a.

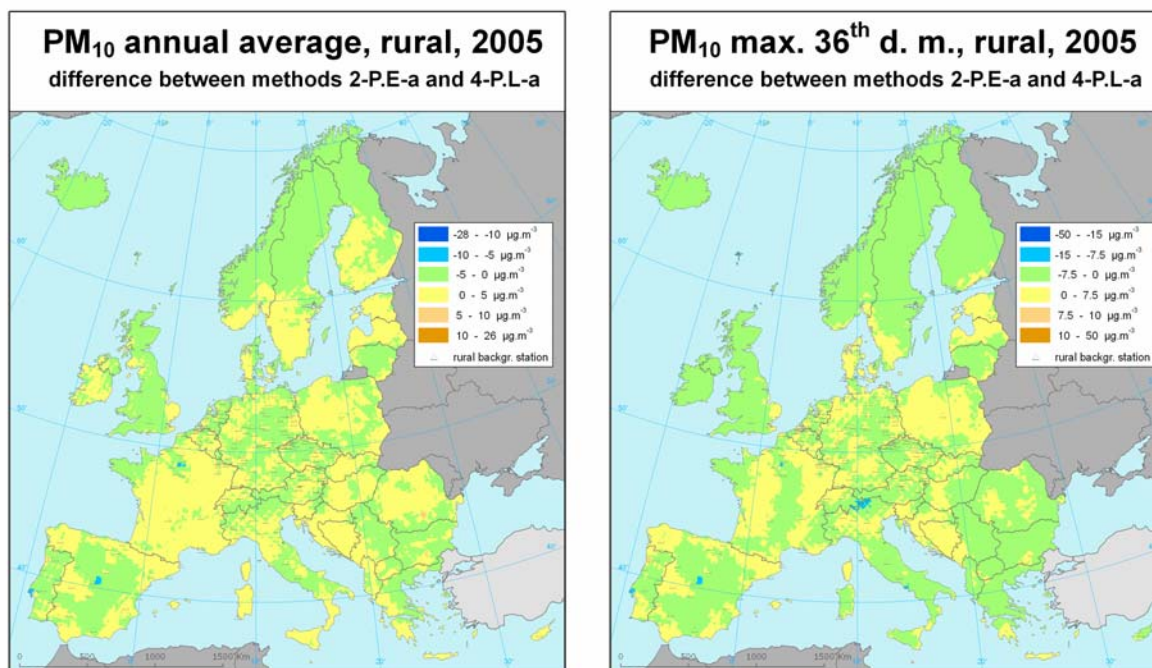


Figure A2.6 Maps showing the difference between the methods using output from the EMEP model (2-P.E-a) and from the LOTOS-EUROS model (4-P.L-a) for PM₁₀ annual average (left) and 36th maximum daily value (right) in $\mu\text{g.m}^{-3}$ on the European scale for rural areas in 2005, 10 x 10 km grid resolution. Negative values show higher concentrations of method 4-P.L-a.

Uncertainty estimated by cross-validation

For the preferred method a more in-depth uncertainty analysis has been made. The basic uncertainty analysis is given by cross-validation. Using RMSE as the most common indicator, the absolute mean uncertainty of the maps in positions without measurement within the areas covered by measurements - i.e. excluding areas lacking monitoring stations such as the Balkan - can be expressed in $\mu\text{g.m}^{-3}$ (see Tables A2.2. and A2.3). The absolute mean uncertainty for method 3-P.Eawr-a of the map of PM₁₀ annual average expressed by RMSE is 5.5 $\mu\text{g.m}^{-3}$ and for 36th maximum daily mean PM₁₀ values is 9.7 $\mu\text{g.m}^{-3}$.

Alternatively, this uncertainty can be expressed as the absolute RMSE uncertainty being a percentage of the mean air pollution indicator value for all stations. The relative mean uncertainty for method 3-P.Eawr-a of the rural map of PM₁₀ annual average is 25.9% and of 36th maximum daily average PM₁₀ values is 26.3%. This uncertainty is slightly higher (of about 2.5%) than the uncertainty of 2004 maps. This relative value is quite good result in comparison with the requirement of minimum relative uncertainty at the level 50% for the modelling of PM₁₀ annual average according to the 1st DD.

Figure A2.7 shows the cross-validation scatter plot for each air pollutant indicator for the selected method 3-P.Eawr-a. The nature of cross-validation (concentration measured in the estimated point is not used for estimation) enables to evaluate the quality of the interpolation at locations without measurements but within the area covered by measurements. The level of R² indicates that about 52% (in the case of annual average), resp. 55% (in the case of 36th maximum daily mean) of the variability is estimated by the interpolation. From the scatter plot the level of underestimation in high values in the places with no measurement can be seen: e.g., the annual average value 45 $\mu\text{g.m}^{-3}$ is for such places without measurement estimated on average by the value of about 35 $\mu\text{g.m}^{-3}$ only.

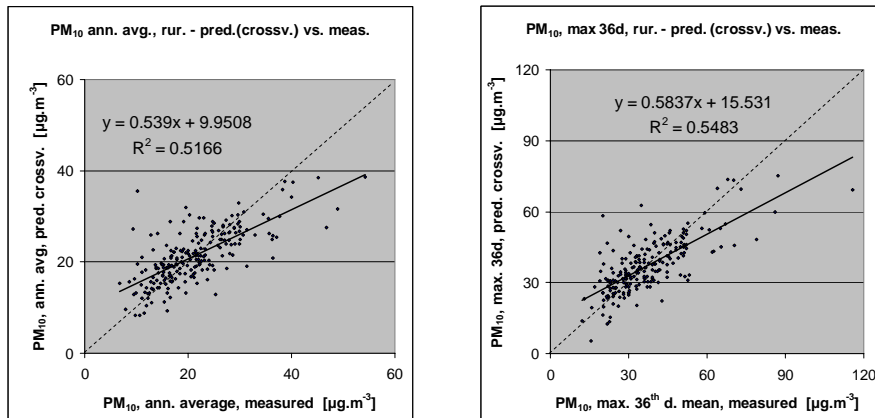


Figure A2.7 Correlation between cross-validation predicted values (y-axis) and measurements (x-axis) for the PM_{10} indicators annual average (left) and 36th maximum daily mean (right) for rural areas in 2005, as a result of the linear regression model P.Eawr and ordinary kriging of its residuals. R^2 and the slope a (from the linear regression equation $y = a \cdot x + c$) should be as close 1 as possible, the intercept c should be as close 0 as possible.

Comparing point measurement values with the predicted grid value

Additional to the cross-validation, a simple comparison between the measured and interpolated values in a 10x10 km grid has been made. By this comparison it can be seen to what extent the predicted value of the corresponding grid cell represents the measured values covered by that cell. As illustration, such simple comparison scatter plot is presented here in this paper only once as Figure A2.8.

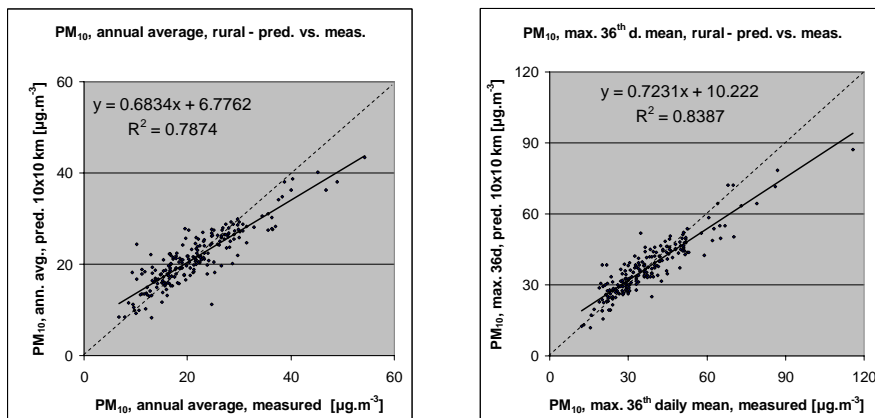


Figure A2.8 Correlation between predicted values for 10x10 grid (y-axis) and measurements (x-axis) for the PM_{10} indicators annual average (left) and 36th maximum daily mean (right) for rural areas in 2005, as a result of the linear regression P.Eawr and ordinary kriging of its residuals.

The results of the cross-validation compared to this gridded validation examination are summarised in Table A2.5. Both figure and table show a better correlated relation between measurement stations and interpolated corresponding grid values for both indicators (i.e. higher R^2 , smaller intercept and the slope closer to 1) than at the cross-validation predictions (Figure A2.7). This has its cause in the fact that the simple comparison of points measurements and gridded interpolated values shows the uncertainty at the stations locations (points) itself, while the cross-validation simulates the behaviour of the interpolation at positions without measurement within the areas covered with measurements. The uncertainty at measurement locations is caused partly by the smoothing effect of interpolation and

partly by the spatial averaging of the values in 10x10 km grid. Similar agreement with the measured data has been found in the analysis of the 2004-data (Horálek et al, 2007).

Table A2.5 Linear regression equation and coefficient of determination R^2 from the scatter plots of the predicted values based on cross-validation (above) and aggregation into 10x10 km grid (bottom) versus the measured values for PM_{10} indicators annual average (left) and 36th maximum daily mean (right) for rural areas in 2005 as a result of the linear regression model P.Earw and ordinary kriging of its residuals.

Indicator		PM ₁₀ , rural areas			
		Annual average		36th max.d.mean	
prediction		equation	R ²	equation	R ²
(i)	Cross-validated predictions	$y = 0.539x + 9.951$	0.517	$y = 0.584x + 15.531$	0.548
(ii)	10x10 km grid predictions	$y = 0.683x + 6.776$	0.787	$y = 0.723x + 10.222$	0.839

Uncertainty maps

Next to the concentration maps (Figure A2.1), the uncertainty maps are constructed (see Figure A2.9). The uncertainty presented here corresponds to the kriging standard error, which is in fact the standard deviation of the predicted values. As expected, both maps show higher uncertainty at areas with lower station density.

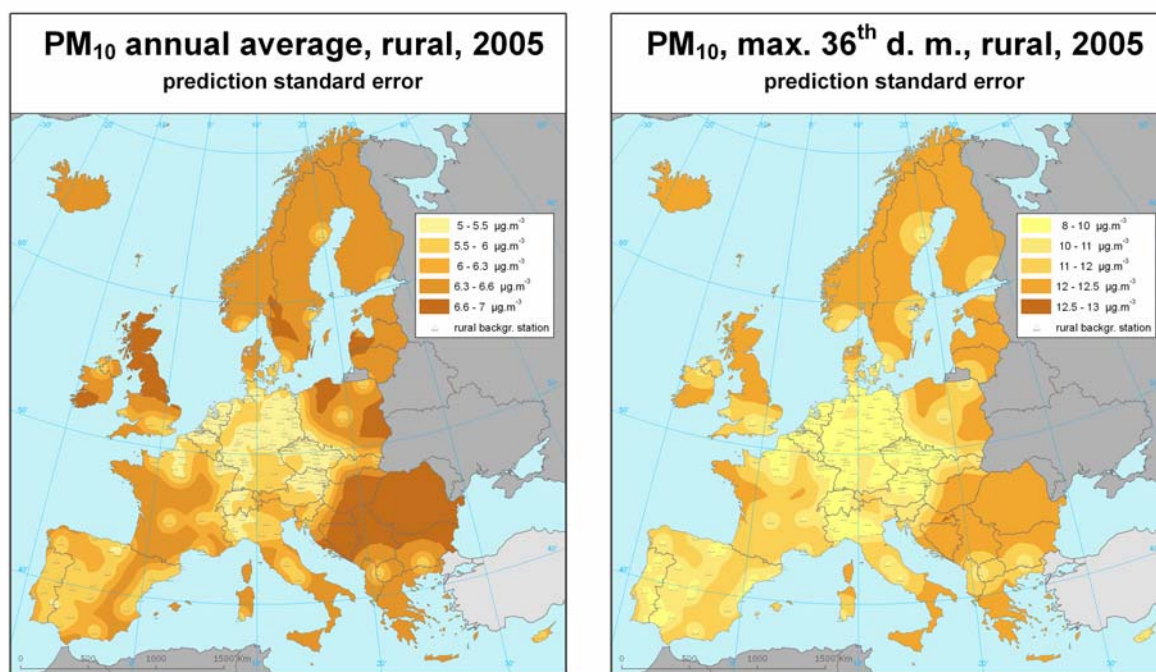


Figure A2.9 Absolute uncertainty maps for maps of PM_{10} indicators annual average (left) and 36th maximum daily mean (right), in $\mu\text{g}\cdot\text{m}^{-3}$ on the European scale for rural areas in 2005, on the 10 x 10 km grid resolution, as a result of the linear regression P.Earw and ordinary kriging of its residuals. The maps are applicable in the rural areas only.

Probability maps

Next, the maps of the probability of the limit value exceedance have been constructed, using the concentration and uncertainty maps (i.e. Figures A2.1 and A2.9) and the limit values (LV, defined in the directive as $40 \mu\text{g}\cdot\text{m}^{-3}$ for the annual average and $50 \mu\text{g}\cdot\text{m}^{-3}$ for the 36th maximum daily mean). The probability map is presented in Figure A2.10. Areas with the probability of limit value exceedance above 75% are marked in red; areas below 25% are marked in green. The red areas indicate areas for

which exceedance may occur very likely due to high concentration close to or already above LV, including such enclosed uncertainty that exceedance is likely. Or lower concentrations with such high uncertainty levels reaching above the LV that exceedance is very likely. Vice versa, in the green areas it is not very likely to have prediction values showing exceedance and/or such enclosed uncertainties that reaching above the LV not very likely.

Areas with 25-50%, resp. 50-75% probability of LV exceedance are marked in yellow and orange. The yellow colour indicates the areas with the estimated values below limit value for which there exists a reasonable chance of exceeding the limit. Contrary, the orange areas are above the limit value according to estimation, but with a chance of non exceedance caused by the uncertainty of the estimation.

Next to the estimation of the probability of the limit value exceedance, the real measured values at the stations are presented in the maps: The stations with the measured values above limit values are marked by red, whereas the stations with the measured values below the limit are marked by green. Neither orange nor yellow is applied in this case: Only the interpolation, not the measurement uncertainty is considered.

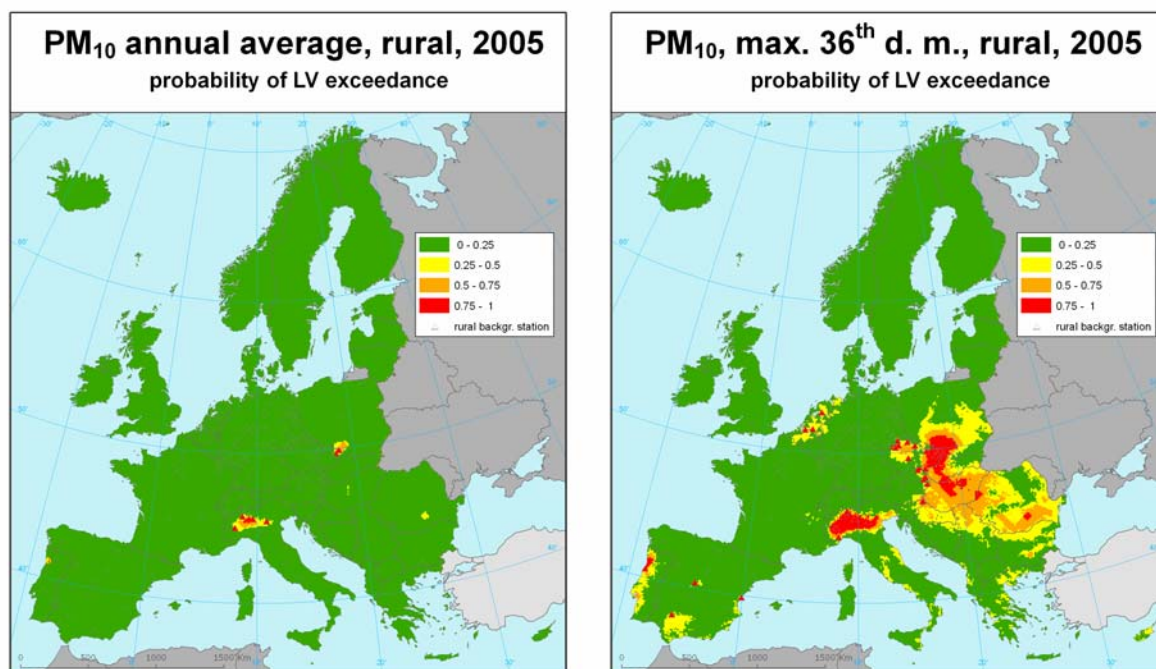


Figure A2.10 Maps with the probability of the limit value exceedance for PM_{10} indicators annual average (left) and 36th maximum daily mean (right), in $\mu g \cdot m^{-3}$ on the European scale for rural areas in 2005, on the 10×10 km grid resolution, as a result of the linear regression P.Earw and ordinary kriging of its residuals. The maps are applicable in the rural areas only.

A2.2 Urban maps

A2.2.1 Linear regression analysis

The same procedure as in Section A2.1.1 is now followed for the urban and suburban areas.

With the use of 2005 data the supplementary parameters selected are, apart from the EMEP model output: surface solar radiation, relative humidity and temperature. The models using EMEP and LOTOS-EUROS modelling output only (coded UP.E resp. UP.L) are examined as well. In Horálek et al (2007) the use of supplementary parameters were not used in the final mapping in the case of urban PM₁₀, so no other set of variables is examined.

Thus, the following linear regression models to be examined are:

Submodel	Input parameters
UP.E	EMEP model output
UP.Erht	EMEP model output, surface solar radiation, relative humidity, temperature
UP.L	LOTOS-EUROS model output

The statistical performance of these three linear regression models is presented in Table A2.6 for both indicators.

Table A2.6 Statistical indicator values of the selected linear regression models indicating the correlation between supplementary data and the annual average and 36th daily maximum mean of the 2005 measurement PM₁₀ concentrations in the urban areas.

Indicator	PM10 annual average, 2005				PM10 max. 36th daily mean, 2005			
	R ²	adjusted R ²	st. error [µg.m ⁻³]	RMSE [µg.m ⁻³]	R ²	adjusted R ²	st. error [µg.m ⁻³]	RMSE [µg.m ⁻³]
UP.E	0.059	0.058	10.23	10.22	0.066	0.063	19.63	19.63
UP.Erht	0.192	0.188	9.50	9.47	0.233	0.229	17.84	17.79
UP.L	0.045	0.044	10.31	10.29	0.011	0.010	20.22	20.19

Table A2.6 shows the results for the PM₁₀ annual average concentration. The values of R² and RMSE for the models of the methodology type 2 (i.e. UP.E) and 3 (UP.Erht) show quite clearly that the addition of supplementary parameters substantially improves the closeness of the regression relation by an increased R² of about 0.13 and a decreased RMSE by approximately 0.7, i.e. of about 7%. Similarly, the R² and RMSE for the models of type 2 (P.E) and 4 (P.L) indicate that the closeness of regression is slightly higher when the EMEP modelled concentration field is used, instead of the LOTOS-EUROS modelled field. However, at both models the correlation between the measured and modelled values is quite poor. This is most likely due to the fact that these models are not developed for the urban areas.

The table shows for the 36th maximum daily average PM₁₀ value that the results are quite similar to those of the annual average. The addition of supplementary parameters substantially improves the closeness of the regression relation by an increased R² of 0.16 and a decreased RMSE of about one tenth. The closeness of the regression improves when output from the EMEP model is used, instead of LOTOS-EUROS model output. However, the correlation between measured and modelled values in case of both models is poor as well.

Conclusions:

- At both indicators the addition of supplementary parameters substantially improves the closeness of the linear regression relation with the indicator values of the PM₁₀ measurements.

- At both indicators the closeness of the linear regression is higher when using the EMEP modelled concentration field instead of the LOTOS-EUROS modelled field.
- However, at both models the correlation between the measured and modelled values is quite poor, most likely due to the fact that both models are not developed for modelling (sub)urban areas.

These conclusions do indicate that the methods using linear regressions most likely will perform better by including additional supplementary parameter next to modelling data in the interpolation methods for (sub)urban PM₁₀ indicators, which will be compared in next section.

A2.2.2 Spatial interpolation

As explained before (introduction, Section 2.1 and A2.1.2) we compare the following interpolation methods on their performance:

1. Interpolation using primarily monitoring data

- Ordinary kriging (OK)
- Lognormal kriging (LK)

2. Interpolation using monitoring data and EMEP model data

Linear regression using EMEP model output (UP.E), followed by interpolation of its residuals using OK.

3. Interpolation using monitoring data, EMEP model data and other supplementary data

Linear regression model using EMEP model output, surface solar radiation, relative humidity, and temperature (UP.Erht), followed by interpolation of its residuals using OK

4. Interpolation using monitoring data and LOTOS-EUROS model data

Linear regression using LOTOS-EUROS model output (UP.L), followed by interpolation of its residuals using OK.

(Neither ordinary nor lognormal cokriging is included, as preliminary analysis proofed to bring no improvement for urban PM₁₀. This is likely due to the weak correlation of PM₁₀ with altitude in urban areas.)

The statistical indicators of the cross-validation of the methods are presented in Table A2.7 for the annual averages and in Table A2.8 for the 36th maximum daily averages. In the same tables the resulting linear regression equations and R² from the cross-validation scatter plots are also presented.

Table A2.7 Comparison of different interpolation methods showing RMSE and the other statistics and linear regression parameters from the cross-validation scatter plots of the predicted values for the PM₁₀ annual averages for 2005 in urban areas. Apart of R² and a, all other statistical indicators are in µg.m⁻³

mapping method		annual average PM ₁₀ [µg.m ⁻³]									
		RMSE	MPE	min. error	max. error	MAE	MedAE	MPSE	linear regr. y=a.x+c		
									a	c	R ²
1-a	interpolation OK	5.51	0.07	-36.73	26.18	3.72	2.32	4.82	0.722	7.660	0.710
1-b	interpolation LK	5.52	0.00	-36.44	26.39	3.71	2.37	4.45	0.710	7.910	0.710
2-UP.E-a	lin. regr. UP.E + OK	5.49	0.01	-36.96	26.73	3.67	2.32	4.93	0.726	7.580	0.714
3-UP.Erht-a	lin. r. m. UP.Erht + OK	5.62	-0.02	-37.29	21.05	3.81	2.50	4.65	0.726	7.460	0.701
4-UP.L-a	lin. regr. UP.L + OK	5.46	0.01	-36.61	26.62	3.65	2.34	4.93	0.722	7.590	0.716

Table A2.8 Comparison of different interpolation methods showing RMSE and the other statistics and linear regression parameters from the cross-validation scatter plots of the predicted values for the PM₁₀ indicator 36th maximum daily averages for 2005 in urban areas. Apart of R² and a, all other statistical indicators are in µg.m⁻³

mapping method		36 th maximum daily average [µg.m ⁻³]									
		RMSE	MPE	min.	max.	MAE	MedAE	MPSE	linear regr. y=a.x+c		
				error	error				a	c	R ²
1-a	interpolation OK	9.98	0.13	-77.69	37.17	6.54	3.86	8.85	0.757	11.3	0.746
1-b	interpolation LK	9.92	-0.01	-77.15	37.19	6.50	3.92	7.63	0.745	11.76	0.749
2-UP.E-a	lin. regr. UP.E + OK	9.91	0.00	-77.59	37.24	6.47	4.02	8.98	0.760	11.09	0.750
3-UP.Erht-a	lin. r. m. UP.Erht + OK	10.32	-0.14	-78.33	37.84	6.87	4.37	9.15	0.759	10.99	0.730
4-UP.L-a	lin. regr. UP.L + OK	9.90	0.06	-77.56	36.59	6.46	3.90	9.05	0.757	11.28	0.751

As indicated in Chapter, 1 inter-annual comparison would be done this in paper for the urban areas in addition to the one for rural areas in Horálek et al. (2007). Table A2.9 shows the RMSE of the cross-validation using the 2005 data for the nominated methods of the four methodology types.

Table A2.9 Comparison of different interpolation methods showing RMSE for the PM₁₀ indicators annual average and 36th maximum daily averages for the years 2004 and 2005 in urban areas. The smaller RMSE means the more accurate the estimation by the mapping method. RMSE is in µg.m⁻³.

mapping method		annual average			36 th max. daily mean		
		2004	2005	avg	2004	2005	avg
1-a	interpolation OK	5.37	5.51	5.44	9.49	9.98	9.73
1-b	interpolation LK	5.38	5.52	5.45	9.50	9.92	9.71
2-UP.E-a	lin. regr. UP.E + OK	5.34	5.49	5.42	9.64	9.91	9.77
3-UP.Erht-a	lin. r. m. UP.Erht + OK	5.40	5.62	5.51	9.54	10.32	9.93

A number of comparison conclusions can be drawn from the results provided in Tables A2.7 - A2.9 for the urban areas:

- When ranking the statistics at both indicators on the 2005 data, very similar results are obtained for the methods of type 1, interpolation with monitoring data only. This is similar to Horálek et al. (2007) on the 2004 data.
- Methods of type 2 and 4, i.e. linear regression using EMEP and LOTOS-EUROS model output respectively, show also quite similar interpolation performance at both PM₁₀ indicators.
- Comparison of the methods of type 1 and 2 shows slightly better overall performance for the method of type 2 (2-UP.E-a, i.e. linear regression without including other supplementary parameter followed by residual interpolation). Concluding, the addition of modelling data improves the interpolation performance slightly.
- The comparison of the method of the type 2 and 3 shows better results for the method of type 2 (2-UP.E-a), based on RMSE and most other statistical indicators. In conclusion: the addition of other supplementary parameters does not improve the interpolation.
- The comparison of the cross-validation scatter plots of the four methods shows quite similar results on slope *a* and intercept *c* and slightly better results for correlation coefficient for the methods of type 2 and 4 than for the other methods.
- An inter-comparison of the methods of the types 1, 2 and 3 shows that the best results for 2005 data are given by method 2-UP.E-a (linear regression model using EMEP model output, UP.E, followed by ordinary kriging of its residuals), based on RMSE, MPE, SDE, MAE and R². Like with the 2005 data, the methods of the type 1 and 2 on 2004 data are quite similar performing with a small advantage for type 1 at the 36th max. daily average.

The conclusions on the linear regression and interpolation analysis designate method 2-UP.E-a (linear regression using EMEP model output only, followed by interpolation of its residuals by ordinary kriging) on the 2005 data as the preferred method for PM₁₀ urban mapping for both indicators. Even though the methods of type 1 do perform almost as good as well on 2005 data, and at 36th max. daily average even slightly better on 2004 data, we prefer 2-UP.E-a for its considerably more complete coverage of the European continent by the EMEP model, especially at areas without measurements (e.g. northern Scandinavia).

The resulting urban maps for the annual mean PM₁₀ concentrations and 36th maximum daily average PM₁₀ using the selected interpolation method 2-UP.E-a are shown in Figure A2.11. Values of the key parameters used for mapping are given in Table A2.10.

Table A2.10 Parameters of the linear regression model and variogram of method 2-UP.E-a used for final mapping of PM₁₀ indicators annual average (left) and 36th maximum daily mean (right) for 2005 in the urban areas, i.e. linear regression model UP.E following by the interpolation on its residuals using ordinary kriging (OK).

linear regr. model P.E + OK on its residuals	annual average	36 th max. daily mean
	coeff.	coeff.
c (constant)	19.0	28.2
a1 (EMEP model 2005)	0.82	0.85
nugget	15	45
sill	65	255
range [km]	390	390

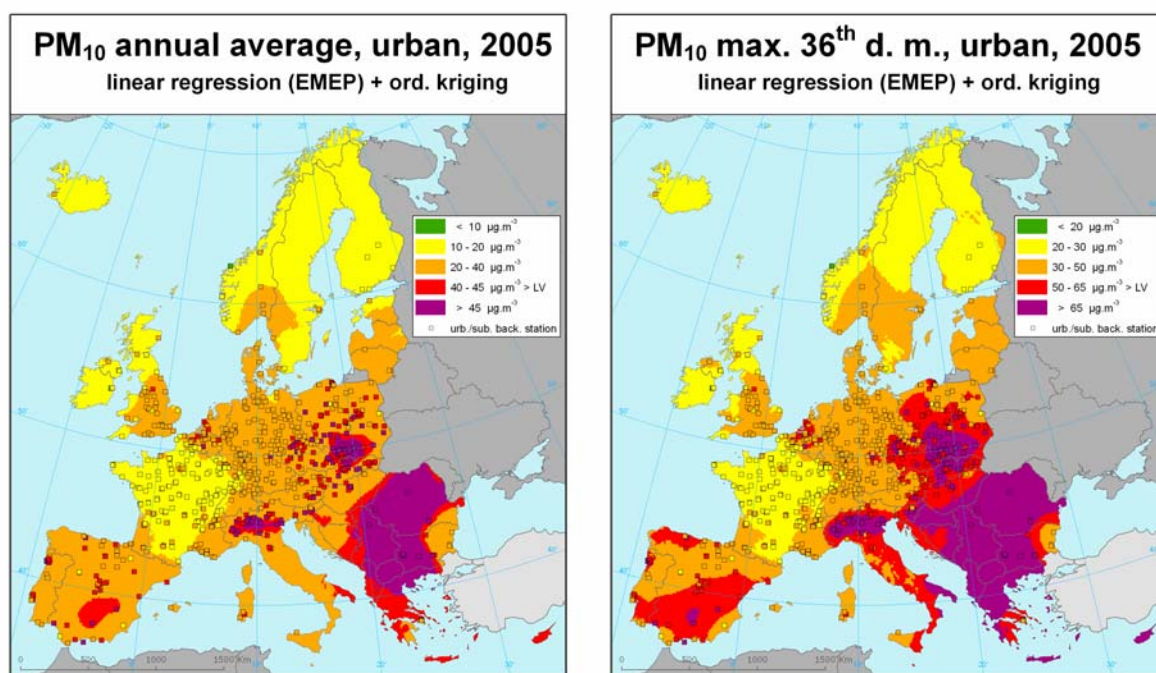


Figure A2.11 Maps showing PM₁₀ indicators annual average (left) and 36th maximum daily mean (right), in $\mu\text{g}\cdot\text{m}^{-3}$ on the European scale for urban areas in 2005, 10 x 10 km grid resolution, as a result of the linear regression UP.E and ordinary kriging of its residuals. Absolute and relative mean uncertainty of these maps expressed by RMSE is $5.5 \mu\text{g}\cdot\text{m}^{-3}$ and 20.0 % (left), and $9.9 \mu\text{g}\cdot\text{m}^{-3}$ and 21.4 % (right). The maps are applicable in the urban areas only. (The reduced concentrations in France compared to its surrounding areas may have its cause in the PM₁₀ correction factors France applied on the measurements of the French monitoring network.)

A2.2.3 Uncertainty analysis

Comparing concentration maps of the interpolation methods

The interpolated maps of urban PM_{10} based on the preferred method 2-UP.E-a as well as methods 1-a, 2UP.Erht-a and 4P.L-a are shown in Figure A2.12 for the annual average and Figure A2.13 for the 36th maximum daily averages. In Figures A2.14 and A2.15 the differences between the selected method 3-P.Eawr-a and the other methods are shown. The urban maps show relative small differences between the individual methods in comparison to what we see at the rural maps in Section A2.1.3. This can be explained by the higher density of the urban monitoring stations throughout the mapping domain. (The lower values in France compared to those in surrounding countries may have its cause in the different approach the French apply the correction factors on PM_{10} measurements of their monitoring networks. Expected is that in future this difference will resolve due to the French intention to adapt their correction procedure.)

Compared to the other maps, the map of method 3-UP.Erht-a shows increased concentrations at mountainous areas such as in Spain and the Alps. This becomes especially clear in the difference maps of Figures A2.14 and A2.15. 3-UP.Erht-a is the only method using meteorological parameters, which may explain the cause of these increased values.

The resulting urban maps obtained by the methods 2-UP.E-a and 4-UP.L-a (i.e. using EMEP and LOTOS-EUROS models) are almost the same, as can be seen in the difference maps of Figure A2.16.

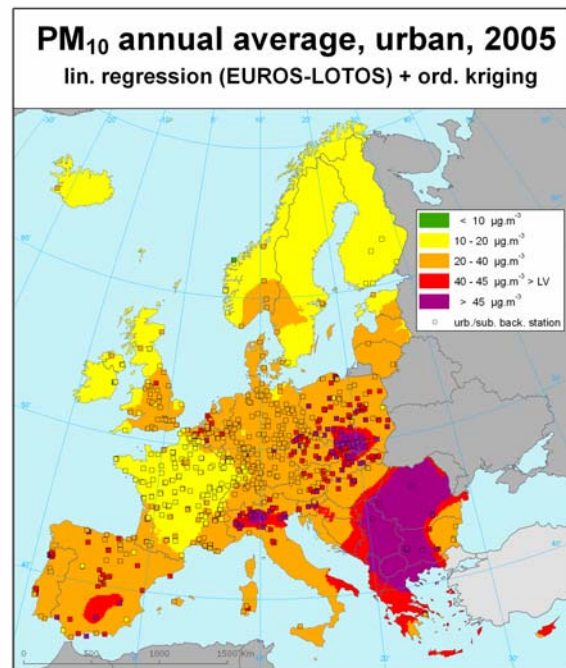
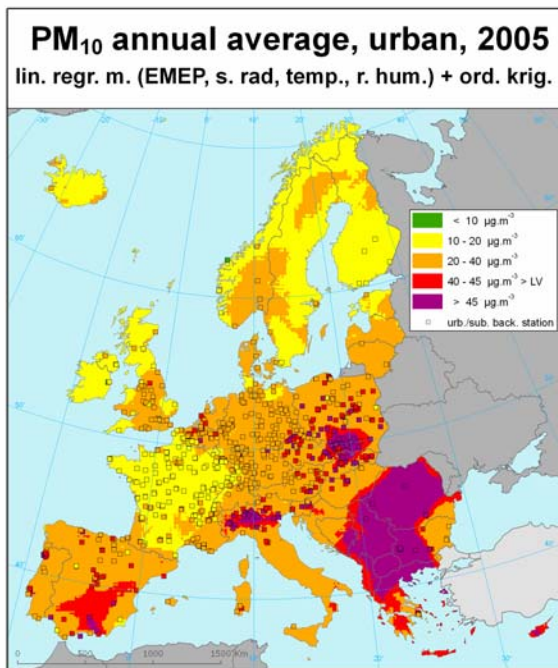
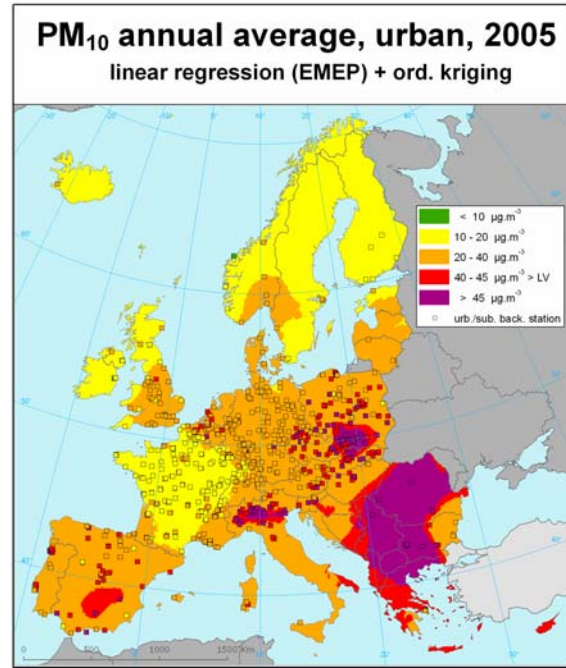
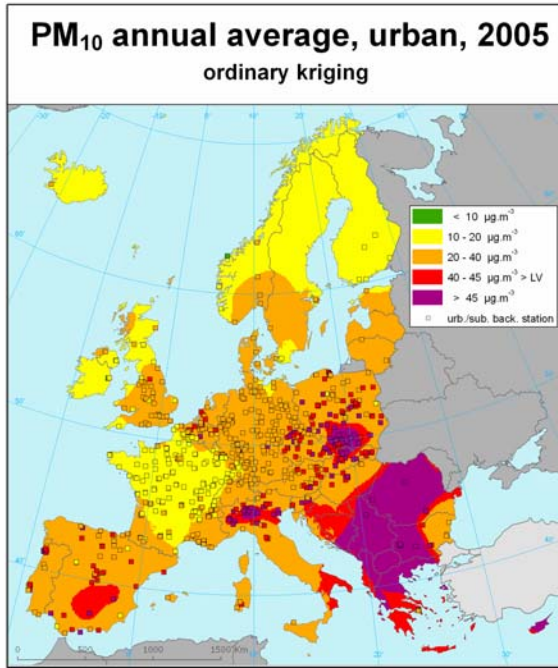


Figure A2.12 Maps showing the annual average PM₁₀ concentration (in $\mu\text{g}\cdot\text{m}^{-3}$) on the European scale for urban areas in 2005, 10 x 10 km grid resolution, as a result of the interpolation methods 1-a (top left), 2-UP.E-a (top right), 3-UP.Erht-a (bottom left) and 4-UP.L-a (bottom right). The maps are applicable in the urban areas only.

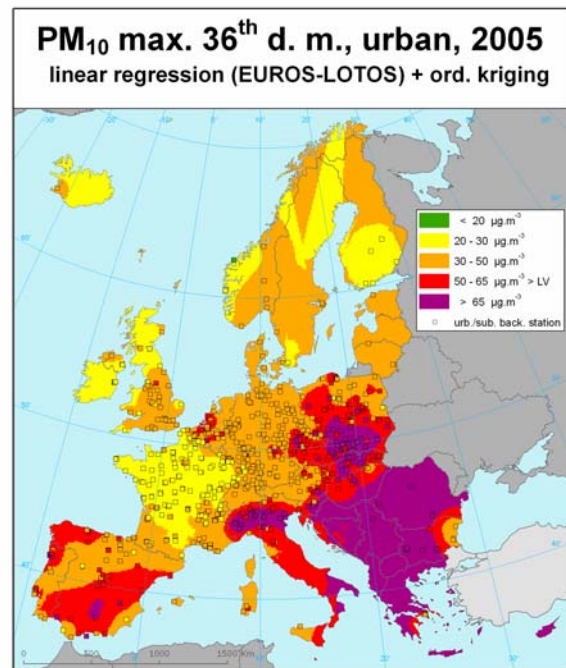
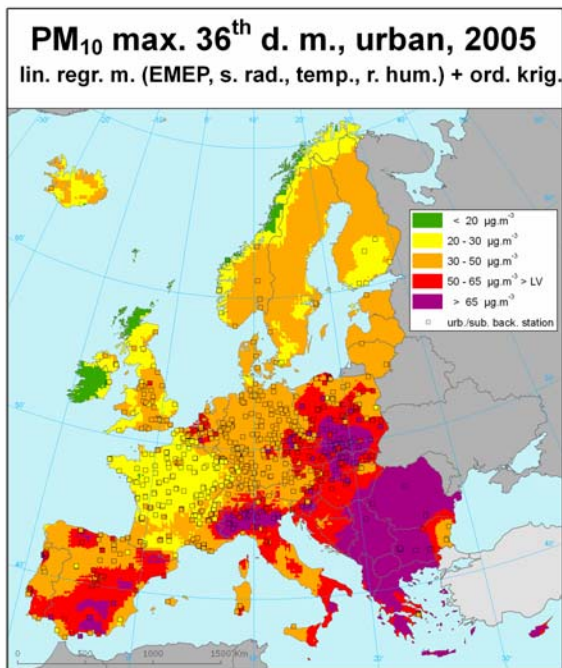
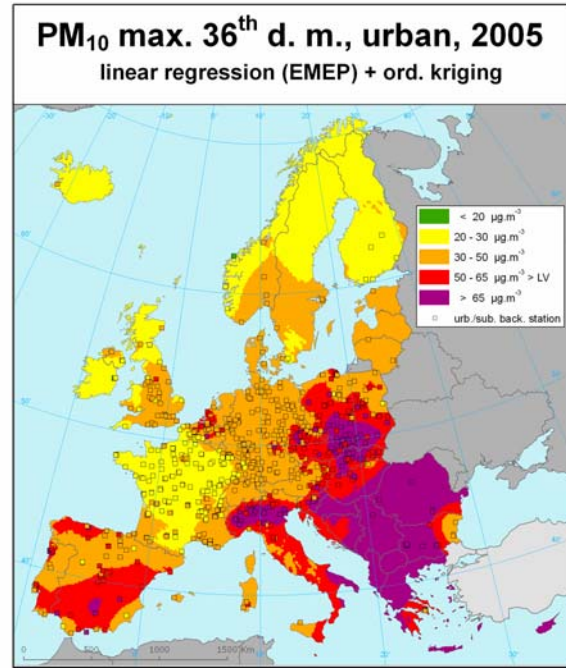
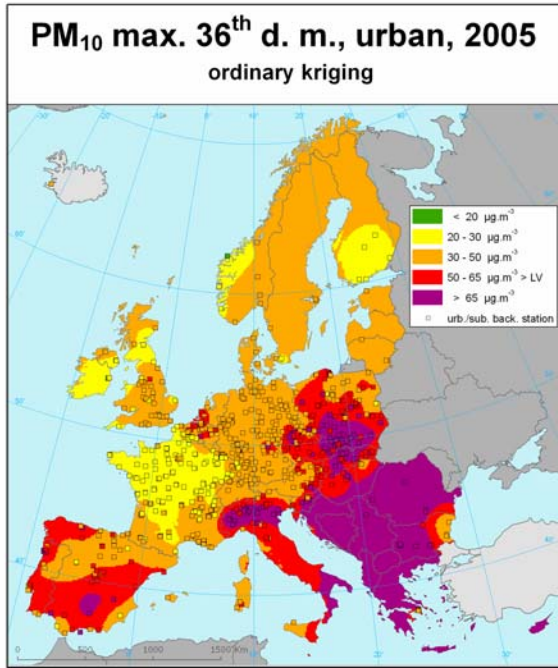


Figure A2.13 Maps showing 36th maximum daily average PM₁₀ concentration (in µg.m⁻³) on the European scale for urban areas in 2005, 10 x 10 km grid resolution, as a result of the interpolation methods 1-a (top left), 2-UP.E-a (top right), 3-UP.Erht-a (bottom left) and 4-UP.L-a (bottom right). The maps are applicable in the urban areas only.

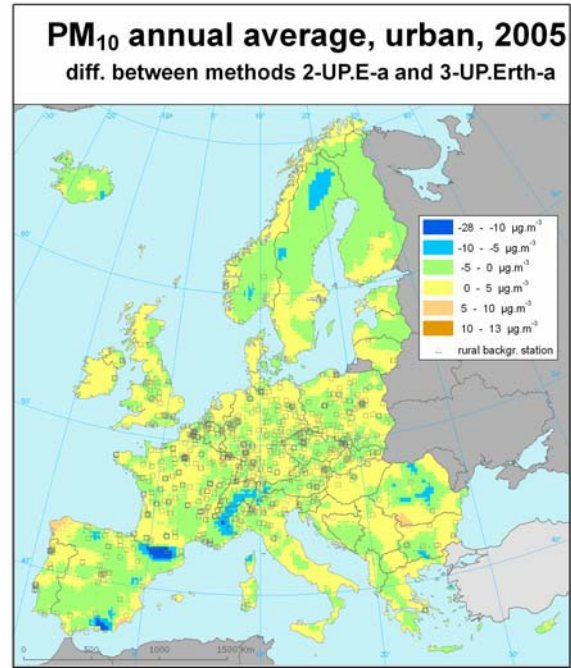
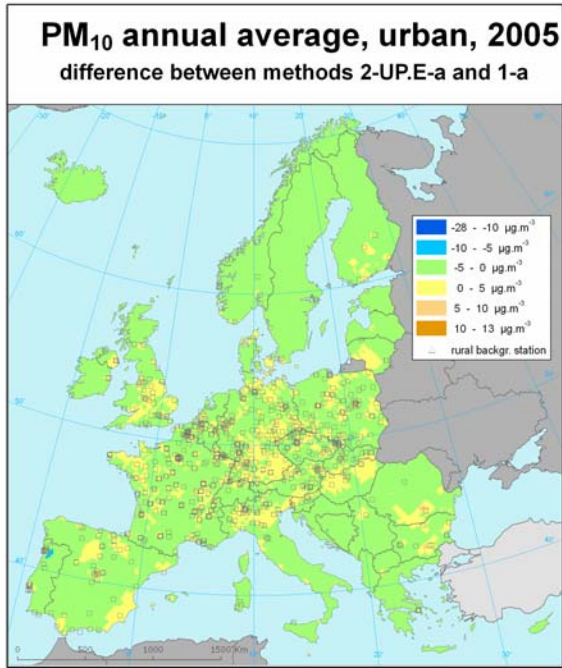


Figure A2.14 Maps showing the difference of the selected method 2-UP.E-a and the method 1-a (left), resp. 3-UP.Erht-a (right) for annual average PM₁₀ concentration (in $\mu\text{g.m}^{-3}$) on the European scale for urban areas in 2005, 10 x 10 km grid resolution. Negative values show up at areas with higher concentrations of the alternative method (1-a left, 3-UP.Erht-a right) compared to the preferred method 2-UP.E-a.

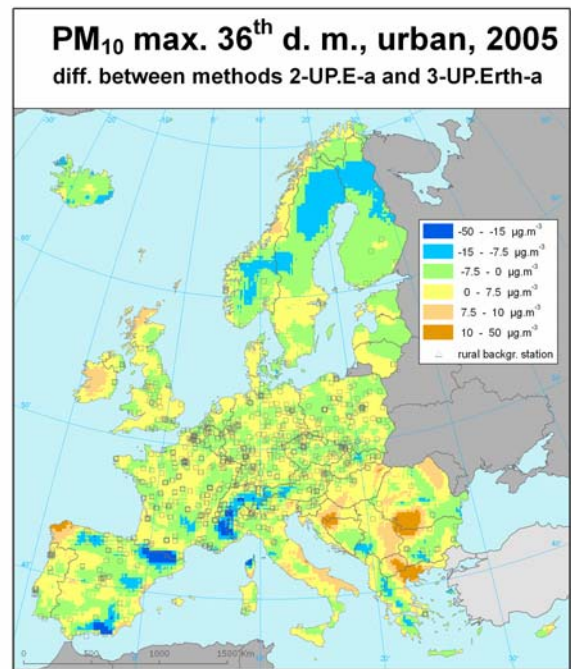
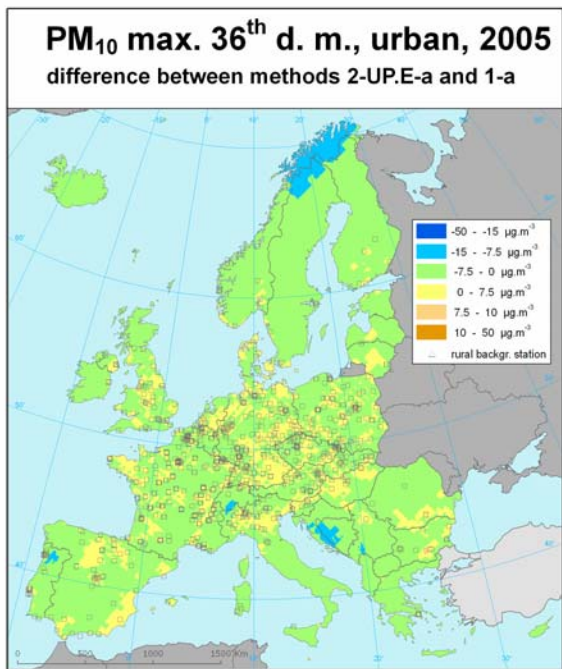


Figure A2.15 Maps showing the difference of the selected method 2-UP.E-a and the method 1-a (left), resp. 3-UP.Erht-a (right) for PM₁₀ indicator 36th maximum daily value (in $\mu\text{g.m}^{-3}$) on the European scale for urban areas in 2005, 10 x 10 km grid resolution. Negative values show up at areas with higher concentrations of the alternative method (1-a left, 3-UP.Erht-a right) compared to the preferred method 2-UP.E-a.

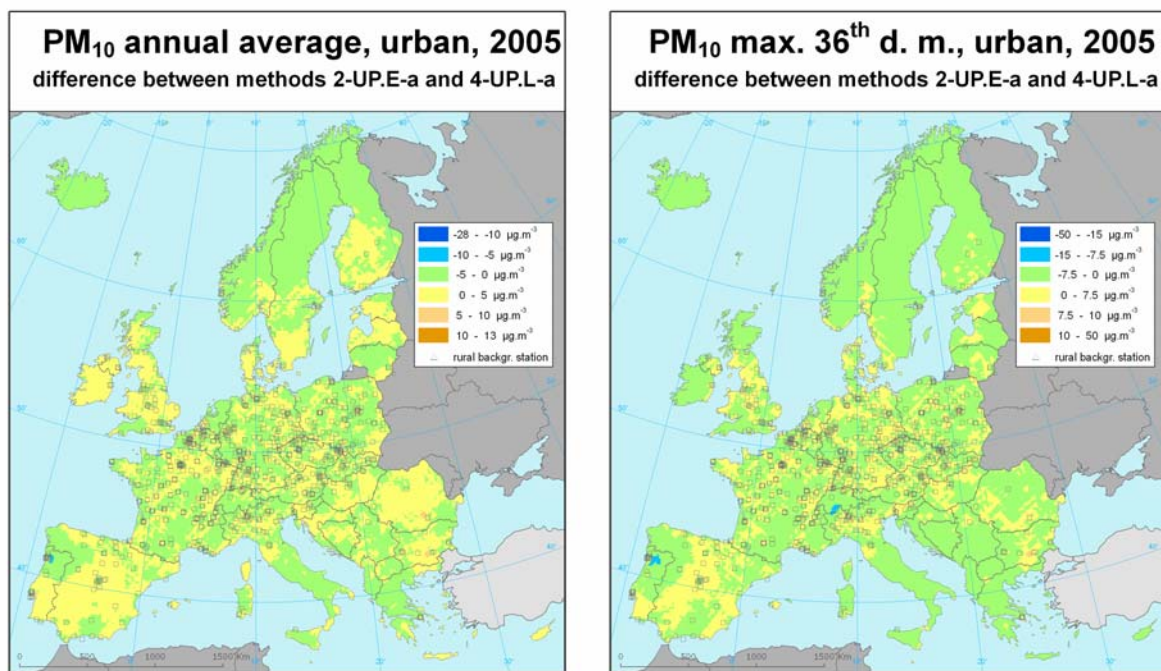


Figure A2.16 Maps showing the difference between the methods using output from the EMEP model (2-UP.E-a) and from the LOTOS-EUROS model (4-UP.L-a) for PM₁₀ annual average (left) and 36th maximum daily value (right) in $\mu\text{g.m}^{-3}$ on the European scale for urban areas in 2005, 10 x 10 km grid resolution. Negative values show higher concentrations of method 4-P.L-a.

Uncertainty estimated by cross-validation

Again but now for urban areas, the RMSE from the cross-validation, in $\mu\text{g.m}^{-3}$, is considered. RMSE is the most common indicator for the uncertainty estimation of the maps in positions without measurement within the areas covered by measurements (see Tables A2.7. and A2.8). The absolute mean uncertainty for the preferred method 2-UP.E-a of the map of PM₁₀ annual average expressed by RMSE is $5.5 \mu\text{g.m}^{-3}$ and of 36th maximum daily mean PM₁₀ values is $9.9 \mu\text{g.m}^{-3}$.

Alternatively, the relative mean uncertainty can be expressed as the percentage of the absolute mean uncertainty value compared to the mean air pollution indicator value for all stations. The relative mean uncertainty of the urban map of PM₁₀ annual average is 20.0% and of 36th maximum daily average PM₁₀ values is 21.4% when method 2-UP.E-a is used for mapping. This uncertainty is slightly better (of about 1%) than the uncertainty of relevant 2004 maps. As in the case of rural areas, the relative uncertainty is quite satisfactory in comparison of the demand of 50% for modelling results according to 1st DD.

In Figure A2.17 the cross-validation scatter plot for the selected method 2-UP.E-a is shown. In comparison with the cross-validation scatter plots for the rural areas (Figure A2.7), the underestimation of interpolation is smaller in the urban areas (given by higher R^2 and slope α). This is caused probably by higher number of urban/suburban stations in comparison with the rural stations. From the figures the level of underestimation of high values in the places with no measurement can be seen, e.g., the annual average $60 \mu\text{g.m}^{-3}$ is estimated in the places without measurement on average as $51 \mu\text{g.m}^{-3}$.

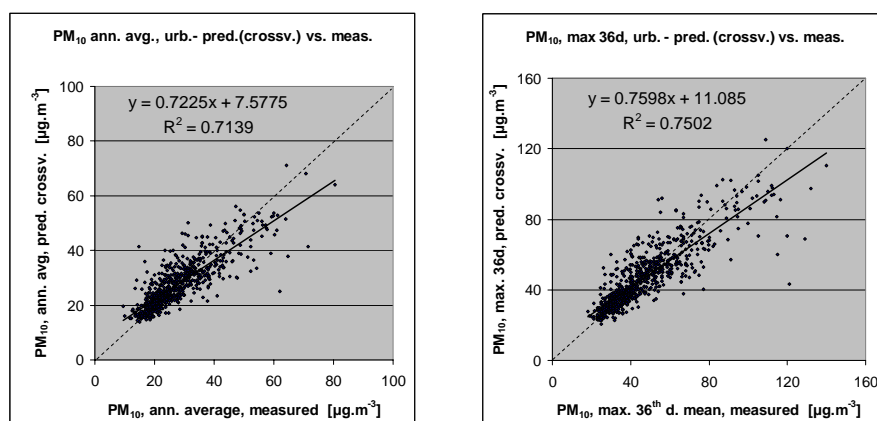


Figure A2.17 Correlation between cross-validation predicted values (*y*-axis) and measurements (*x*-axis) for the PM_{10} indicators annual average (left) and 36th maximum daily mean (right) for urban areas in 2005, as a result of the linear regression P.E and ordinary kriging of its residuals. R^2 and the slope *a* (from the linear regression equation $y = a \cdot x + c$) should be as close 1 as possible, the intercept *c* should be as close 0 as possible

Comparing point measurement values with the predicted grid value

Additionally to the cross-validation, a simple comparison between the measured and interpolated values in a 10 x 10 km grid has been made. This comparison shows to what extent the predicted value of the corresponding grid cell represents the measured point values covered by that cell. The regression results of this comparison are presented in Table A2.12, together with the regression results of the cross-validation scatter plots.

This simple comparison with gridded predictions shows the uncertainty at locations with measurements itself, while cross-validation simulates the behaviour of interpolation in the positions with no measurements within the area covered by measurements. The uncertainty at measurement locations is caused partly by the smoothing effect of interpolation and partly by the spatial averaging of the values in 10x10 km grid. As expected, the correlation between stations measurements and corresponding predicted grid values is better at of the simple comparison (higher R^2 , slope closer to 1, lower intercept) compared to the cross-validation predictions, see Table A2.12. All table parameters show better conformity between measured and interpolated values in urban areas, compared to those in Table A2.5 for the rural areas (according all parameters, i.e. R^2 , slope and the intercept). The agreement of the measured values with the estimated values is somewhat better than has been found for the 2004-data.

Table A.2.12 Linear regression equation and coefficient of determination R^2 from the scatter plots of the predicted values based on cross-validation (above) and aggregation into 10x10 km grid (bottom) versus the measured values for PM_{10} indicators annual average (left) and 36th maximum daily mean (right) for urban areas in 2005 as a result of the linear regression model UP.E and ordinary kriging of its residuals.

Indicator	PM ₁₀ , rural areas			
	Annual average		36th max.d.mean	
prediction	equation	R ²	equation	R ²
(i) Cross-validated predictions	$y = 0.723x + 7.578$	0.714	$y = 0.759x + 11.085$	0.750
(ii) 10x10 km grid predictions	$y = 0.822x + 4.870$	0.877	$y = 0.846x + 7.509$	0.896

Uncertainty maps

Next to the concentration maps (Figure A2.11), again the uncertainty maps in Figure A2.18 are constructed. The maps show higher uncertainty in areas with lower density of urban and suburban stations. The uncertainty increases the further away from the stations. Similar effect occurred at the

rural stations used for mapping uncertainty in rural areas. The areas with the highest uncertainty are southern Italy, west Balkan and the northern Scandinavia.

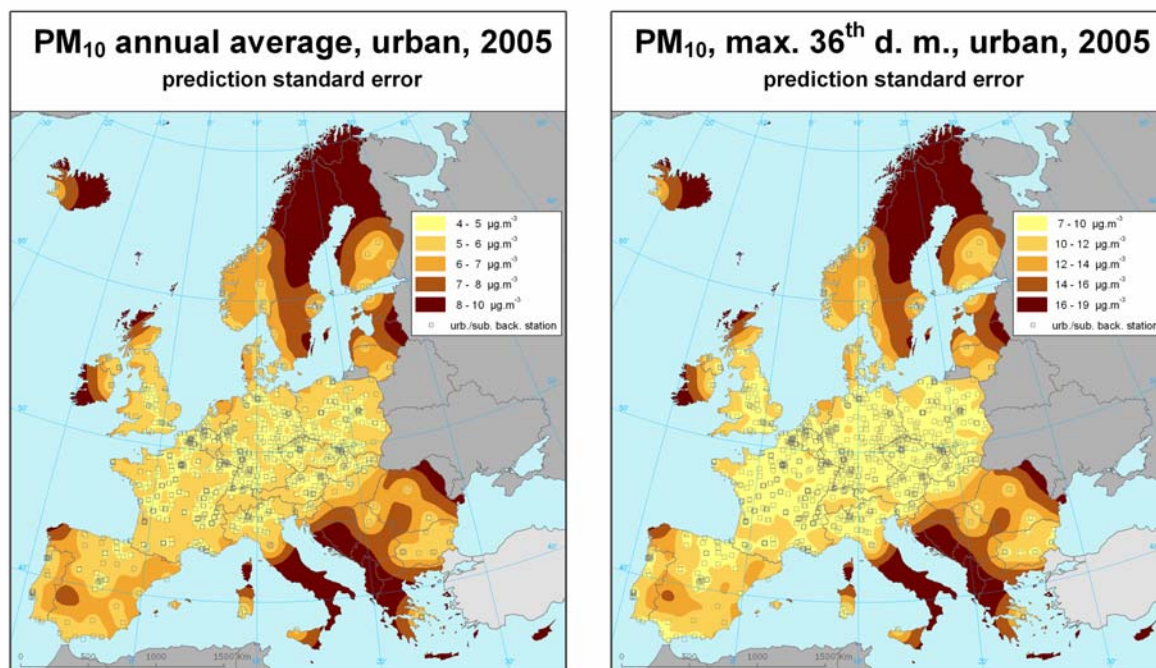


Figure A2.18 Uncertainty maps for maps of PM₁₀ indicators annual average (left) and 36th maximum daily mean (right), in $\mu\text{g.m}^{-3}$ on the European scale for urban areas in 2005, 10 x 10 km grid resolution, as a result of the linear regression UP.E and ordinary kriging of its residuals. The maps are applicable in the urban areas only.

Probability maps

Next, the maps of the probability of the limit value exceedance in urban areas have been constructed, using concentration and uncertainty maps (i.e. Figures A2.11 and A2.18) and the limit values (LV, i.e. $40 \mu\text{g.m}^{-3}$ for the annual average and $50 \mu\text{g.m}^{-3}$ for the 36th maximum daily mean) The probability map is presented in Figure A2.19. The urban annual average shows high likelihood of exceedances in areas of south-east Europe, south Poland, Italian Po Valley and south Spain. The rest of Europe shows a likelihood of exceedance of less than 25%. Concerning the daily probability of exceedance the areas with high likelihood of annual based exceedance are now much more extended, covering the whole of eastern Europe, Italy as a whole and large additional areas in north-western Spain, Portugal and the Benelux. Furthermore are there a considerable increased number of measurement stations with a daily limit exceedance than with an annual limit exceedance (station values above the limit value are marked red and station values below are in green, as explained in Section 2.3).

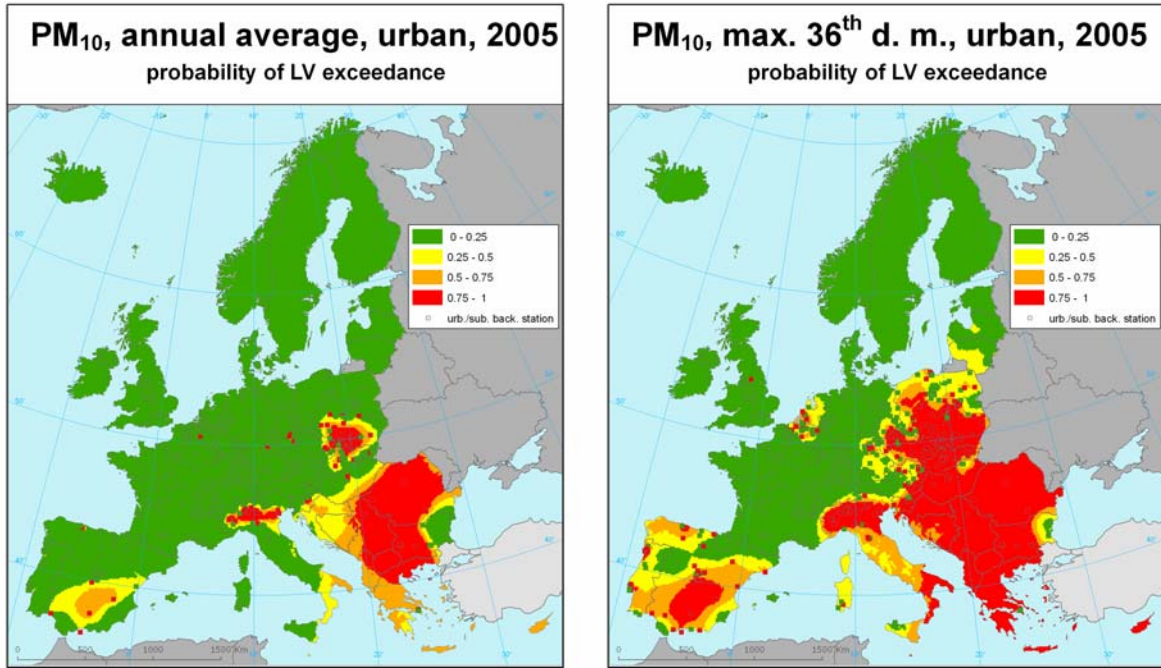


Figure A2.19 Probability of the limit value exceedance maps for PM₁₀ indicators annual average (left) and 36th maximum daily mean (right), in $\mu\text{g}\cdot\text{m}^{-3}$ on the European scale for urban areas in 2005, 10 x 10 km grid resolution, as a result of the linear regression U.P.E and ordinary kriging of its residuals. The maps are applicable in the urban areas only.

Annex 3 Ozone spatial analysis

The same procedures as described in Annex 2 are followed for the ozone indicators as well.

The following ozone indicators are examined:

- human health: 26th highest daily maximum 8-hour average concentration and SOMO35
- vegetation: AOT40 for crops and AOT40 for forests

For the health-related indicators the most suitable and preferred method for interpolated mapping of each indicator of the rural and urban areas are analysed again separately. Out of the separate rural and urban maps based on the selected interpolation method, the final combined indicator map is created. For the vegetation-related indicators only rural maps are considered. The spatial analysis, method selection and uncertainty analysis for the rural mapping is described in Section A3.1 and for the urban mapping in Section A3.2. See for details in the procedure the introduction of Annex 2. The creation of the combined map for each indicator is covered by Chapter 4.

A3.1 Rural maps

A3.1.1 Linear regression analysis

In Horálek et al. (2007) the linear regression model selected for rural ozone mapping of 2004 data was used for the SOMO35 only. That model used, apart from air pollution modelling output data, the supplementary parameters altitude and surface solar radiation (coded below as O.Ear). This model is included in the comparison with 2005 data again.

With the 2005 data the selection of the supplementary data parameters - apart from the EMEP model output - fitting the linear regression significantly best are altitude and relative humidity (coded O.Eah) for 26th highest daily maximum 8-hour average concentration and AOT40 for forests. Altitude and solar radiation (coded O.Ear) are the best for SOMO35 and AOT40 for crops.

The linear regression models using EMEP and LOTOS-EUROS modelling output only (coded O.E resp. O.L) are examined as well. Its purpose was to inter-compare the performance of the contribution of different dispersion model data as input. It was limited to the health indicators only to keep it within time and resources limits.

Thus, the following linear regression models to be examined are:

Submodel	Input parameters
O.E	EMEP model output
O.Ear	EMEP model output, altitude, surface solar radiation
O.Eah	EMEP model output, altitude, relative humidity
O.L	LOTOS-EUROS model output

The statistical performance of these four different linear regression models is presented in Table A3.1 for the human health indicators and Table A3.2 for the vegetation indicators.

Table A3.1 Statistical indicator values of the selected linear regression models indicating the correlation between supplementary data and the 26th highest daily maximum 8-hour mean and SOMO35 of the 2005 measurement ozone concentrations in the rural areas

Indicator	Ozone, 26th h.d.max.8-hr, 2005				Ozone, SOMO35, 2005			
	R ²	adjusted R ²	st. error [µg.m ⁻³]	RMSE [µg.m ⁻³]	R ²	adjusted R ²	st. error [µg.m ⁻³]	RMSE [µg.m ⁻³]
O.E	0.319	0.317	14.48	14.46	0.326	0.324	2673	2666
O.Ear	0.449	0.446	13.05	12.99	0.509	0.506	2286	2275
O.Eah	0.461	0.458	12.91	12.85	0.501	0.498	2304	2293
O.L	0.077	0.074	16.86	16.82	0.214	0.212	2886	2880

Table A3.2 Statistical indicator values of the selected linear regression models indicating the correlation between supplementary data and the AOT40 for crops and the AOT40 for forests of the 2005 measurement ozone concentrations in the rural areas.

Indicator	Ozone, AOT40 crops, 2005				Ozone, AOT40 forests, 2005			
	R ²	adjusted R ²	st. error [µg.m ⁻³]	RMSE [µg.m ⁻³]	R ²	adjusted R ²	st. error [µg.m ⁻³]	RMSE [µg.m ⁻³]
O.E	0.338	0.337	9378	9357	0.367	0.365	14665	14632
O.Ear	0.537	0.534	7860	7825	0.519	0.516	12812	12755
O.Eah	0.530	0.527	7917	7882	0.526	0.523	12720	12663

Tables A3.1 and A3.2 show at all four indicators better values of R² and RMSE for the linear regression models of the methodology type 2 (i.e. O.E) and 3 (O.Eah and O.Ear) then for type 1 (O.E) or 4 (O.L), indicating that the addition of supplementary parameters results in a substantially better linear regression model.

For the human health indicators we inter-compared the output of dispersion models as the only regression variable. At both indicators the R² and RMSE for the regression model of methodology types 2 (O.E) and 4 (O.L) indicate that the closeness of regression is higher when the EMEP modelled concentration field is used, instead of the LOTOS-EUROS modelled field.

Conclusions:

- At all for indicators the addition of supplementary parameters substantially improves the closeness of the linear regression relation with the measured ozone indicators.
- For both health indicators the EMEP model performs better than the LOTOS-EUROS model.

These conclusions indicate that the methods using linear regressions most likely will perform better by including additional supplementary parameter and the EMEP modelling data. However, the regression residual interpolations will have to be compared to the interpolation methods (in next section) on the primary monitoring data to explicitly appoint the best or preferred method for the final mapping.

A3.1.2 Spatial interpolation

From the four methodological types we examine the most promising interpolation methods by comparing the RMSE and other statistical indicators from the cross-validation. (Neither lognormal kriging nor lognormal cokriging has been examined, because preliminary analysis showed worse results than ordinary kriging and ordinary cokriging at all ozone indicators. Furthermore, ozone indicators do not have a lognormal distribution in space, so there would be no improvement in the results). Only for the health-related indicators we compare the use of EMEP modelled output against that of LOTOS-EUROS due to limited time and resources within the project.

The four methods we examine are:

1. Interpolation using primarily monitoring data

a. Ordinary kriging (OK)

c. Ordinary cokriging (OC)

2. Interpolation using monitoring data and EMEP model data

Linear regression using EMEP model output (O.E), followed by interpolation of its residuals using OK.

3. Interpolation using monitoring data, EMEP model data and other supplementary data

Linear regression model using EMEP model output, altitude and surface solar radiation (O.Ear), followed by interpolation of its residuals using OK

Linear regression model using EMEP model output, altitude and relative humidity (O.Eah), followed by interpolation of its residuals using OK

4. Interpolation using monitoring data and LOTOS-EUROS model data

Linear regression using LOTOS-EUROS model output (O.L), followed by interpolation of its residuals using OK

The statistical indicators of the cross-validation of the methods are presented per ozone indicator in a separate table (Tables A3.3 to A3.6). All the statistical indicators, with exception of R^2 , are expressed in the same units as the relevant ozone indicator. In the same tables the linear regression equations and R^2 from the cross-validation scatter plots with the measurements on the x axis, and the predicted values on the y axis are given.

Table A3.3 Comparison of different interpolation methods showing RMSE and the other statistics and linear regression parameters from the cross-validation scatter plots of the predicted values for ozone indicator 26th highest daily maximum 8-hour average value, for 2005 in rural areas. Apart from R^2 and a , all other statistical indicators are in $\mu\text{g}\cdot\text{m}^{-3}$.

mapping method		26 th highest maximum daily 8-hour mean [$\mu\text{g}\cdot\text{m}^{-3}$]									
		RMSE	MPE	min.	max.	MAE	MedAE	MPSE	linear regr. $y=a\cdot x+c$		
				error	error				a	c	R^2
1-a	interpolation OK	12.4	0.0	-75.4	108.5	7.8	5.5	12.1	0.514	57.89	0.499
1-c	interpolation OC	12.2	0.0	-70.1	108.8	7.7	5.4	9.4	0.556	52.88	0.516
2-O.1-a	lin. regr. O.E + OK	13.0	-0.1	-77.8	105.0	8.3	5.9	12.5	0.511	58.20	0.459
3-O.Ear-a	lin. r. m. O.Ear + OK	12.3	-0.1	-71.1	106.5	7.5	5.0	11.9	0.541	54.58	0.511
3-O.Eah-a	lin. r. m. O.Eah + OK	12.3	-0.1	-72.1	107.8	7.5	5.1	11.7	0.540	54.71	0.507
4-O.L	lin. regr. O.L + OK	12.6	-0.2	-76.9	108.4	7.9	5.4	12.3	0.524	56.57	0.487

Table A3.4 Comparison of different interpolation methods showing RMSE and the other statistics and linear regression parameters from the cross-validation scatter plots of the predicted values for ozone indicator SOMO35, for 2005 in rural areas. Apart from R^2 and a , all other statistical indicators are in $\mu\text{g}\cdot\text{m}^{-3}\cdot\text{days}$.

mapping method		SOMO35 [$\mu\text{g}\cdot\text{m}^{-3}\cdot\text{d}$]									
		RMSE	MPE	min.	max.	MAE	MedAE	MPSE	linear regr. $y=a\cdot x+c$		
				error	error				a	c	R^2
1-a	interpolation OK	2425	-35	-21111	8446	1492	938	2322	0.423	3492	0.443
1-c	interpolation OC	2137	-36	-17476	8948	1329	843	1388	0.591	2465	0.568
2-O.1-a	lin. regr. O.E + OK	2507	-69	-21809	9175	1575	1001	2185	0.440	3358	0.407
3-O.Ear-a	lin. r. m. O.Ear + OK	2173	-59	-18743	9038	1299	833	1845	0.553	2679	0.552
3-O.Eah-a	lin. r. m. O.Eah + OK	2207	-43	-18936	9310	1331	860	1735	0.545	2739	0.538
4-O.L	lin. regr. O.L + OK	2487	-76	-21220	9141	1533	919	2018	0.468	3179	0.419

Table A3.5 Comparison of different interpolation methods showing RMSE and the other statistics and linear regression parameters from the cross-validation scatter plots of the predicted values for ozone indicator AOT40 for crops, for 2005 in rural areas. Apart from R^2 and a , all other statistical indicators are in $\mu\text{g.m}^{-3}.\text{hours}$.

mapping method		AOT40 for crops [$\mu\text{g.m}^{-3}.\text{h}$]									
		RMSE	MPE	min.	max.	MAE	MedAE	MPSE	linear regr. $y=a.x+c$		
				error	error				a	c	R^2
1-a	interpolation OK	7807	1	-62177	36947	4672	2721	7105	0.544	8594	0.541
1-c	interpolation OC	7647	22	-55115	36149	4667	3013	5762	0.585	7843	0.561
2-O.1-a	lin. regr. O.E + OK	8558	-68	-65507	42839	5217	3168	6344	0.556	8316	0.465
3-O.Ear-a	lin. r. m. O.Ear + OK	7677	-42	-62481	39380	4639	2851	6692	0.577	7968	0.556
3-O.Eah-a	lin. r. m. O.Eah + OK	7666	-71	-63262	39979	4599	2961	6324	0.591	7664	0.558

Table A3.6 Comparison of different interpolation methods showing RMSE and the other statistics and linear regression parameters from the cross-validation scatter plots of the predicted values for ozone indicator AOT40 for forests, for 2005 in rural areas. Apart from R^2 and a , all other statistical indicators are in $\mu\text{g.m}^{-3}.\text{hours}$.

mapping method		AOT40 for forests [$\mu\text{g.m}^{-3}.\text{h}$]									
		RMSE	MPE	min.	max.	MAE	MedAE	MPSE	linear regr. $y=a.x+c$		
				error	error				a	c	R^2
1-a	interpolation OK	13035	-59	-107958	56866	7692	4354	11388	0.503	14880	0.499
1-c	interpolation OC	12643	-9	-97501	56085	7618	4388	9058	0.544	13713	0.529
2-O.1-a	lin. regr. O.E + OK	13744	-239	-121907	60747	8153	4643	10793	0.496	14953	0.448
3-O.Ear-a	lin.r.m. O.Ear + OK	12474	-215	-107927	58678	7276	4337	10510	0.550	13354	0.541
3-O.Eah-a	lin.r.m. O.Eah + OK	12514	-312	-112626	57611	7202	4422	10205	0.545	13412	0.538

A number of comparison conclusions can be drawn from the results provided in Tables A3.3 - A3.6 for the rural areas:

- When ranking the statistics (RMSE, SDE, MAE, R^2 and MPSE) of the interpolation methods of methodology type 1, i.e. using 2005 monitoring data only, the best results are obtained with ordinary cokriging, method 1-c, at all ozone indicators for the rural areas. This confirms the results from Horálek et al. (2007) on the 2004 data.
- When ranking the statistics for the methods of methodology type 3, at both human health indicators the best results are obtained by the linear regression model using EMEP model output, altitude and solar radiation, followed by its residual interpolation using ordinary kriging (method 3-O.Ear-a). The same was concluded in Horálek et al. (2007) on the 2004 data, however, only for SOMO35. (The health indicator 26th highest daily maximum 8-hour average was not examined due to lack of the EMEP model data availability).
- Furthermore, this ranking of the statistics for the methods of methodology type 3 shows at the vegetation indicators, that the results for method 3-O.Ear-a and 3-O.Eah are about equal. At AOT40 for crops method 3-O.Eah-a performs negligible better, while at AOT40 for forests of that is the case for method 3-O.Ear-a. We consider both methods as equally performing for the vegetation indicators.
- The comparison of the method of the types 2 and 4 (i.e. use of EMEP or LOTOS-EUROS model) shows better results for the type 2 (i.e. use of EMEP), based on RMSE (and all other statistical indicators). However, the difference is only 2% and consider them equally performing in their contribution to the linear regression model, followed by its residuals interpolation.
- The comparison of the method of the methodology types 2 and 3 shows better results for the methods of type 3 (i.e. including other supplementary parameter) for all ozone indicators, based on RMSE (and almost all statistical indicators). It confirms that for the 2005 data the

addition of supplementary parameters improves the interpolations. In Horálek et al. (2007) on 2004 data it was not so obvious to conclude that for all indicators.

- The comparison of the scatter plots shows that the methods 1-c and both the examined methods of type 3 give the best results. The method 1-c at both health indicators performs slightly better for slope a (highest), i.e. it is expected this method will show the smaller underestimations for high values in areas with no measurements. Its intercept at both indicators is smallest, i.e. expected is the method will show the smallest overestimations of predicted values at low values in areas without measurements. Also its correlation coefficient (R^2) values are highest, meaning method 1-c provides also the best correlation with the measured values and expectedly the best representation of predicted for areas without measurements. For AOT40 for forests this is valid for method 3-O.Ear-a; for AOT40 for crops the method 1-c gives the best results in the case of R^2 , while the method 3-O.Eah-a for slope and intercept. Nevertheless, the results of the methods 1-c, 3-O.Ear-a and 3-O.Eah-a for all indicators are quite close to each other and therefore not driving the appointment of the best method.
- An inter-comparison of the methods of the types 1, 2 and 3 shows that the best results for 2005 data are given by both methods of type 1 (ordinary cokriging on monitoring data only) and both of type 3 (linear regression model with supplementary parameters, following by ordinary kriging of its residuals). The methods of the type 1 are just slightly better at human health indicators and AOT40 for crops, while the methods of the type 3 are just slightly better at AOT40 for forests.

Concluding from the above, the selection of most preferred method needs clearly to be taken from the methods of the types 1 and 3. Additionally, methods of type 3 have the advantage of providing a more complete European coverage, especially at areas lacking monitoring stations. Taking furthermore into account the slightly better performance of method 3-O.Ear-a, as one of the two of type 3, at both health indicators and at the AOT40 for forests, with very close 2nd best performance at the AOT40 for crops, we prefer to use for the rural mapping for all four indicators this method 3-O.Ear-a.

Other considerations leading to this selection are related to the results with 2004 data. On the 2004 data method 3-O.Ear-a was selected also as best for the health indicator SOMO35, in absence of the 26th highest daily maximum 8-hr mean (Horálek et al., 2007). Furthermore, the results on both AOT40 vegetation indicators showed quite equal or even better performance at methods of type 3 (3-O.Ear-a) compared to the method of type 1, ordinary kriging using monitoring data including altitude in the EEA indicator on exposure of ecosystems to air pollution (CSI005). For consistency in the indicator assessment over the years (1996 – 2004) the type 1 method was still prolonged. However, current comparison with 2005 data confirms method 3-O.Ear-a to be the best, leading to the decision to switch methods for the indicator CSI005 analysis.

The resulting rural maps for the 26th highest daily maximum 8-hour average concentration and for SOMO35 using the selected interpolation method 3-O.Ear-a are shown in Figure A3.1. Figure A3.2 shows the vegetation indicators AOT40 for crops and AOT40 for forests using the same method 3-O.Ear-a. Values of the parameters used for mapping are given in Table A3.7.

Table A3.7 Parameters of the linear regression model and variogram of method 3-O.Ear-a used for final mapping of ozone measurement parameters 26th highest daily maximum 8-hour average values, SOMO35, AOT40 for crops and AOT40 for forests for 2005 in the rural areas, i.e. linear regression model O.Ear following by the interpolation on its residuals using ordinary kriging (OK).

linear regr. model O.Ear + OK on its residuals	high. 26 th max. d. 8h	SOMO35	AOT40 for crops	AOT40 for forests
	coeff.	coeff.	coeff.	coeff.
c (constant)	21.82	-2089	-11877	-22328
a1 (EMEP model 2005)	0.659	0.452	1.178	0.427
a2 (altitude GTOPO)	0.0131	3.201	8.821	12.512
a3 (s. solar radiation 2005)	1.57	405	1836	2984
nugget	125	3.1E+06	4.3E+07	1.0E+08
sill	160	3.6E+06	4.6E+07	1.2E+08
range [km]	530	510	960	510

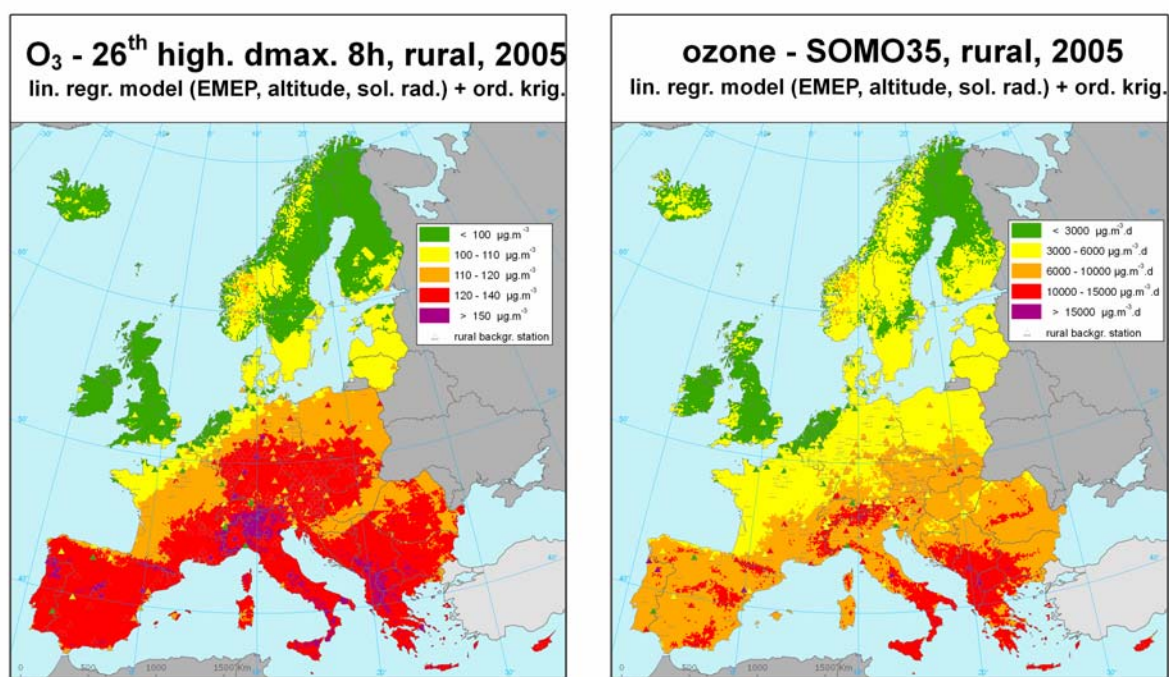


Figure A3.1 Maps showing health ozone indicators 26th highest daily maximum 8-hour average values (left, in $\mu\text{g.m}^{-3}$) and SOMO35 (right, in $\mu\text{g.m}^{-3}.\text{days}$) on European scale for rural areas in 2005, 10 x 10 km grid resolution, as a result of the linear regression model O.Ear and ordinary kriging of its residuals. Absolute and relative mean uncertainty of these maps expressed by RMSE is 12.3 $\mu\text{g.m}^{-3}$ and 10.3 % (left), and 2173 $\mu\text{g.m}^{-3}$ and 35.5 % (right).

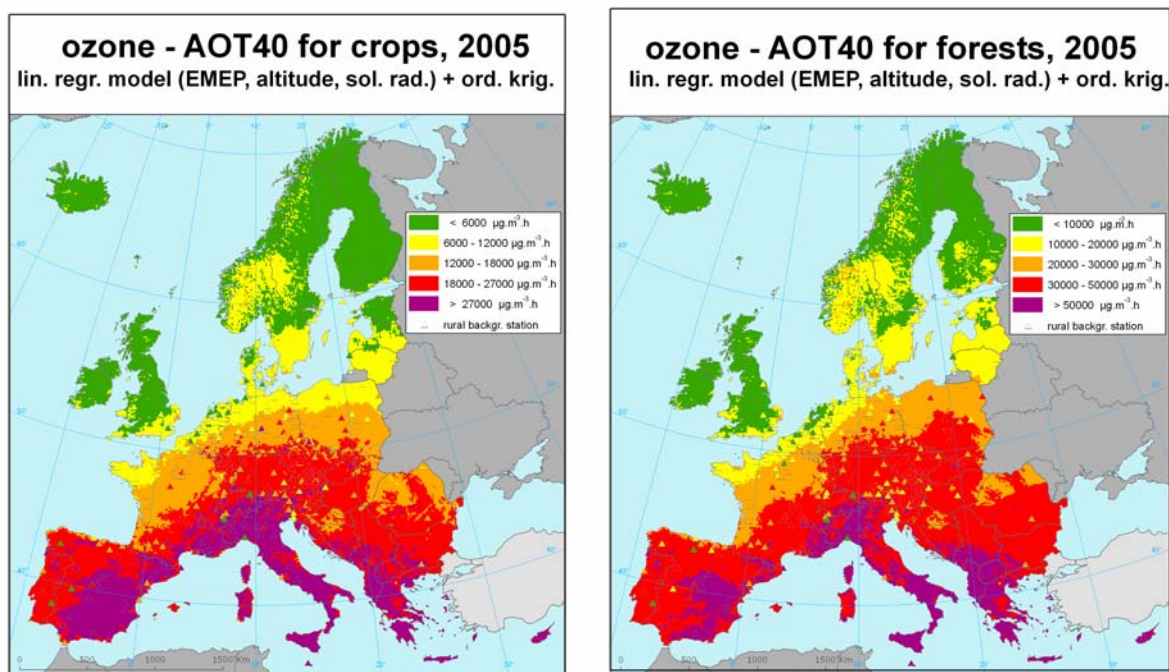


Figure A3.2 Maps showing vegetation ozone indicators AOT40 for crops (left) and AOT40 for forests (right), in $\mu\text{g.m}^{-3}.\text{h}$) on European scale for rural areas in 2005, 10 x 10 km grid resolution, as a result of the linear regression model O.Ear and ordinary kriging of its residuals. Absolute and relative uncertainty of these maps expressed by RMSE is $7677 \mu\text{g.m}^{-3}.\text{h}$ and 40.7 % (left), and $12474 \mu\text{g.m}^{-3}.\text{h}$ and 41.5 % (right).

A3.1.2 Uncertainty analysis

Comparing concentration maps of the interpolation methods

The interpolated maps of rural ozone health indicators based on the preferred method 3-O.Ear-a as well as methods 1-c, 2O.E-a and 4O.L-a are shown in Figure A3.3 for the 26th highest daily maximum 8-hour average and Figure A3.4 for the SOMO35. In Figures A3.7 and A3.8 the differences between the selected method 3-O.Ear-a and the other methods are shown. Due to its poor measurement station coverage in the south-east of Europe we excluded this area from the interpolation on monitoring data only (method 1-c). The patterns of the four methods are quite similar, except that the concentration levels differ between methods. At the preferred method 3-O.Ear-a the contribution of parameter altitude is clearly visible with more elevated ozone concentrations at the orogenetic areas. This may be caused by the dependency of ozone to altitude.

Figure A3.9 illustrates for both indicators the differences between method 2-O.E-a (EMEP) and the corresponding method 4-O.L-a (LOTOS-EUROS). Both ozone health indicators have a pattern in the methods being quite similar, with EMEP showing somewhat higher concentrations in Scandinavia and LOTOS-EUROS tending to have higher concentrations in the south of Europe, and more specifically south Balkan and Greece.

The interpolated maps of rural ozone vegetation indicators based on the preferred method 3-O.Ear-a as well as methods 1-c, are shown in Figure A3.5 for the AOT40 for crops and Figure A3.6 for the AOT40 for forests. In Figure A3.10 the differences between the selected method 3-O.Ear-a and the other method 1-c are shown. Methods 2O.E-a and 4O.L-a have not been examined and inter-compared on the vegetation indicators. (The basic aim was to examine the interpolation behaviour when using a different dispersion model then the EMEP model which we used so far only. We limited this inter-

comparison to health indicators only). At the interpolation on monitoring stations only, the Balkan region was excluded from the mapping calculations due to its poor measurement station coverage.

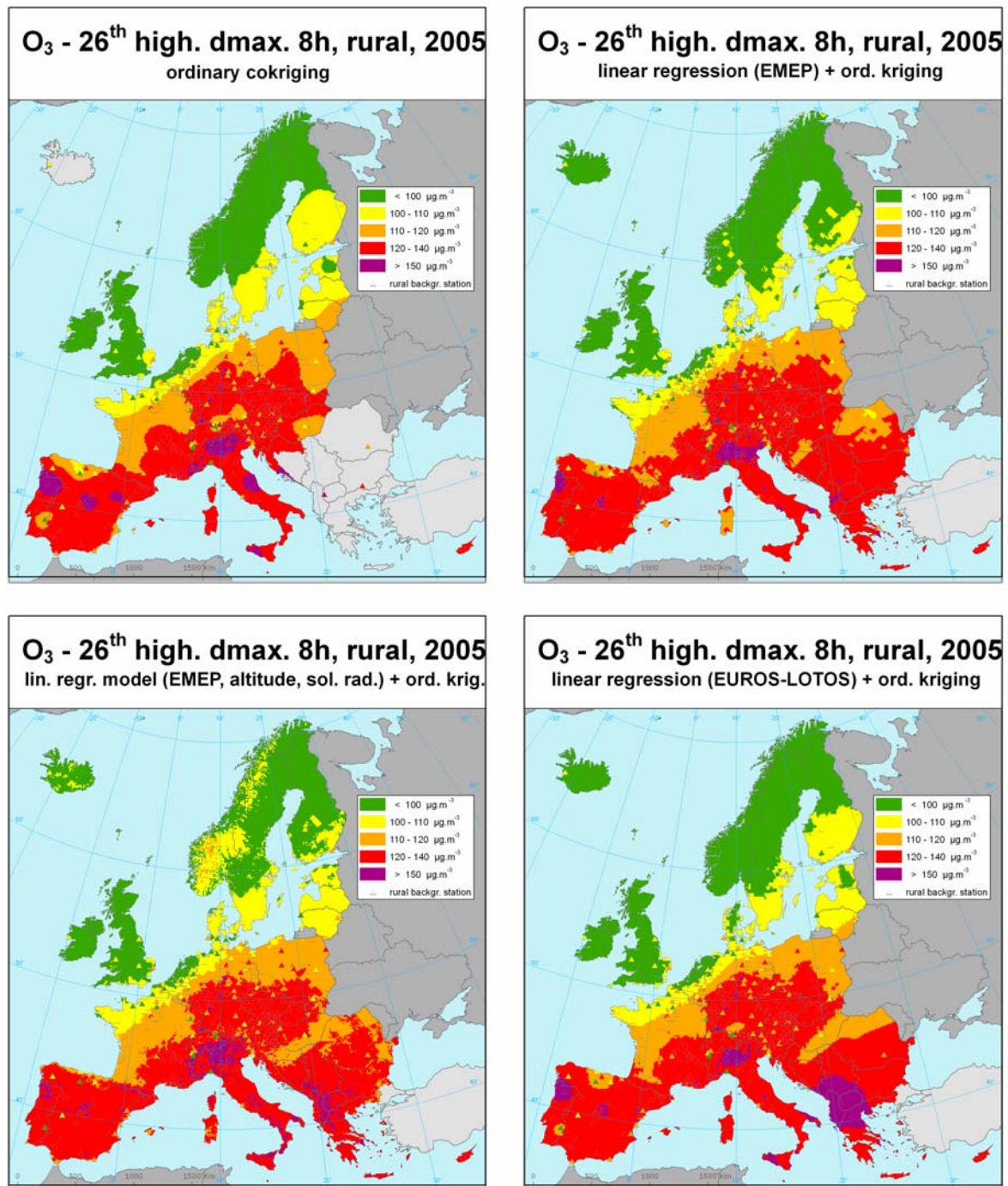


Figure A3.3 Maps showing ozone 26th highest daily maximum 8-hour average values (in $\mu\text{g.m}^{-3}$) on European scale for rural areas in 2005, 10 x 10 km grid resolution, as a result of interpolation method 1-c (top left), 2-O.E-a (top right), 3-O.Ear-a (bottom left) and 4-O.L-a (bottom right).

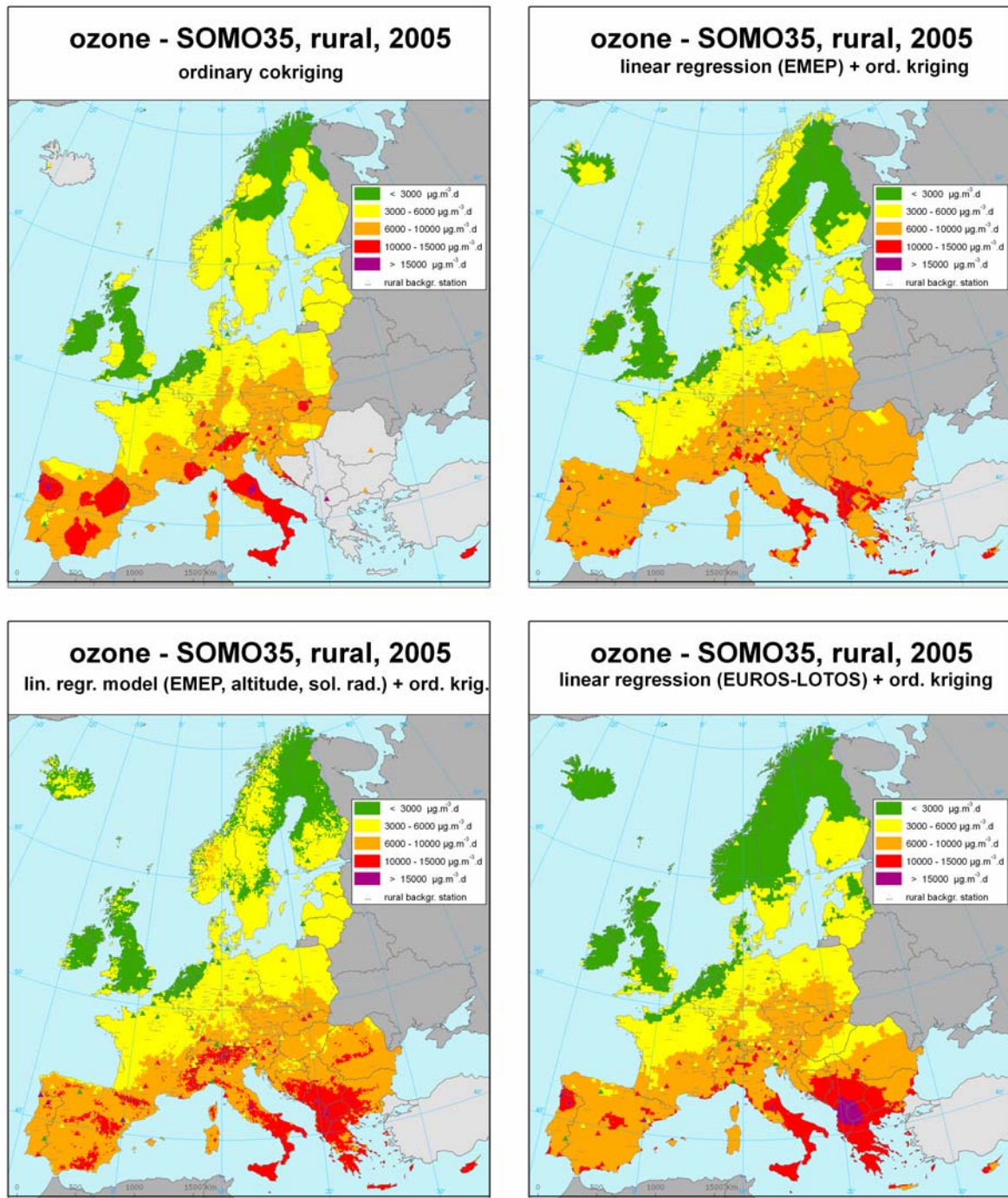


Figure A3.4 Maps showing of ozone SOMO35 (in $\mu\text{g.m}^{-3}.\text{days}$) on European scale for rural areas in 2005, 10 x 10 km grid resolution, as a result of interpolation method 1-c (top left), 2-O.E-a (top right), 3-O.Ear-a (bottom left) and 4-O.L-a (bottom right).

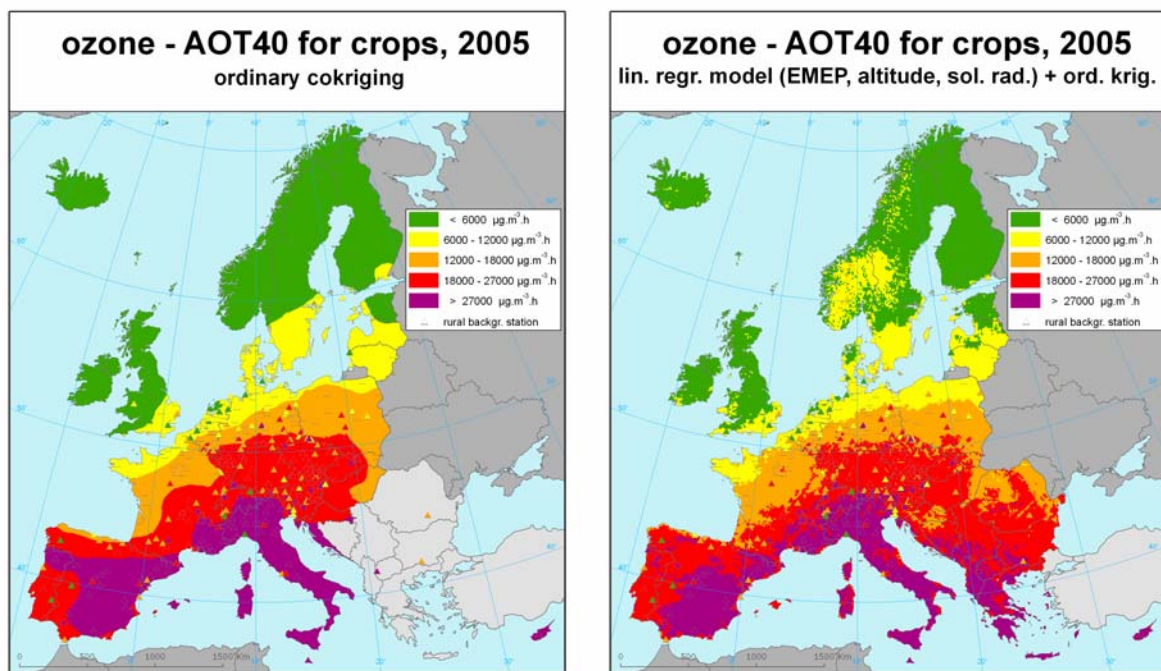


Figure A3.5 Maps showing ozone AOT40 for crops (in $\mu\text{g.m}^{-3}.\text{h}$) on European scale for rural areas in 2005, 10 x 10 km grid resolution, as a result of interpolation method 1-c (left) and 3-O.Ear-a (right).

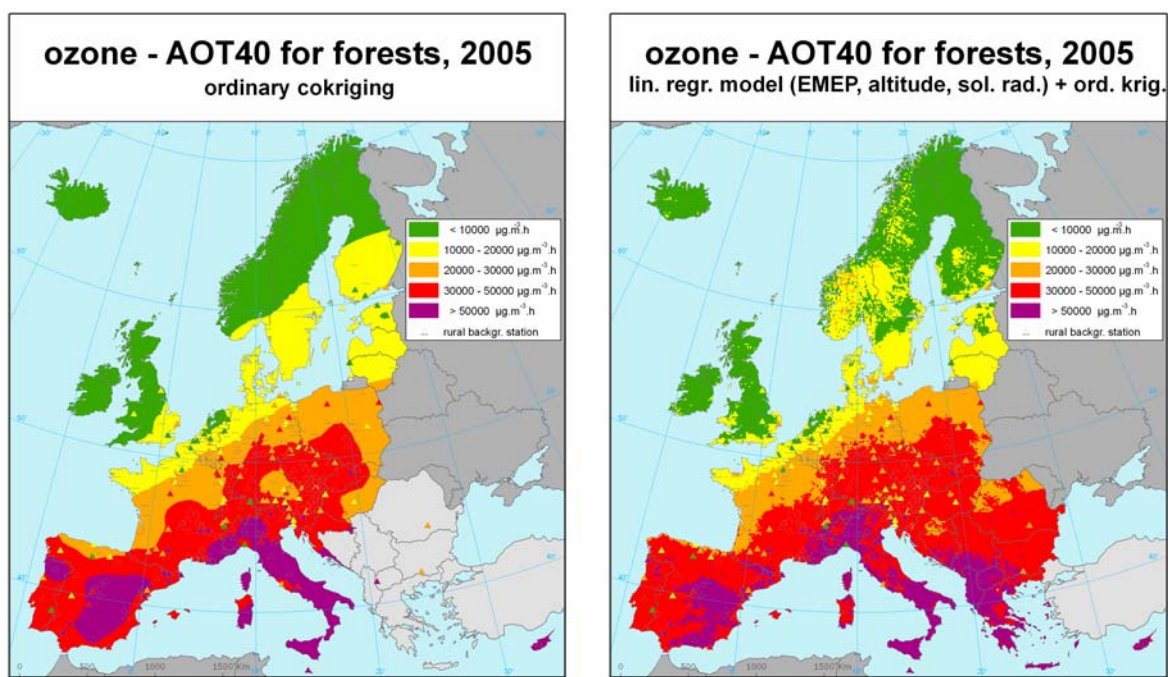
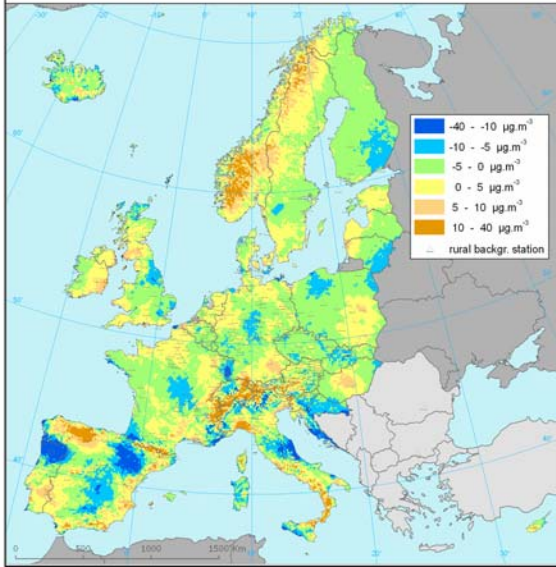


Figure A3.6 Maps showing ozone AOT40 for forests (in $\mu\text{g.m}^{-3}.\text{h}$) on European scale for rural areas in 2005, 10 x 10 km grid resolution, as a result of interpolation method ordinary cokriging 1-c (left) and 3-O.Ear-a (right).

O₃ - 26th high. dmax. 8h, rural, 2005
 difference between methods 3-O.Ear-a and 1-c



O₃ - 26th high. dmax. 8h, rural, 2005
 difference between methods 3-O.Ear-a and 2-O.E-a

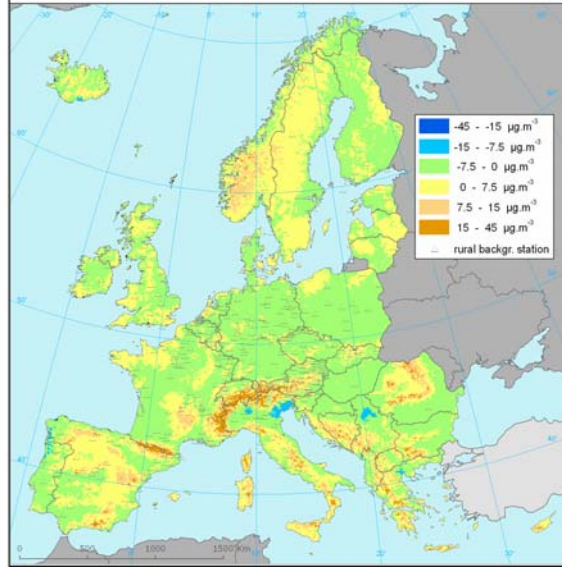
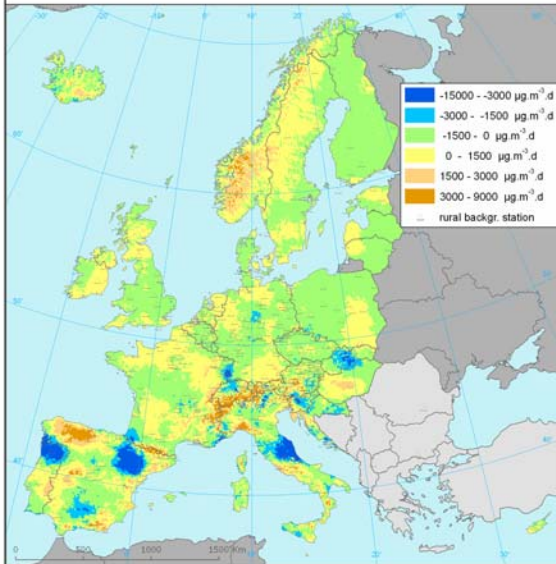


Figure A3.7 Maps showing the difference of the selected method 3-O.Ear-a and the method 1-c (left), resp. 2-O.E-a (right) for 26th highest daily maximum 8-hour average values (in $\mu\text{g.m}^{-3}$) on the European scale for rural areas in 2005, 10 x 10 km grid resolution. Negative values show up at areas with higher concentrations of the alternative method (1-c left, 2-O.E-a right) compared to the preferred method 3-O.Ear-a.

Ozone - SOMO35, rural, 2005
 difference between methods 3-O.Ear-a and 1-c



ozone - SOMO35, rural, 2005
 difference between methods 3-O.Ear-a and 2-O.E-a

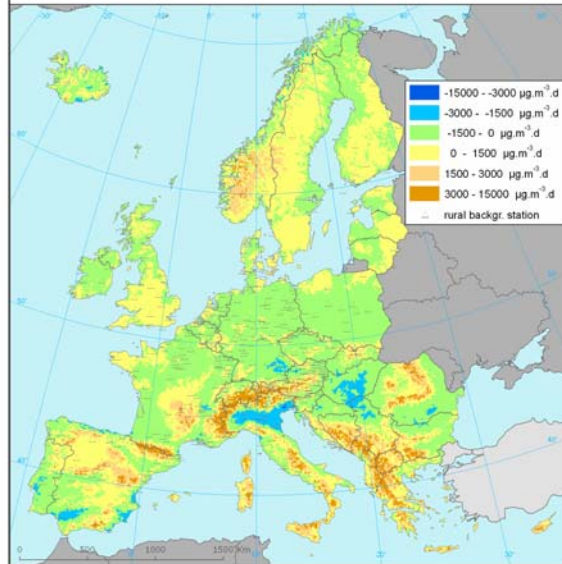


Figure A3.8 Maps showing the difference of the selected method 3-O.Ear-a and the method 1-c (left), resp. 2-O.E-a (right) for SOMO35 (in $\mu\text{g.m}^{-3}.\text{days}$) on the European scale for rural areas in 2005, 10 x 10 km grid resolution. Negative values show up at areas with higher concentrations of the alternative method (1-c left, 2-O.E-a right) compared to the preferred method 3-O.Ear-a.

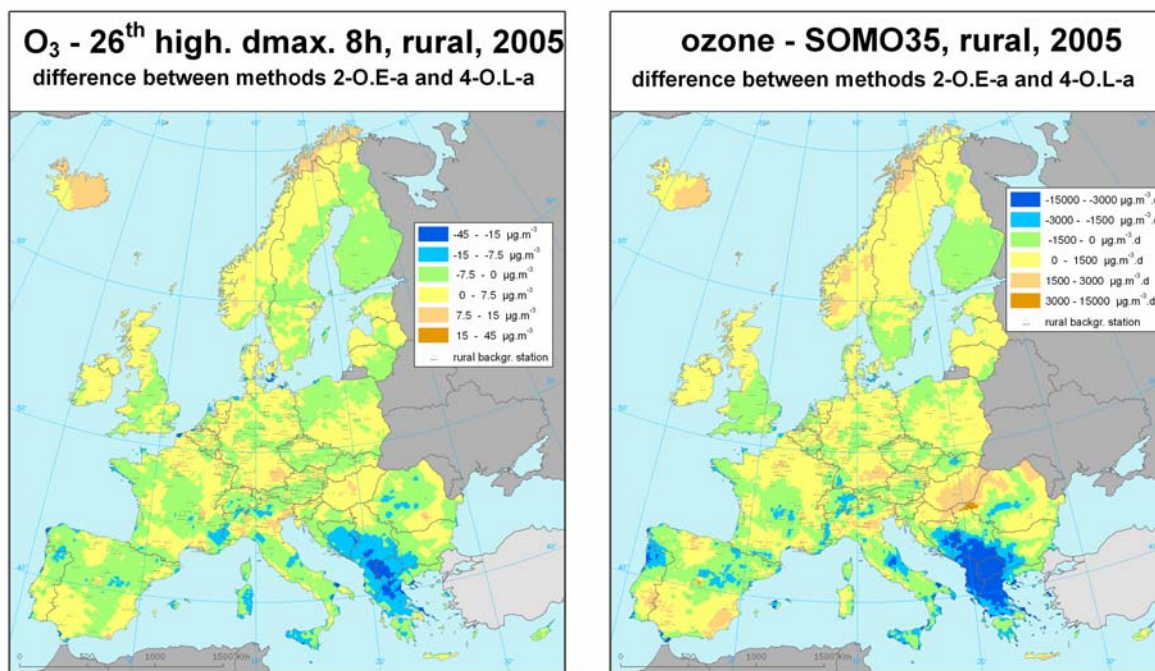


Figure A3.9 Maps showing the difference between the methods using output from the EMEP model (2-O.E-a) and from the LOTOS-EUROS model (4-O.L-a) for 26th highest daily maximum 8-hour average in $\mu\text{g.m}^{-3}$ (left) and SOMO35 in $\mu\text{g.m}^{-3}.\text{day}$ (right) on the European scale for rural areas in 2005, 10 x 10 km grid resolution. Negative values show higher concentrations of method 4-O.L-a.

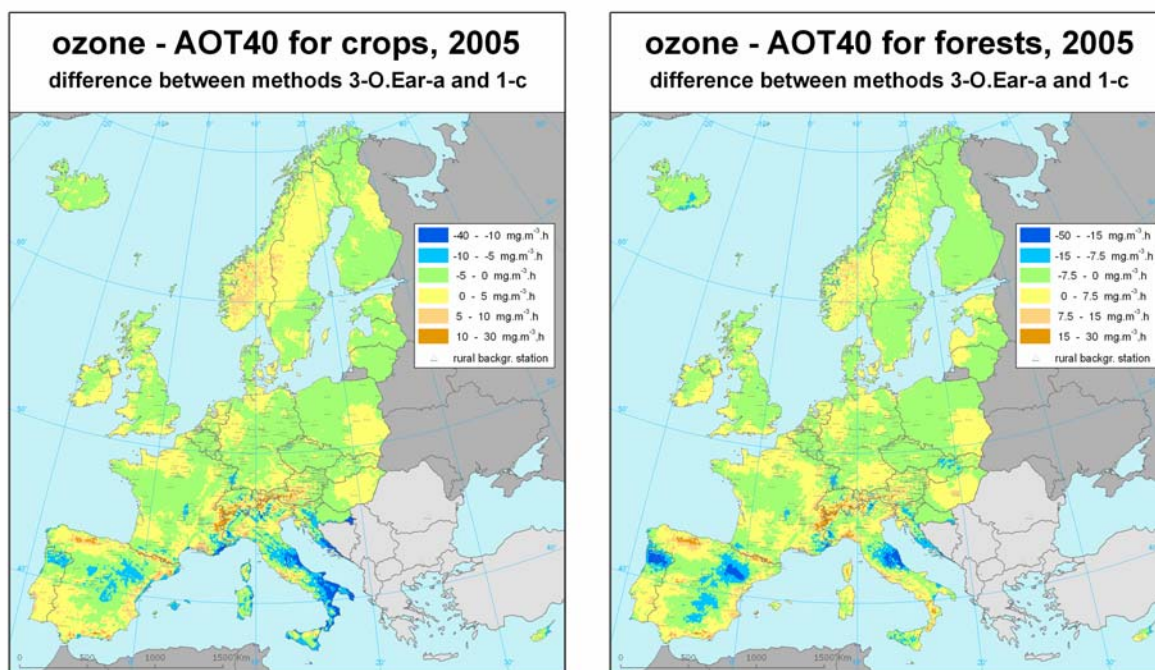


Figure A3.10 Maps showing the difference of the selected method 3-O.Ear-a and the method 1-c for AOT40 for crops (left) and AOT40 for forests (right) in $\text{mg.m}^{-3}.\text{hours}$ on the European scale for rural areas in 2005, 10 x 10 km grid resolution. Negative values show up at areas with higher concentrations of the alternative method 1-c compared to the preferred method 3-O.Ear-a.

Uncertainty estimated by cross-validation

The absolute mean uncertainty in the rural maps in the areas covered by measurements is estimated by RMSE from the cross-validation as the most common indicator. The values are expressed in the units of its indicator (see Tables A3.3 – A3.6).

The absolute mean and relative mean uncertainty using the preferred method 3-O.Ear-a to create the rural map for all four indicators is given in Table A3.8. The relative mean uncertainty is the percentage of the absolute mean uncertainty value compared to the mean air pollution indicator value for all stations.

Table A3.8 Absolute and relative mean uncertainty in the 2005 rural maps created with 3-O.Ear-a of the four ozone indicators, expressed as RMSE of the cross-validation.

Ozone, rural, 2005, method 3-O.Ear-a	Uncertainty (RMSE of cross-validation)	
	Absolute units	Relative (%)
26th h.d.max.8hr avg	12.3 $\mu\text{g.m}^{-3}$	10.3
SOMO35	2173 $\mu\text{g.m}^{-3}.\text{days}$	35.5
AOT40c	7677 $\mu\text{g.m}^{-3}.\text{hours}$	40.7
AOT40f	12474 $\mu\text{g.m}^{-3}.\text{hours}$	41.5

In the Figures A3.11 and A3.12 the cross-validation scatter plots for the selected method 3-O.Ear-a are shown. The figures demonstrate the level of the underestimation of high values in the positions with no measurement within the areas covered by measurements. For example, the 26th highest maximum daily 8-hour value at the level $140 \mu\text{g.m}^{-3}$ is for such places estimated on average by the value of about $130 \mu\text{g.m}^{-3}$ only.

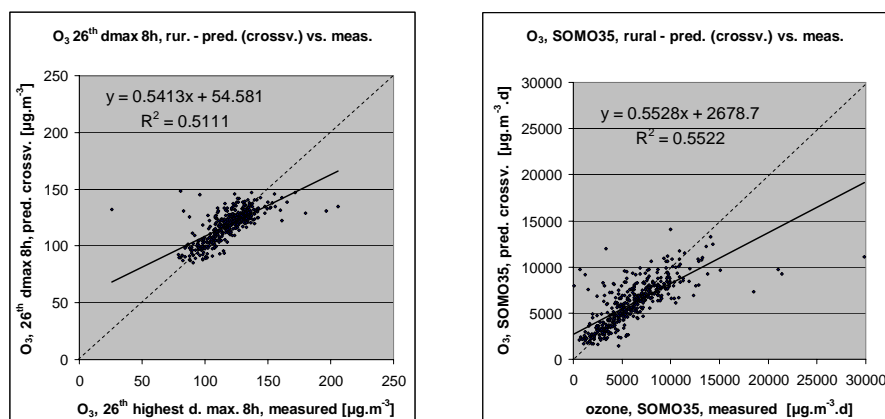


Figure A3.11 Correlation between cross-validation predicted values (y-axis) and measurements (x-axis) for the ozone health indicators 26th highest daily maximum 8-hour average values (left) and SOMO35 (right) for rural areas in 2005, as a result of the linear regression model O.Ear and ordinary kriging of its residuals.

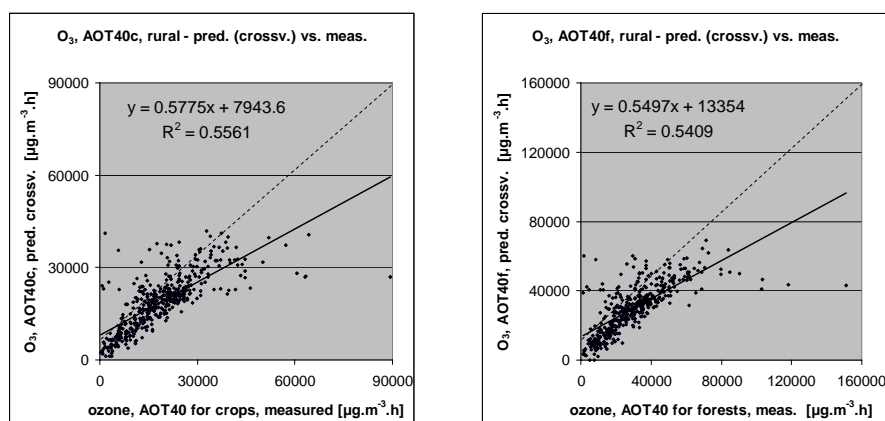


Figure A3.12 Correlation between cross-validation predicted values (y-axis) and measurements (x-axis) for the ozone vegetation indicators AOT40 for crops (left) and AOT40 for forests (right) for rural areas in 2005, as a result of the linear regression O.Ear and ordinary kriging of its residuals.

Comparing point measurement values with the predicted grid value

Additionally to the cross-validation, a simple comparison between the measured and interpolated values in a 10x10 km grid has been made. This comparison shows to what extent the predicted value of the corresponding grid cell represents the measured values covered by that cell. The regression results of the cross-validation compared to this gridded validation examination are summarised in Tables A3.9 and A3.10. The results of this simple comparison are quite poor, compared to both the cross-validation results (smaller improvement than expected) and last year's results, with e.g. a R^2 for SOMO35 of 0.77.

The table shows (except AOT40 for crops) better correlated relation between simple comparison of measurement stations and interpolated corresponding grid values for indicators (i.e. higher R^2 , smaller intercept and the slope closer to 1) than at the cross-validation predictions (Figure A3.11 and A3.12). This has its cause in the fact that the simple comparison between points measurements and gridded interpolated values shows the uncertainty at the stations locations (points) itself which tends to include less uncertainty than the cross-validation, simulating the behaviour of the interpolation at positions without measurement within the areas covered with measurements. The uncertainty at measurement locations is caused partly by the smoothing effect of interpolation and partly by the spatial averaging of the values in 10x10 km grid. Similar agreement with the measured data has been found in the analysis of the 2004-data (Horálek et al, 2007).

Table A3.9 Linear regression equation and coefficient of determination R^2 from the scatter plots of the predicted values based on cross-validation (above) and aggregation into 10x10 km grid (bottom) versus the measured values for ozone indicators 26th highest daily maximum 8-hour average values (left) and SOMO35 (right) for rural areas in 2005 as a result of the linear regression model O.Eaw and ordinary kriging of its residuals.

Indicator	ozone, rural areas			
	26 th high. d. 8-hr mean		SOMO35	
prediction	equation	R^2	equation	R^2
(i) Cross-validated predictions	$y = 0.5413x + 54.581$	0.5111	$y = 0.5528x + 2678.7$	0.5522
(ii) 10x10 km grid predictions	$y = 0.5726x + 50.884$	0.6053	$y = 0.5663x + 2591.5$	0.6014

Table A3.10 Linear regression equation and coefficient of determination R^2 from the scatter plots of the predicted values based on cross-validation (above) and aggregation into 10x10 km grid (bottom) versus the measured values for ozone indicators AOT40 for crops (left) and AOT40 for forests (right) for rural areas in 2005 as a result of the linear regression model O.Eaw and ordinary kriging of its residuals.

Indicator		ozone, rural areas			
		AOT40 for crops		AOT40 for forests	
prediction		equation	R^2	equation	R^2
(i)	Cross-validated predictions	$y = 0.5775x + 7943.6$	0.5561	$y = 0.5497x + 13354$	0.5409
(ii)	10x10 km grid predictions	$y = 0.5707x + 8045.1$	0.5707	$y = 0.5776x + 12480$	0.6145

Uncertainty maps

Next to the concentration maps (Figures A3.1 and A3.2), the uncertainty maps are constructed, see Figures A3.13 on the health indicators and Figure A3.14 on the vegetation indicators. The uncertainty presented corresponds to the kriging standard error, which is in fact the standard deviation of the predicted values. As expected, both figures show higher uncertainty at areas with lower rural station density and uncertainty increases the further away from the stations, e.g. in the Balkan, Scandinavia, Spain, Scotland, Iceland and southern Italy.

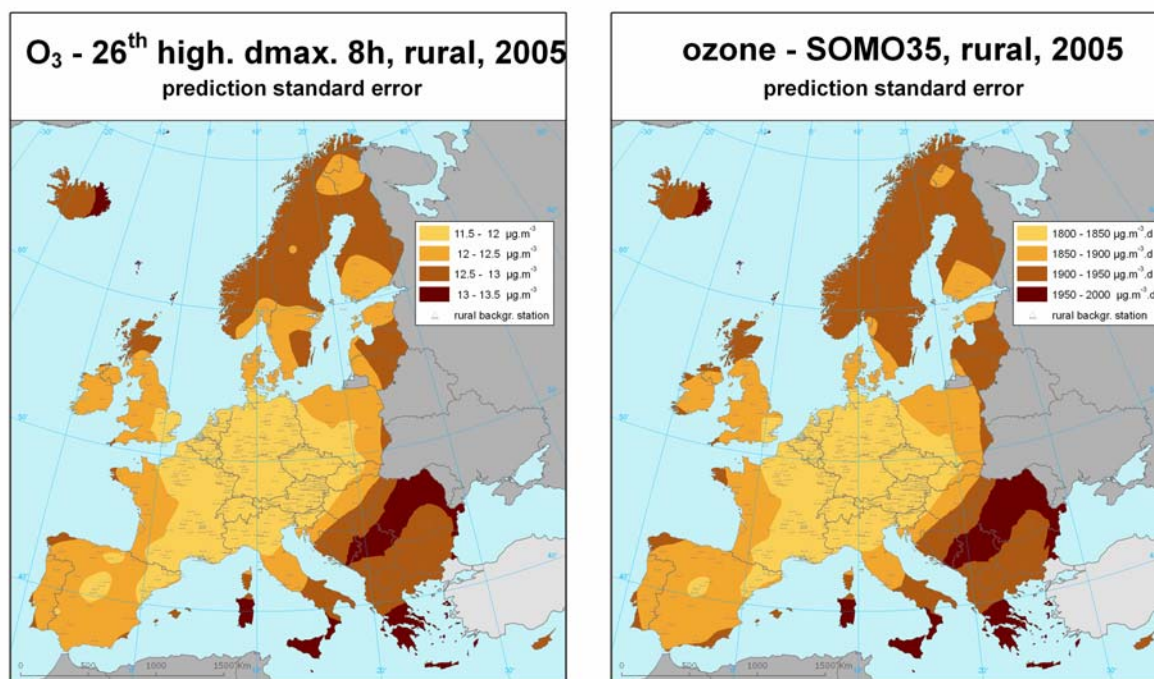


Figure A3.13 Uncertainty maps for the maps of the ozone health indicators 26th highest daily maximum 8-hour average values (left, in $\mu\text{g.m}^{-3}$) and SOMO35 (right, in $\mu\text{g.m}^{-3}.\text{days}$) on European scale for rural areas in 2005, 10 x 10 km grid resolution, as a result of the linear regression model P.Ear and ordinary kriging of its residuals.

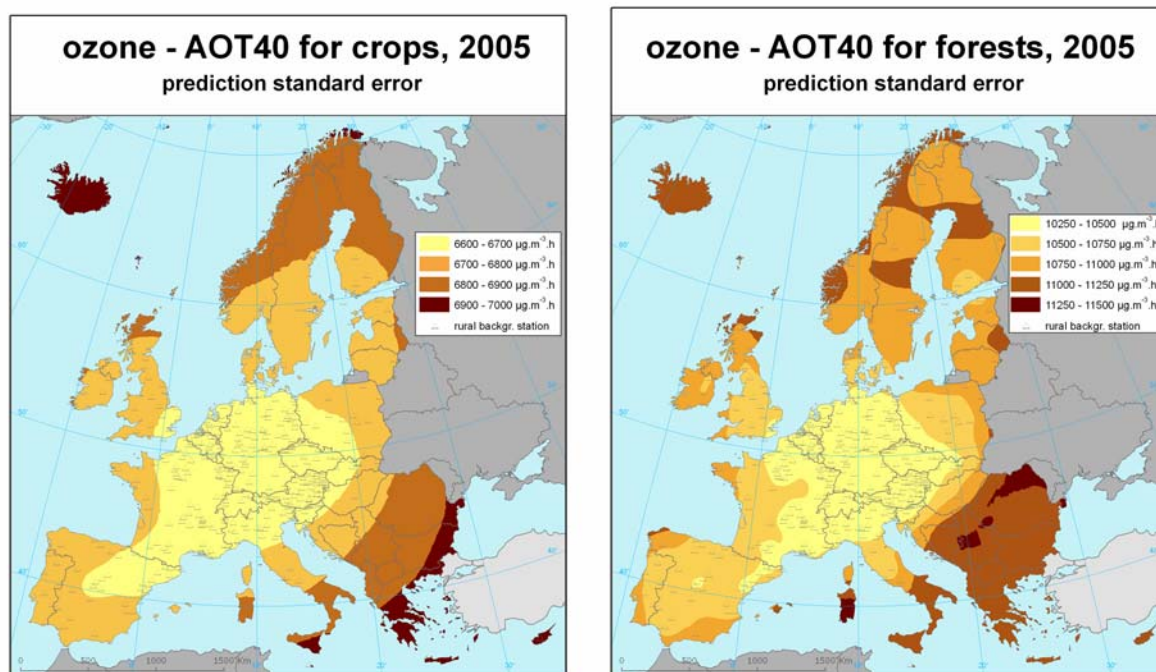


Figure A3.14 Uncertainty maps for the maps ozone vegetation indicators AOT40 for crops (left) and AOT40 for forests (right), in $\mu\text{g}\cdot\text{m}^{-3}\cdot\text{h}$ on European scale for rural areas in 2005, 10 x 10 km grid resolution, as a result of the linear regression model P.Ear and ordinary kriging of its residuals.

Probability map

Next, the maps of the probability of the target value exceedance in rural areas has been constructed, see Figure A3.15, using concentration and uncertainty maps (i.e. Figures A3.1 left and Figure A3.13 left) and the target values (TV, i.e. $120 \mu\text{g}\cdot\text{m}^{-3}$) for the 26th highest daily maximum 8-hour mean. The map shows high (> 75%) likelihood of daily mean exceedance in south Europe and to some less extend (> 50%) in central Europe, with more moderate likelihood (25-50%) more north-west ward, reaching relative modest (<25%) likelihood of exceedance in the north-west part of Europe.

The probability of target value of exceedance map in Figure A3.15 for AOT40 for crops has been composed from its concentration map (Figure A3.2), its uncertainty map (Figure A3.14 left) and its target value (TV, i.e. $18,000 \mu\text{g}\cdot\text{m}^{-3}\cdot\text{h}$).

The ozone directive does not define a target value for the AOT40 for forests; therefore no probability of exceedance map has been prepared. No limit or target value is set for the (WHO recommended) ozone health indicator SOMO35, therefore no probability of exceedance map could be prepared.

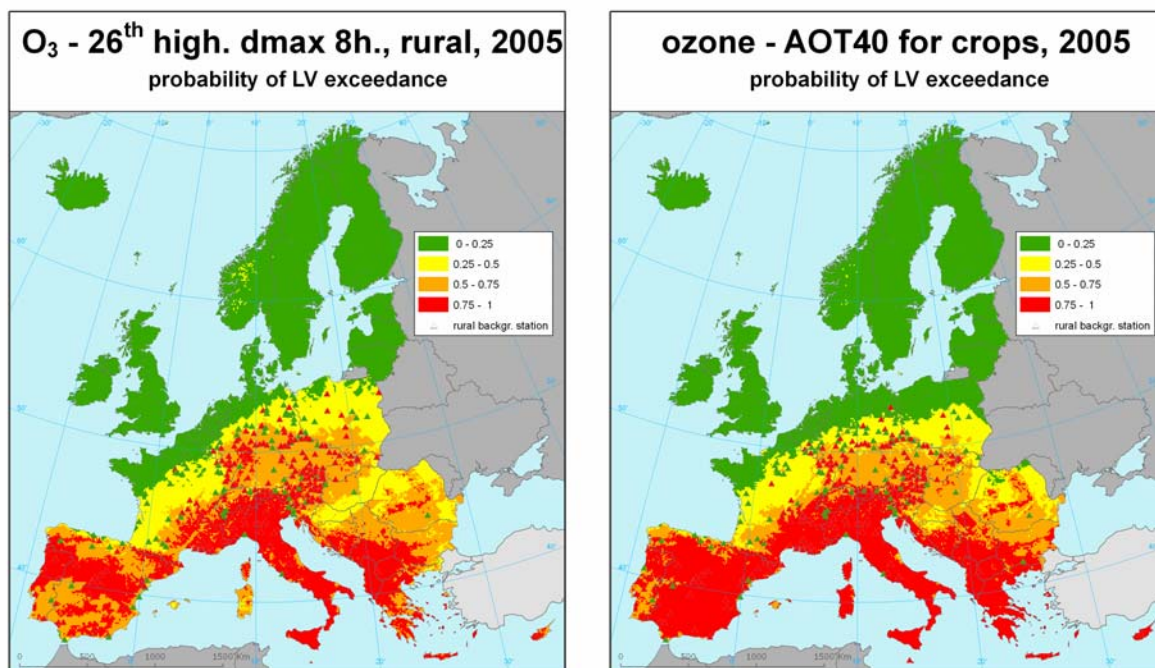


Figure A3.15 Probability of the limit value exceedance map for ozone health indicator 26th highest daily maximum 8-hour average values (in $\mu\text{g}\cdot\text{m}^{-3}$, left) and vegetation indicator AOT40 for crops ($\mu\text{g}\cdot\text{m}^{-3}\cdot\text{h}$, right) on European scale for rural areas in 2005, 10 x 10 km grid resolution, as a result of the linear regression model P.Ear and ordinary kriging of its residuals.

A3.2 Urban maps

A3.2.1 Linear regression analysis

The same procedure as in Section A3.1.1 is now followed for the urban and suburban areas for both health-related ozone indicators.

Horálek et al. (2007) used as mapping method the ordinary kriging on 2004 monitoring data only; no supplementary parameters were used in the final mapping in the case of urban ozone. Therefore, no method using a linear regression model or supplementary data is nominated here again.

With the use of 2005 data the supplementary parameters useful for further analysis of the linear regression model performance selected are, apart from EMEP model output: wind speed and relative humidity (coded UO.Ewh). For consistency with the rural mapping, another comparative set of variables is considered, i.e. solar radiation instead of relative humidity: wind speed and surface solar radiation (coded UO.Ewr). The models using EMEP and LOTOS-EUROS modelling output only (coded UO.E resp. UO.L) are examined as well.

Thus, the following linear regression models to be examined are:

Submodel	Input parameters
UO.E	EMEP model output
UO.Ewh	EMEP model output, wind speed, relative humidity
UO.Ewr	EMEP model output, wind speed, surface solar radiation
UO.L	LOTOS-EUROS model output

The statistical performance of these four linear regression models is presented in Table A3.11 for both human health indicators.

Table A3.11 Statistical parameter values for the selected linear regression models indicating their correlation between the ozone measurements based 26th highest daily maximum 8-hour mean and SOMO35 ozone concentration for 2005 in the urban areas.

Indicator	Ozone, 26th h.d.max.8-hr, 2005				Ozone, SOMO35, 2005				
	Linear regr. model	R ²	adjusted R ²	st. error [µg.m ⁻³]	RMSE [µg.m ⁻³]	R ²	adjusted R ²	st. error [µg.m ⁻³]	RMSE [µg.m ⁻³]
UO.E		0.413	0.413	12.19	12.17	0.455	0.454	1666	1664
UO.Ewh		0.526	0.525	10.96	10.94	0.502	0.500	1594	1590
UO.Ewr		0.514	0.512	11.10	11.07	0.488	0.486	1617	1613
UO.L		0.108	0.107	15.0	15.0	0.291	0.290	1900	1897

Table A3.11 shows the results for the 26th highest daily maximum 8-hour average ozone concentration. The values of R² and RMSE for the models of the methodology type 2 (i.e. UO.E) and 3 (UO.Ewh and UO.Ewr) show quite clearly that the addition of supplementary parameters substantially improves the closeness of the regression relation by an increased R² of about 0.11 and a decreased RMSE by approximately 1.4, i.e. one tenth. Similarly, the R² and RMSE for the models of type 2 (UO.E) and 4 (UO.L) indicate that the closeness of regression is considerably higher when the EMEP modelled concentration field is used, instead of the LOTOS-EUROS modelled field.

The table shows for SOMO35 quite similar results as for the first indicator, however, with smaller differences between the models. The addition of supplementary parameters improves the closeness of the regression relation by a maximum R² increase of 0.05 and a decreased RMSE of about 4%. The closeness of the regression improves considerably when output from the EMEP model is used, instead of LOTOS-EUROS model output.

Conclusions:

- At both indicators the addition of supplementary parameters improves the closeness of the linear regression relation with the indicator values of the ozone measurements.
- At both indicators the closeness of the linear regression is considerably higher when using the EMEP modelled concentration field instead of the LOTOS-EUROS modelled field. Despite the models are not developed for urban modelling purposes the EMEP shows still reasonable correlation (R^2 just above 0.4), whereas LOTOS-EUROS shows indeed rather poor correlation for ozone.

These conclusions do indicate that the methods using linear regressions most likely will perform better by including additional supplementary parameter next to EMEP modelling data in the interpolation methods on (sub)urban ozone indicators, which will be compared in next section.

A3.2.2 Spatial interpolation

From the four methodological types we examine the most promising interpolation methods by comparing the RMSE and other statistical indicators from the cross-validation. (Neither lognormal kriging nor lognormal cokriging has been examined, because preliminary analysis showed worse results than ordinary kriging and ordinary cokriging at both health-related ozone indicators.)

The four methods we examine are:

1. Interpolation using primarily monitoring data

a. Ordinary kriging (OK)

c. Ordinary cokriging (OC)

2. Interpolation using monitoring data and EMEP model data

Linear regression using EMEP model output (UO.E), followed by interpolation of its residuals using OK.

3. Interpolation using monitoring data, EMEP model data and other supplementary data

Linear regression model using EMEP model output, wind speed and relative humidity (UO.Ewh), followed by interpolation of its residuals using OK

Linear regression model using EMEP model output, wind speed and surface solar radiation (UO.Ewr), followed by interpolation of its residuals using OK

4. Interpolation using monitoring data and LOTOS-EUROS model data

Linear regression using LOTOS-EUROS model output (UO.L), followed by interpolation of its residuals using OK

The statistical indicators of the cross-validation of the methods are presented in Table A3.12 for the 26th highest daily maximum 8-hour average ozone concentration and in Table A3.13 for SOMO35. All the statistical indicators, with exception of R^2 , are expressed in the same units as the relevant ozone indicator.

Table A3.12 Comparison of different interpolation methods showing RMSE and the other statistics and linear regression parameters from the cross-validation scatter plots of the predicted values for ozone indicator 26th highest daily maximum 8-hour average value for 2005 in urban areas. Apart of R² and a, all other statistical indicators are in µg.m⁻³

mapping method		26 th highest maximum daily 8-hour mean [µg.m ⁻³]									
		RMSE	MPE	min.	max.	MAE	MedAE	MPSE	linear regr. y=a.x+c		
				error	error				a	c	R ²
1-a	interp. OK	10.25	0.00	-42.08	67.23	7.09	5.16	8.20	0.609	44.15	0.603
1-c	interp. OC	10.24	-0.01	-42.78	67.18	7.10	5.27	7.89	0.613	43.69	0.603
2-UO.E-a	lin. regr. UO.E + OK	10.11	0.04	-39.18	58.48	7.20	5.23	9.60	0.628	42.14	0.597
3-UO.Ew h-a	lin. regr. UO.Ew h + OK	10.12	-0.04	-39.18	54.62	7.21	5.14	7.86	0.642	40.44	0.598
3-UO.Ew r-a	lin. regr. UO.Ew r + OK	10.01	0.09	-39.16	52.99	7.13	5.05	9.11	0.638	41.02	0.605
4-UO.L-a	lin. regr. UO.L + OK	10.09	-0.11	-44.60	69.43	7.01	5.19	8.25	0.636	41.07	0.600

Table A3.13 Comparison of different interpolation methods showing RMSE and the other statistics and linear regression parameters from the cross-validation scatter plots of the predicted values for ozone indicator SOMO35 for 2005 in urban areas. Apart of R² and the slope a, all other statistical indicators are in µg.m⁻³.days.

mapping method		SOMO35 [µg.m ⁻³ .days]									
		RMSE	MPE	min.	max.	MAE	MedAE	MPSE	linear regr. y=a.x+c		
				error	error				a	c	R ²
1-a	interp. OK	1473	2	-7097	10260	1001	692	1303	0.583	1882.8	0.576
1-c	interp. OC	1470	0	-6814	10252	1000	687	1307	0.585	1868.7	0.578
2-UO.E-a	lin. regr. UO.E + OK	1486	0	-7036	9781	1015	690	1363	0.595	1829.4	0.567
3-UO.Ew h-a	lin. r. m. UO.Ew h + OK	1474	1	-6783	9223	1004	659	1295	0.598	1818.7	0.574
3-UO.Ew r-a	lin. r. m. UO.Ew r + OK	1459	4	-6690	9421	1000	664	1312	0.605	1792.0	0.582
4-UO.L-a	lin. regr. UO.L + OK	1510	-5	-7361	10919	1018	686	1257	0.604	1784.6	0.555

As indicated in Chapter 1, inter-annual comparison would be done this in paper for the urban areas in addition to the one for rural areas in Horálek et al. (2007). Table A3.14 shows the RMSE of the cross-validation using the 2005-data for the nominated methods of the five methodology types. This comparison could only be performed for SOMO35, while no 2004-data output of the EMEP model output was available for the 26th highest daily maximum 8-hour averages.

Table A3.14 Comparison of different interpolation methods showing RMSE for the ozone indicator SOMO35 for the years 2004 and 2005 in urban areas. The smaller RMSE means the more accurate the estimation by the mapping method. RMSE is in µg.m⁻³.days.

mapping method		SOMO35 [µg.m ⁻³ .days], RMSE		
		2004	2005	avg
1-a	interpolation OK	1413	1473	1443
1-c	interpolation OC	1372	1470	1421
2-UO.E-a	lin. regr. UO.E + OK	1464	1486	1475
3-UO.Ehw-a	lin. r. m. UO.Ehw + OK	1434	1474	1454
3-UO.Erw-a	lin. r. m. UO.Erw + OK	1426	1459	1443

A number of comparison conclusions can be drawn from the results provided in Tables A3.12 – A3.14 for the urban areas:

- When ranking the statistics (RMSE, SDE, MAE, R² and MPSE) of the methods of methodology type 1, interpolation using 2005 monitoring data only, slightly better results for both ozone indicators are obtained with ordinary cokriging, method 1-c. This is similar to Horálek et al. (2007) as far as it was examined on the 2004 data.

- When ranking statistics within the methods of methodology type 3, slightly better results are obtained by the linear regression model using EMEP output, wind speed and surface solar radiation, followed by residual interpolation by ordinary kriging, method 3-UO.Ewr-a.
- The statistics of methods of both methodology type 1 and 3 show very comparable performances. As such these statistical indicators do not provide the driving arguments for the selection of the method to use best or preferred for urban ozone health indicator interpolated mapping. Methods of type 3 have the advantage of providing a more complete European coverage, especially at areas lacking monitoring stations.
- The comparison of the method of the types 2 and 4 (i.e. use of EMEP or LOTOS-EUROS model) shows quite similar results at both ozone indicators, with EMEP providing slightly better results at SOMO35 and LOTOS-EUROS slightly better at the 26th highest daily maximum 8-hour mean. Preference would go to EMEP due to its better regression performance in Section A3.2.1.
- The comparison of the method of the methodology types 2 and 3 shows better results for the methods of type 3 (i.e. linear regression including next to modelling output also other supplementary parameter) for both ozone indicators, based on RMSE (and almost all statistical indicators). The addition of supplementary parameters improves the interpolation on 2005 data, which was not a clear-cut case at the use of 2004 data in Horálek et al. (2007).
- The linear regression results of cross-validation scatter plots show that the smoothing effect of the interpolation is lowest for methods 1-c and 3-UO.Ewr which show similarly highest R², they show similar lowest overestimated predictions (lowest intercepts) at the lower indicator values, and they show smallest underestimated predictions at the higher indicator values (slope closest to 1). The slightly better results are given by the method UO.Ewr.
- An inter-comparison of the methods of the types 1, 2, 3 shows that overall slightly better results are obtained with the methods of type 3 (linear regression model including supplementary data, following ordinary kriging of its residuals) for 2005 data, and within that type the method 3-UO.Ewr-a (linear regression using EMEP output, wind speed and surface solar radiation) performs best.

Concluding from the above the selection of the most preferred method for urban ozone mapping is 3-UO.Ewr-a at both health indicators. It shows overall the best statistical indicators for both health indicators. Furthermore, it has the advantage of providing European coverage, also at areas without measurements. Finally, it uses the same meteorological supplementary parameter as the method (3-O.Ear-a) selected for interpolated mapping of both ozone health indicators for the rural areas.

The resulting urban maps for the 26th highest daily maximum 8-hour mean and for SOMO35 using the selected interpolation method 3-UO.Ewr-a are shown in Figure A3.16. Values of the key parameters used for mapping are given in Table A3.15.

Table A.3.15 Parameters of the method used for final mapping of ozone measurement parameters 26th highest daily maximum 8-hour average values(left) and SOMO35 (right) for 2005 in the urban areas, i.e. linear regression model O.Ewr following by the interpolation on its residuals using ordinary kriging (OK).

linear regr. model UO.Ewr + OK on its residuals	highest 26 th max. d. 8h	SOMO35
	coeff.	coeff.
c (constant)	51.93	-41.8
a1 (EMEP model 2005)	0.577	0.525
a2 (wind speed 2005)	-5.744	-376.2
a3 (s. solar radiation 2005)	1.170	245.6
nugget	60	1.2E+06
sill	100	2.0E+06
range [km]	140	100

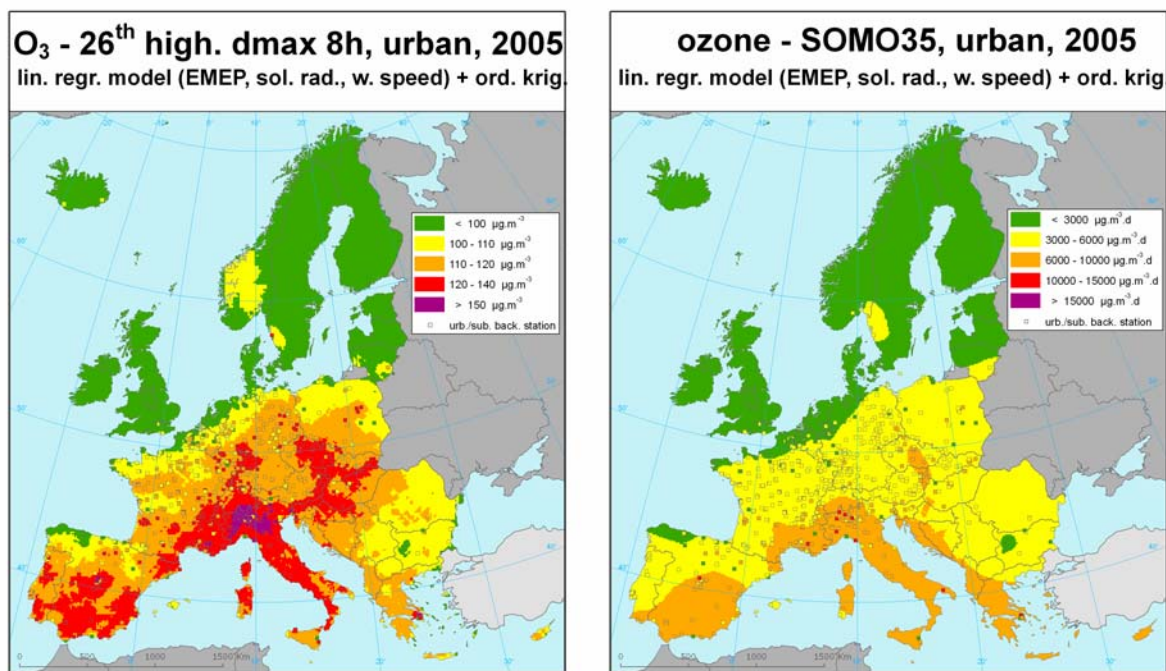


Figure A3.16 Maps showing ozone health indicators 26th highest daily maximum 8-hour average values (left, in $\mu\text{g.m}^{-3}$) and SOMO35 (right, in $\mu\text{g.m}^{-3}.\text{days}$) on European scale for urban areas in 2005, 10 x 10 km grid resolution, as a result of interpolation method 3-UO.Ewr-a. Absolute and relative uncertainty of these maps expressed by RMSE is 10 $\mu\text{g.m}^{-3}$ and 8.9 % (left), and 1459 $\mu\text{g.m}^{-3}.\text{days}$ and 32.4 % (right). The maps are applicable in the urban areas only.

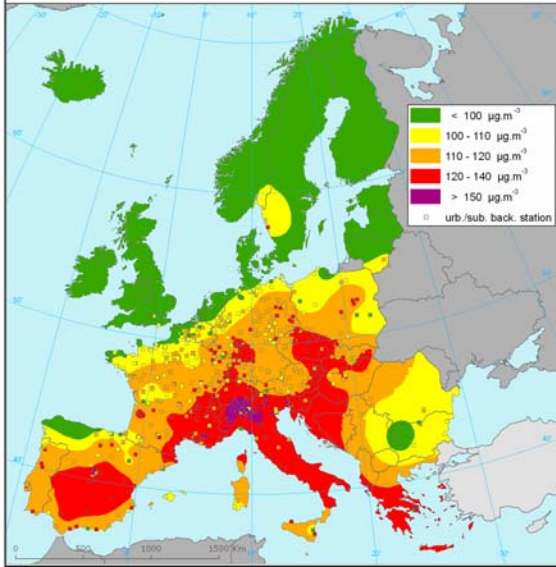
A3.2.3 Uncertainty analysis

Comparing concentration maps of the interpolation methods

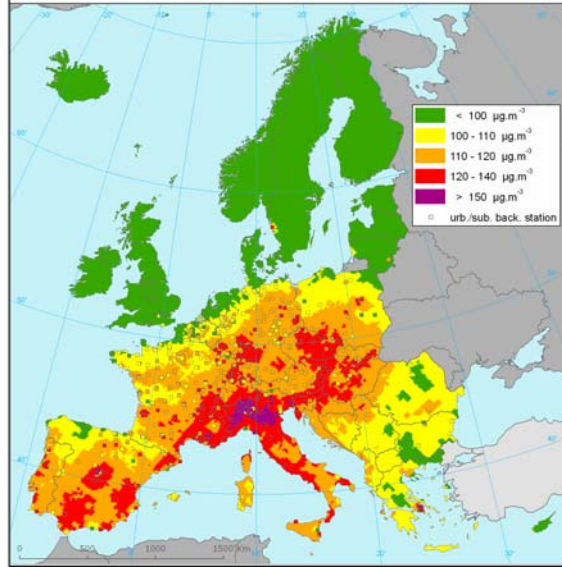
The interpolated maps of urban ozone health indicators based on the preferred method 3-UO.Ewr-a as well as methods 1-c, 2UO.E-a and 4UO.L-a are shown in Figure A3.17 for the 26th highest daily maximum 8-hour average and Figure A3.18 for the SOMO35. In Figures A3.19 and A3.20 the differences between the selected method 3-UO.Ewr-a and other methods are shown. The patterns of the four methods are quite similar: the maps all show a reducing concentration gradient from southern to northern Europe. The difference maps show some regional differences between the concentration levels of the preferred method 3-UO.Ewr-a and method 1-c and 2UO.e-a. The difference with 1-c may be explained by reduced interpolation accuracy away from the stations, whereas the difference with for 2-UO.E-a is most likely determined by the meteorological parameters at the daily based indicator.

Figure A3.21 illustrates for both indicators the difference between method 2-O.E-a (EMEP) and the corresponding method 4-O.L-a (LOTOS-EUROS). Both ozone health indicators show a pattern in the methods being quite similar, with EMEP showing somewhat higher concentrations in northern Scandinavia and LOTOS-EUROS tending to have somewhat higher concentrations in south Sweden with a typical emphasize at the region Oslo-Göteborg. Furthermore, at several regions in the south of Europe, and more specifically south Balkan, Greece and central Spain, LOTO-EUROS tends to show higher concentrations. In comparison with the rural maps, the urban differences are smaller between the methods, having their main cause in the higher number of urban stations than there rural stations being used in the interpolations. However, particular differences such as for Greece are related to differences in the interpolation methods itself.

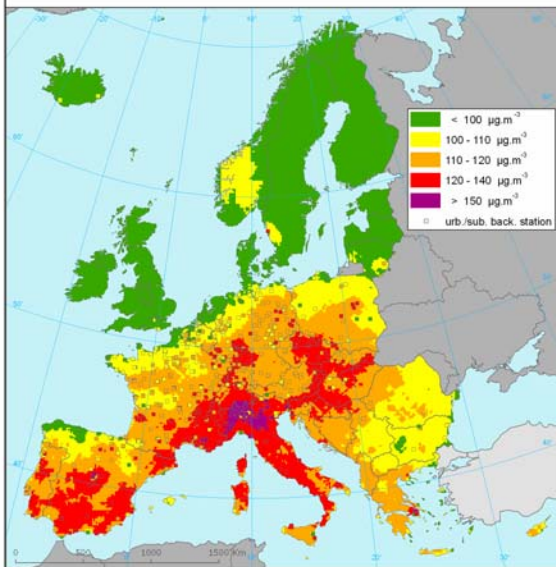
O₃ - 26th high. dmax 8h, urban, 2005
ordinary cokriging



O₃ - 26th high. dmax 8h, urban, 2005
linear regression (EMEP) + ord. kriging



O₃ - 26th high. dmax 8h, urban, 2005
lin. regr. model (EMEP, sol. rad., w. speed) + ord. krig.



O₃ - 26th high. dmax 8h, urban, 2005
lin. regression (EUROS-LOTOS) + ord. kriging

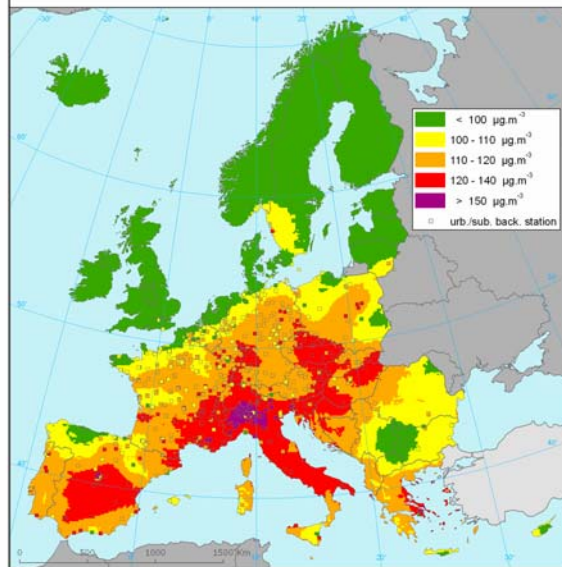


Figure A3.17 Maps showing ozone 26th highest daily maximum 8-hour average values (in $\mu\text{g}\cdot\text{m}^{-3}$) on European scale for urban areas in 2005, 10 x 10 km grid resolution, as a result of interpolation method 1-c (top, left), 2-UO.E-a (top, right), 3-UO.Ewr-a (bottom, left) and 4-UO.L-a (bottom, right).

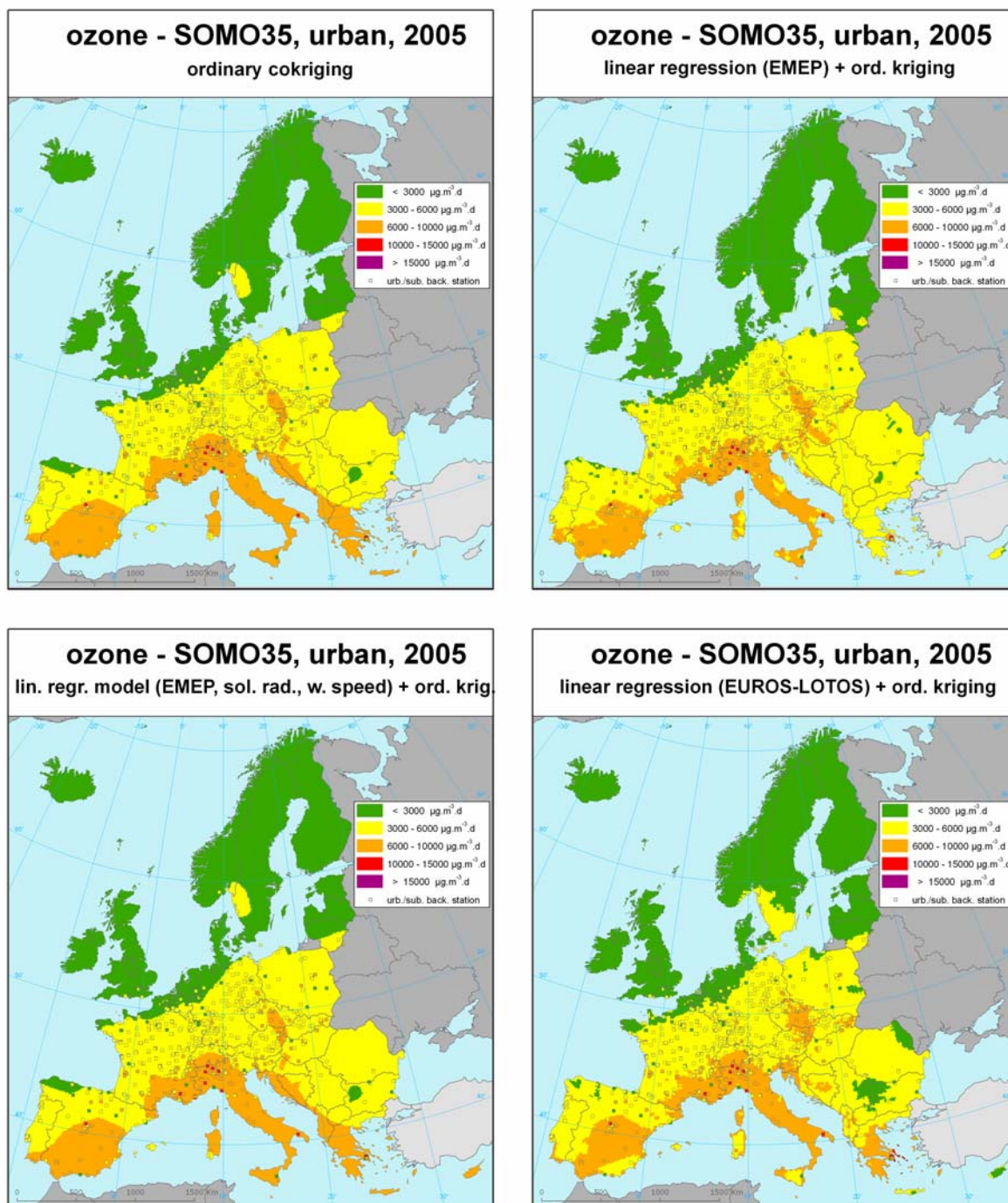
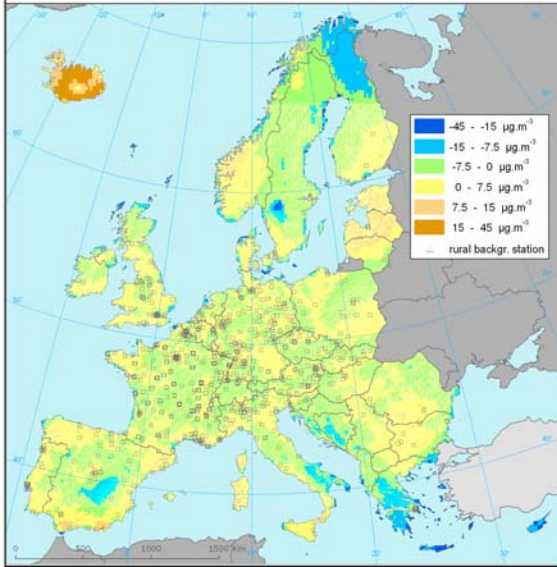


Figure A3.18 Maps showing ozone SOMO35 (in $\mu\text{g.m}^3.\text{days}$) on European scale for urban areas in 2005, 10 x 10 km grid resolution, as a result of interpolation method 1-c (top, left), 2-UO.E-a (top, right), 3-UO.Ewr-a (bottom, left) and 4-UO.L-a (bottom, right).

O₃ - 26th high. dmax 8h, urban, 2005
 difference between methods 3-UO.Ewr-a and 1-c



O₃ - 26th high. dmax 8h, urban, 2005
 differ. between methods 3-UO.Ewr-a and 2-UO.E-a

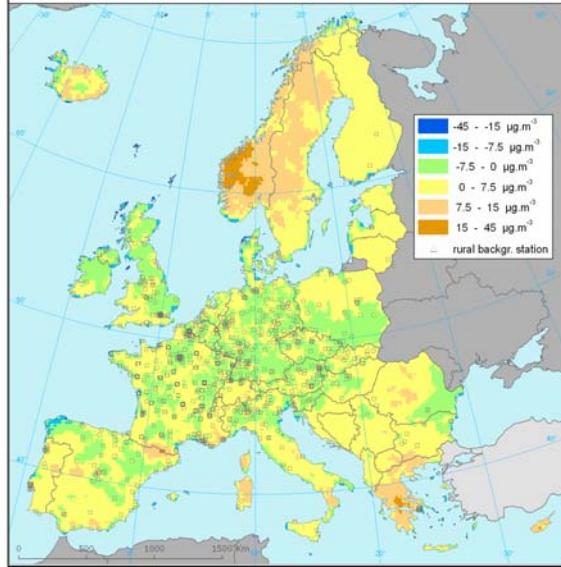
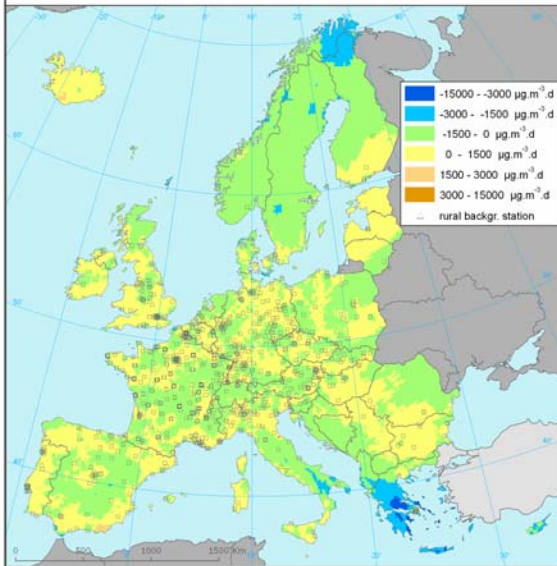


Figure A3.19 Maps showing the difference of the selected method 3-UO.Ewr-a and the method 1-c (left), resp. 2-UO.E-a (right) for 26th highest daily maximum 8-hour average values (in µg.m⁻³) on the European scale for urban areas in 2005, 10 x 10 km grid resolution. Negative values show up at areas with higher concentrations of the alternative method (1-c left, 2-UO.E-a right) compared to the preferred method 3-UO.Ewr-a.

ozone - SOMO35, urban, 2005
 difference between methods 3-UO.Ewr-a and 1-c



ozone - SOMO35, urban, 2005
 diff. between methods 3-UO.Ewr-a and 2-UO.E-a

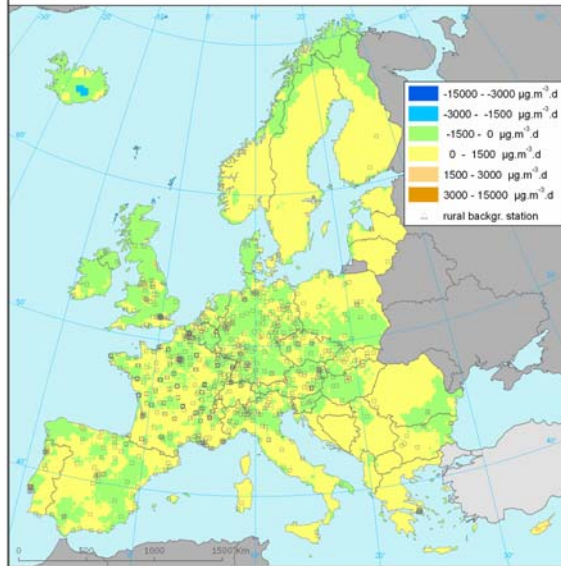


Figure A3.20 Maps showing the difference of the selected method 3-UO.Ewr-a and the method 1-c (left), resp. 2-UO.E-a (right) for SOMO35 (in µg.m⁻³.days) on the European scale for urban areas in 2005, 10 x 10 km grid resolution. Negative values show up at areas with higher concentrations of the alternative method (1-c left, 2-UO.E-a right) compared to the preferred method 3-UO.Ewr-a.

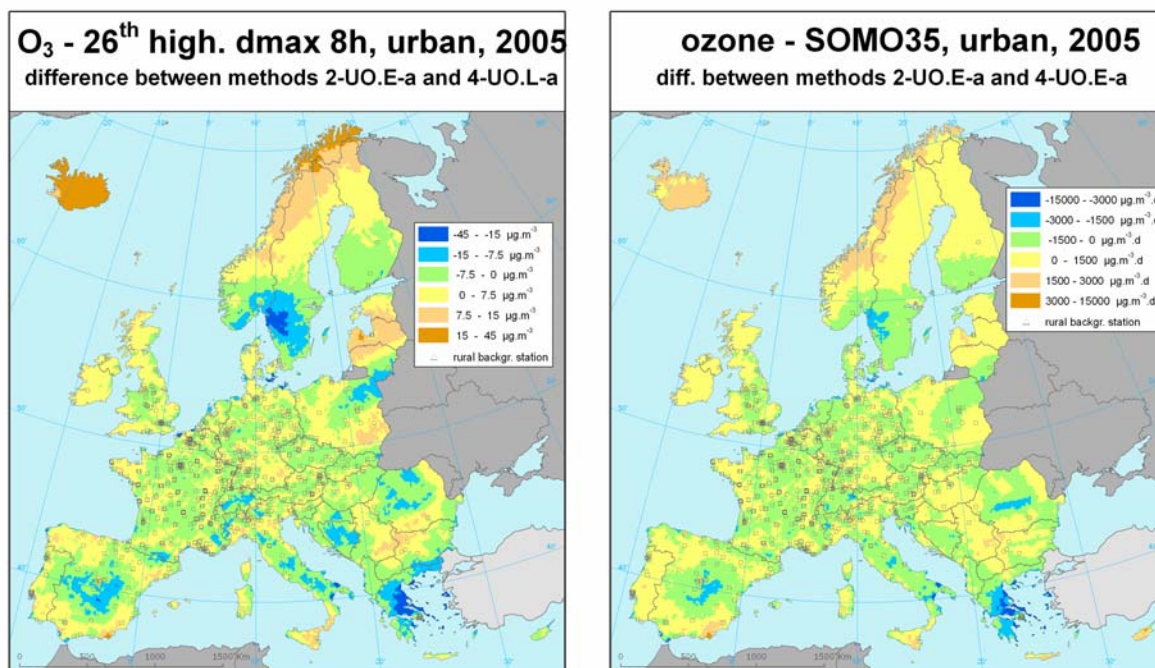


Figure A3.21 Maps showing the difference between the methods using output from the EMEP model (2-UO.E-a) and from the LOTOS-EUROS model (4-UO.L-a) for 26th highest daily maximum 8-hour average in $\mu\text{g.m}^{-3}$ (left) and SOMO35 in $\mu\text{g.m}^{-3}\cdot\text{day}$ (right) on the European scale for rural areas in 2005, 10 x 10 km grid resolution. Negative values show higher concentrations of method 4-UO.L-a.

Uncertainty estimated by cross-validation

The RMSE from the cross-validation is the most common indicator for the absolute mean uncertainty of the maps in the areas covered by measurements (see Tables A3.12 and A3.13). Using the preferred method 3-UO.Ewr-a, the absolute mean uncertainty of the urban map of the 26th highest daily maximum 8-hour average concentration is $10 \mu\text{g.m}^{-3}$ and for the the urban map of SOMO35 it is $1459 \mu\text{g.m}^{-3}\cdot\text{days}$.

Alternatively, this uncertainty can be also expressed as the relative mean uncertainty, being the percentage the absolute mean uncertainty indicator value is compared to the mean indicator value for all stations. The relative mean uncertainty of the urban map of the 26th highest daily maximum 8-hour average concentration is 8.9 % and of the urban map of SOMO35 is 32.4 % in case method 3-UO.Ewr-a is used for mapping.

The Figure A3.22 presents the cross-validation scatter plot regression results for the urban areas. It shows the smoothing effect of the interpolation (preceded with or without linear regression) is lowest for method 1-c and 3-UO.Ewr. The figures demonstrate the level of underestimation of high values in positions without measurement within the areas covered by measurements: for example, the value of SOMO35 at the level of $10,000 \mu\text{g.m}^{-3}\cdot\text{day}$ is estimated in the places without measurement on average as about $7900 \mu\text{g.m}^{-3}\cdot\text{day}$.

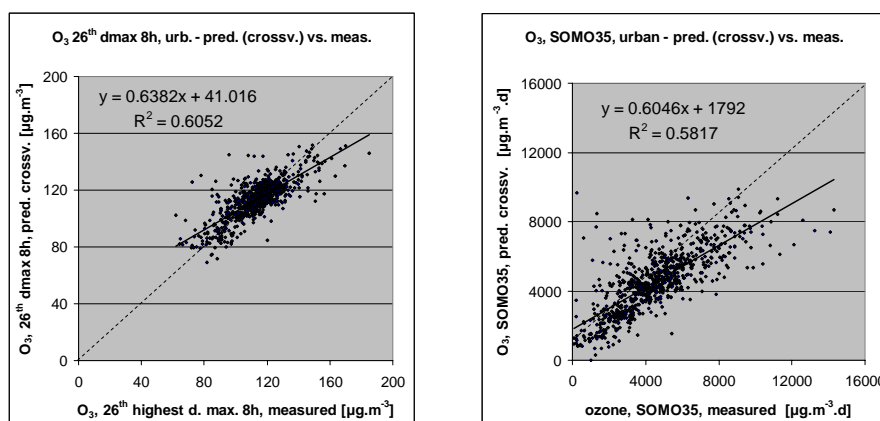


Figure A3.22 Correlation between cross-validation predicted values (y-axis) and measurements (x-axis) for the ozone indicators 26th highest daily maximum 8-hour average values (left) and SOMO35 (right) for urban areas in 2005, as a result of the linear regression model UO.Ewr and ordinary kriging of its residuals.

Comparing point measurement values with the predicted grid value

Additionally to cross-validation, a simple comparison between the measured and interpolated values in a 10x10 km grid has been made. This comparison shows to what extent the predicted value of the corresponding grid cell represents the measured values covered by that cell. The regression results of the cross-validation compared to this gridded validation examination are summarised in Table A3.16.

This simple comparison shows at both urban indicators better correlation between stations measurements and corresponding predicted grid values (higher R^2 , slope closer to 1, lower intercept) than the cross-validation predictions. This has its cause in the fact that the simple comparison between points measurements and gridded interpolated values shows the uncertainty at the stations locations (points) itself which tends to include less uncertainty than the cross-validation, simulating the behaviour of the interpolation at positions without measurement within the areas covered with measurements. The uncertainty in the simple comparison is determined partly by the smoothing effect of interpolation and partly by the spatial averaging of the values in 10x10 km grid.

The agreement of the measured and estimated values is better than in the case of rural areas; it is quite the same (for 26th highest max. daily 8-hor mean), resp. slightly worse (for SOMO35) in comparison with 2004 data in the case (R^2 was 0.78, resp. 0.85).

Table A3.16 Linear regression equation and coefficient of determination R^2 from the scatter plots of the predicted values based on cross-validation (above) and aggregation into 10x10 km grid (bottom) versus the measured values for ozone indicators 26th highest daily maximum 8-hour average values (left) and SOMO35 (right) for urban areas in 2005 as a result of the linear regression model UO.Ewr and ordinary kriging of its residuals.

Indicator	O ₃ , rural areas			
	26 th high. max. d. 8-hr mean		SOMO35	
prediction	equation	R ²	equation	R ²
(i) Cross-validated predictions	y = 0.6382x + 41.016	0.6052	y = 0.6047x + 1791.5	0.5816
(ii) 10x10 km grid predictions	y = 0.7324x + 30.391	0.7774	y = 0.7185x + 1280.9	0.7862

Uncertainty maps

Next to the concentration maps (Figure A3.16), the uncertainty maps are constructed, see Figure A3.23. The uncertainty is higher in areas with the lower density and increasing further away from the urban and suburban stations. The urban maps show a lower uncertainty compared to the rural uncertainty maps in Figure A3.13, for two reasons: (1) ozone concentrations tend to be lower in urban

areas compared to rural areas due to reductions caused by nitrogen emissions from the higher traffic intensity in urbanised areas, and (2) the higher number and therefore higher density of the urban (and suburban) stations in the mapping areas reduce the uncertainties between the stations.

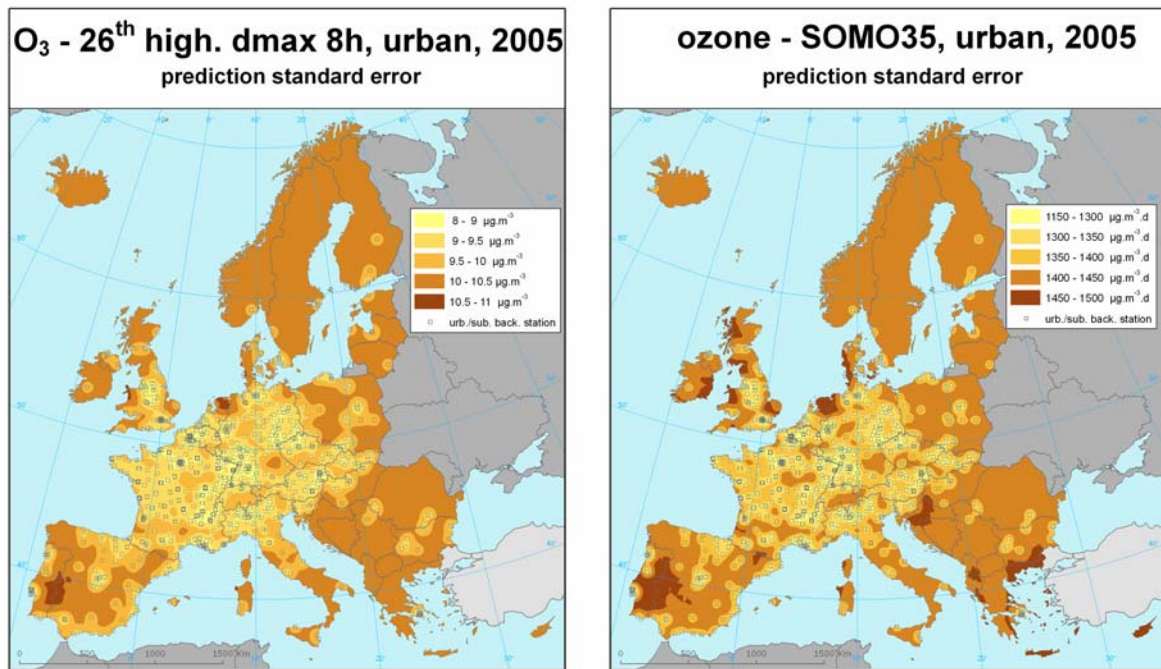


Figure A3.23 Uncertainty maps for the maps showing values of ozone parameters 26th highest daily maximum 8-hour average values (left, in $\mu\text{g.m}^{-3}$) and SOMO35 (right, in $\mu\text{g.m}^{-3}.\text{days}$) on European scale for urban areas in 2005, 10 x 10 km grid resolution, as a result of interpolation method 3-UO.Ewr-a. The maps are applicable in the urban areas only.

Probability map

Next, the map of the probability of the target value exceedance in rural areas has been constructed for the health indicator 26th highest daily maximum 8-hour average value, using the urban concentration and uncertainty map (i.e. Figures A3.16 left, and A3.23 left) with a ozone directive defined target values of $120 \mu\text{g.m}^{-3}$. The probability of exceedance map is presented in Figure A3.24.

The map shows high (> 75%) likelihood of daily mean exceedance in a large region consisting of northern Italy, the southern and western Alps, the French and northern Spanish mediteranean coastal zone. Furthermore regions in central and southern Spain, central Germany and the region of Rome-Napels. Large parts of south and central Spain, parts of Portugal, Italy and central-eastern Europe show quite moderate probability levels (> 50%) with 25-50% in the periphery of these regions. More north and north-westward bound the levels reach relative modest (<25%) likelihood of exceedance.

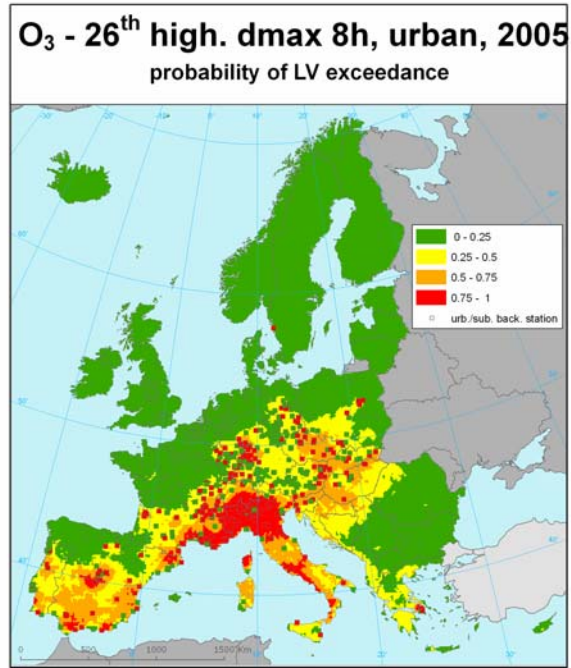


Figure A3.24 Probability of the limit value exceedance map for ozone parameter 26th highest daily maximum 8-hour average values (in $\mu\text{g}\cdot\text{m}^{-3}$) on European scale for urban areas in 2005, 10 x 10 km grid resolution, as a result of interpolation method 3-UO.Ewr-a. The maps are applicable in the urban areas only.

Annex 4 SO₂ spatial analysis

The two SO₂ ecosystem-related indicators are examined here: annual average and winter average SO₂ concentrations. It concerns vegetation that is considered only to occur at rural areas and therefore we focus on mapping of rural areas only in this Annex.

A4.1 Rural maps

A4.1.1 Linear regression analysis

In Horálek et al. (2007) only the annual average has been examined and mapped on 2004 data, using a linear regression model with EMEP output only, followed by residual interpolation by ordinary kriging. This method is nominated for examination here again (coded S.E).

With the 2005 data the selection of the supplementary parameters, apart from the EMEP model output, that fit the linear regression significantly are: wind speed, surface solar radiation and temperature (coded S.Ewrt) for both indicators.

Thus, the following linear regression models to be examined are:

Submodel	Input parameters
S.E	EMEP model output
S.Ewrt	EMEP model output, wind speed, surface solar radiation, temperature

The statistical performance of these two linear regression models is presented in Tables A4.1 for both indicators.

Table A4.1 Statistical indicator values of the selected linear regression models indicating the correlation between supplementary data and the annual average and winter average of the 2005 measurement SO₂ concentrations in the rural areas.

Indicator	SO ₂ Annual average, 2005				SO ₂ winter average, 2005			
	R ²	adjusted R ²	st. error [µg.m ⁻³]	RMSE [µg.m ⁻³]	R ²	adjusted R ²	st. error [µg.m ⁻³]	RMSE [µg.m ⁻³]
S.E	0.269	0.266	2.44	2.44	0.323	0.321	3.01	3.00
S.Ewrt	0.344	0.335	2.33	2.30	0.409	0.400	2.83	2.80

Table A4.1 shows at the two indicators better values of R² and RMSE for the linear regression model of the methodology type 3 (S.Ewrt) than for the one of type 2 (i.e. S.E), indicating that the regression relation improves when supplementary parameters are included. For SO₂ annual average the R² increases by 0.07 and RMSE decreases by approximately 5%. For the SO₂ winter average R² increases by 0.08 and RMSE decreases by about 6%.

Conclusion:

- At both indicators the addition of supplementary parameters show limit improvement, compared to the majority of other air pollution indicators, in the closeness of the linear regression relation with the measurement based indicator values.

This conclusion indicates that the interpolation methods using linear regressions have limited profit of the inclusion of additional supplementary parameter.

A4.1.2 Spatial interpolation

The four most promising methods of the three methodological types we examine (no cokriging method is examined because of lacking relation of SO₂ concentrations with altitude), by comparing the RMSE and other statistical indicators from the cross-validation, are:

1. Interpolation using primarily monitoring data

a. Ordinary kriging (OK)

b. Lognormal kriging (LK)

2. Interpolation using monitoring data and EMEP model data

Linear regression using EMEP model output (S.E), followed by interpolation of its residuals using OK.

3. Interpolation using monitoring data, EMEP model data and other supplementary data

Linear regression model using EMEP model output, altitude and surface solar radiation (S.Ewrt), followed by interpolation of its residuals using OK

The statistical indicators of the cross-validation of the methods are presented in Table A4.2 for the annual average SO₂ concentration and in Table A4.3 for winter annual average SO₂ concentration. The main criterion is RMSE, followed by MAE, MPE, MedAE and other indicators. All the indicators, with exception of R², are expressed in µg.m⁻³.

Table A4.2 Comparison of different interpolation methods showing RMSE and the other statistics and linear regression parameters from the cross-validation scatter plots of the predicted values for the SO₂ annual averages for 2005 in rural areas. Apart of R² and a, all other statistical indicators are in µg.m⁻³

mapping method		RMSE	MPE	min. error	max. error	MAE	MedAE	MPSE	linear regr. y=a.x+c		
									a	c	R ²
1-a	interp. OK	2.12	0.04	-9.75	4.51	1.42	0.93	1.91	0.472	1.96	0.447
1-b	interp. LK	2.08	-0.03	-9.87	4.30	1.36	0.84	1.87	0.497	1.80	0.470
2-S.E-a	lin. regr. S.E + OK	1.93	0.00	-9.93	5.35	1.29	0.89	1.71	0.592	1.49	0.547
3-S.Ewrt-a	lin. r. m. S.Ewrt + OK	1.93	-0.01	-9.66	5.94	1.32	0.96	1.80	0.610	1.42	0.548

Table A4.3 Comparison of different interpolation methods showing RMSE and the other statistics and linear regression parameters from the cross-validation scatter plots of the predicted values for the SO₂ winter season averages for the season 2004/2005 in rural areas. Apart of R² and a, all other statistical indicators are in µg.m⁻³

mapping method		winter season average SO ₂ [µg.m ⁻³]							linear regr. y=a.x+c		
		RMSE	MPE	min. error	max. error	MAE	MedAE	MPSE	a	c	R ²
1-a	interp. OK	2.44	0.04	-14.99	6.23	1.61	0.98	2.20	0.563	1.91	0.551
1-b	interp. LK	2.35	-0.02	-14.47	6.32	1.57	1.04	2.16	0.582	1.77	0.584
2-S.E-a	lin. regr. S.E + OK	2.32	-0.06	-12.68	5.83	1.51	0.96	2.44	0.617	1.59	0.596
3-S.Ewrt-a	lin. r. m. S.Ewrt + OK	2.37	-0.08	-12.77	5.87	1.58	1.00	2.52	0.624	1.55	0.585

A number of comparison conclusions can be drawn from the results provided in Tables A4.2 and A4.3:

- When ranking the statistics of the methods for within each indicator it can be concluded the methods give results quite close to each other, at for both the annual average and the winter average.
- Ranking the statistics within the methods of methodology type 1, interpolation with 2005 monitoring data only, the best results are obtained by the lognormal kriging, method 1-b. This is in line with the results in Horálek et al. (2007) on the 2004 data.

- When ranking the statistics for the method of the methodology types 2 and 3 shows no improvement for the type 3, i.e. including other supplementary parameter. It even tends to decrease the performance slightly as is most convincing to be seen at the winter average statistics. The addition of supplementary parameters next to the EMEP model output does not improve the interpolation.
- The statistics in the tables for the cross-validation scatter plots of predicted against the measured values show that the winter average show slightly higher correlation (higher R^2), somewhat lower overestimation at the lower values (smaller intercept) and a smaller underestimation at the higher values (slope closer to 1), then annual average. This indicates that the winter average might be a more accurate indicator than the annual averages. However, the statistical estimates of errors (Tables A4.2 and A4.3) show slightly higher values at the winter average.
- An inter-comparison of the methods of the types 1, 2 and 3 shows that the best results for 2005 data are given by method 2-S.E-a, i.e. linear regression model using only EMEP model output (S.E), followed by ordinary kriging of its residuals). This the same method as was used for the SO₂ annual average mapping on the 2004 data in Horálek et al. (2007) and confirms may therefore support its robustness.

Concluding from the above, the preferred method for the rural interpolated maps for the annual average SO₂ concentrations and the annual average SO₂ concentrations is the linear regression model using only EMEP output, followed by residual interpolation with ordinary kriging, method 3-S.E-a. The use of the EMEP modelled data is preferred, to guarantee the best European coverage of areas lacking measurements. No additional supplementary data sources are useful to improve the interpolations. The interpolated maps are shown in Figure A4.1. Values of the key parameters used for mapping are given in Table A4.4.

In case one would like to aim for one indicator for inter-annual trend analysis in the reduction of SO₂ exceedances, one should consider the winter average concentrations. Despite their higher concentrations then the annual average and their slightly worse performance on the error statistics, they show more accurate behaviour when comparing predicted values against measured values.

Table A4.4 Parameters of the method used for final mapping of SO₂ indicators annual average for 2005 (left) and winter average for the season 2004/2005 (right) in the rural areas, i.e. linear regression model S.E following by the interpolation on its residuals using ordinary kriging (OK).

linear regression model S.E + OK on its residuals	annual average	winter average
	coeff.	coeff.
c (constant)	1.549	1.009
a1 (EMEP model 2005)	0.812	0.916
nugget	1.0	1.5
sill	5.5	8.5
range [km]	270	130

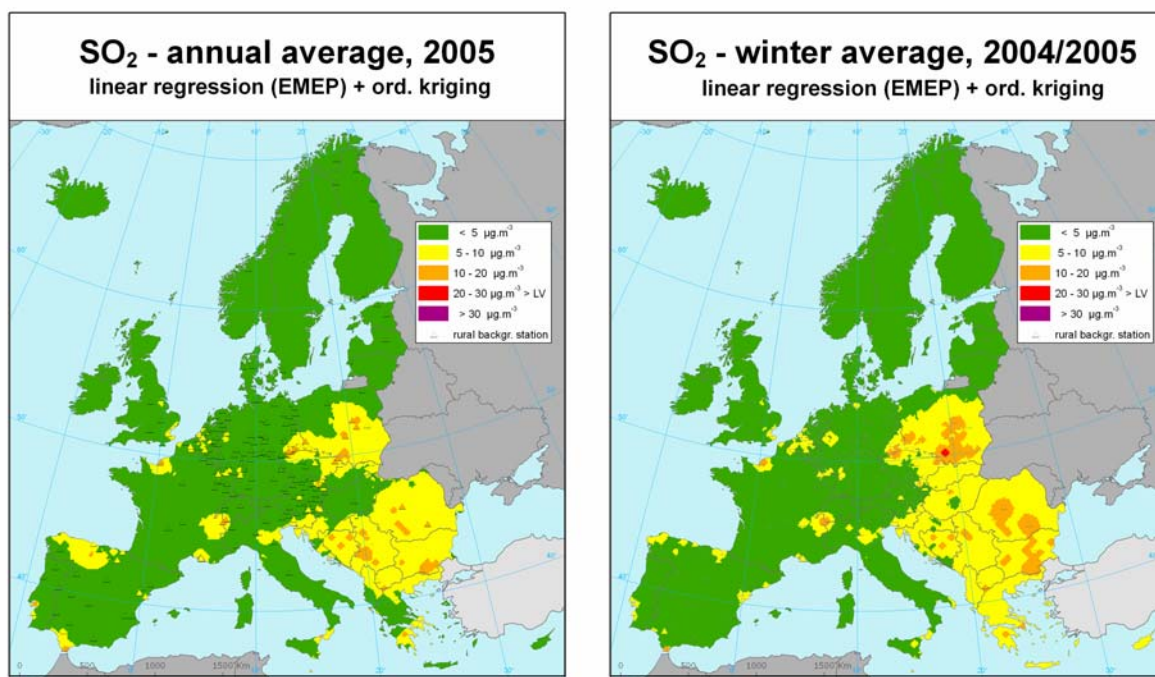


Figure A4.1 Maps showing the SO_2 indicators annual average concentration in the year 2005 (left) and winter average concentration for the season 2004/2005 (in $\mu g.m^{-3}$) on European scale for rural areas, 10×10 km grid resolution, as a result of interpolation method 3-S.E-a. Absolute and relative uncertainty of these maps expressed by RMSE is $1.9 \mu g.m^{-3}$ and 53.1 % (left) and $2.3 \mu g.m^{-3}$ and 54.3 % (right).

A4.1.3 Uncertainty analysis

Comparing concentration maps of the interpolation methods

In the Figures A4.2 and A4.3 the maps created by the preferred method 2-S.E-a and the alternative method 1-b are presented. In Figure A4.4 the differences between the selected method 2-S.E-a and the other method 1-b are shown. The differences between the methods are caused by the inclusion of EMEP dispersion model in the selected method. One can still recognise the EMEP grids and with support of this model data the limit value exceedance in specific areas is more refined determined and estimated in the map, for example the Katowice area in southern Poland.

Due to its poor measurement station coverage in the south-east of Europe we excluded this area from the interpolation on monitoring data only (method 1-b).

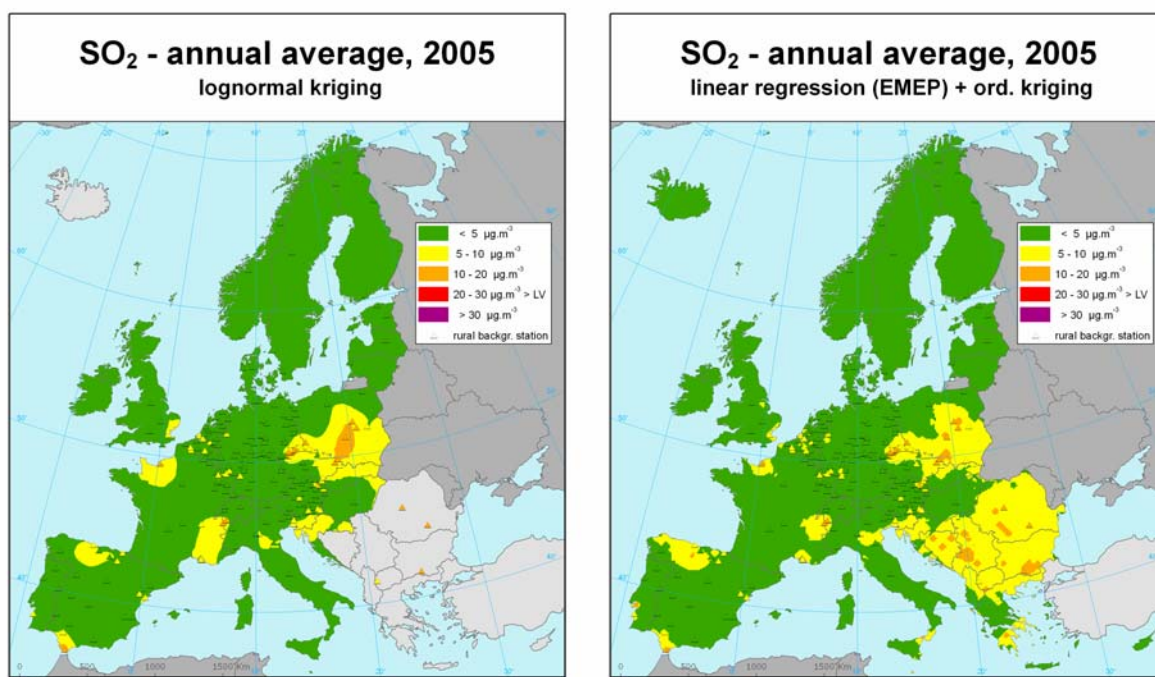


Figure A4.2 Maps showing the annual average SO_2 concentration (in $\mu g.m^{-3}$) on European scale for rural areas in 2005, 10 x 10 km grid resolution, as a result of interpolation method 1-b (left) and 2-S.E-a (right).

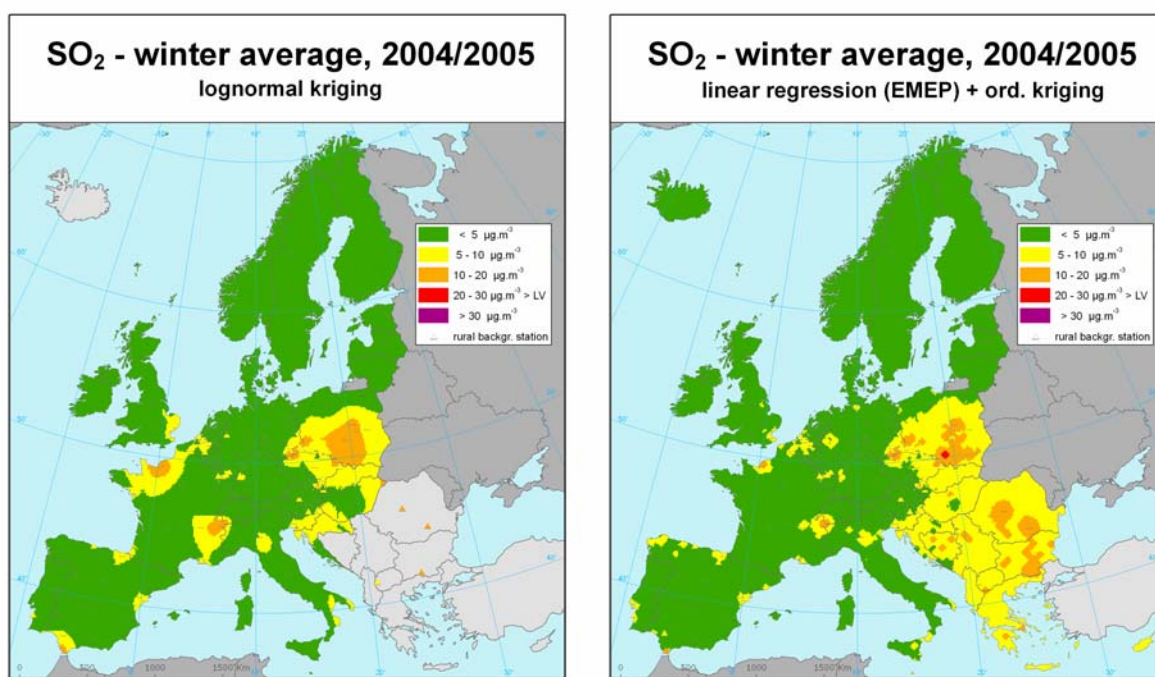


Figure A4.3 Maps showing the winter average SO_2 concentration (in $\mu g.m^{-3}$) on European scale for rural areas for winter season 2004/2005, 10 x 10 km grid resolution, as a result of interpolation method 1-b (left) and 2-S.E-a (right).

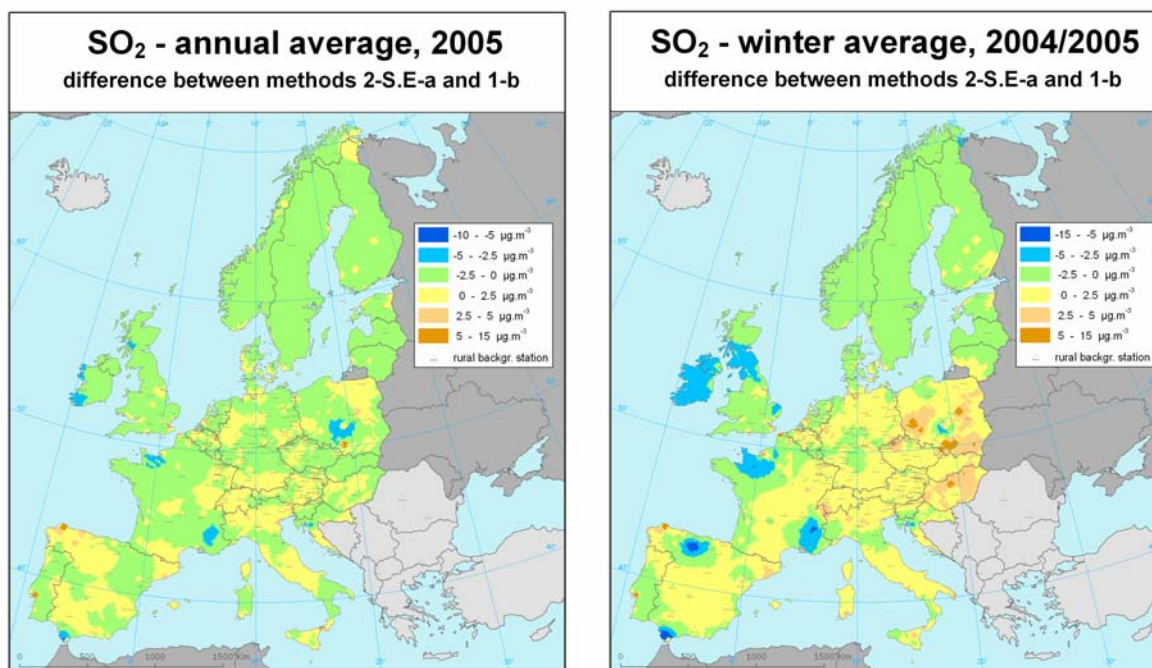


Figure A4.4 Maps showing the difference of the selected method 2-S.E-a and the method 1-b for the SO₂ indicators annual average in 2005 (left) and winter average in season 2004/2005 (right) in $\mu\text{g.m}^{-3}\cdot\text{hours}$ on the European scale for rural areas in 2005, 10 x 10 km grid resolution. Negative values show up at areas with higher concentrations of the alternative method 1-b compared to the preferred method 2-S.E-a.

Uncertainty estimated by cross-validation

The RMSE from the cross-validation is the most common indicator for the absolute mean uncertainty of the maps in the areas covered by measurements (see Tables A4.2. and A4.3). Using 2-S.E-a, this uncertainty of the rural map of the SO₂ annual average is $1.9 \mu\text{g.m}^{-3}$; and of SO₂ winter average is $2.3 \mu\text{g.m}^{-3}$.

Alternatively, this uncertainty can be also expressed as the relative mean uncertainty, being the percentage the absolute mean uncertainty is compared to the mean of the indicator values based on the measurements for all rural background stations. The relative uncertainty of the rural SO₂ annual average map is 53.1% and of the rural SO₂ winter average map it is 54.3%, in case method 3-S.E-a is used for mapping. This relative uncertainty is quite big – however, this is caused especially by generally small values of SO₂.

In the Figure A4.5 the cross-validation scatter plot for the selected method 3-S.E-a is shown. The nature of cross-validation (i.e. measured concentration in the point of estimation is excluded from the estimation) enables to evaluate the quality of the interpolation in the positions with no measurement within the areas covered by measurements. The level of the smoothing effect can be explained by the behaviour of parameters of its linear regression $y = a \cdot x + c$: high intercept c means overestimation at the lower concentrations and a flat slope a means underestimation at the higher concentrations. The figure shows a certain amount of such smoothing effect, e.g. at a measurement value of $10 \mu\text{g.m}^{-3}$ shows the annual average a predicted value of about $7 \mu\text{g.m}^{-3}$ and the winter average about the same, $7.5 \mu\text{g.m}^{-3}$, which is clearly an underestimation at the higher values.

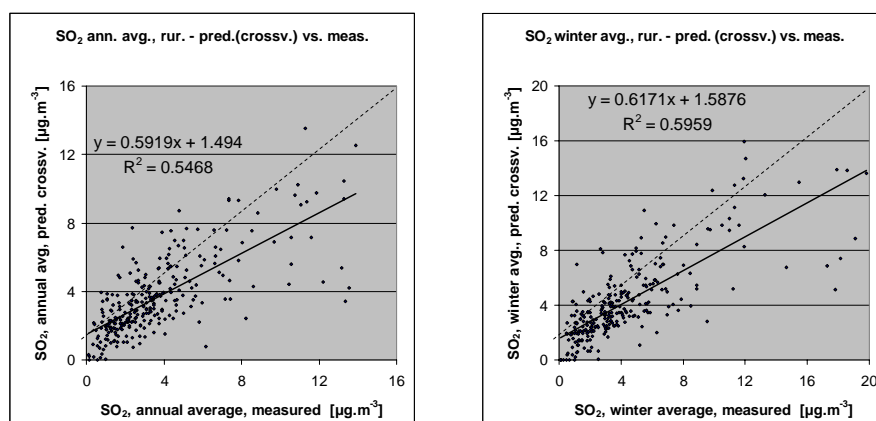


Figure A4.5 Correlation between cross-validation predicted values (y-axis) and measurements (x-axis) for the SO₂ indicators annual average in 2005 (left) and winter average for the season 2004/2005 (right) for rural areas, as a result of the linear regression S.E and ordinary kriging of its residuals

Comparing point measurement values with the predicted grid value

Additionally to cross-validation, a simple comparison between the measured and interpolated values in a 10x10 km grid has been made. This comparison shows to what extent the predicted value of the corresponding grid cell represents the measured values covered by that cell. The regression results of the cross-validation compared to this gridded validation examination are summarised in Table A4.5. This simple comparison shows at both indicators better correlation between stations measurements and corresponding predicted grid values (higher R², slope closer to 1, lower intercept) than the cross-validation predictions. This has its cause in the fact that the simple comparison between point measurements and gridded interpolated values shows the uncertainty at the stations locations (points) itself which tends to include less uncertainty than the cross-validation, simulating the behaviour of the interpolation at positions without measurement within the areas covered with measurements. The uncertainty in the simple comparison is determined partly by the smoothing effect of interpolation and partly by the spatial averaging of the values in 10x10 km grid.

The table values show that the agreement between point measurements and the estimated values at (in the points of measurements is very good: R² is larger than 0.9, the slope is larger than 0.8 and the intercept is around 0.5 µg.m⁻³. This small underestimation between at point measurement and predictions is also confirmed by the small value of nugget value in Table A4.4.

Table A4.5 Correlations between the predicted values of (i) the cross-validation and (ii) the 10x10 km grid respectively, and the measurements for the SO₂ indicators annual average and winter average for rural areas in 2005, as a result of the linear regression model S.E and ordinary kriging of its residuals.

Indicator	SO ₂ , 2005			
	Rural			
	annual average		winter average	
Mapping method	equation	R ²	equation	R ²
2-S.E-a lin. regr. S.E + OK				
(i) Cross-validated predictions	y = 0.5919x + 1.494	0.5468	y = 0.6171x + 1.5876	0.5959
(ii) 10x10 km grid predictions	y = 0.8405x + 0.5715	0.9248	y = 0.8800x + 0.4986	0.9557

Uncertainty maps

Next to the concentration maps (see Figure A4.1), the uncertainty maps are constructed, see Figure A4.6. As expected, the uncertainty is higher in areas with the lower density and increasing further away from the urban and suburban stations. The relative low density of SO₂ measurement stations used

in the interpolations lead to the higher uncertainty values especially at areas further away from the stations.

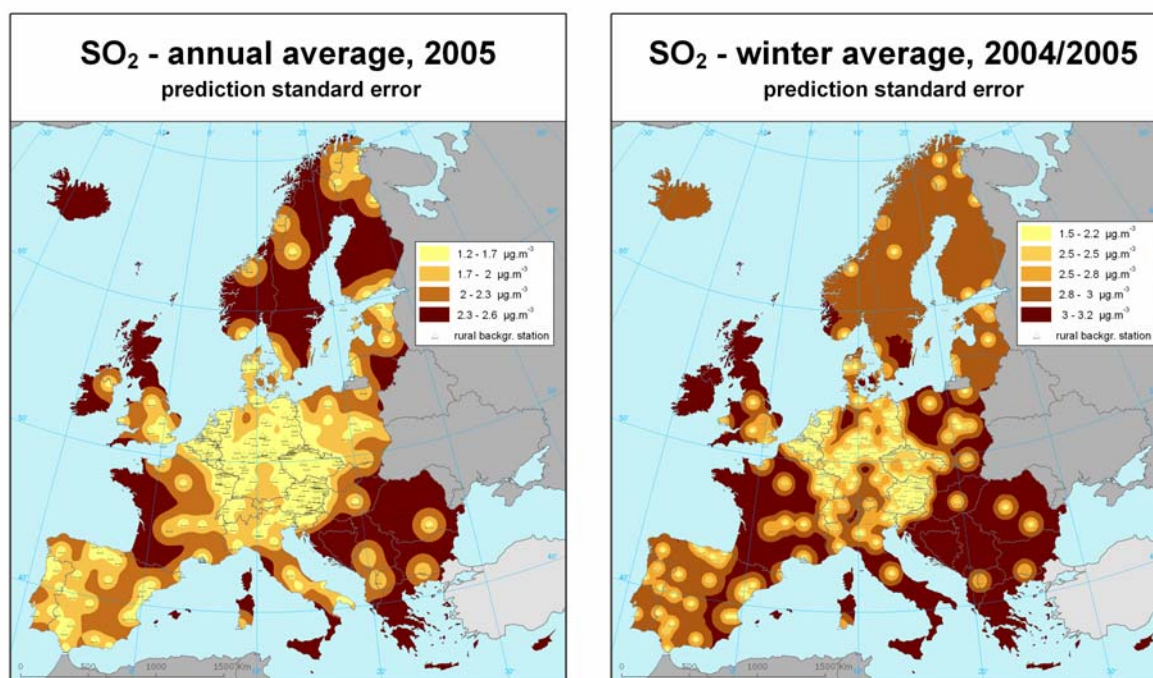


Figure A4.6 Uncertainty maps for the maps showing values of the SO₂ indicators annual average concentration in the year 2005 (left) and winter average concentration for the season 2004/2005 (in $\mu\text{g.m}^{-3}$) on European scale for rural areas, 10 x 10 km grid resolution, as a result of interpolation method 3-S.E-a.

Probability maps

Next, the maps of the probability of the limit value exceedance are constructed, using concentration and uncertainty maps (i.e. Figures A4.1 and A4.6) and the limit values (i.e. $20 \mu\text{g.m}^{-3}$ for both SO₂ vegetation-related indicators), see Figure A4.7. The maps show that there is only a small location in Bulgaria where the limit value of the annual average may be exceeded with a probability of 25 - 50 %. The other small location is at Katowice, south Poland, where the limit value for the winter season average may be exceeded with a probability larger than 75 %.

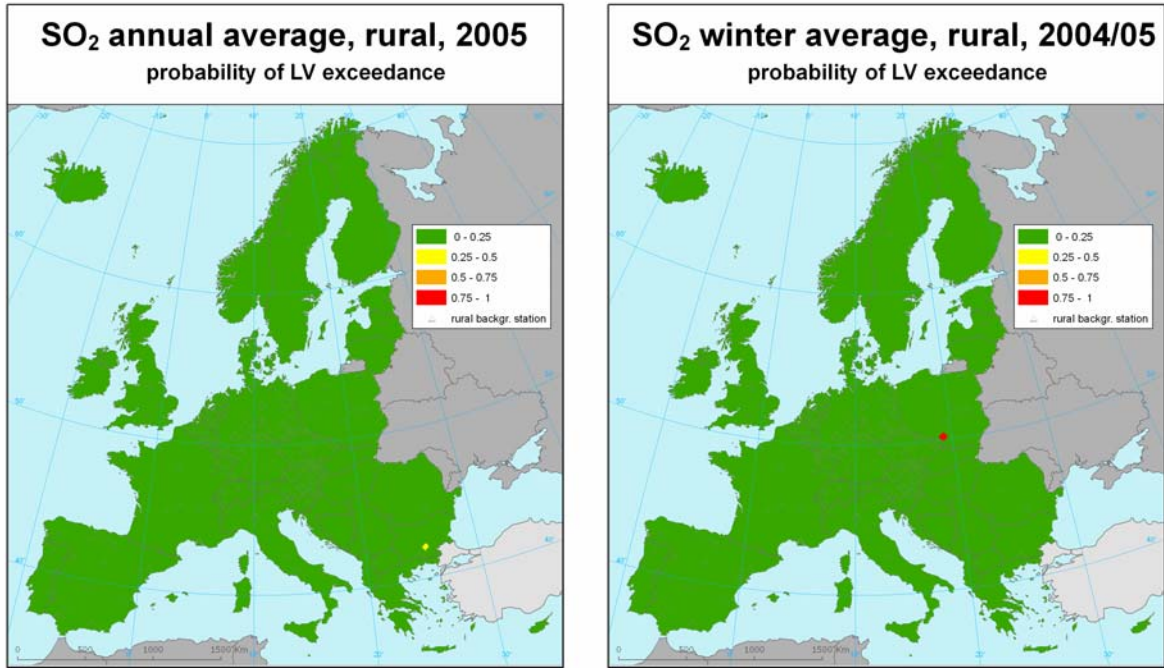


Figure A4.7 Probability of the limit value exceedance map for the SO₂ indicators annual average concentration in the year 2005 (left) and winter average concentration for the season 2004/2005 (in $\mu\text{g}\cdot\text{m}^{-3}$) on European scale for rural areas, 10 x 10 km grid resolution, as a result of interpolation method 3-S.E-a.

Annex 5 NO_x spatial analysis

One NO_x vegetation-related indicator is examined here: annual average NO_x concentrations. It concerns vegetation that is considered only to occur at rural areas and therefore we focus on mapping of rural areas only in this Annex.

A5.1 Rural maps

A5.1.1 Linear regression analysis

In Horálek et al. (2007) for the mapping of the 2004 annual average NO_x indicator a linear regression model using EMEP model output and altitude has been used. This method is nominated for examination here again (coded N.Ea).

With the 2005 data the selection of the supplementary parameters, apart from the EMEP model output, that fit the linear regression significantly are: wind speed, relative humidity and solar radiation. (Additional supplementary parameter would be surface pressure. However, it was decided not to use this parameter in final mapping: NO_x is the only pollutant for which the use of surface pressure tends to improve the regression, but its improvement in the map results would be very limited compared to the additional computational capacity involved for preparing the surface pressure data).

Thus, the following linear regression models to be examined are:

Submodel	Input parameters
N.E	EMEP model output
N.Ea	EMEP model output, altitude
N.Eawr	EMEP model output, altitude, wind speed, and surface solar radiation

The statistical performance of these three linear regression models is presented in Table A5.1.

Table A5.1 Statistical indicator values of the selected linear regression models indicating the correlation between supplementary data and the annual average of the 2005 measurement NO_x concentrations in the rural areas. R² (and adjusted R²) should be as close as possible to 1; RMSE (and standard error) should be as low as possible.

Indicator	NOx annual average, 2005			
	R ²	adjusted R ²	st. error [µg.m ⁻³]	RMSE [µg.m ⁻³]
N.E	0.150	0.147	12.56	12.52
N.Ea	0.179	0.174	12.35	12.30
N.Eawr	0.387	0.379	10.71	10.63

Table A5.1 shows better values of R² and RMSE for the linear regression models of the methodology type 3 (N.Ea and N.Eawr) than for the one of type 2 (i.e. N.E), indicating that the regression relation improves when supplementary meteorological parameters are included: R² increases by about 0.21 and RMSE decreases by about 14%. Altitude shows only little improvement.

Conclusions:

- The addition of only altitude as supplementary parameter just slightly improves the linear regression the closeness of the linear regression relation with the indicator values of the measurements.
- Whereas the extra addition of supplementary meteorological parameters considerably improves the closeness of the linear regression relation with the indicator values of the measurements.

These conclusions do indicate that the methods using linear regressions model performance improves significantly by including additional supplementary parameter altitude and especially meteorological parameters as wind speed and solar radiation, next to EMEP modelling data, in the interpolation methods on rural NO_x indicators. The individual models will be compared in next section.

A5.1.2 Spatial interpolation

Three types of the methods are examined. These methods are compared with each other using RMSE and other statistical indicators from cross-validation.

1. Interpolation using primarily monitoring data

- | | |
|----------------------------|-----------------------------|
| a. Ordinary kriging (OK) | b. Lognormal kriging (LK) |
| c. Ordinary cokriging (OC) | d. Lognormal cokriging (LC) |

2. Interpolation using monitoring data and EMEP model data

Linear regression using EMEP model output (N.E) and interpolation of its residuals using OK.

3. Interpolation using monitoring data, EMEP model data and other supplementary data

Linear regression model using EMEP model output and altitude (N.Ea), followed by interpolation of its residuals using OK

Linear regression model using EMEP model output, altitude, wind speed, surface solar radiation (N.Eawr), followed by interpolation of its residuals using OK

The statistical indicators of the cross-validation of the methods are presented in Table A5.2. The main criterion is RMSE, followed by MAE, MPE, MedAE and other indicators. All the indicators, with exception of R², are expressed in µg.m⁻³.

Table A5.2 Comparison of different interpolation methods showing RMSE and the other statistics and linear regression parameters from the cross-validation scatter plots of the predicted values for the NO_x annual averages for 2005 in rural areas. Apart of R² and a, all other statistical indicators are in µg.m⁻³

mapping method		annual average NO _x [µg.m ⁻³]										
		RMSE	SDE	MPE	min. error	max. error	MAE	MedAE	MPSE	linear regr. y=a.x+c		
										a	c	R ²
1-a	interp. OK	10.66	10.66	0.09	-51.04	25.40	7.16	4.62	11.10	0.385	10.72	0.383
1-b	interp. LK	10.59	10.59	0.01	-51.30	26.16	6.99	4.61	15.23	0.394	10.48	0.391
1-c	interp. OC	10.49	10.48	0.41	-49.99	25.91	7.03	4.54	10.92	0.427	10.31	0.405
1-d	interp. LC	9.48	9.46	0.56	-45.09	25.03	6.26	4.04	9.95	0.503	9.14	0.514
2-N.E-a	lin. regr. N.E + OK	10.31	10.31	0.04	-48.98	24.14	6.63	4.00	10.79	0.426	9.96	0.423
3-N.Ea-a	lin. r. m. N.Ea + OK	9.71	9.71	0.05	-46.87	24.48	6.21	3.91	10.63	0.456	9.44	0.491
3-N.Eawr-a	lin. r. m. N.Eawr + OK	9.66	9.66	0.04	-46.68	26.64	6.51	4.38	9.48	0.535	8.21	0.506

A number of comparison conclusions can be drawn from the results provided in Tables A5.2:

- When ranking the of the methods of interpolation with 2005 monitoring data only (methodology type 1), the best results with regard to RMSE and most other indicators are obtained with lognormal cokriging, method 1-d.
- When ranking statistics within the methods of methodology type 3, slightly better results are obtained by the linear regression model using EMEP output, altitude, wind speed and solar radiation, followed by residual interpolation by ordinary kriging, method 3-N.Eawr-a.
- The comparison of statistics of the methods of the methodology types 2 and 3 shows the improvement for the type 3 (i.e. including other supplementary parameter), based on RMSE and almost all other statistical indicators. The addition of supplementary parameters next to the EMEP model output improves the interpolation.
- The statistics of the best performing methods of both methodology type 1 (1-d) and 3 (3-N.Eawr-a) show very comparable performance. However, for the other methods of type 1 and 3, type 3 shows clearly better performances. In combination with previous bullet this tends to provide more confidence in concluding that addition of supplementary parameters next to the EMEP model output improves the interpolation.
- The statistics in Table A5.2 for the cross-validation scatter plots of predicted against the measured values shows that the predicted annual average according method 3-N.Eawr-a has highest correlation (higher R^2), lowest overestimation at the lower values (lowest intercept) and the smallest underestimation at the higher values (slope closest to 1). This method shows the smallest smoothing effect of its linear regression providing the best fit of predicted values at the locations of the measurement based values.
- An inter-comparison of the methods of the types 1, 2 and 3 shows that the best results are given by methods of methodological types 1 (lognormal cokriging using altitude) and 3 (linear regression model N.Eawr, followed by ordinary kriging of its residuals) for 2005 data (3-N.Eawr-a). The good results of lognormal cokriging (despite it is not more than an interpolation of measurement data only) are given by the fact that this method uses logarithmic transformation which corresponds to a logarithmic-normal distribution of NO_x . However, good results of RMSE in the case of the method 1-d are balanced by its very bad results of MPE.

Concluding from the above the selection of the best and most preferred interpolation method for rural NO_x vegetation indicator mapping is 3-N.Eawr-a. Its meteorological parameters improve the interpolation. Furthermore provides this method coverage of European areas without measurement stations, something that second best performing method 1-d does not facilitate in. The resulting rural map for the annual average NO_x concentrations using 3-N.Eawr-a is shown in Figure A5.1.

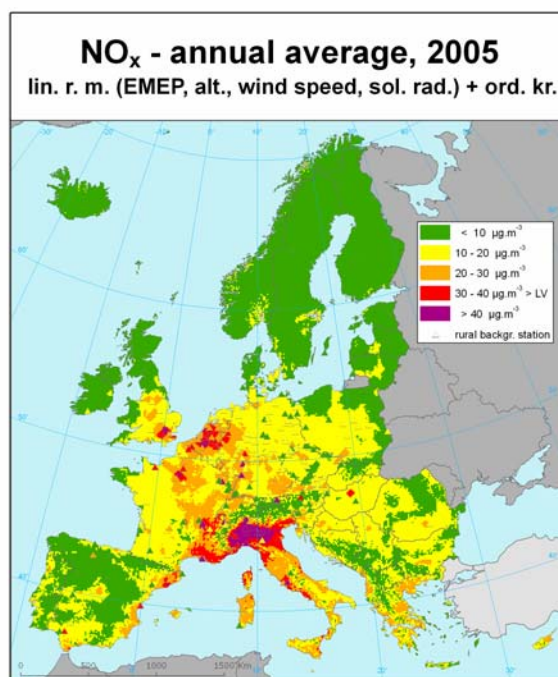


Figure A5.1 Map showing the annual average NO_x concentration (in $\mu\text{g.m}^{-3}$) on ecosystems on European scale for rural areas in 2005, 10 x 10 km grid resolution, as a result of interpolation method 3-N.Eawr-a. Uncertainty of these maps expressed by RMSE is $9.7 \mu\text{g.m}^{-3}$, i.e. 55.9 %.

Table A5.3 Parameters of the method used for final mapping of NO_x indicator annual average for 2005 in the rural areas, i.e. linear regression model N.Eawr following by the interpolation on its residuals using ordinary kriging (OK).

linear regr. model N.Eawr + OK on its residuals	annual average
	coeff.
c (constant)	20.32
a1 (EMEP model 2005)	0.995
a2 (altitude GTOPO)	-0.0140
a3 (wind speed 2005)	-5.753
a4 (s. solar radiation 2005)	1.165
nugget	80
sill	190
range [km]	3500

A5.1.3 Uncertainty analysis

Comparing concentration maps of the interpolation methods

In Figure A5.2 the maps created by the two other methods, 1-d and 2-N.E-a, are presented. These maps can be compared with the one of the preferred method 3-N.Eawr-a presented of Figure A5.1. In Figure A5.3 the differences between the selected method 3-N.Eawr-a and other methods are shown. It can be seen that method 1-d overestimates predicted concentrations values on the northern parts of the British Island and Ireland. This may be explained by the relative small number of rural stations present in this region. The effect of including altitude in the interpolation at the preferred method 3-N.Eawr-a

is also clearly visible for its lower values in the mountainous areas, such as the Pyrenees, Alps and in the Balkan.

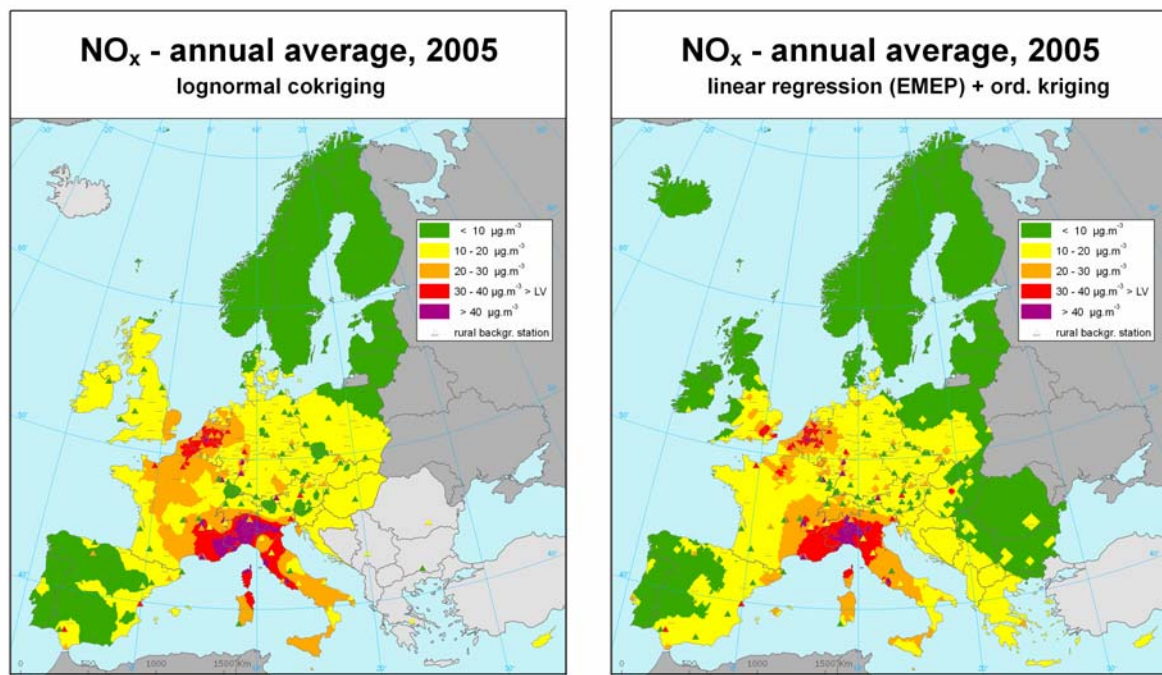


Figure A5.2 Maps showing the annual average NO_x concentration (in $\mu\text{g}\cdot\text{m}^{-3}$) on European scale for rural areas in 2004, $10 \times 10 \text{ km}$ grid resolution, as a result of interpolation method 1-d (left) and 2-N.E-a (right).

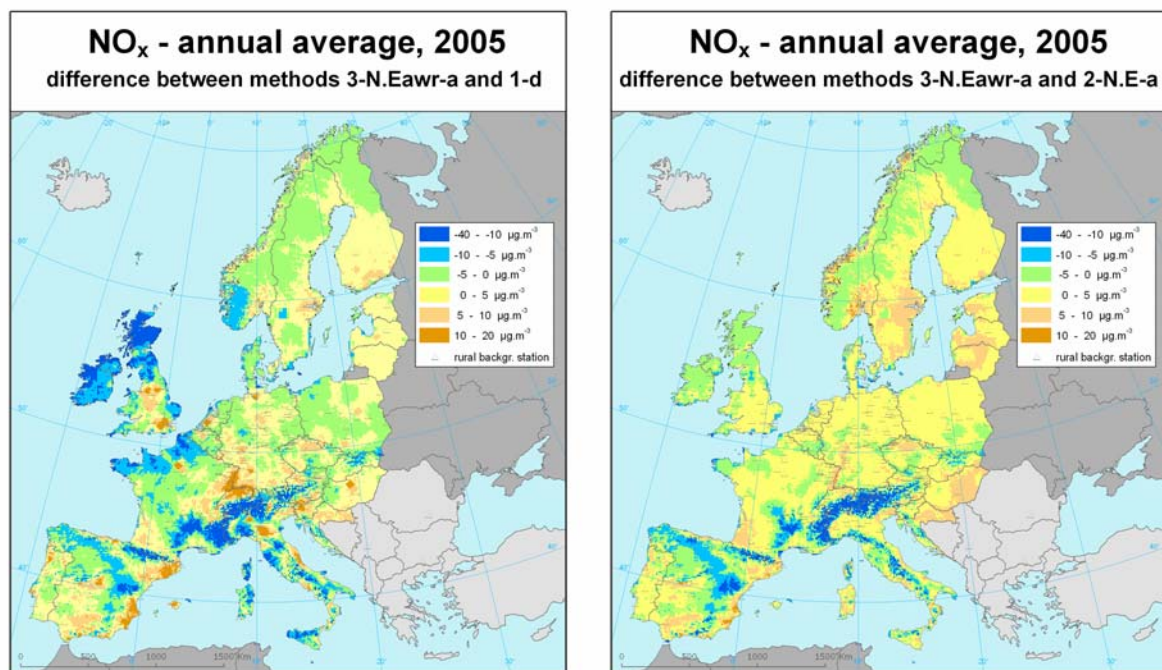


Figure A5.3 Maps showing the difference of the selected method 3-N.Eawr-a and the method 1-d (left), resp. 2-N.E-a (right) for the annual average NO_x concentration (in $\mu\text{g}\cdot\text{m}^{-3}$) on the European scale for rural areas in 2005, $10 \times 10 \text{ km}$ grid resolution. Negative values show up at areas with higher concentrations of the alternative method (1-d left, 2-N.E-a right) compared to the preferred method 3-N.Eawr-a.

Uncertainty estimated by cross-validation

The RMSE from the cross-validation is the most common indicator for the absolute mean uncertainty of the maps in the areas covered by measurements (see Table A5.2). The absolute mean uncertainty of the preferred method 3-N.Eawr-a for the rural map of NO_x annual average expressed by RMSE is 9.7 µg.m⁻³.

Alternatively, this uncertainty can be also expressed as the relative mean uncertainty, being the percentage the absolute mean uncertainty is compared to the mean of the indicator values based on the measurements for all rural background stations. The relative uncertainty of the rural NO₂ annual average map is 55.9% for method 3-N.Eawr-a.

In the Figure A5.4 the cross-validation scatter plot for the selected method 3-N.Eawr-a is shown. The nature of cross-validation (i.e. measured concentration in the point of estimation is excluded from the estimation) enables to evaluate the quality of the interpolation in the positions with no measurement within the areas covered by measurements. The level of the smoothing effect can be explained by the behaviour of the parameters of its linear regression $y = a \cdot x + c$: high intercept c means overestimation at the lower concentrations and a flat slope a means underestimation at the higher concentrations. The figure shows a certain amount of such smoothing effect, e.g. the annual average shows at 30 µg.m⁻³ measurement value a predicted value of about 24 µg.m⁻³, which is clearly an underestimation at the higher values.

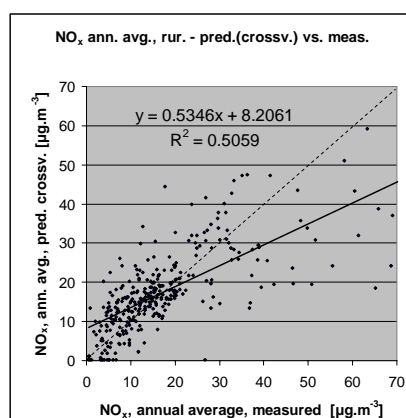


Figure A5.4 Correlation between cross-validation predicted values (y-axis) and measurements (x-axis) for the NO_x indicator annual average for rural areas in 2005, as a result of the linear regression N.Eawr and ordinary kriging of its residuals.

Comparing point measurement values with the predicted grid value

In addition to cross-validation, a simple comparison between the measured and interpolated values in a 10x10 km grid has been made. It shows to what extent the predicted value of the corresponding grid cell represents the measured values covered by that cell. The regression results of the cross-validation compared to this gridded validation examination are summarised in Table A5.4. This simple comparison shows a slightly correlation between stations measurements and corresponding predicted grid values (higher R², slope closer to 1, lower intercept) than the cross-validation predictions. The uncertainties between point measurements and gridded interpolated values shows the uncertainty at the stations locations (points) itself and are of almost the same order of uncertainty of the cross-validation, simulating the behaviour of the interpolation at positions without measurement within the areas covered with measurements.

Table A5.4 Correlations between the predicted values of (i) the cross-validation and (ii) the 10x10 km grid respectively, and the measurements for the NO_x indicators annual average for rural areas in 2005, as a result of the linear regression model N.Eawr and ordinary kriging of its residuals.

Indicator		NO _x rural	
		annual average	
prediction		equation	R2
(i)	Cross-validated predictions	$y = 0.5431x + 7.933$	0.498
(ii)	10x10 km grid predictions	$y = 0.5563x + 7.716$	0.508

Uncertainty maps

Next to the concentration map (see Figure A5.1), the uncertainty map is constructed, see Figure A5.5. Again, the uncertainty is higher in the areas with lower density of the rural stations, especially the areas without rural background station with NO_x measurements, such as Iceland and Cyprus. In central Europe where the density is highest the uncertainty levels are lowest.

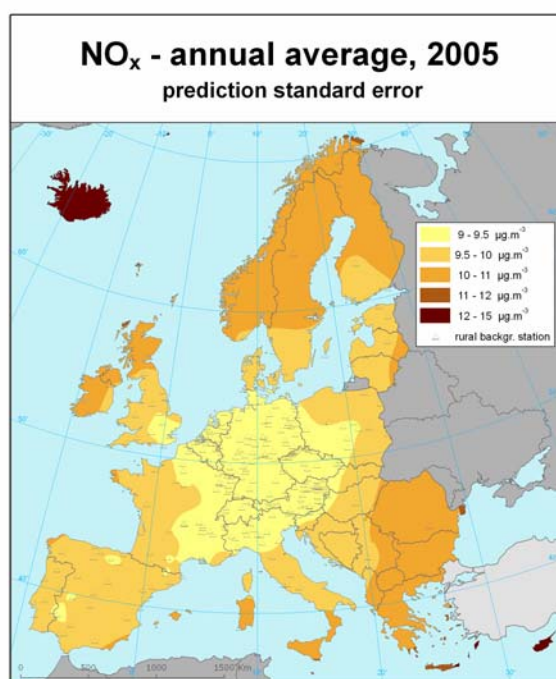


Figure A5.5 Uncertainty map for map showing the annual average NO_x concentration (in $\mu\text{g.m}^{-3}$) on European scale for rural areas in 2005, 10 x 10 km grid resolution, as a result of interpolation method 3-N.Eawr-a.

Probability maps

Next, the map of the probability of the NO_x limit value exceedance is constructed, using concentration and uncertainty maps (i.e. Figures A5.1 and A5.4) and the limit value (i.e. $30 \mu\text{g.m}^{-3}$), see Figure A5.6.

The highest probability of limit value exceedance is at locations and regions with large agglomerations, such as London, Ruhr Gebiet, Paris, Rhone Valley in France, Rhine valley in Germany, the Italian Po Valley, and the Benelux. Also the Italian, French, Spanish Mediterranean coastal zone elevated probability of exceedance.

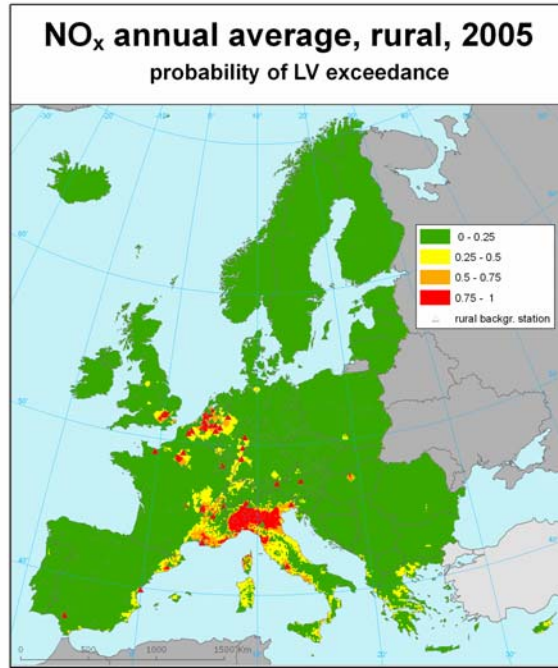


Figure A5.6 Probability of the limit value exceedance map for the annual average NO_x concentration (in $\mu\text{g.m}^{-3}$) on European scale for rural areas in 2005, 10 x 10 km grid resolution, as a result of interpolation method 3-N.Eawr-a.

Annex 6 Formulas of statistical indicators and other calculations

Statistical indicators

In the report, many statistical indicators are used:

Linear regression

In the linear regression analysis the indicators R^2 , *adjusted R^2* , *standard error of estimation* and *RMSE* are applied, according to the equations

$$R^2 = \frac{\left(\sum_{i=1}^N (Z(s_i) - \bar{Z})(\hat{Z}(s_i) - \bar{\hat{Z}}) \right)^2}{\sum_{i=1}^N (Z(s_i) - \bar{Z})^2 \cdot \sum_{i=1}^N (\hat{Z}(s_i) - \bar{\hat{Z}})^2} = 1 - \frac{\sum_{i=1}^N (Z(s_i) - \hat{Z}(s_i))^2}{\sum_{i=1}^N (Z(s_i) - \bar{Z})^2} \quad (A6.1)$$

$$\text{adjusted } R^2 = R^2 - \frac{p-1}{(N-p)} \cdot (1 - R^2) \quad (A6.2)$$

$$\text{st.error} = \sqrt{\frac{1}{N-p} \sum_{i=1}^N (Z(s_i) - \hat{Z}(s_i))^2} \quad (A6.3)$$

$$\text{RMSE} = \sqrt{\frac{1}{N} \sum_{i=1}^N (Z(s_i) - \hat{Z}(s_i))^2} \quad (A6.4)$$

where $Z(s_i)$ is the measured concentration at the i -th point, $i = 1, \dots, N$,
 $\hat{Z}(s_i)$ is the estimated concentration at the i -th point using other points,
 \bar{Z} is the arithmetic average of $Z(s_1), \dots, Z(s_N)$,
 $\bar{\hat{Z}}$ is the arithmetic average of $\hat{Z}(s_1), \dots, \hat{Z}(s_N)$,
 N is the number of the measuring points,
 p is the number of parameters of the lin. regr. model including constant.

R^2 and adjusted R^2 should be as close to 1 as possible. Standard error of estimation and RMSE should be as small as possible.

Cross-validation

The particular indicators used in cross-validation are the following: Root mean squared error (RMSE), mean prediction error (MPE) which is the same as the average bias, standard deviation of error (SDE), mean absolute error (MAE), minimum error, maximum error, median of absolute error (MedAE), and mean prediction standard error (MPSE). These indicators are calculated according to the equations

$$\text{RMSE} = \sqrt{\frac{1}{N} \sum_{i=1}^N (Z(s_i) - \hat{Z}(s_i))^2} \quad (A6.5)$$

$$\text{MPE} = \frac{1}{N} \sum_{i=1}^N (Z(s_i) - \hat{Z}(s_i)) \quad (A6.6)$$

$$SDE = \sqrt{\frac{1}{N} \sum_{i=1}^N \left((Z(s_i) - \hat{Z}(s_i)) - \frac{1}{N} \sum_{i=1}^N (Z(s_i) - \hat{Z}(s_i)) \right)^2} \quad (A6.7)$$

$$MAE = \frac{1}{N} \sum_{i=1}^N |Z(s_i) - \hat{Z}(s_i)| \quad (A6.8)$$

$$\min. \text{ error} = \min \{ Z(s_i) - \hat{Z}(s_i); i = 1 \dots N \} \quad (A6.9)$$

$$\max. \text{ error} = \max \{ Z(s_i) - \hat{Z}(s_i); i = 1 \dots N \} \quad (A6.10)$$

$$MedAE = \text{median} \{ |Z(s_i) - \hat{Z}(s_i)|; i = 1 \dots N \} \quad (A6.11)$$

$$MPSE = \frac{1}{N} \sum_{i=1}^N PSE(s_i) \quad (A6.12)$$

where $Z(s_i)$ is the measured concentration at the i -th point, $i = 1, \dots, N$,

$\hat{Z}(s_i)$ is the estimated concentration at the i -th point using other information, without the measured concentration at the i -th point,

$PSE(s_i)$ is the kriging standard error at the i -point,

N is the number of the measuring points.

RMSE, *SDE*, *MedAE*, *MAE* and *MPSE* should be as small as possible. *MPE*, *minimum error* and *maximum error* values should be as close to zero as possible. The *SDE* is in most cases of this report almost equal to *RMSE*, inherent to the fact that at in most cases the *MPE* (being part of *SDE* equation) is close to zero.

Coefficient of determination R^2 of cross-validation scatter plot is calculated similarly as in eq. (A6.1).

Kriging and variograms

Kriging

Kriging is a statistical interpolation method, which makes use of the assumption that the spatial variance of the value being interpolated can be described as a function of distance. In other words, the further away a point is from a measurement then the larger the uncertainty is in its value. Kriging exploits this assumption, which is described by the semi-variogram model and its parameters of nugget, sill and range (see below), by trying to minimise the variance at the interpolation point, i.e. the most likely value at that point given the surrounding measurements.

The spatial variance of the value to be interpolated, and described using the semi-variogram, is scale dependent. It depends on the spatial variability of the value and is also dependent on the spatial sampling frequency of that value. For the application described here, for instance, there are very few observations of air quality data at a rural scale that are within 20 km of each other, thus no information is known concerning the variability on spatial scales less than this. Even for the urban scale there are few observations of air quality within 5 km of each other, and so the variance on scales less than this is unknown. As a result the kriging methodology attributes a certain variance to these smaller scales, which is based on the variance at the lower limit of the resolved scales. This is termed, in kriging, the 'nugget' value. If this was 0 then measurements close to each other would vary very little from each other. If this value was, for instance, $100 \text{ } (\mu\text{g}\cdot\text{m}^{-3})^2$ then even measurements close to each other would vary with a standard deviation of $10 \text{ } \mu\text{g}\cdot\text{m}^{-3}$.

When interpolations are carried out on a 10 x 10 km grid then the interpolation at that grid point is strongly weighted by the nearest measurements (possibly within the grid itself). When the nugget value is 0 then the grid point interpolation will be very close to the value of the nearest measurement. If there are 2 equally nearby measurements then the grid point will be close to their average value. However, if the nugget value becomes larger then the nearby measurements are weighted less, in regard to points further away, with the result that deviations from the very local measurements will occur in the interpolation, affected by measurements further away.

When scatter plots are made of the observations against the gridded interpolations at the same point in space then their difference depends strongly on the relative weighting, as described above, resulting from the nugget value (more precisely the ration of the nugget to sill value). If the nugget is 0 then there will be very good correlation with very low RMSE. If nugget is high then there will be more deviation and a tendency towards a filtering of the results. In this way the nugget determines the error seen in the scatter plots. However, the nugget is itself based on a fit to available data (and to some extent on an optimisation of the method to reduce RMSE). In this way the nugget represents the uncertainty in the spatial representativeness at scales below the sampling scale, or at the lower limit of the sampling scale. For this reason I expect, and this could be confirmed by Jan, that the MSE found with this sort of comparison is very close to the nugget value used for the interpretations.

Variogram parameters

The basic parameters of the variogram are called nugget, sill and range, see Figure A6.1.

Sill is the value at which the spatial variability doesn't change with distance (plateau); range is the distance at which the spatial variability doesn't change. The range gives information about the size of the search window as it is not interesting to account for those points where spatial variance is not related to distance. If the range is large, the long-range variation dominates; if small then the short distances dominate the variation. Nugget is the y-intercept, which represents the spatial uncorrelated noise and errors, since at zero distance we would expect no variability. The difference sill-nugget is sometimes called partial sill.

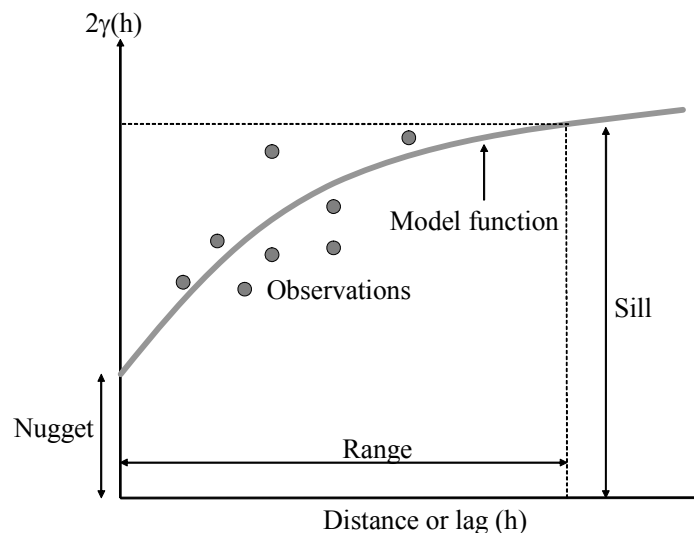


Figure A6.1 Diagram showing the important parameters that describe the variogram, $2\gamma(h)$, used in kriging

Merging criteria of rural and urban maps into combined concentration maps

The European-wide population density grid is used for merging the rural and urban maps into one combined air quality indicator map. Both the rural map and the urban map are created for the whole of Europe. The population density grid helps to determine for which part of the area the respective map is used.

For areas with population density less than the defined value of α_1 , the rural map is applied, and for areas with population density grids greater than the defined value α_2 , the urban map is applied. For areas with population density within the interval (α_1, α_2) the following relation is applied

$$\hat{Z}(s) = \frac{\alpha_2 - \alpha(s)}{\alpha_2 - \alpha_1} \cdot R(s) + \frac{\alpha(s) - \alpha_1}{\alpha_2 - \alpha_1} \cdot U(s) \quad (\text{A6.13})$$

where $\hat{Z}(s)$ is the resulting value of concentration at the point s ,

$R(s)$ is the concentration at the point s for the rural map,

$U(s)$ is the concentration at the point s for the urban map,

$\alpha(s)$ is the density of population at the point s .

Combining criteria of rural and urban uncertainty map for the combined probability map

The combined map of probability of exceedance is derived composed from the combined map of concentrations and the combination of the rural and urban uncertainty map according a merging criterion as described in Section 2.3. It explains how the combined uncertainty is derived according the standard error propagation calculation on the level of grid cells.

The uncertainty in the probability maps accounts only for the uncertainties caused by the interpolation. Uncertainties in the measurements, the supplementary data, linear regression and those caused by the urban/rural combination are not included.

Annex 7 PM_{2.5} in relation to PM₁₀

In many countries the monitoring network for PM_{2.5} are still under development. The number of operational PM_{2.5} stations is relatively small. In particular, the number of rural background stations is too low for constructing a rural PM_{2.5} map. As PM_{2.5} and PM₁₀ measurements show a high correlation it was investigated whether, after a proper transformation, the more widely available PM₁₀ data could be used as surrogate PM_{2.5} measurements.

Co-located PM_{2.5} and PM₁₀ measurements have been reported in 2004 and 2005 for 274 stations but not all stations cover the full two-year period. The data available from AirBase has been used as such, that is, it is assumed that, where needed, all PM data has been corrected for a non-reference method. Information on PM₁₀ methods and correction factors is given in by Buijsman and de Leeuw (2004) and de Leeuw (2005); this information is, however, not up-to-date. Information on the applied PM_{2.5} correction factors is not available. This lack of information hampers the comparison of results between countries. Any conclusion regarding PM_{2.5}/PM₁₀ relation should be handled with caution in light of this uncertainty, see below. Data has been analysed with minimum data coverage of 75% on a daily basis.

The correlation between co-located PM_{2.5} and PM₁₀ measurements is generally high (averaged over all stations R=0.86 (2004) and R=0.88 (2005)). The inter-annual variations in correlation are small. There are striking differences between the countries. The Nordic countries (Denmark, Finland, Iceland, Norway, and Sweden) show a correlation which is clearly lower than in the more southern countries. The more frequent use of studded tyres and winter sanding in these countries may lead to increased coarse fraction during parts of the year, affecting the correlation between PM_{2.5} and PM₁₀. Although there are only two (2004) or three (2005) operational rural background stations in the Nordic region, these two stations show a better correlation than found at the five (2004) or six (2005) (sub)urban background and at the eleven traffic stations.

For all available stations, the correlation at (sub)urban background stations (R= 0.89) and rural background stations (R=0.89) is similar and better than at traffic stations (R=0.81).

In Figure AIII.1 the annual mean concentrations of PM₁₀ and PM_{2.5} are given as function of the station

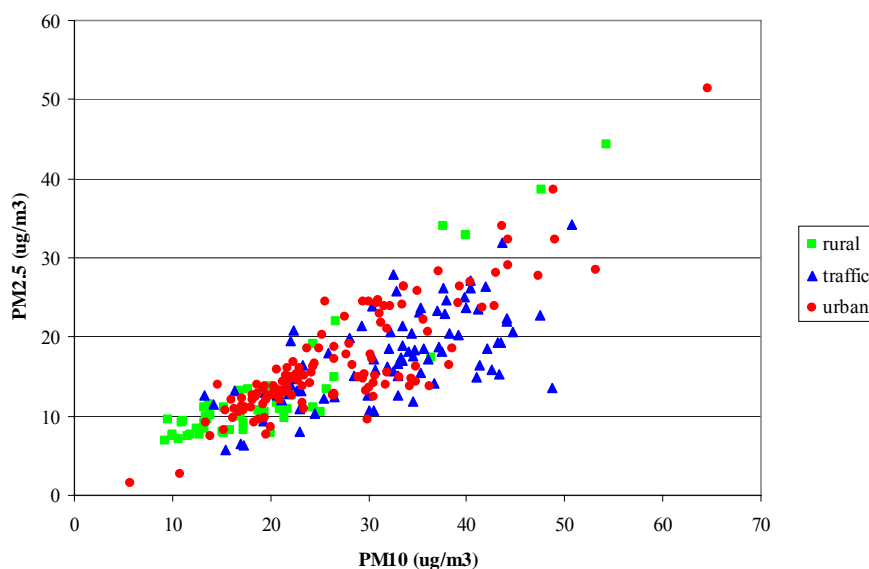


Figure AIII.1 Annual mean concentrations of PM₁₀ and PM_{2.5} (period 2004-2005)

classification. The figure indicates a wide spread in $PM_{2.5} / PM_{10}$ ratios; the ratio clearly depends on the type of station.

There are various options to calculate the $PM_{2.5} / PM_{10}$ ratio. The simplest approach is to calculate it from the annual mean values:

$$ratio = \bar{C}_{PM_{2.5}} / \bar{C}_{PM_{10}} \quad \text{or} \quad ratio = \frac{1}{n} \sum C_{PM_{2.5}} / \frac{1}{m} \sum C_{PM_{10}} \quad [M1]$$

where \bar{C} is the annual mean value. The averaging is over n and m days, respectively. The number of days is not necessarily the same for PM_{10} and $PM_{2.5}$.

A second approach is to estimate the ratio as the slope of a linear regression of daily concentrations:

$$C_{PM_{2.5}} = ratio C_{PM_{10}} + b$$

where C is the daily mean value and b is the intercept which could – optionally – be forced to zero. In this case, the ratio is obtained from:

$$ratio = \frac{1}{k} \sum C_{PM_{2.5}} \cdot C_{PM_{10}} / \frac{1}{k} \sum C_{PM_{10}}^2 \quad [M2]$$

where the averaging is over the k days with simultaneous measurements of PM_{10} and $PM_{2.5}$.

In the third approach the ratio is calculated on a daily basis and next averaged over the full year:

$$ratio = \frac{1}{k} \sum (C_{PM_{2.5}} / C_{PM_{10}}) \quad [M3]$$

In further analysing of the data, two stations have been excluded as preliminary calculations indicated unrealistic ratios of more than 1.1 or smaller than 0.07. Calculations for each of the two years showed that the inter-annual variations in ratio are small. The results of the two years are therefore combined in further processing.

Comparing the three methods generally results in similar ratios, see figure AIII.2. The largest differences are found when in method M1 the data coverage in calculating the annual means of $PM_{2.5}$

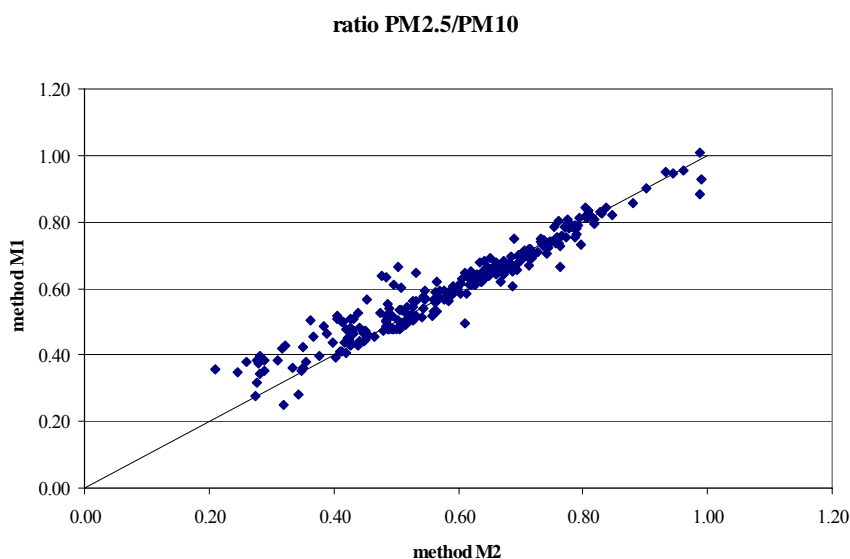


Figure AIII.2 Comparison between method M1 and M2 in calculating the $PM_{2.5} / PM_{10}$ ratio. The line corresponds to the 1:1 line.

and PM₁₀ show relatively large differences. Method M2 will result in the best fit between PM_{2.5} and PM₁₀ concentrations and is therefore to prefer.

A closer look at the ratios suggests, next to the dependency on station type, a geographical dependency. To evaluate this, Europe has been divided in four regions (not all countries have reported valid paired PM_{2.5} and PM₁₀ time series. Countries not included in the current analyses are printed in *italic*):

1. Northern Europe: Norway, Sweden, Finland, *Estonia, Lithuania, Latvia*, Denmark and Iceland
2. North-western Europe: United Kingdom, Ireland, *the Netherlands*, Belgium, *Luxembourg*, France north of 45 degrees latitude
3. Central and Eastern Europe: Germany, Poland, Czech Republic, Slovakia, *Hungary*, Austria, Switzerland, Liechtenstein
4. Southern Europe: France south of 45 degrees latitude, Portugal, Spain, *Andorra, Monaco*, Italy, *San Marino, Slovenia, Croatia*, Greece, *Cyprus, Malta*.

Results (method M2) are presented in Table AIII.1 and Figure AIII.3. The ratios are in the range of 0.4 to 0.8. In North and Central-East there is a clear tendency for lower ratios in the order rural-urban-traffic. This indicates an increasing contribution of locally emitted coarse particles at urban and traffic sites. In Southern Europe there is no such significant tendency. The rural stations in North-Western Europe (4 time series in the UK, one in Belgium) have a ratio which is surprisingly low compared to the ratio at urban and traffic sites in this region. The low number of time series may a role here.

Table AIII.1 PM_{2.5}/PM₁₀ ratios and available number of time series as function of region and station type

region	PM _{2.5} /PM ₁₀ ratio			number of time series		
	rural	urban	traffic	rural	urban	traffic
North	0.78	0.46	0.39	5	11	22
North-West	0.53	0.61	0.59	5	54	17
Central-East	0.76	0.70	0.64	13	45	22
South	0.56	0.55	0.54	28	19	24
Total	0.63	0.62	0.54	51	129	85

The ratio at rural stations is much lower in North-western and Southern Europe than in North and Central-East. A possible explanation is the importance of sea spray particles (NW Europe) and mineral (Sahara) dust (S Europe).

The ratios presented here indicate some clear dependencies. However, as uncertainties in the ratios are large, one should be careful to draw conclusions. As mentioned above, detailed information how measurements using a non-reference method are treated is lacking; different procedure for PM_{2.5} and PM₁₀ will be reflected in large differences in ratios. The ratio shows large station-to-station variability, see the standard deviations plotted in Figure AIII.3. For each station type the number and location of stations differs widely within a region (and also within a country). For example, in North-western Europe, 4 (out of 5) rural time series are located in the UK while 43 (out of 54) urban time series are in France.

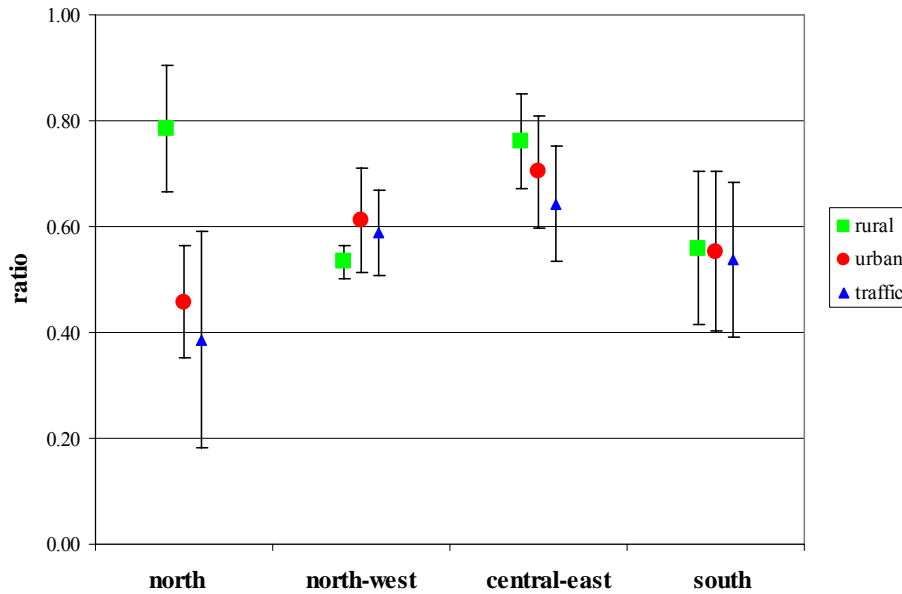


Figure AIII.3. $PM_{2.5}/PM_{10}$ ratios averaged per region and station type. The error bars indicate plus/minus one standard deviation.

As Horálek et al (2007) discussed, the availability of $PM_{2.5}$ monitoring data in 2004 is too low to produce a European concentration map. Over 2005 the number of stations has been increased but still not more than 33 rural stations provide a valid annual mean (data coverage > 75%). Relaxing the data coverage criteria to 50% is no solution: it will increase the number to 39 which is still too low for the interpolation procedure. It has been suggested to increase this number of stations by introducing pseudo- $PM_{2.5}$ stations. At these stations the $PM_{2.5}$ concentration has been estimated from a $PM_{2.5}/PM_{10}$ ratio and the PM_{10} concentrations measured at the station.

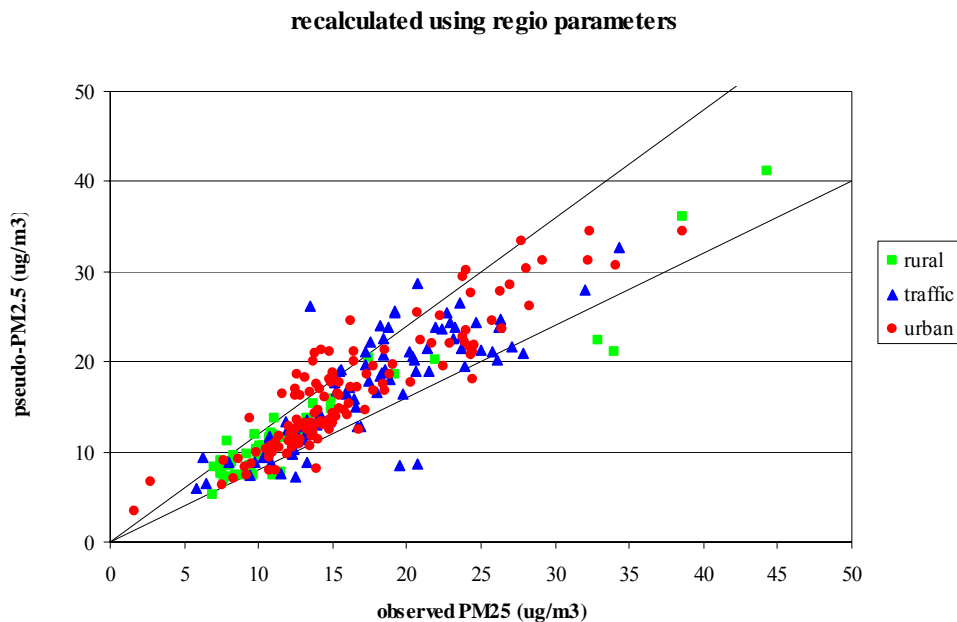


Figure AIII.4 Scatter plot of observed and calculated $PM_{2.5}$ concentrations. Calculations are based on region/station type specific ratios. The two lines correspond to $y=1.2x$ and $y=0.8x$

This approach was tested here for annual mean concentrations. Using the here derived region/station type specific ratio and the observed PM_{10} concentrations, the pseudo- $PM_{2.5}$ concentrations have been

estimated. The calculated values are compared with the observed values in Figure AIII.4 and Table A.2. The bias, between observed and calculated values - defined as $bias = \frac{1}{n} \sum (C_{obs} - C_{calc})$ - is negligible. However, the root-mean-square error (RMSE) is $3.1 \mu\text{g}/\text{m}^3$ (19% of the grand average of $16.1 \mu\text{g}/\text{m}^3$). The two lines in the scatter plot corresponds to $y=1.2x$ and $y=0.8x$, that is, for data points within the two lines the error between observed and calculated $\text{PM}_{2.5}$ values is less than 20%. It is evident that in the range of $10\text{-}20 \mu\text{g}/\text{m}^3$ –the range of the most frequently observed concentrations – a large number of data points fall outside this 20%-range.

Table A.2 Comparison between observed and calculated $\text{PM}_{2.5}$ concentrations using region and country specific ratios.

Parameter(1)	Region specific	Country specific	Perfect fit
RMSE	3.06	2.41	0
bias	0.01	0.07	0
MAE	2.17	1.65	0
a	0.90	0.97	1
sa	0.03	0.02	0
b	1.54	0.38	0
sb	0.46	0.37	0
MARE (%)	14	11	0
observed averaged	16.2	16.2	-

The following parameters are given:

$$\text{RMSE: root mean square error} = \sqrt{\sum \frac{1}{n} (C_{obs} - C_{calc})^2}$$

$$\text{Bias} = \frac{1}{n} \sum (C_{obs} - C_{calc})$$

$$\text{MAE: Mean absolute error} = \frac{1}{n} \sum |C_{obs} - C_{calc}|$$

Slope (a) and intercept (b) and their standard error (sa, sb) of the regression:
 $C_{calcs} = a C_{obs} + b$

$$\text{MARE: mean absolute relative error} = 100\% \cdot \frac{1}{n} \sum |C_{obs} - C_{calc}| / C_{obs}$$

The estimation of the pseudo $\text{PM}_{2.5}$ concentrations can be improved by applying ratios with a higher spatial resolution, that is, averaged at the country level instead of the region level. Although the fit between observed and calculated concentrations improves - the RMSE drops to $2.4 \mu\text{g}/\text{m}^3$ (15% of the grand average), see figure 5 and Table 2- this improvement is limited considering the increase in the number of parameters from 15 region/station type specific ratios to 47 country/station type specific ratios.

Considering that in the above applications the same data set is used both for parameterisation and for validation, it is to be expected that when the approach is used to estimated $\text{PM}_{2.5}$ concentrations at the locations of the more than 2000 PM_{10} stations available in AirBase, the error in these estimates will largely exceed the 15-20% error found here. In combination with the uncertainties in the PM_{10} measurements itself, the constructed pseudo $\text{PM}_{2.5}$ data will most likely not fulfil the data quality objectives as given in the first daughter directive.

The application of the country/station type depending ratios is further hampered by the fact that only 47 of the required 99 ratios (33 countries providing information to AirBase and 3 stations type) can be estimated. Gap filling of the missing ratios, e.g. by introducing the median or averaged value from the region, will certainly enhance the error.

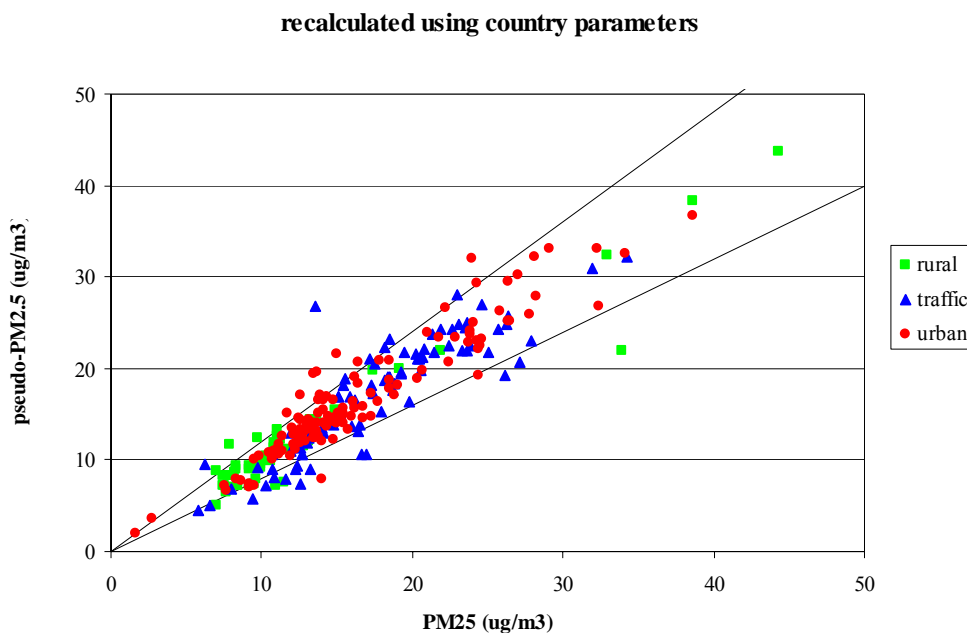


Figure AIII.5. Scatter plot of observed and calculated PM_{2.5} concentrations. Calculations are based on country/station type specific ratios. The two lines correspond to $y=1.2x$ and $y=0.8$

The use of a PM_{2.5}/PM₁₀ ratio to generate “pseudo”PM_{2.5} data from the widely available PM₁₀ measurement should be discouraged.

References to Annex 7

- Buijsman E. and de Leeuw F.A.A.M. (2004) Correction factors and PM₁₀ measurements in AIRBASE, ETC/ACC technical paper - draft.
http://air-climate.eionet.europa.eu/docs/meetings/041122_9th_EIONET_AQ_WS/05d_PM10_corr_factors_in_Air_Base_Nov2004-TempDraft.pdf.
- de Leeuw F.A.A.M. (2005) PM₁₀ measurement methods and correction factors in AirBase 2004 status report. ETC/ACC Technical Paper 2005/6. Available from:
http://air-climate.eionet.europa.eu/reports/ETCACC_TechPaper_2005_6_PM10_CorrFactors2004
- Horálek, J., Denby, P., de Smet, P., de Leeuw, F., Kurfürst, P., Swart, R., van Noije, T. (2007). Spatial mapping of air quality for European scale assessment. ETC/ACC Technical paper 2006/6.
http://air-climate.eionet.europa.eu/docs/ETCACC_TechPaper_2006_6_Spat_AQ.pdf

